HAWKE'S BAY
REGIONAL COUNCIL

Heretaunga Aquifer Groundwater Model

Development Report

May 2018
HBRC Report No. RM18-14
Publication No. 4997

Resource Management Group

ISSN 2324-4127 (PRINT)
ISSN 2324-4135 (ONLINE)

HAWKE'S BAY REGIONAL COUNCIL

159 Dalton Street . Napier 4110
Private Bag 6006 Napier 4142
Telephone (06) 835 9200
Fax (06) 835 3601
Regional Freephone (06) 0800 108 838

Environmental Science - Groundwater

Heretaunga Aquifer Groundwater Model

Development Report

May 2018
HBRC Report No. RM18-14 – 4997

Prepared By:

Pawel Rakowski
Matthew Knowling (GNS)

Reviewed By:

Jeff Smith

Hugh Middlemis

Approved By:

Stephen Swabey

ISSN 2324-4127 (PRINT)
ISSN 2324-4135 (ONLINE)

Contents

Tables

Figures

Executive summary

Content of this report

This report documents the development of a groundwater model for Heretaunga Aquifer System.

This report contains the following:

- Hydrogeological conceptualisation, including detailed discussion and summary of historical and recently acquired data;
- Detailed description of model design;
- Detailed description of model calibration using automated model calibration software PEST;
- Discussion of model limitations and capabilities.

A standalone executive summary for this report is provided as a separate document (Rakowski, 2018) and provides a comprehensive description of study findings, in particular related to hydrogeological conceptualisation.

A brief summary of content of the report is provided below.

Purpose of the study

The overall purpose of the groundwater model is to simulate the Heretaunga Plains gravel aquifer system and associated surface water resources to allow technically defensible groundwater and surface water allocation and water quality limits to be established. A detailed discussion of the objectives is provided in Section 0.

Context of the study

The work documented in this report is a part of a larger groundwater modelling study, which includes modelling scenarios, contaminant transport modelling and uncertainty estimation, which will be documented in separate reports. This groundwater modelling study is in turn a part of a series of studies supporting the Plan Change for catchments of TANK (**T**utaekuri, **A**huriri, **N**garuroro and **K**aramu Rivers). The Plan change for the TANK catchments will ensure that appropriate limits are established for water resources within the management zones.

Hydrogeological conceptualisation

The study provides a revised hydrogeological conceptualisation and groundwater budget for the Heretaunga Aquifer System, on basis of historical and recent studies and data including:

- Comprehensive review of surface water – aquifer interaction;
- Comprehensive review of groundwater pumping data;
- Irrigation demand and recharge study;
- 3D geological model;
- Groundwater age, and isotopic and hydrochemical composition of groundwater;
- Piezometric surveys;

- Groundwater level monitoring.

A detailed discussion of hydrogeological conceptualisation is provided in Section 0.

Description of groundwater model

Detailed description of the model set-up is given in Section 0.

MODFLOW-2005 was used to simulate groundwater flow under both steady-state and transient conditions. The model was designed to cover the period from 1 July 1980 until 30 June 2015, with a monthly stress period, but for model calibration purposes this time discretisation was modified to reduce model run time. The model covers the area of the Heretaunga Plains and surrounding river valleys that are considered to contain aquifers in hydraulic connection with the Heretaunga Aquifer. The model domain was extended approximately 1.5 km east, to include the sea and enable simulation of submarine springs. The total active area is 506 km^2. The model area is discretised into a 100 m x 100 m uniform grid. The grid consists of 302 rows and 501 columns and the domain contains 87,594 active cells.

The aquifer was discretised vertically into two model layers. Layer 1 represents the combined Holocene gravels (mainly fan gravels, where present in unconfined area) and the underlying Last Glacial Gravels (Quaternary isotope stages Q2-Q4, approximately 12,000 years ago to 71,000 years ago). Layer 2 represents the deeper deposits of the main Heretaunga aquifer (geologically defined as deposits below the Last Glacial Gravels or Q5-Q7 deposits, 71,000 years ago to 303,000 years ago), to a maximum depth of about 250 m. Both layers are set as Type 3 using the MODFLOW BCF package which allows for conversion between confined and unconfined conditions. The confining layer above the Heretaunga Aquifer - consisting predominantly of low permeability marine clays and silts - was not included in the model layer thicknesses, but its confining effect on the gravel aquifers was represented.

Rivers, streams and springs are represented using the “River” boundary condition (RIV), with main rivers using variable river stage. The Coastal boundary was represented as line of “General Head Boundary” condition cells (GHB). Land surface rainfall and/or irrigation recharge is represented by the “Recharge” (RCH) boundary condition. Pumping from the aquifer was simulated using the MODFLOW “Well” package (WEL). Parameterisation of spatial variability in Kh, Kz, Sy, and Ss was achieved using pilot points. Diffuse drainage in the confined aquifer was represented using the “drain” package (DRN).

Model calibration

Estimation of model parameters through calibration was performed using the industry-standard Parameter Estimation software PEST. The process of calibration is described in detail in section 0.

Observations

Observations used in model calibration included:

- Groundwater levels
- Groundwater level changes
- Long-term trends
- Vertical head differences
- River losses and gains during different times

Overall, over 6000 observations were used.

Parameters

Model parameters included:

- Aquifer properties (Kh, Kz, Sy, and Ss) as pilot points;
- River conductances;
- Land surface recharge and irrigation demand multipliers;
- Coastal boundary conductances;
- Drain conductances.

Overall, over 800 parameters were used.

Regularisation technique was used to improve calibration process.

PEST runs

Due to long model run time and a large number of parameters, PEST runs had to be undertaken using a high performance computing facility, and a total of nearly 50,000 processing hours was used during PEST runs.

Calibration outcome

The final calibrated model is able to replicate the observed dynamic of groundwater system (i.e. match seasonal and long-term groundwater level changes, as well as observed spring flows and river losses). Although this match is not perfect, in practice better level of fit is rarely achieved in groundwater modelling. Therefore, the model can be considered suitable for simulating the effects of groundwater pumping on river flows, along with and seasonal and long-term changes of groundwater levels.

Limitations

Due to the possibility that the model solution developed is not unique, despite a reasonable calibration, there is a residual uncertainty remaining. This uncertainty has been explored using calibration-constrained Monte Carlo analysis and its impact on model predictions will be explored in a subsequent report.

Limitations of the model calibration also include:

- Poor match to observation data in some areas;
- Limited observation data in some areas;
- Conceptual uncertainty;
- Uncertainty related to rate of recharge during high rainfall events.

1 Study Context and Scope

Hawke's Bay Regional Council (HBRC) is a local government body in New Zealand that has responsibility for developing policies and regulatory plans to ensure the sustainable management of resources within the region. HBRC is currently (ie, in 2018) reviewing policy underpinning management of land and water resources in the TANK catchments. This catchment-wide approach to managing water and land includes groundwater resources underlying the Heretaunga Plains, and is intended to result in changes to the HBRC Regional Resource Management Plan (RRMP).

Heretaunga Plains is an alluvial plain, located on the east coast of the North Island of New Zealand, with an area of about 300 km^2. The Plains have been formed by sediments deposited by the Ngaruroro, Tukituki and Tutaekuri Rivers (Dravid & Brown, 1997). The Heretaunga Aquifer is a deep sedimentary basin underlying Heretaunga Plains. The Heretaunga Aquifer System includes the Aquifer and several connected peripheral valley aquifers.

The groundwater model study area includes the entire Heretaunga Aquifer System and is shown on Figure 1-1.

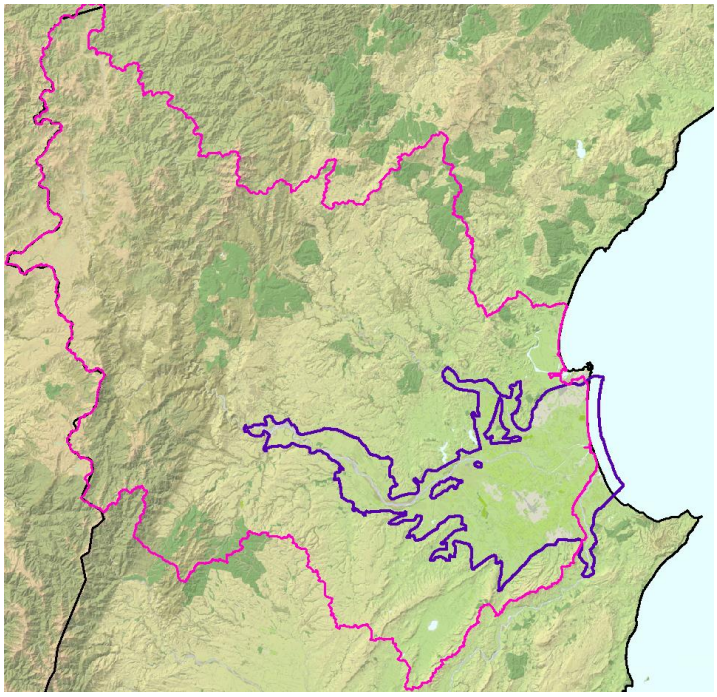

Figure 1-1: Study area (pink – surface water model and TANK catchment model boundary, blue – Heretaunga Aquifer System boundary)

The study modelled groundwater resources of the Heretaunga Aquifer System, including connected surface water resources. This study is part of the larger project covering the catchments of TANK – the collective acronym for the **T**utaekuri, **A**huriri, **N**garuroro and **K**aramu catchments (Figure 1-1).

1.1 Project drivers

Recently the National Policy Statement for Freshwater Management directed all regional councils to establish water allocation limits and water quality targets, and to ensure that attributes defining ecological and community values will be met. The Plan change for the TANK catchments will ensure that appropriate limits are established for water resources within the management zones. The Plan change is scheduled for notification in 2018.

In 2012 the Council established a large stakeholder group with about 30 representatives from the wider community, to agree on a framework for managing land and water resources of the TANK catchments.

The Group has met regularly and has considered presentations on new science to improve understanding of the ways that land and water use affects the TANK area.

A key part of the science programme was the development of surface water and groundwater models for the catchment. Work on these components commenced in 2015.

1.2 Modelling framework

This study focuses on development of a groundwater model for the Heretaunga Aquifer System. However, it is part of a larger TANK project and closely linked to other components of the broader project.

The modelling framework includes several components for modelling groundwater and surface water flows, and nutrients in those environments (Figure 1-2 and Table 1-1). In particular, the groundwater model relies on inputs from several other models. These are discussed below.

MODFLOW groundwater flow model

MODFLOW is the industry standard groundwater flow modelling code, developed by the U.S. Geological Survey (Harbaugh et al., 2017).

MODFLOW allows for computer simulation of groundwater flow processes through the aquifer, including key hydrological stresses such as groundwater recharge, surface water and groundwater interaction, and groundwater pumping.

MODFLOW was used to simulate groundwater flow in the Heretaunga Aquifer System.

SOURCE surface water flow, and nutrient routing model

SOURCE is an integrated water resource management software, developed in Australia by eWater[1]. It includes rainfall runoff, stream flow routing and nutrient flow components. (Carr & Podger, 2012)

A SOURCE surface water model was independently developed to simulate surface water flow and nutrient transport in the entire TANK catchment, which included areas outside of the domain of the groundwater model, as shown in Figure 1-1 (Diack & Williamson, 2018). The SOURCE Model has capability for modelling surface water abstraction and incorporating flow dependent abstraction bans.

This model is loosely linked with the Heretaunga groundwater model within the groundwater model domain, because the groundwater model provides groundwater-surface water flows to the SOURCE model, and the SOURCE model provides some surface water data to the groundwater model. The SOURCE modelling architecture includes sub-catchment level groundwater flow capability, but this is achieved using a very simplistic approach compared to MODFLOW and it is not suitable for representing complex river-aquifer interactions, such as in the Heretaunga Aquifer System. Therefore, the SOURCE groundwater component is only used in the upper catchments of TANK (outside the main MODFLOW groundwater model domain) and in the shallow aquifer overlying the confined Heretaunga aquifer.

[1] Further information on SOURCE and software downloads are available at https://ewater.org.au/products/ewater-source/ (accessed 22 March 2018)

The SOURCE model also provides data to the groundwater water model. Depending on scenarios being modelled, this may include river stage or flow, nutrient loading in streams, or days with pumping restrictions. The SOURCE model also relies on an IrriCalc model (Rajanayaka & Fisk, 2016a,b) to provide irrigation demand for surface water takes, but uses its own rainfall-runoff model to calculate groundwater recharge.

The SOURCE model is also used to simulate transport of nutrients, except for the unconfined aquifer area where nutrient flux is simulated directly by the groundwater model.

IrriCalc soil water balance model

IrriCalc is a farm-scale, daily soil water balance model (AEI, 1991) that is capable of estimating irrigation requirement for various crops and soils, along with aquifer recharge under variable climatic conditions. IrriCalc was used by Aqualinc Research Limited to produce recharge and irrigation demand data for the Heretaunga groundwater model and irrigation demand for the SOURCE surface water model (Rajanayaka & Fisk, 2016a,b).

The use of the IrriCalc model was necessary because of:

- Lack of sufficient pumping records from irrigation wells, which are understood to have a significant contribution to aquifer water budget; and
- Spatial variability of soil and land use, along with temporal variability of rainfall inputs.

OVERSEER nutrient budgeting model

OVERSEER is an agricultural management tool, based on a nutrient budget, that assists in examining nutrient use and movement within a farm, to optimise production and reduce nutrient losses from the farm (Watkins & Selbie, 2015). OVERSEER was used to calculate and map nutrient loading to the TANK catchments, including the Heretaunga Aquifer System (Millner, 2017).

The nutrient loads were later used in a groundwater transport model and surface water flow model.

MT3DMS groundwater nutrient transport model

MT3DMS is a modular three-dimensional transport model for the simulation of advection, dispersion, and chemical reactions of dissolved constituents in groundwater systems (Zheng & Wang, 1999; Zheng, 2010). This is industry standard modelling code for simulating multi-species contaminant transport in groundwater.

MT3DMS requires an underlying groundwater flow model, which in this case was the Heretaunga MODFLOW model. Nutrient transport modelling also requires nutrient loads, which were provided from OVERSEER results. Inputs from surface water (e.g. losing rivers) were also provided.

MT3DMS outputs are groundwater concentrations. The outputs may include concentrations in groundwater discharging to springs, which may be imported to the SOURCE model.

MODPATH particle-tracking model

MODPATH is a particle-tracking model that computes three-dimensional flow paths using output from groundwater flow simulations based on MODFLOW (Pollock, 2012).

MODPATH was used to calculate groundwater travel times and estimate groundwater age, for the purpose of groundwater model calibration (Knowling, 2018).

PEST uncertainty analysis tool

PEST is an industry standard model calibration and uncertainty analysis tool in groundwater modelling (Doherty, 2016a). PEST was used to undertake calibration and uncertainty analysis of the Heretaunga groundwater model, to match model outputs to observed groundwater levels and spring flows.

Table 1-1: Modelling Framework.

Framework element	Model	Spatial domain	Processes	General description	Purpose	Description
GW model	MODFLOW 2005[1]	Heretaunga Aquifer System	Groundwater (GW) flow, GW/Surface Water (SW) interaction	Industry standard groundwater flow modelling tool	Modelling of groundwater flow in the Heretaunga Aquifer	2 layer. 100x100m grid. 35 year calibration period. Transient/steady state. Variable timesteps (sub-daily/monthly/yearly). Parametrised using pilot points over 800 parameters. Thousands of observation points (water levels, spring flows, water level changes, long-term trends, seasonal water level fluctuations).
Surface water model	SOURCE	TANK	SW flow, minor GW, contaminant transport, flow statistics, resource management (e.g. bans)	Integrated water resource management software.	Modelling of surface water flow and nutrient transport (provides inputs to MODFLOW GW model)	137 subcatchments. Daily timestep. Calibrated to available flow and water quality data. 35 years run time. Modelling of abstraction rules (e.g. pumping bans). Integrated with MODFLOW
Recharge and irrigation demand	IRRICALC	TANK	recharge, irrigation demand	Calculates soil moisture, water use, and drainage for irrigation systems in New Zealand.	Irrigation demand and recharge model	Daily soil moisture balance model to calculate groundwater recharge and irrigation demand. Variables include soil type, land use, irrigation type, daily rainfall and potential evapotranspiration (thousands of combinations).
Nutrient loading from land use	OVERSEER[4]	TANK	nutrient loading from land use	Calculates full nutrient budget analysis for farm systems,	Nitrate loading model	Model calculating nutrient loading (Nitrogen and Phosphorus) for given land use, soil, and climate combination (steady state).
GW nutrient transport	MT3D[5]	TANK	GW nutrient transport	Industry standard groundwater transport modelling tool.	Nutrient transport in groundwater model.	Calibrated and nutrient concentration, Nutrient predictions Steady state
Particle tracking	MODPATH	Heretaunga Aquifer System	GW travel time	Particle-tracking model that computes three-dimensional flow paths	Calibrating to groundwater age	Calibration to groundwater age
GW model calibration	PEST[6]	Heretaunga Aquifer System	GW model calibration	Model calibration and uncertainty analysis software.	Industry standard inverse method in groundwater modelling.	Used for calibration and uncertainty analysis of MODFLOW and MT3D models,

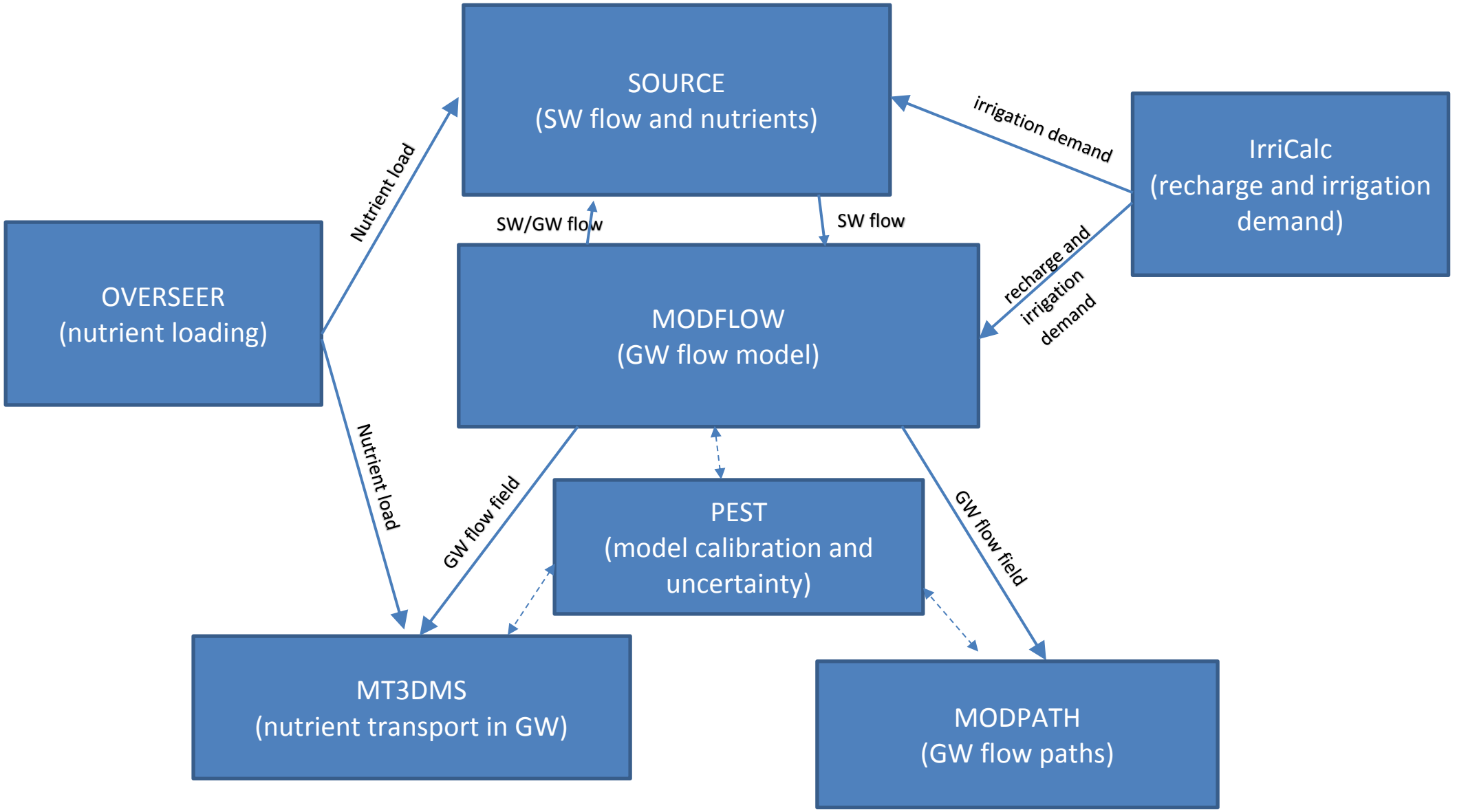

Figure 1-2: Modelling Framework. GW – groundwater, SW – surface water

1.3 Scope of this report

This report presents a description of model development including:

- Modelling objectives;
- Hydrological conceptualisation, including review of available data;
- Model design;
- Model calibration;
- Capability and limitations of the model.

1.4 Other reports

The following reports will be published separately:

- Management scenarios – predictive modelling report;
- Stream depletion modelling report;
- Model uncertainty analysis report;
- Predictive uncertainty report.

2 Modelling objectives

2.1 Original objectives

Modelling objectives were originally defined in a model scoping report (Trewartha, 2014), which suggested the following overall objectives of the model:

"The overall purpose of the numeric model is to simulate the Heretaunga Plains gravel aquifer system and associated surface water resources to an extent that will allow technically defensible groundwater and surface water allocation and water quality limits to be established. Ideally the model will be able to simulate the Heretaunga Plains aquifer at a scale that would allow highly localised management issues to be simulated as well, including well-interference effects and the effects of pumping of one or a few closely associated bores on surface water flows in local stream reaches or spring flows." It was acknowledged that this would be a long-term goal that may not be achievable with the initial development of the groundwater model documented in this report.

More specific definition of objectives was also provided:

(1) Simulate surface water flows and groundwater levels in response to abstraction and seasonal factors at the regional scale. Additionally, simulate the effects of groundwater pumping on surface water flows (springs, streams and rivers) at the sub-catchment spatial scale (similar to Tukituki scale).

(2) Simulate the effects of climate change on Heretaunga Basin and effects this may have on future groundwater allocation and abstraction limits. The extent that this can be simulated will be based on available data.

(3) Simulate the effects of current and future groundwater pumping on the seawater/freshwater interface (to establish seawater intrusion risk) at the sub-regional aquifer scale. The extent that this can be simulated will be based on available data.

(4) Simulate groundwater flow pathways of the Heretaunga Plains aquifers, taking into account seasonal effects, allowing transient times (time of travel) for groundwater to be estimated at a sub-catchment scale.

(5) Simulate groundwater travel times for the Heretaunga Plains aquifers, which is the time of travel for water emerging as springs, streams and rivers to be estimated at sub-catchment scale.

(6) Estimate the effects of individual or localised groups of groundwater takes on local groundwater levels, or linked stream or spring flows at a sub-catchment scale and over seasonal timeframes.

(7) Simulate the fate and likely future of groundwater contaminant concentrations in the Heretaunga Plains aquifer.

2.2 Discussion of objectives

The original objectives were broad and ambitious, and were subsequently refined. This section discusses how the objectives impact on model development, before the next section discusses the final set of objectives that were developed, in consultation with the TANK Group.

Objective 1 requires:

- A transient model that runs on a sub-seasonal time scale;
- Fine model grid to simulate surface water features.

Objective 2 requires:

- Climate change data to define future scenarios;
- Transient model running on a long time scale.

This objective is unclear, as is does not define how the future allocation and abstraction limits may be set, or what criteria are to be used, or indeed what climate scenarios to simulate.

Objective 3 requires much finer vertical discretisation, but does not necessarily need fine time discretisation. The model that could fully incorporate this objective, along with all other objectives, would most likely be impractical to build and execute, due to long run times. However, saline intrusion risk can may be to roughly assess using a simpler model (as developed for this study). If necessary (that is if this risk is estimated to be significant), a separate, purpose built model may be more suitable to fully meet this objective.

Objectives 4 and 5 may require detailed vertical discretisation. Objective 5 requires full contaminant transport simulation. Such simulations are known to be difficult (or even impossible) to set up and run on a regional scale, particularly in transient mode. The objective is vague as to what contaminants are to be simulated, and the type of contaminant may be important factor in model design.

In addition, during model development some additional objectives were generated. These included:

- Calibrate the model to available observed water level and springs flows;
- Produce a stochastic model to robustly estimate uncertainty of predictions;
- Calibrate to water age and nitrate data;
- Evaluate effectiveness of various mitigation strategies on stream flow (e.g. pumping bans, artificial recharge, stream augmentation) and security of supply for abstraction;
- Determine zones of high stream depletion potential;
- Evaluate impact of land use scenarios on water quality.

2.3 Final objectives

During the development and calibration of the model it became apparent that the original objectives needed to be redefined to make them clearer, achievable and complete. Some of the objectives relating to dual density modelling (for seawater intrusion) and contaminant transport modelling required use of a separate modelling tool.

The final objectives have been defined in Table 2-1.

Table 2-1: Final objectives for the Heretaunga groundwater modelling.

Objective number	Objective description	Comment
1	Ability to evaluate impact of stresses (such as pumping from individual wells or groups of takes, climate impacts) on groundwater levels and individual stream flows, accounting for seasonal effects, for historical and future scenarios	
2	Ability to evaluate the effects of various allocation strategies, in terms of spring flows and water levels	
3	Ability to evaluate climate impacts on water levels and spring flows	
4	Ability to evaluate effectiveness of various management strategies on stream flow and groundwater levels (e.g. pumping bans, artificial recharge, stream augmentation), along with security of supply	
5	Calibrate to water level and spring flow data since 1980, along with matching observed trends	
6	Determine zones of high stream depletion potential	
7	Produce a stochastic model to robustly estimate uncertainty of predictions	
8	Assessment of seawater intrusion potential	(separate density dependent model)
9	Calibrate to observed water age and nitrate concentrations	(separate MT3D and MODPATH models)
10	Evaluate impact of land use scenarios on water quality	(separate MT3D model)

3 Hydrogeological conceptualisation

3.1 Geography of the area

The study area comprises the Heretaunga Plains and surrounding valleys. The Heretaunga Plains are derived mainly from deposition of gravels from three major catchments: the Ngaruroro, Tutaekuri and Tukituki Rivers. These rivers drain the Ruahine and Kaweka mountain ranges, carrying a load of eroded materials that are generally greywacke gravels. The rivers converge at the coastline near the township of Clive.

The Heretaunga Plains are relatively flat, sloping gently from an elevation of about 60 m above mean sea level (AMSL) in the west, to just below sea level at the coast. The plains are bounded by steep hills, with an abrupt boundary between hills and the plains, which formed 7,000 years ago when the area of the Heretaunga Plains was an estuary (Dravid & Brown, 1997).

Land use in the plains is dominated by irrigated agriculture, including orchards, vineyards and cropping.

In contrast, the TANK catchments upstream of the groundwater study area are dominated by mountain ranges and hill country with land cover mostly pasture, forestry and native bush.

3.2 Climate

The Heretaunga Plains have a maritime-temperate climate, with approximately 800 mm of rainfall and 2150 sunshine hours per year (Chappell, 2013) . The seasonality of rainfall is small, but there are high evaporation rates through summer, which increase water demand for irrigation. The ranges west of the Heretaunga Plains (e.g. Ruahine, Kaweka) capture high rainfall from westerly weather systems. The colder and wetter climates in the ranges generate higher flows in the mainstem rivers (Ngaruroro, Tukituki, Tutaekuri), compared to lowland areas, and this contrast is more pronounced through summer and autumn.

The low rainfall increases the dependence of horticulture on irrigation. Most irrigation water for the Heretaunga Plains is sourced from groundwater (Wilding, 2014). Intensive development of the Heretaunga gravel aquifers provides irrigation water for orchards, vineyards and crops, alongside town and industrial water supplies.

The above description is adapted from Wilding's (2017) report.

3.3 Geology of the area

Basement Geology and structure

The Heretaunga Plains is a fault bounded, deep sedimentary basin (Figure 3-1), reaching at least 900 m depth (perhaps as deep as 1,600 m) below ground level (mbgl) (Lee et al., 2014). The basin has been created by tectonic deformation and subsequent infilling with river and marine sediments (Dravid & Brown, 1997).

Hill country surrounding the plains is mostly Pliocene limestone and sandstone, with Late Miocene rocks (sandstone and mudstone) occurring around Tukituki River and Ocean Beach (Lee et al., 2014). Around Havelock North and Cape Kidnappers, there are younger Quaternary rocks, mainly of the Kidnappers Group, which consist of a sequence of marginal marine to non-marine conglomerate, sandstone, carbonaceous mudstone, tephra and ignimbrite beds (Lee et al., 2014). Under the

Heretaunga Plains, the base of the Kidnappers Group has been estimated to a depth of 1300 mbgl (Lee et al., 2014).

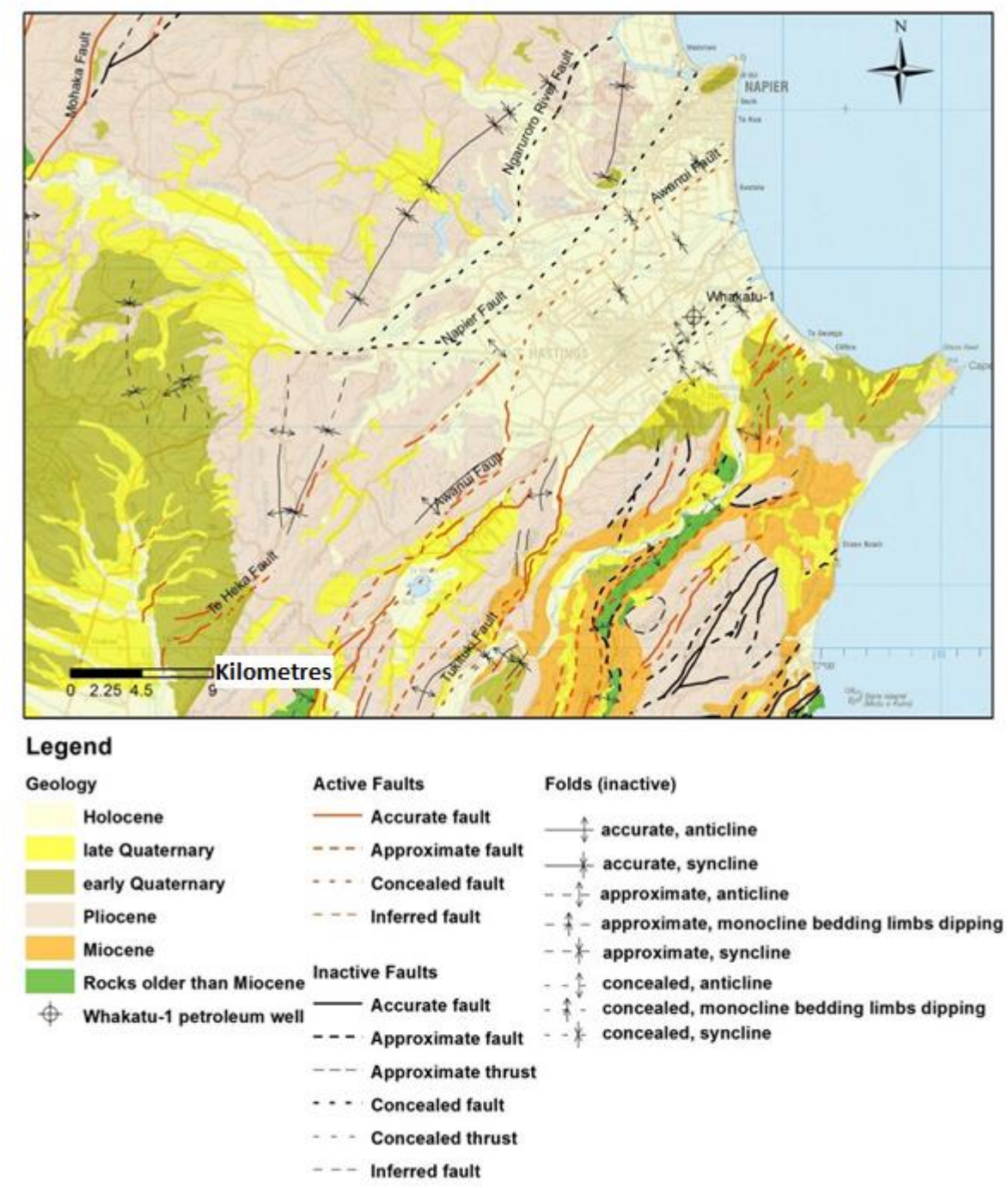

Figure 3-1: Geology of Heretaunga Plains. Figure after Lee (2014)

Quaternary Alluvial deposits

Above Kidnappers Group there is a sequence of younger Quaternary alluvial interglacial and glacial deposits. These were grouped into several units estimated to be present to depths of 250 m below the Heretaunga Plains (Lee et al., 2014):

Q7 - Penultimate Interglacial 245,000 years ago until 186,000 years ago

Q6 - Penultimate Glacial deposits	186,000 years ago until 128,000 years ago
Q5 - Last Interglacial deposits	128,000 years ago until 71,000 years ago
Q2-Q4 - Last Glacial deposits	71,000 years ago until 12,000 years ago

The Last Glacial deposits consist mainly of river gravels deposited between 71,000 years and 12,000 years ago, and form a layer of considerable thickness (Lee et al., 2014). This layer was deposited when the sea level was 150 m lower than at present, and the coast line would have been 60 km offshore (Dravid & Brown, 1997).

Table 3-1: Gravel deposits thicknesses.

	Thickness of deposit (m)		
	Flaxmere	Tollemache	Awatoto
Holocene gravels	59.5	35	28.5
Q2 (Last Glacial Gravels)	36.8	24.1	53
Q5-Q7		>160.9	>132.5

The thicknesses of last glacial gravels and Q5-Q7 deposits are known from three deep exploratory bores (Dravid & Brown, 1997). The thickness of last glacial gravels is estimated to be between 24 m and 53 m, while Q5-Q7 material may be greater than 160 m thick (Table 3-1). Last glacial gravels are also present at the surface of the Ngaruroro River terraces upstream of Maraekakaho, and are up to 15 m thick (Lee et al., 2014).

Holocene Alluvial fans and beach gravels

Marine/estuarine deposits

Sea level rise after the last glacial period resulted in deposition of a wedge of marine, estuarine and lagoon sediments over the permeable deposits of last glacial gravels. This wedge forms a confining layer over the underlying artesian gravel aquifer: at Awatoto, reaching a thickness of 30 m (Dravid & Brown, 1997).

Alluvial fan deposits

After the sea level stabilised following the last glacial period about 7,000 years ago, the Ngaruroro, Tutaekuri and Tukituki rivers began depositing sand and gravel; forming alluvial fans on entry to Heretaunga Plains (Lee et al., 2014). A layer of Ngaruroro fan gravel up to 30 m thick has been identified in the Roys Hill area, lying directly on top of last glacial gravels, and forming an unconfined aquifer (Lee et al., 2014).

Tukituki fan gravels have been identified near Havelock North. This fan interfingers and is in places overlain by Holocene marine sediments, and lies directly on top of the Last Glacial Gravels (Lee et al., 2014). Fan gravels have been also identified for the Tutaekuri River (Lee et al., 2017).

Other fluvial Holocene gravels

A 3D geological model (Lee et al., 2014, 2017) includes delineated volumes of Ngaruroro, Tutaekuri and Tukituki river gravels. However, radiocarbon age data from deep bores reported by Dravid & Brown (1997) indicates Holocene fluvial gravel deposits directly on top of the Last Glacial Gravels in all three deep bores, in areas outside of the fan gravels delineated in Leapfrog. This suggests widespread presence of younger gravels across the Heretaunga Plains; not restricted to areas of delineated fan gravels. Thicknesses of these Holocene gravel deposits are listed in Table 3-1.

Beach Gravels

Holocene beach gravels are formed along the coast by re-deposition of river gravels, between Napier and Awatoto, and between Haumoana and Te Awanga. These gravels form a layer about 10 m thick, and are overlain and underlain by Holocene marine silt and clay: possibly lying directly on top of the Last Glacial Gravels near Te Awanga (Lee *et al.*, 2014).

3.3.1 Geological model

General description

The 3D geological model of Heretaunga Plains developed using Leapfrog software (Lee et al., 2014) was later refined (Lee et al., 2017). The purpose of the Leapfrog model was to inform development of a numerical groundwater flow model. The model was built using Leapfrog Geo software (version 1.4.2, ARANZ Geo Ltd).

The following data sources have been used:

- Topographic data;
- 1:250,000 Geological map of Hawke's Bay;
- Land Information New Zealand 1: 250 000 scale Topo50 map;
- Radiocarbon age data;
- HBRC bore logs;
- Deep bore logs (Dravid & Brown, 1997);
- Published seismic lines.

The model was developed at a horizontal resolution of 100 m by 100 m.

A 3D geological model consists of a series of 3D geological unit volumes organised according to their age and structural relationships. 3D geological volumes are defined by bottom surfaces of the units (Lee et al., 2014). For the Heretaunga Plains model, these bottom surfaces have been defined by using surface geology data and manually drawn polylines based on interpretation of bore data, and other available data.

Example cross-section generated in Leapfrog is presented in Figure 3-2, and other cross-sections presented in relevant sections of the report, for example Figure 3-14 and Figure 3-16 in Section 0.

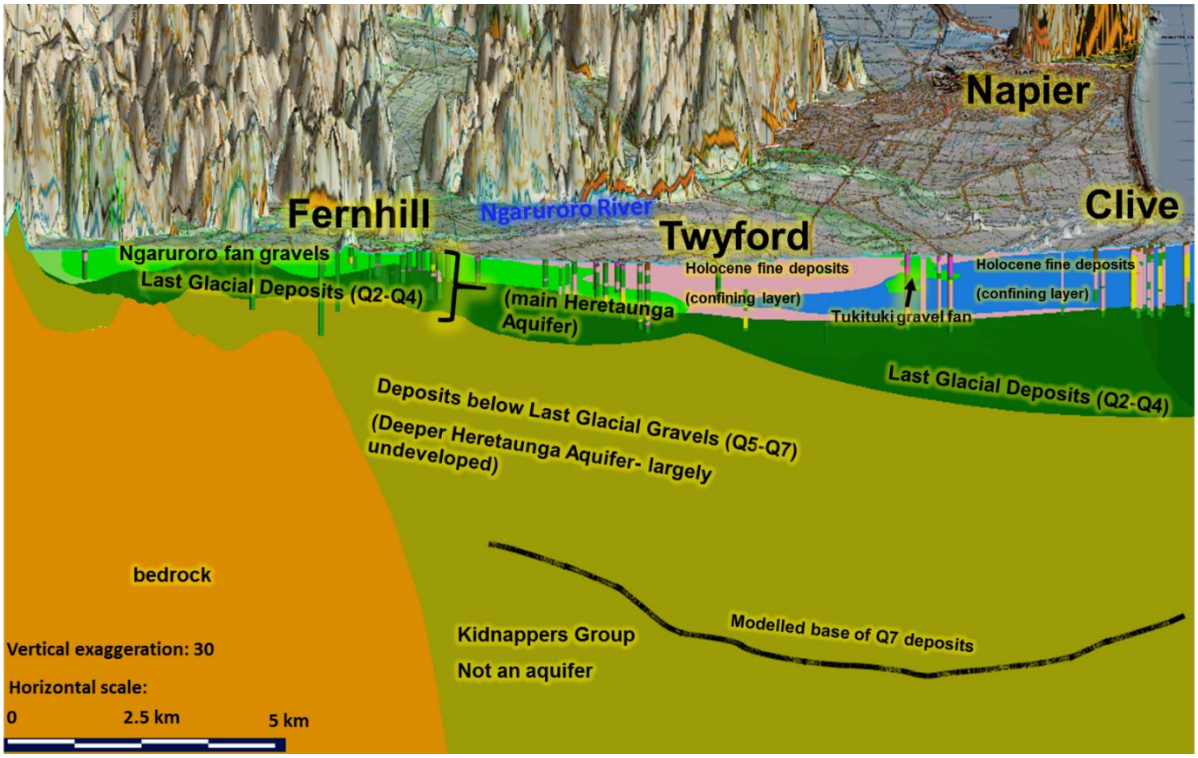

Figure 3-2: Leapfrog 3D geological model. Example of cross-section between Fernhill and Clive Last Glacial Gravels. Horizontal scale is approximate as this is 3D oblique view.

Despite a large number of bores in the Heretaunga Plains that potentially penetrate to the Last Glacial Gravels, there is limited bore data available that could provide information on the bottom of it and distinguish it from younger gravel deposits. This is because most of the bores have been drilled as water supply wells and were terminated when sufficient supply was tapped, rather than at the base of the unit. Most of the driller's logs contain only very basic lithological information and are not suitable to accurately determine age. In fact, only a handful of bores have deposits present that have been comprehensively dated: Flaxmere (ID 3698), Tollemache (ID 3697) and Awatoto (ID 3699).

According to the Leapfrog model documentation (Lee et al., 2014), the subsurface extent was determined using bore logs and radiocarbon age data from Dravid and Brown (1997).

Radiocarbon samples provide age estimates for deposits, but available samples from the Heretaunga Plains were less than 12,000 years old (a sample from Hospital Hill is not informative of aquifer age). The Last Glacial Gravels are between 12,000 and 71,000 years, so all dated samples are of Holocene age (ie, less than 12,000 years in age). This means available radiocarbon ages can only help indirectly to identify the top of the Last Glacial Gravels (e.g. when shallower deposits are 12,000 years, deeper deposits can be expected to be older and could belong to the Last Glacial Gravels), but not in determining the bottom of that layer.

The base of the Last Glacial Gravels is more difficult to identify, because there is little data (apart from three deep bore logs and seismic data that is not directly informative of layer age). This has not been stated explicitly in the Leapfrog model documentation. In addition, spatial coverage of dating is poor.

Dravid and Brown (1997) interpreted ages for three deeper exploratory bores (using radiocarbon dating from Awatoto and Tollemache and pollen interpretation from Flaxmere). The Leapfrog model is only in agreement with one of them (Awatoto bore) regarding the base of the Last Glacial Gravels. For the two other bores, the Leapfrog model shows a Q2-Q4 layer in Holocene (ie, Q1) gravel deposits, as interpreted by Dravid & Brown (1997). The Leapfrog model Q2-Q4 layers appear to also include

Holocene gravels that lie on top of the Last Glacial Gravels. The documentation does not explain this setup, so possibly it is a result of an error.

The Q2-Q4 unit in the Leapfrog model appears to be representative of a first layer of fluvial gravels (including Holocene) and this boundary with the overlying finer Holocene deposits is likely to be accurately defined because there is plenty of bore data and distinction between fine and coarse deposits is easy. However, the base of the unit would be arbitrary and based on very limited data, as noted above. From a groundwater modelling (rather than strict geology) perspective, if gravels of different ages are connected, they can be modelled as one unit and their age has no impact on model setup.

The Last Glacial Gravels have also been delineated in the Leapfrog model for a section of the Ngaruroro River outside of Heretaunga Plains; between Maraekakaho and Whanawhana. However, the delineation in this area appears very simplistic. In particular, the Q2-Q4 deposits on terraces in this area are known to be only around 15 m thick and lie on the terrace top, but the geological model shows them as a layer over 100 m thick, and extending below the base of the valley.

Units below last glacial gravels

The Leapfrog geological model documentation (Lee et al., 2014) notes that all the units below (older than) the Last Glacial Gravels (Q5-Q7) have been defined crudely, because only three deep bores were available. The basement, representing the boundary with hard sedimentary rock below the Heretaunga Plains alluvial basin, was estimated from interpretation of seismic lines.

Holocene deposits

According to the Leapfrog geological model documentation (Lee et al., 2014), Holocene alluvial fans and beach gravels have been identified from bore logs. However, little detail has been provided on how the younger Holocene gravels have been distinguished from older Last Glacial Gravels lying directly below them. As explained in the previous section, there is only limited radiocarbon data and its coverage (along with all ages being younger than Holocene) would make this task nearly impossible.

The Leapfrog geological model documentation explains that these structures have been delineated via bore logs using manually drawn polylines around large patches of gravel (presumably distinguished from fine Holocene sediments). Structures delineated this way would give a reasonable representation of distribution of coarser, more permeable materials in the vicinity of finer material forming a confining layer of the aquifer.

This is important from a groundwater modelling perspective, so the Holocene fan gravel and beach gravel units remain useful for flow modelling, despite uncertainties about their distinction from the last glacial gravel unit.

In fact, Tukituki and Ngaruroro gravels fans (as delineated in the Leapfrog model) correspond remarkably well with losing sections of rivers, along with areas of spring discharges, which have been explored independently. This gives confidence in the ability of the Leapfrog model to represent key hydrogeological structures.

However, the location of delineated Tutaekuri fan gravels does not match with hydrological data (despite the modelled large gravel fan, no river losses or gains/springs have been observed in this area). This may be due to limitations of Leapfrog to represent local scale features, or other limitations as explained in later in this report.

Hydrological data is further discussed in Section 3.4.

Fine Holocene deposits that form a confining layer above the aquifer are represented reasonably accurately by the geological model, as this unit is defined by topography and intersection with Last Glacial Gravels or Holocene Gravels (and plentiful bore data is available that defines this top of Last Glacial Gravels and extent of Holocene Gravels as explained earlier).

Limitations of the geological model

The geological model is not a full representation of the subsurface, as its accuracy is limited by various factors such as data availability and coverage, bore log quality and consistency, software limitations for representing complex structures, and interpretation (John Begg, GNS Science, pers. comm.). The complex depositional nature of the Heretaunga Plains, which were created over thousands of years from shifting river channels depositing gravels, along with multiple marine transgressions, may be impossible to represent numerically with great accuracy.

It appears that the Leapfrog model has achieved a reasonable representation of shallow gravel aquifer and confining layers. However, the base of the Last Glacial Gravels and details of the deeper aquifer system are represented crudely.

Also, some shallow deposits that may have a strong impact on hydrology (e.g. spring discharges) have not been included in the model. Shallow surface gravels in the Irongate area have not been delineated, and it appears that these gravels form pathways for spring flows. Similarly, the confining layer in the Moteo valley has not been delineated and this layer appears to be related to the presence of large springs in the area. Also, a layer of pumice in the Karewarewa area has not been delineated and this layer may be important for flows in the local streams. See Section 3.4.4 for detail.

Figure 3-3 shows bore data overlaid with the geological model cross-section. It can be seen that the model does not always fully agree with the bore data. Because of these limitations, there remains some uncertainty regarding the exact nature of flow pathways. Nevertheless, the Leapfrog geological model is useful for informing a conceptual understanding of the subsurface.

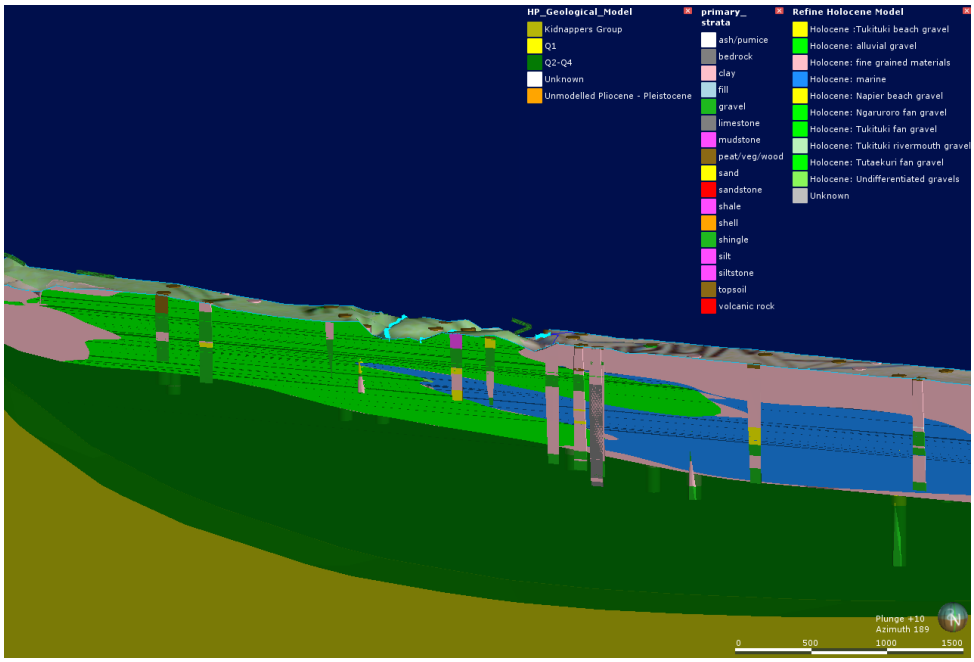

Figure 3-3: Comparison of the geological model with bore data from west (left) to east across the Heretaunga Plains.

Verification of the model with new data

Since the Leapfrog geological model has been produced, new drilling data has become available and this can be used to validate the model.

This includes new bore 16383, which is an exploratory bore almost 150 m deep drilled by Hastings District Council (HDC) near Havelock North. The purpose of the bore was exploration for a deeper public water supply source to replace shallower water supply bores, in an attempt to reduce the stream depletion effect on nearby Mangateretere stream (Dylan Stuijt, HDC, pers. comm.). The bore encountered several gravel aquifers separated by clay layers, with a gravel aquifer present at 150 m. This suggests that Q5-Q7 Quaternary deposits may be present at that depth. Unfortunately, the deposits have not been dated, so their age remains uncertain. This location is reasonably close to the Heretaunga Plains perimeter, so such a depth is surprising. This is deeper than interpreted in the Leapfrog model, which has Kidnappers group at a depth of 50 metres. This indicates that the Leapfrog geological model underestimated depth of the basin in this area.

Bore 16300, which has been drilled to depth of 109 m in the Twyford area, identified mostly gravelly layers separated by minor clay layers. The depth to top of the Kidnappers group is estimated to be 150 m in the Leapfrog model, which means that this new data supports the model.

3.4 Hydrology of the area

3.4.1 Overview

On the Heretaunga Plains and surrounding valleys there is a complex network of rivers, streams and drains that interact with the underlying Heretaunga Aquifer System. This network is presented in Figure 3-4.

Rivers originating in the mountains outside of the Heretaunga Plains enter the plains and begin losing water, providing recharge to the aquifer. There are also springs, spring-fed streams and artificial drains that receive discharge from the aquifer. This interaction is very important for understanding water resources of the Heretaunga Aquifer System.

This interaction has been discussed in detail by Dravid & Brown (1997) and more recently by Wilding (2017). Wilding's (2017) work is of particular importance for this study, as it included a comprehensive and systematic review of the entire stream network of Heretaunga Plains and identified all significant river losses and spring locations. Wilding (2017) identified 64 locations where flow is either losing or gaining. He describes a variety of methods used to identify and quantity these flows; including aerial photographs, visual inspections, flow gaugings, electrical conductance surveys, temperature surveys and heavy water isotopes. Wilding (2017) also discusses sources of water in the springs. It is unlikely that there are undiscovered areas with significant river losses or springs, except for tidally affected rivers and coastal discharges.

The section below provides more detail of this interaction, based on Wilding (2017).

3.4.2 Stream network delineation

An initial stream network map (as shown on Figure 3-4) was created using the Heretaunga Drains layer available in HBRC GIS data. This drain layer was originally created by engineers in the HBRC Asset Management Group to assist with the management of drains in the Heretaunga Plains.

This layer was then edited and refined, along with extension of the network to the Heretaunga Model boundary. Editing focussed on achieving alignment with the LiDAR terrain map to enable extraction of stream elevations. The stream layer was also pruned to remove ephemeral streams and drains.

Perennial streams were identified from field surveys, aerial photos and Google street view (time series). Editing was also completed to honour various topological rules (e.g. reach intersections touching, correct flow direction, etc.).

Reaches were delineated from confluences, pronounced changes in channel slope, and boundaries of losses and gains from groundwater. Elevations for each reach were then extracted from the 2003 LiDAR data. Reach minimum elevations were extracted in ARCMAP using 3D analyst. Various problems with identifying maximum elevation necessitated the use of the minimum elevation from the next reach upstream to define the maximum.

Stream widths were estimated from aerial photos. Polygons were manually drawn from aerial photographs to determine total reach area, then divided by reach length to obtain width. This width was reduced for braided rivers to obtain an estimate of mean width (width/2.8), but no correction was necessary for other stream types. Water surface elevation is from the LiDAR. Stream bed elevation was approximated by subtracting an estimate of river depth (0.5 m, 1.0 m, 1.5 m or 2.5 m) from the water surface elevation (this is detailed below).

The stream network includes river widths estimated (using the polygon method above) for most river/stream reaches throughout the network (as detailed above). River widths for several small tributaries throughout the network and 4 braided reaches in the Upper Ngaruroro were unable to be estimated. For these reaches, generalised river widths (explained below under target river flow sites) were used to provide an alternative estimate of width.

The stream network includes river depths for every river/stream reach throughout the network. River depths for each reach were estimated using the following methods:

- Single, Tidal and Wetland Reaches – Generalised river depths (explained below under target river flow sites) were used as an estimate of river depth.
- Braided Reaches – River depth was calculated as 2.5% of river width (with 8 exceptions – generalised river depths were used for the 4 braided reaches in the Upper Ngaruroro with generalised river widths, 3 braided reaches on the Maraekakaho and 1 braided reach on the Kikowhero).

The stream network includes minimum and maximum river water level elevations estimated for every river/stream reach throughout the network. Minimum and maximum river bed elevations for each reach were calculated by subtracting the river depth from the minimum and maximum water level elevations.

3.4.3 Main rivers

There are three main rivers that flow across the Heretaunga Plains: the Ngaruroro, Tutaekuri and Tukituki Rivers, as shown in Figure 3-4. These rivers originate in the mountain ranges to the west and have braided gravel bed characteristics. The river flows are characterised by high floods and low summer flows, as shown in Table 3-2.

The Ngaruroro river loses water as it flows over the Heretaunga Aquifer System and this river is the largest contributor to Heretaunga groundwater recharge – losing 4.4 m^3/s to the groundwater system (

Table 3-3) (Wilding, 2017).

Note that the Tukituki River is not part of the TANK catchments, but nevertheless it flows across the Heretaunga Plains and is in hydraulic connection with the Heretaunga Aquifer, so it was included here.

The Tutaekuri River loses water to an underlying aquifer and most of this water appears to re-emerge as spring flow in the Moteo valley (see Section 3.4.4). However, a connection of Moteo valley to the main Heretaunga Aquifer is likely (see discussion in Section 3.5.2).

Table 3-2: Main river flow statistics (in m^3/s). (Waldron & Kozyniak, 2017)

	Period	7-Day Minimum	Maximum	Mean	Q_5	Median	Q_{95}
Ngaruroro	1976-2014	1.1	1781.3	34.4	102.7	19.8	4.2
Tukituki	1968-2014	2.9	3044.3	44.6	138.2	21.7	5.7
Tutaekuri	1968-2014	2.1	1588.0	14.7	36.6	8.6	3.6

Table 3-3: Main river losses to the Heretaunga Aquifer System.

	Estimated loss to aquifer m^3/s
Ngaruroro	4.4
Tukituki	0.8
Tutaekuri	0.78
Total	**5.98**

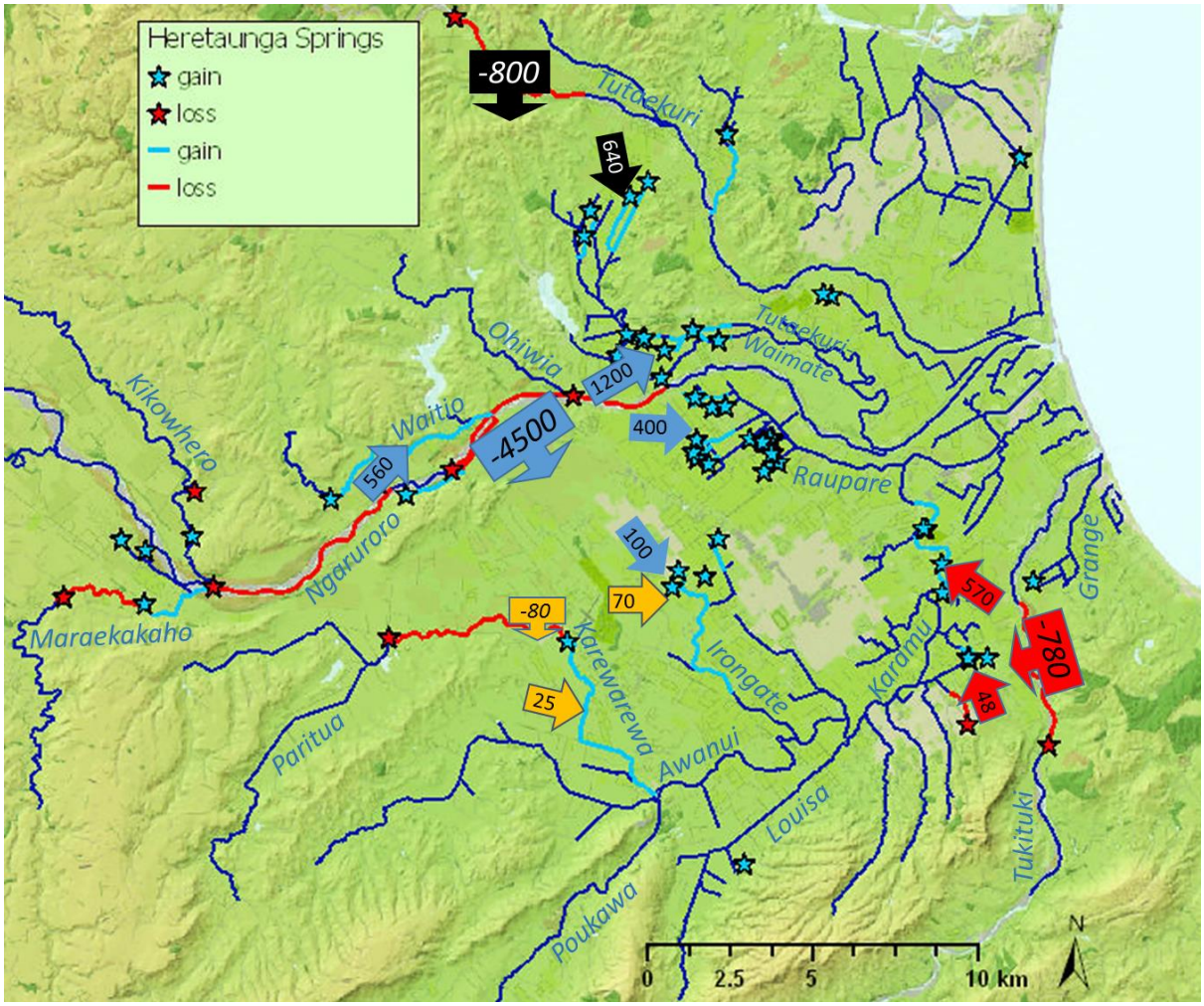

Figure 3-4: Heretaunga Plains hydrology and flows in L/s (Wilding, 2017). Red sections of waterways indicate losing reaches, while bright blue sections are gaining reaches.

Ngaruroro

This text is adapted from Wilding's (2017) report.

The lower Ngaruroro River typically loses more than 4,000 L/s to groundwater. This recharges the Heretaunga aquifer which, in turn, feeds many of the springs on the Heretaunga Plains. Losing sections of the Ngaruroro River are above the unconfined Heretaunga Aquifer, which geologically is formed by Ngaruroro fan gravels.

The Ngaruroro is the most intensively gauged river on the Heretaunga Plains (Grant, 1965; Dravid & Brown, 1997), with flow losses measured from 336 concurrent gaugings dating back to 1952. This is in addition to 1,392 gaugings at monitoring sites on the Ngaruroro River (Fernhill, Whanawhana and Chesterhope). Flow gaugings are the only way to observe flow losses at present, because the loss of water has little effect on chemical characteristics of the river water (compared to gaining reaches, where discharge of groundwater may affect river chemistry).

Most of the flow loss from the Ngaruroro occurs between Roys Hill and Fernhill, with a median loss of 4,250 L/s (based on 107 concurrent gaugings with median gauged flow of 7,020 L/s at Fernhill). This 5 km length of river is termed the "major loss" reach (Figure 3-5). The material underlying this reach includes unconfined gravels. The concurrent gaugings show some variability in the amount of water lost from the river (interquartile range 3900 L/s to 4600 L/s loss). Some of this variability is attributable

to measurement error and the magnitude of absolute measurement error (in L/s) increases with flow (e.g. 10% error equates to ±100 L/s error at 1,000 L/s river flow; or ±10,000 L/s error at 100,000 L/s river flow).

In addition, the true loss from the river can change over time. When groundwater levels are lower, more water may be lost from the Ngaruroro River (Dravid & Brown, 1997). Theoretically, higher river flows can also increase the amount of flow lost, by increasing the pressure head and the area of wetted gravel through the losing reaches. However, there was no correlation between flow loss and the total river flow, or groundwater level (R^2 = 0.02 and 0.01 respectively). Likewise, lower groundwater levels did not increase the likelihood of more loss. It is still possible that loss of river flow increases at higher flows, but this increase is confounded by the increasing absolute error at flows sufficient to inundate the gravel bed. Factors unrelated to river level and groundwater level can also affect flow-loss, including clogging of the riverbed by silt.

An additional flow loss was often detected downstream of Fernhill, which was smaller and more variable than the major loss (median 120 L/s loss, interquartile range 410 L/s loss to 110 L/s gain, from 46 concurrent gaugings at a median gauged flow of 5,010 L/s at Fernhill). This is termed the "variable loss" reach, which extends up to 3 km downstream of Fernhill (Figure 3-5).

An additional "minor loss" reach may also occur upstream of the major-loss reach (Figure 3-5). Dravid and Brown (1997) estimated the minor loss at 800 L/s. A similar magnitude of loss was estimated for this report, using different methods. Inflows were measured from the mainstem (Ngaruroro at Whanawhana), in addition to tributaries between Whanawhana and Ohiti (Poporangi, Otamauri, Mangatahi, Kikowhero, Maraekakaho). Using eight concurrent gaugings that included sites on all tributaries, the median loss was 450 L/s (interquartile range 350 L/s to 750 L/s).

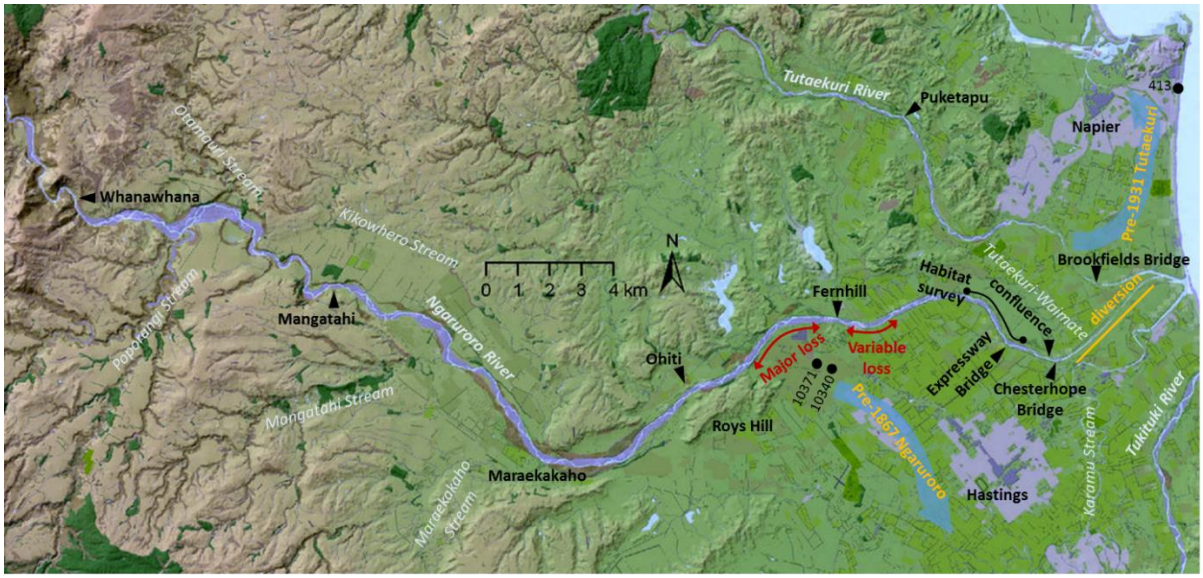

Figure 3-5: Lower Ngaruroro River. Map of the lower Ngaruroro River showing the location of continuous flow monitoring sites (Fernhill and Chesterhope Bridge) and reaches that lose flow to groundwater (Minor loss, Major loss and Variable loss).

Tutaekuri

This text is an adapted from Wilding's (2017) report.

The Tutaekuri River downstream of the Mangaone confluence loses flow to groundwater, most of which appears to feed tributaries of the Tutaekuri-Waimate Stream. More recent calculations support a flow loss from the Tutaekuri of approximately 820 L/s.

Similarly to the Ngaruroro River, the loss occurs to an unconfined aquifer.

The location of the loss was investigated using concurrent gaugings between the Mangaone confluence and Puketapu. These confirm the loss occurred between Hakowai and Silverford (Figure 3-6), with flow conserved between Silverford and Puketapu (from 8 concurrent gaugings with a median gauged flow of 7,560 L/s at Puketapu). This location conflicts with Dravid and Brown (1997), who indicated the loss occurred downstream of Silverford. However, their Table 6.4 contains flows labelled as Silverford, which do not match same day gaugings archived for Silverford in the HBRC Hilltop Allsites database. This suggests there may be an error in Dravid and Brown's locations.

Dravid and Brown (1997) noted an absence of flow losses downstream of Puketapu, which was confirmed by more recent concurrent gaugings. Only 5 out of 30 concurrent gaugings measured a flow loss between Puketapu and Brookfields bridge.

The loss of flow from the Tutaekuri River makes it a potential source of the groundwater feeding springs in neighbouring catchments (e.g. Tutaekuri-Waimate Stream, Section 3.4.4) and potentially contributing to the main Heretaunga Aquifer.

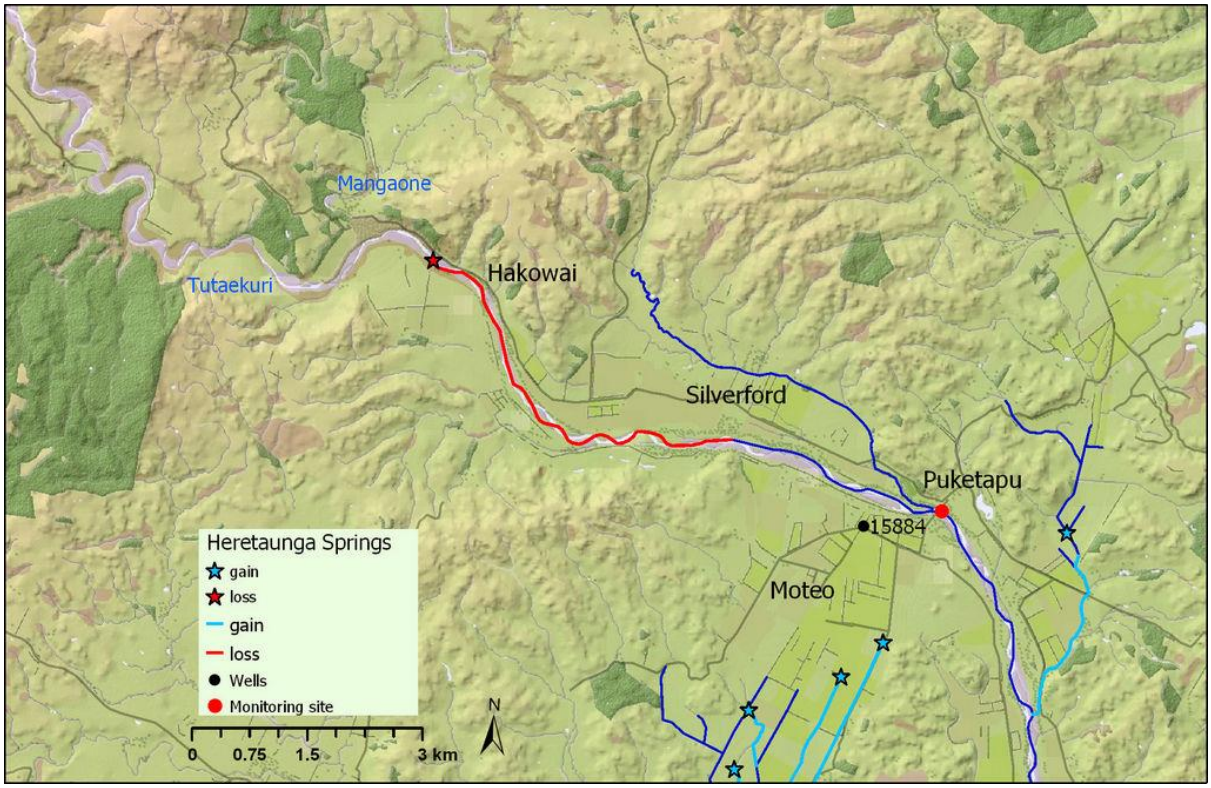

Figure 3-6: Tutaekuri River. The median flow loss from the Tutaekuri River was 820 L/s over the losing reach (approximated as a red line).

Tukituki

This text is an adapted from Wilding's (2017) report.

Concurrent gaugings along the lower Tukituki River traversing the Heretaunga Plains revealed a loss of river flow to groundwater. This flow loss is less adequately quantified than the Ngaruroro loss, with only ten concurrent gaugings completed to date (five of those in the last five years). There are insufficient data to quantify how this loss varies over time. However, 14 data pairs were compiled by using stage-to-flow data from Red Bridge together with gaugings compiled from two downstream sites (Black Bridge and Tennant Rd, in order of preference). Using this expanded dataset, the median flow loss was 910 L/s, with an interquartile range of 640 L/s to 1050 L/s. There are no known surface water takes in this reach that could have affected the loss calculation.

Concurrent gaugings were also used to estimate where the flow loss occurs (Figure 3-7). Available information indicates that flow loss is mostly confined to the section of river between River Road and Tennant Rd.

Similarly to Ngaruroro and Tutaekuri, the loss occurs to an unconfined aquifer, which in this location is formed by Tukituki fan gravels. In fact, there is a remarkable match between the losing section identified from concurrent gaugings and an independently delineated surface extent of Tukituki fan gravels (Figure 3-10)

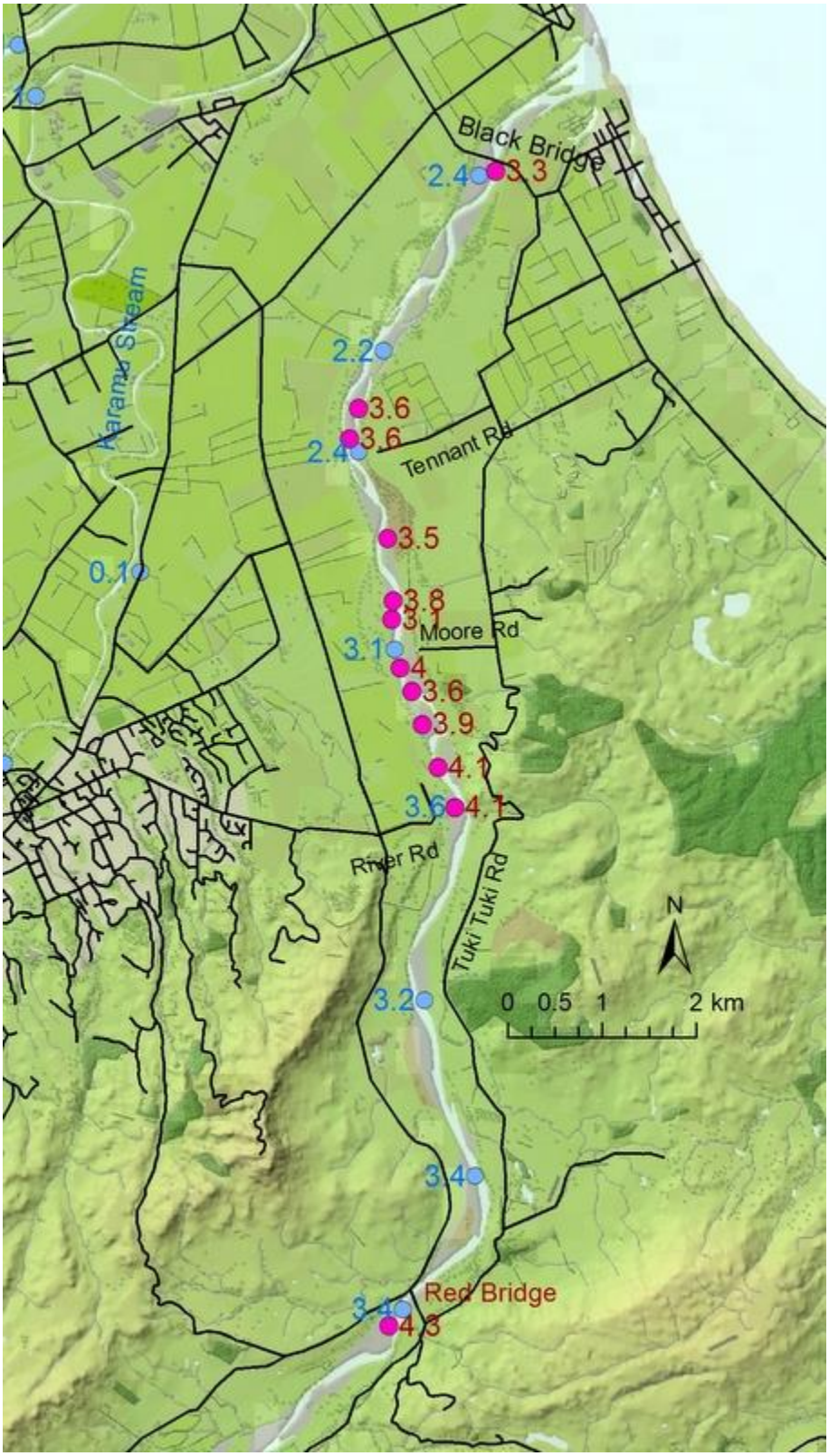

Figure 3-7: Lower Tukituki gaugings. Concurrent gaugings along the lower Tukituki River on 27 March 2013 (blue dots, left label) and 5 February 2015 (red dots, right label). Flows are labelled in m^3/s.

3.4.4 Springs, Spring-fed Streams and Drains

There are numerous springs and spring-fed streams in the Heretaunga Plains and surrounding valleys.

The most significant spring fed streams and their typical summer discharges are summarised in Table 3-4, using data collected by Wilding (2017), and are discussed in sections below.

Table 3-4: Summer spring discharges in Heretaunga Plains.

Stream	Typical summer spring flow L/s
Tutaekuri -Waimate	1831
Karamu	575
Waitio	566
Raupare	402
Irongate	168
Mangateretere	46
Karewarewa	25
Paritua	-100 (losing section)
Other streams	15
Total	**3528**

Tutaekuri –Waimate

This text is adapted from Wilding's (2017) report.

Description

The Tutaekuri-Waimate is a spring-fed stream tributary of the Ngaruroro River, originating in the Moteo Valley, which is a valley formed by an abandoned buried channel of the Tutaekuri River.

Spring Flow

Springs emerge in two distinct areas:

The first area is in the middle section of the valley, where the aquifer becomes confined. The mean annual low flow (MALF) of spring discharges here was estimated at 640 L/s, with a median flow of 750 L/s. This median flow of 750 L/s is slightly less than the median loss from the Tutaekuri River (820 L/s). The flow represented by this difference may continue to move south towards the Heretaunga Aquifer, but some, or perhaps all, of this water may exit the aquifer through groundwater pumping. For example, total pumping from this area in January 2013 is estimated to be 129 L/s on average, which would balance out inputs and outputs, leaving no additional flow to the Heretaunga Aquifer system.

The second area of spring discharges is located outside the Moteo valley, on the Heretaunga Plains, with total spring discharge approximately 1,000 L/s.

Spring Origin

The Tutaekuri-Waimate appears to be fed by two gravel aquifers – the Moteo Valley aquifer and the Heretaunga aquifer. Evidence for there being two sources includes distinct chemistry and differing water levels at which the springs arise. In the Moteo Valley, springs discharge water with higher electrical conductance compared to springs on the Heretaunga Plains. The Moteo springs probably

originate from the Tutaekuri River upstream of Puketapu, which has higher electrical conductance than groundwater in the Heretaunga aquifer. The electrical conductance of springs in Moteo valley is slightly higher than Tutaekuri river water, which may be explained by some contribution from limestone hill country to Moteo groundwater.

The Tutaekuri is connected to the Tutaekuri-Waimate via a gravel aquifer that feeds springs in the Moteo Valley (Dravid & Brown, 1997; Hughes, 2009a; Levy, 2016). Median flow losses from the Tutaekuri were estimated at 820 L/s (see Section 3.4.3), which recharges the Moteo gravels. Groundwater is confined to deeper gravels by clays in the downstream (southern) part of the valley. Springs are expected to arise near the edge of that confining layer, where artesian pressure becomes positive and the confining clays are thin and imperfect.

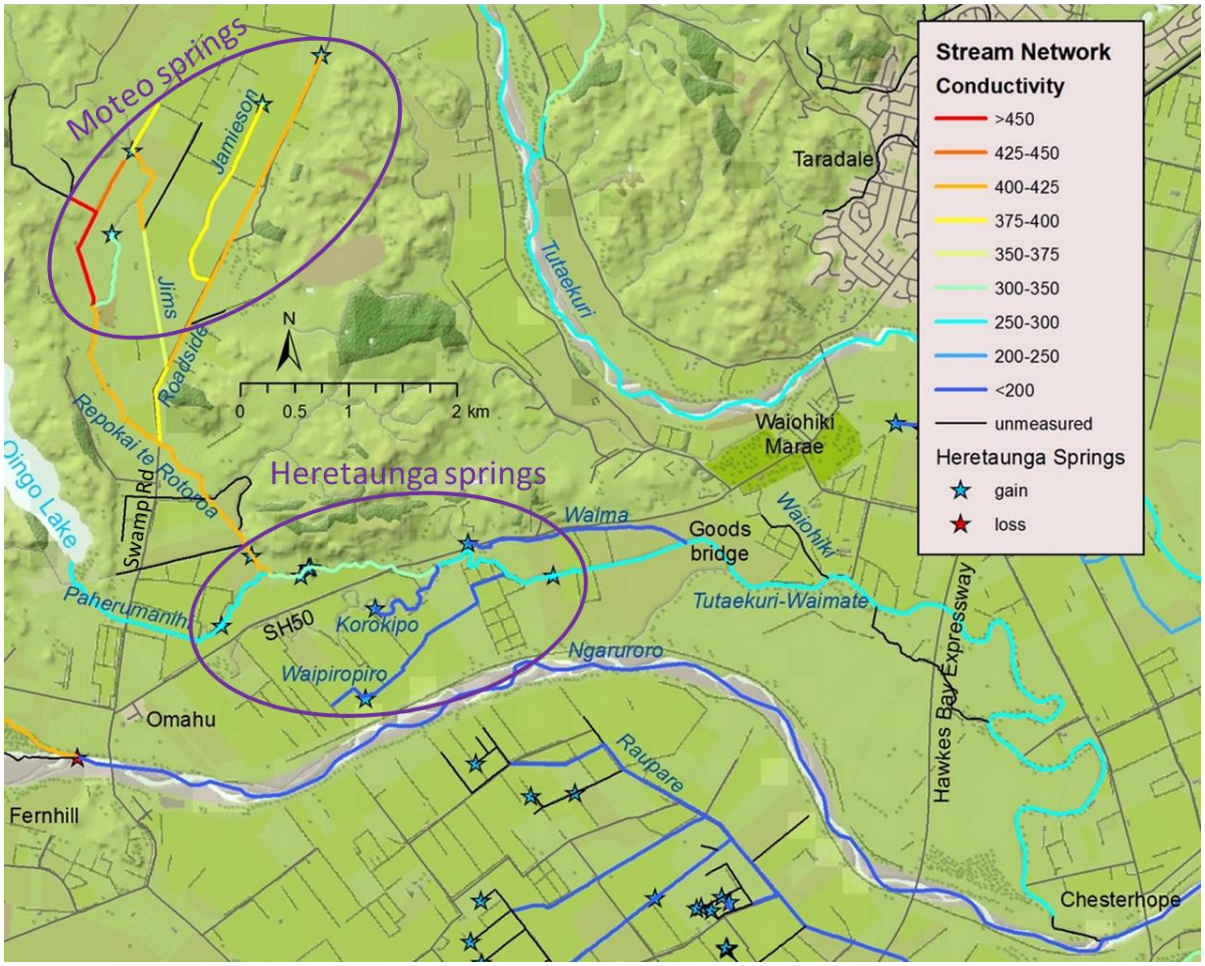

Figure 3-8: Tutaekuri-Waimate springs. Streams are mapped with lines colour-coded using electrical conductance (µS/cm at 25°C). Lower conductance springs originate on the Heretaunga Plains (blue colours), compared to the higher conductance water from Moteo Valley (where the Repokai te Rotoroa exits Moteo). The red dots represent spring locations that take the form of point springs or gaining sections.

Karamu

This text is adapted from Wilding's (2017) report.

Description

The Karamu Stream is a slow flowing waterway, generally represented by the section of the stream below the confluence with Irongate and Awanui Streams (Figure 3-9), and upstream of the confluence with the Raupare Stream. The mean summer flow of the Karamu Stream is 1.4 m^3/s.

Spring Flow

A large component of flow in the Karamu Stream cannot be accounted for by tributary inflows alone, with the shortfall estimated to be between 570 L/s and 920 L/s. Recent work indicates that this shortfall is a result of groundwater inflows, as described below. While Dravid and Brown (1997) postulated that this shortfall is due to irrigation losses, this appears unlikely. The locations of flow gains were estimated from longitudinal kayak surveys of electrical conductance.

Spring Origin

The two most likely sources of groundwater inflows are losses from the Tukituki River, or losses from the Ngaruroro River (via the Heretaunga Aquifer).

A potential hydraulic connection exists between the Tukituki River and the Karamu springs. The gaining section of the Karamu Stream passes within 2 km of the Tukituki River. As described in Section 3.4.3, the Tukituki River loses water from this adjacent reach, and the flows are similar in magnitude to the Karamu gains. A Leapfrog geological model of Heretaunga Plains (Lee et al., 2014, 2017), shows that the Tukituki River has deposited a gravel fan in this area. The surface extent of this gravel fan coincides with the Tukituki River losing section. Furthermore, the Karamu springs and Mangateretere springs coincide with the surface or underground extent of the fan (Figure 3-10).

This gravel fan provides a potential conduit between the Tukituki River and the springs (Figure 3-11). Also, the geological model shows the gravel fan to be in direct contact with the underlying Heretaunga Aquifer, which suggests that it could provide a conduit between the Karamu Stream and the Heretaunga aquifer, and consequently the Ngaruroro River (Figure 3-11).

The Karamu Stream is lower in elevation than the Tukituki River, providing the necessary gradient for groundwater to flow from the Tukituki to the Karamu.

Observations of electrical conductance for the spring-inputs to the Karamu are consistent with the contribution changing over time from the Tukituki to the Ngaruroro.

Isotope composition shows a consistent difference between water samples from the Ngaruroro and Tukituki rivers. The isotope ratios for the Karamu spring inflows identified the Tukituki as being the dominant source during summer low flows, with increasing inputs from the Ngaruroro during winter. However, these results are based on limited sampling data, and are subject to interpretation.

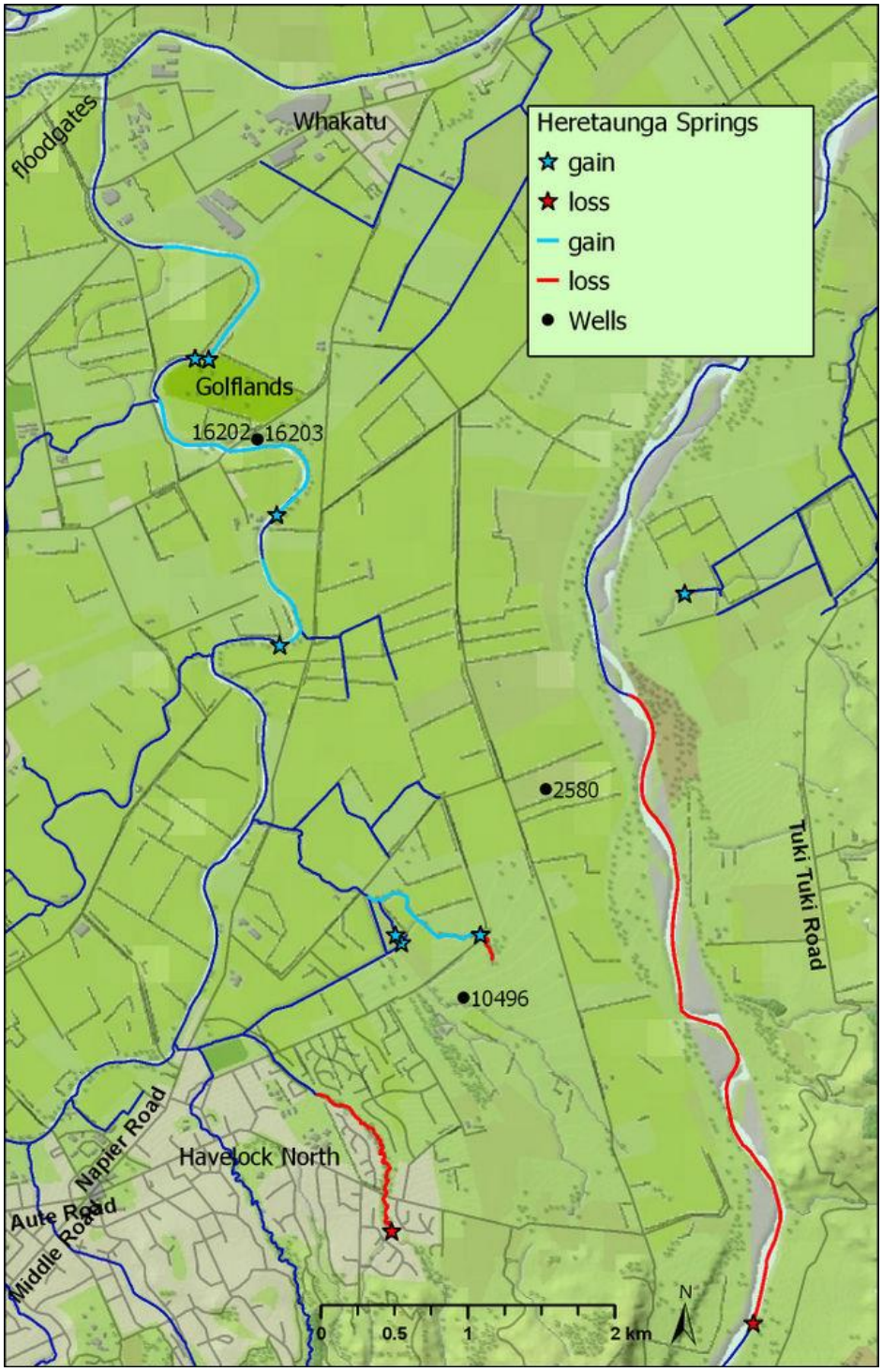

Figure 3-9: Flow gains and losses mapped for the Karamu Stream. . Springs were located using changes in electrical conductance, with blue stars indicating the start of a gaining section. The losing section of the Tukituki River (red star at start) was located using concurrent gaugings (see Section 3.4.3). Selected monitoring wells are mapped.

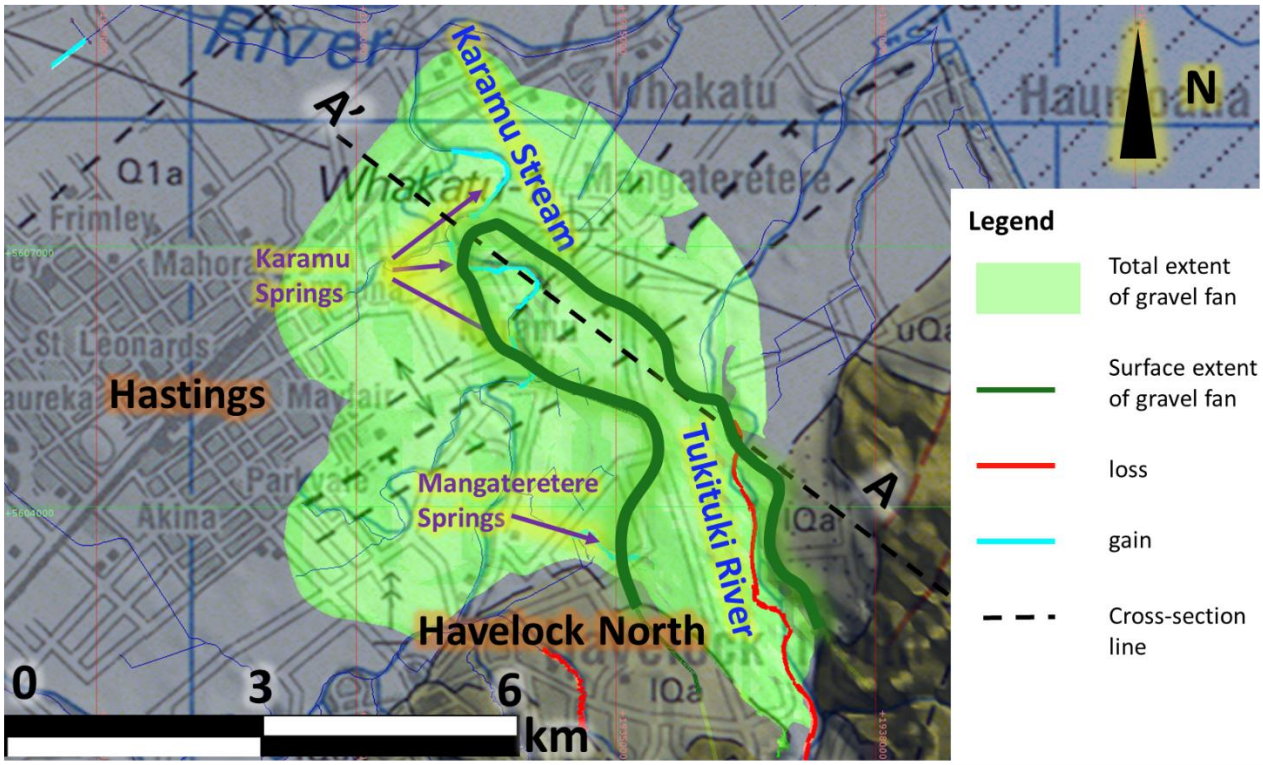

Figure 3-10: Karamu Stream Springs Geology - plan view. Geological model developed by GNS Science **(Lee *et al.*, 2017)**

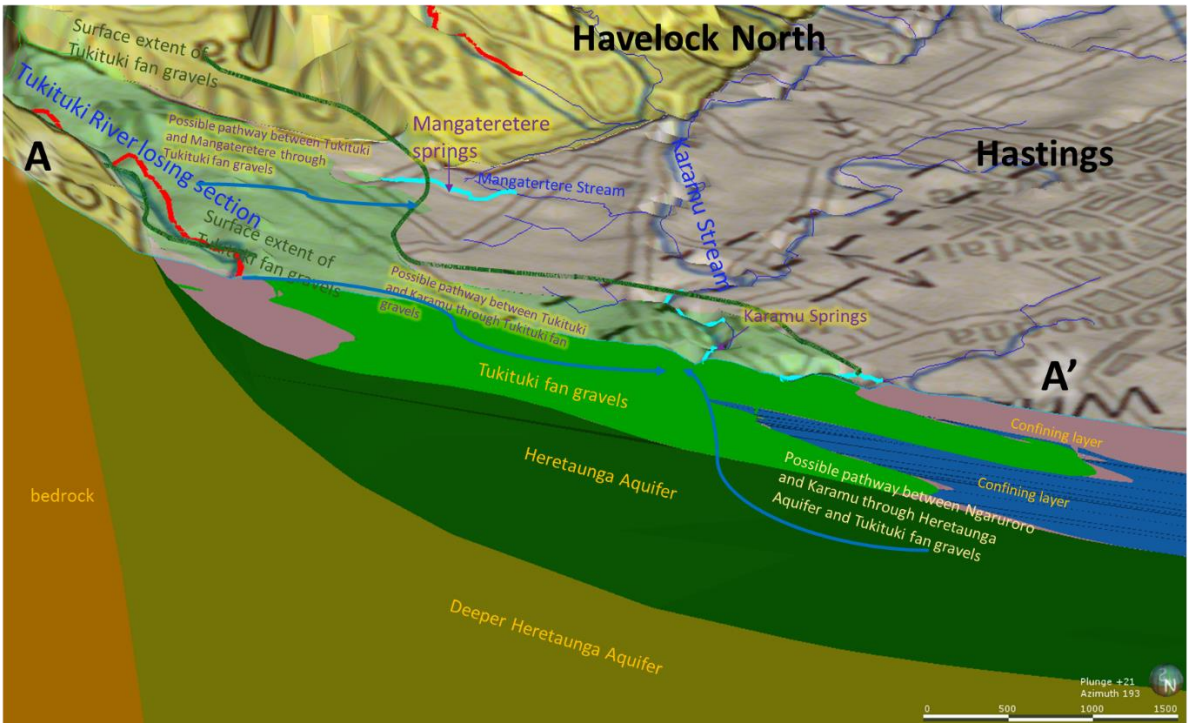

Figure 3-11: Karamu Stream Springs Geology - Cross-section. Geological model developed by GNS Science **(Lee *et al.*, 2017)**

Mangateretere

This text is adapted from Wilding's (2017) report.

Description

The Mangateretere Stream is a major tributary of the Karamu Stream. Springs emerge, mostly as diffuse discharges, downstream of Brookvale Road (Figure 3-9).

Spring Flow

The combined outflow from these springs generates a mean annual low flow (MALF) of 48 L/s, with a median flow of 180 L/s, at the Napier Rd monitoring site.

Spring Origin

The two most likely sources of groundwater inflows are losses from the Tukituki River, or losses from the Ngaruroro River (through the Heretaunga aquifer).

Local rainfall recharge cannot account for the magnitude of flow originating from the Mangateretere springs. In addition, a large portion of flow is taken from the Mangateretere by stream-depleting groundwater takes (e.g. average 140 L/s metered use from the Brookvale municipal bores on 27/2/2013)

Because the surface-catchment inflows can only explain a fraction of the spring flow, groundwater inflows from neighbouring catchments are likely to form the bulk of the flow. This is further supported by the low electrical conductance of the Mangateretere, compared to tributaries lacking trans-basin groundwater inputs (median 244 µS/cm for the Mangateretere at Napier Rd, compared to 714 µS/cm for Awanui at Flume).

Dravid and Brown (1997, 167) proposed that the shallow groundwater feeding the Mangateretere Stream originated from the Tukituki River, with increasing inputs of Ngaruroro sourced water during winter when water levels in the Heretaunga aquifer were elevated. Stable oxygen and deuterium/hydrogen isotopes collected during winter and summer in the Mangateretere Stream support this.

A potential connection exists between the Tukituki and Ngaruroro rivers and the Mangateretere springs, through a Tukituki gravel fan, as described in an earlier subsection describing Karamu springs.

The Mangateretere springs are at an elevation similar to the end of the Tukituki losing reach, creating the gradient necessary for Tukituki sourced groundwater to flow toward the Mangateretere Stream.

Electrical conductance measured in the Mangateretere Stream is slightly higher than in Tukituki River water, indicating some contribution from limestone hill country to groundwater feeding the Mangateretere Stream.

Intermittent springs (i.e. in stream reaches that change seasonally from gaining to losing) have been identified in the Mangateretere Stream, which have the potential to become a conduit for contaminants to enter groundwater (DIA, 2017).

Raupare

This text is adapted from Wilding's (2017) report.

Description

The Raupare is a spring-dominated stream that arises close to the variable-loss reach of the Ngaruroro River, and then joins Karamu Stream which becomes the Clive River. The springs emerge as large point-springs with boiling sands, or as diffuse discharges. The springs emerge in the confined area of the Heretaunga aquifer, close to the confined/unconfined boundary (sometimes referred as a semi-confined aquifer).

Spring flow

The combined outflow of these springs, measured at Ormond Road (2014-2016), produce a MALF of 400 L/s.

Spring origin

Stable isotopes from Raupare Stream are similar to groundwater recharged by the Ngaruroro River, and indicate that the Ngaruroro River is the primary source of Raupare Stream flow.

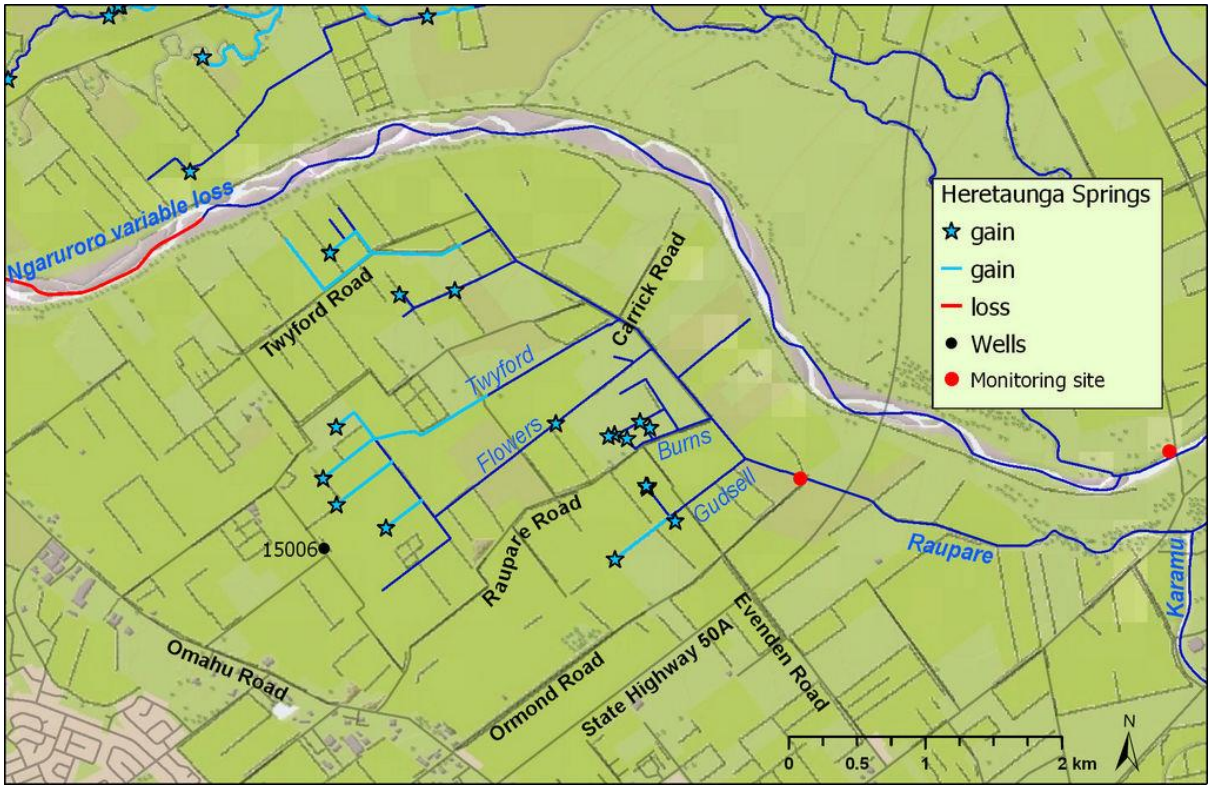

Figure 3-12: Raupare Stream map. Springs were mapped in the Raupare catchment, with point springs shown as blue stars and more diffuse springs identified with light blue lines to provide an indication of the length of gaining stream. The soil depth (cm) down to the top of a layer of Taupo pumice/ash sand is represented by coloured polygons from Griffiths (2001). The flow monitoring site at Ormond Road is marked with a red dot, and selected groundwater monitoring wells with black dots.

Irongate

This text is adapted from Wilding's (2017) report.

Description

The Irongate Stream is a spring dominated stream and is a tributary of Karamu Stream (Figure 3-13). While point-springs were not observed in the Irongate catchment, groundwater seeps through the bed of Irongate Stream as diffuse springs.

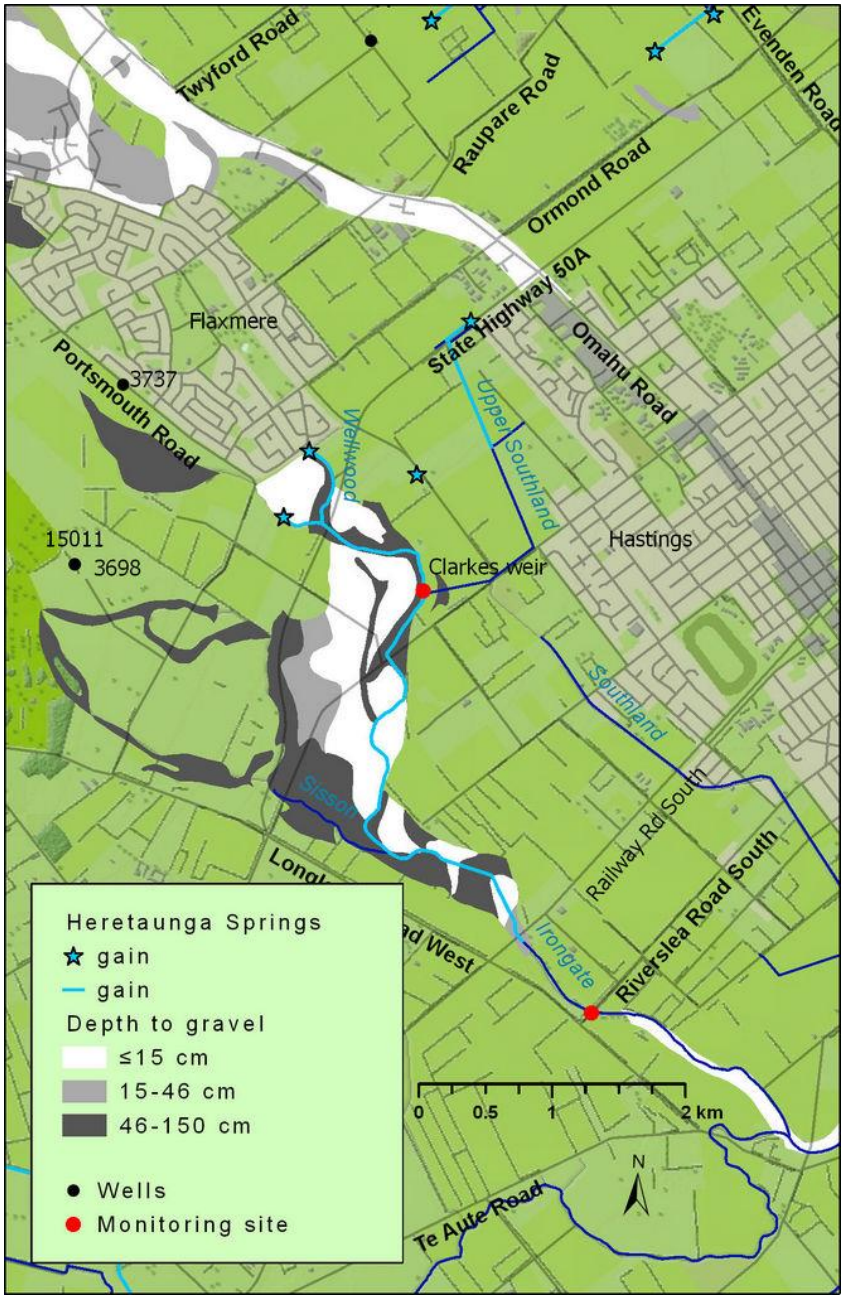

Figure 3-13: Irongate Stream. Perennial streams are shown as blue lines, with the start of perennial springs shown as blue stars. For Irongate, the springs are diffuse and extend all the way down to Railway Road (light blue line). Shallow gravels from soil maps are displayed as shaded polygons (e.g. white polygons represent gravel within 15 cm of the soil surface), (Griffiths, 2001).

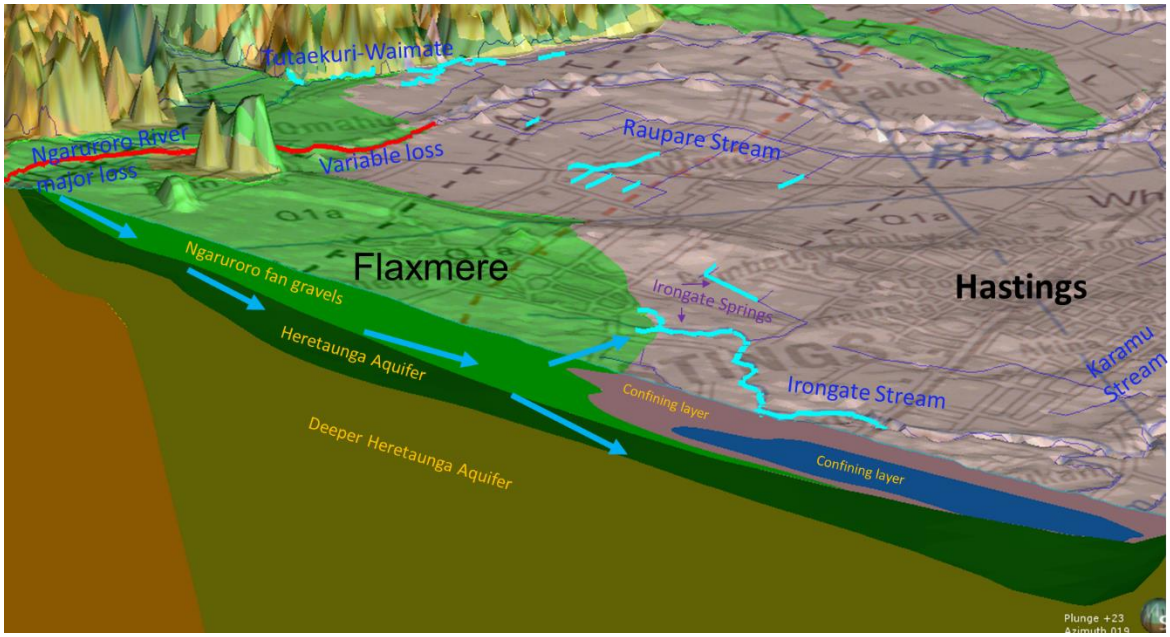

Figure 3-14: Irongate Stream conceptual model.

Spring Flow

The Irongate has a MALF of 100 L/s at Clarkes weir (Waldron & Kozyniak, 2017), which would equate to 170 L/s MALF at Railway Rd (from concurrent gaugings).

Spring Origin

Water in the Irongate springs appears to originate from both the Ngaruroro River and local rainfall in the unconfined aquifer.

Much of the gradual increase in flow occurs downstream of a layer of clay that confines groundwater within the Heretaunga (Figure 3-14). Above the confining layer sits a shallow layer of river gravel (Figure 3-13) which was left behind when the Ngaruroro River abandoned this flowpath in 1867[1] (HBRC, 2004). Well logs indicate this gravel layer is about 2.5 m to 5 m thick (e.g. drilling logs for bores 10799 and 3322), transitioning to a similar thickness of pumice sand to the west of Hawke's Bay Expressway (e.g. bore 8373). The gaining reaches of the Irongate Stream, as mapped for this study (Figure 3-13), terminate at the downstream end of the shallow gravels that were included in soil maps by Griffiths (2001).

This shallow layer of gravels has not been included in the 3D geological model of the Heretaunga Aquifer (Lee et al., 2014, 2017), presumably because this is a local feature of relatively small scale.

Shallow gravels are connected to the unconfined part of the Heretaunga Aquifer. A 3D geological model (Lee et al., 2014, 2017) indicates that the unconfined part of the Heretaunga Aquifer consists of Ngaruroro fan gravel and is underlain by deeper and older aquifer deposits. This gravel fan provides a pathway for water between the losing section of the Ngaruroro River and Irongate stream. It also provides a pathway for rainfall recharge to discharge into Irongate Stream.

Stable isotopes in water collected from the Irongate Stream in March 2015 indicate that source of water could be mixed rainfall recharge (40%) and Ngaruroro River water (60%) at the time of sampling.

[1] http://hwe.niwa.co.nz/event/May-June_1867_Hawkes_Bay_Flooding

Paritua-Karewarewa

Description

The Paritua Stream drains limestone hill-country (sandstone, limestone and mudstone of marine origin) before flowing across the Heretaunga Plains. Downstream of Bridge Pa the Paritua becomes the Karewarewa Stream.

On the Heretaunga Plains, there are two distinct sections of the stream. The upper section, below Washpool Station bridge loses water for around 7.5 km. This section can become dry at times. These losses occur where the stream flows across unconfined gravels that are perched several metres above the groundwater table (Rabbitte, 2009).

Hughes (2009b) considered the rate of loss to be slow for the losing reach, concluding the streambed sediments had low permeability. Investigations revealed a coating of tufa that weakly cemented the cobbles and gravels together, lowering the streambed permeability.

A gaining section begins near Raukawa Road, although the exact location depends on groundwater levels in the area. The start of the gaining section coincides with the edge of the confining layer and with a change from unconfined gravels to a shallow layer of Taupo pumice sand and ash. From well records, the layer of the pumice sand is typically 4 m thick (e.g. well numbers 8512, 668, 10522) and this layer can be seen in eroded stream banks. Separating this layer of pumice sand from the deeper gravel-aquifer is a layer of confining marine clays that thickens southeast of Bridge Pa (Dravid & Brown, 1997). Therefore, downstream of Bridge Pa is where this layer of pumice sand could provide a conduit for groundwater moving laterally to streams (e.g. Karewarewa, Awanui and Louisa streams), together with nutrients leached from overlying land use.

A 3D geological model (Lee et al., 2014, 2017) shows (Figure 3-16) that the losing section of Paritua Stream is located on a Ngaruroro fan gravel unit (which coincides with an unconfined aquifer), and the gaining section of Karewarewa Stream is located on a gaining reach of the confining unit (fine Holocene materials). The layer of pumice has not been represented on the 3D geological model, presumably because this is a local feature of relatively small scale.

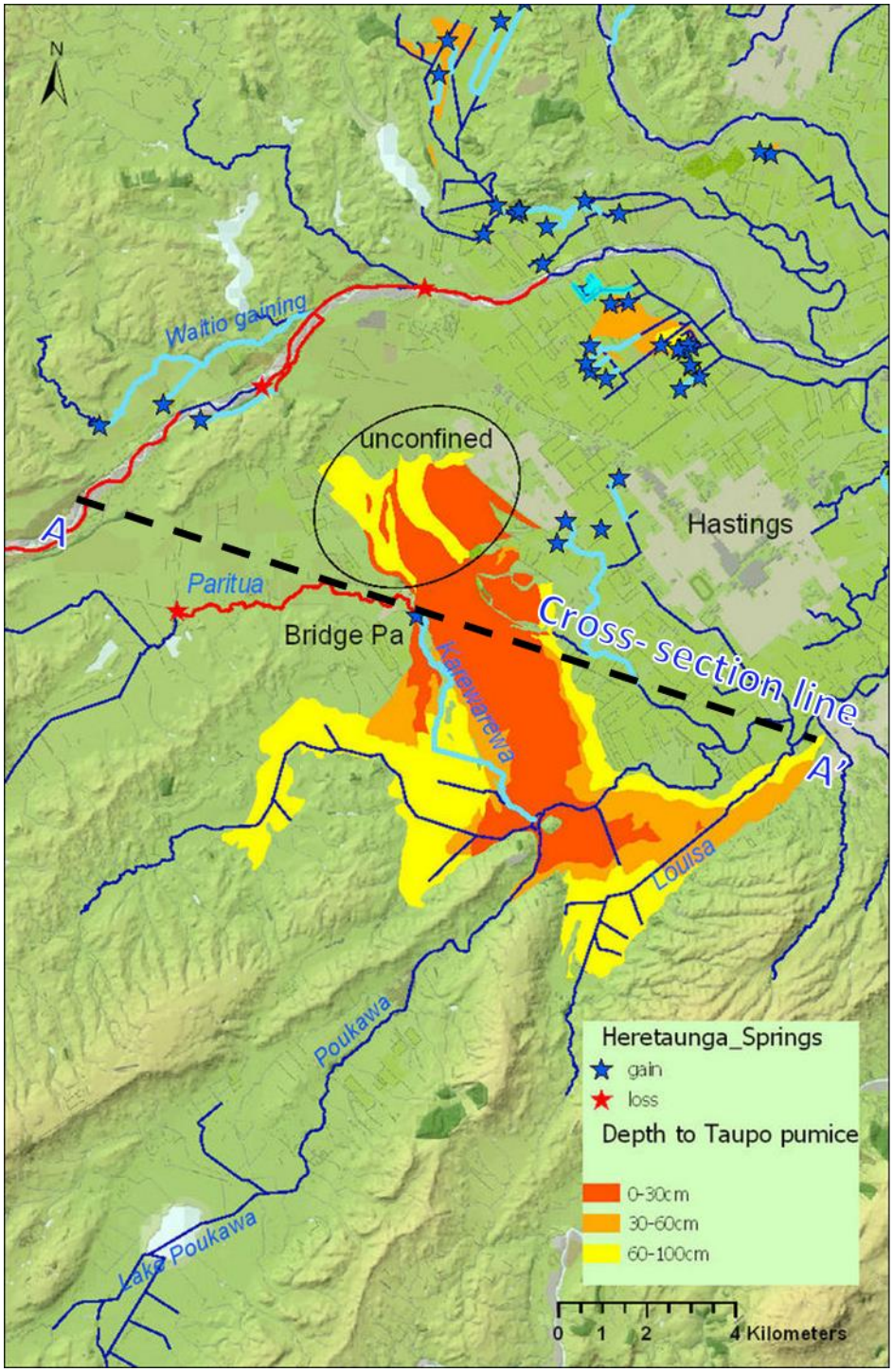

Figure 3-15: Taupo pumice sand layer. The soil depths (cm) to top of the Taupo pumice/ash sand layer are represented by coloured polygons (darker orange for shallow soil overlaying pumice). The polygons and soil-depths are from Griffiths (2001). Marine clays separate the pumice layer from deeper gravels, with the exception of the area north of Bridge Pa (labelled "unconfined").

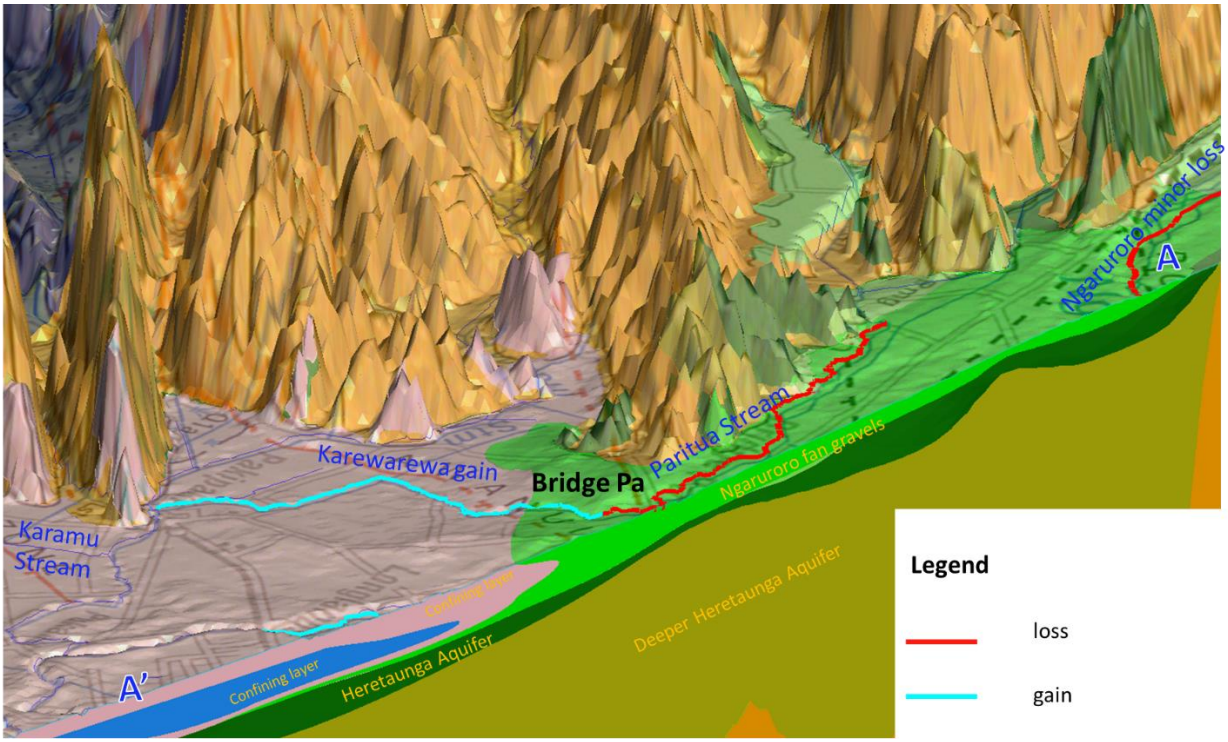

Figure 3-16: Cross-section along Paritua and Karewarewa streams.

Spring Flow

The typical magnitude of loss for Paritua Stream was 100 L/s. The typical magnitude of gain for the Karewarewa Stream under low flow conditions was estimated as 25 L/s at Pakipaki.

Spring Origin

Ngaruroro fan gravel can potentially provide a pathway for local rainfall recharge and water lost from the minor Ngaruroro River losing section upstream of Roys Hill (see Section 3.4.3). However, the high electrical conductance and stable isotopes of the Karewarewa Stream are not consistent with a Ngaruroro source. Stable isotopes in the Karewarewa provide a closer match with streams in warmer, lowland catchments, indicating that the Karewarewa Stream may be recharged by groundwater sourced locally from losing streams (including the Paritua) or by direct rainfall recharge on the plains.

Maraekakaho

Description

The Maraekakaho Stream drains limestone hill-country (sandstone, limestone and mudstone of marine origin) together with some old river terraces, before flowing across more recent alluvial terraces as it approaches the Ngaruroro River (Figure 3-17). This transition to the more recent alluvial terraces occurs downstream of Tait Road, coinciding with changes in the surface-groundwater interactions for the Maraekakaho. The Maraekakaho Stream loses flow to groundwater over the reach downstream of Tait Road. Complete drying of the Maraekakaho Stream can occur over a section starting about 2 km upstream of Kereru Rd. When this section is dry, the stream starts flowing again around 0.5 km further downstream and regains much of its flow before reaching the Ngaruroro River.

Spring flow

Losses and gains were estimated to be 120 L/s.

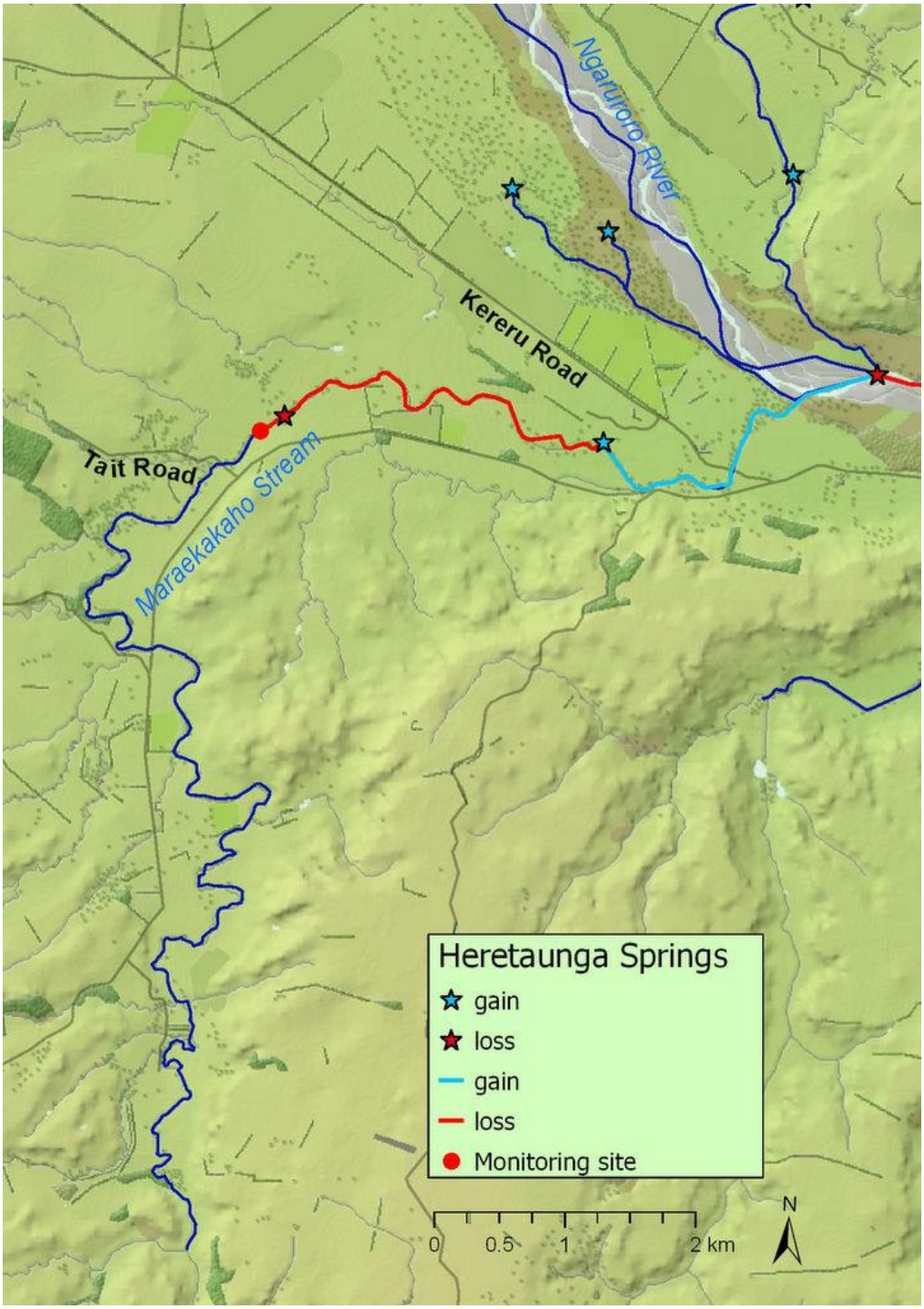

Figure 3-17: Maraekakaho Stream. The flow gauging site is located downstream of Tait Rd. The section of stream that loses flow to groundwater is displayed as a red line, while the gaining reach is a light-blue line

Waitio

Description

Waitio Stream drains the Ohiti area on the true left of the Ngaruroro River and gains flow from springs as it crosses the Heretaunga Plains (Figure 3-18).

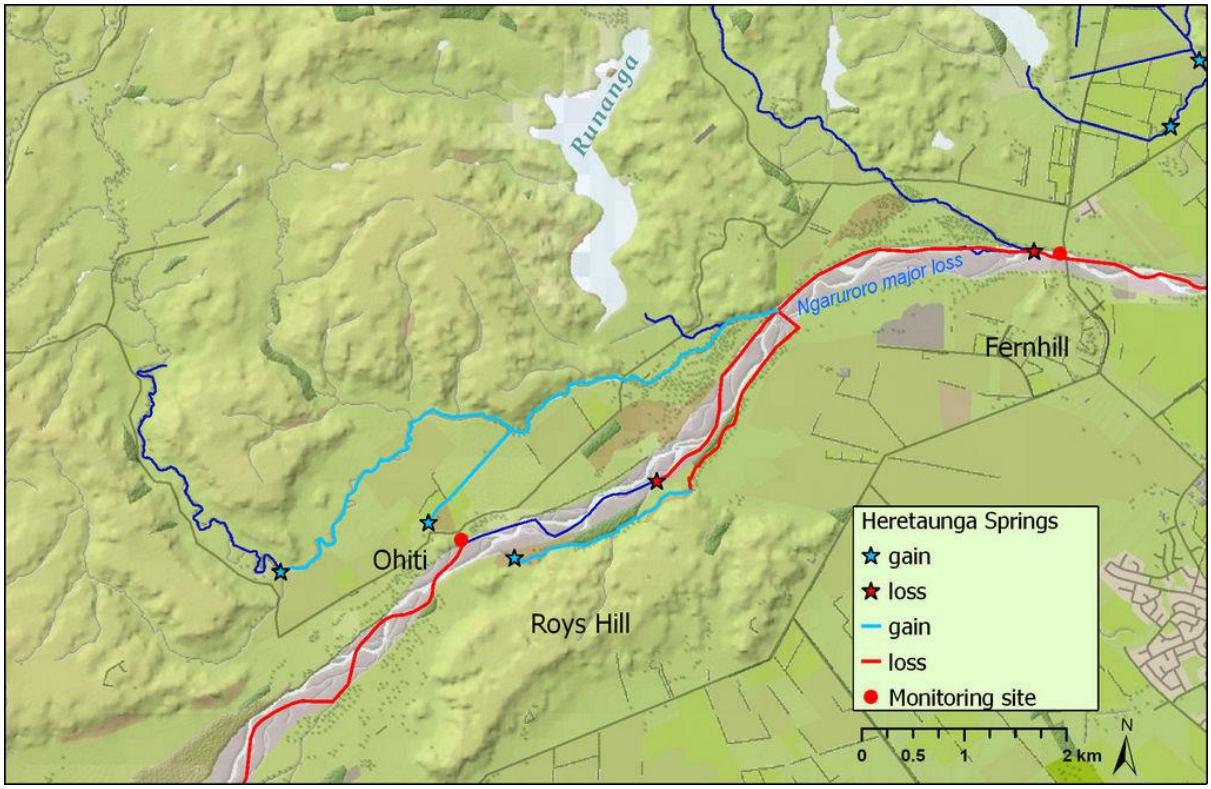

Figure 3-18: Waitio Stream. Spring inflows were detected where the stream flows across the Heretaunga Plains.

Spring Flow

MALF increases from <10 L/s as the Waitio Stream leaves the hill country, to 570 L/s before its confluence with the Ngaruroro River

Spring Origin

Evidence for the additional water originating from the Ngaruroro River includes a physical elevation gradient between the two (Waitio gaining section starts at 45 m elevation compared to 59 m in the Ngaruroro), separated by alluvial gravels. Further evidence comes from a decrease in electrical conductance of the Waitio. Stable isotopes in water sampled from the Waitio matched the Ngaruroro sourced groundwater.

Other stream and springs

Awanui

Awanui Stream drains a large area of peat wetlands and limestone hill-country (limestone, mudstone and sandstone of marine origin). This stream is not spring dominated (except for the Karewarewa tributary described earlier in this report) and there is a lack of evidence for spring discharges from the Heretaunga aquifer to Awanui Stream. Consequently, for the Awanui Stream, the spring survey did not go beyond mapping of the stream network.

Louisa and Te Waikaha

The Te Waikaha Stream drains a narrow catchment of limestone hill country (limestone, mudstone and sandstone of marine origin), including the western slopes of the highest peak in the Karamu catchment (Mt Erin, 490 m AMSL). After entering the Heretaunga Plains, the stream name changes to Louisa Stream. Springs were not surveyed in this catchment, beyond mapping the extent of wetted channels from aerial photographs, as there is a lack of evidence for noteworthy spring inputs from Heretaunga Aquifer to Louisa Stream.

Kikowhero

The headwaters of the Kikowhero Stream drain hill country that receives more rainfall than the Heretaunga Plains. Much of the stream flow originates from that wetter hill country. After leaving foothills, the stream path then follows the border between the Ngaruroro river terraces and the hill country. The Kikowhero flows through a small gully with the stream-bed cutting down into white sedimentary rock in places, interspersed by some gravel substrates. No increase in flow was detected over the long section of stream flowing alongside the river terraces.

A loss of flow probably occurs downstream of Omapere Rd, where the Kikowhero changes course and crosses river terraces to reach the Ngaruroro River. This 2 km of losing-reach can dry completely, as demonstrated by a dry braided channel visible from aerial photos. This losing reach is also elevated above the Ngaruroro River. Springs occur downstream of the drying reach, from the start of the gaining section. The start of the gaining reach coincides with channel elevation dropping to the same level as the Ngaruroro River. The magnitude of flow gain prior to the Ngaruroro confluence has not been quantified. Channel substrate appears to be gravel through the losing and gaining reaches, transitioning from white sedimentary rock somewhere upstream of Matapiro Road.

Ohiwia

There is no evidence of springs that originate from the Heretaunga aquifer and discharge to the Ohiwia Stream. Evidence for limited interaction includes negligible drop in electrical conductance and little change in observed flows along Ohiwia Stream.

Roys Hill

This stream is adjacent to the Ngaruroro River, with flow increased by channel excavation (i.e. by artificially dropping the bed level below the groundwater level). Spring inflows were mapped from aerial photographs after a visit to the stream (Figure 3-18). The flow was originally diverted into an artificial groundwater recharge scheme. However, that scheme no longer operates (Brooks, 1999; Gordon, 2009a). The channel now runs back toward the Ngaruroro River. It is possible that flow returns to the ground before reaching the Ngaruroro, given that it traverses gravels adjacent to the major loss reach of the Ngaruroro River.

Grange

Grange Creek appears to arise from springs adjacent to the Tukituki River within 5 km of the coast, and flows to its confluence with the Tukituki estuary at Haumoana (Figure 3-7). Flow was measured at 4 L/s during a single flow gauging. These springs may be sourced from shallow groundwater fed by flow losses from the Tukituki River.

Karituwhenua

The Karituwhenua Stream was walked on several occasions. The stream was dry for the entire length through Havelock North on at least one occasion. However, more often the stream was flowing upstream of Te Mata Road and gradually lost flow before drying completely downstream of Te Mata

Road. The channel is incised within old river terraces and intersects a layer of gravel in the area where it appears to lose flow. A losing reach was mapped based on these observations (Figure 3-9).

Ruahapia

Ruahapia Stream is a small tributary of the Karamu catchment, with median flow of 21 L/s. The source of flow for this stream was not identified. However, there is evidence that suggests the source of this stream may not be spring flow, but discharges from industrial activity in the Hastings area.

Turirau and Wharerangi

The headwaters of the Turirau Stream were historically diverted into the Ahuriri Estuary via a channel that was excavated through a hill with explosives. The headwaters are called the Wharerangi Stream, which flows through a small valley before reaching the diversion into the Ahuriri. Spring inputs to the Turirau and Wharerangi have not been investigated.

Georges

This small urban stream is sustained by saline groundwater. Georges Stream is separated from the Heretaunga gravel aquifer by a thick confining layer. A geological model (Lee *et al.*, 2014) reveals a lens of beach gravel and sand on the true-right bank that may connect Georges Stream with the ocean.

Groundwater level – spring flow relationship

A typical head/spring flow relationship is linear, so that spring flow increases proportionally with increases in groundwater levels. A non-linear relationship, where flow increases more rapidly than groundwater head, is typical for springs where seepage area increases (Rushton, 2004). Conceptually, this could occur by increasing a length of the spring-fed stream (Figure 3-19), or by increasing width and activation of elevated pathways to the stream during high groundwater levels (Figure 3-20).

The relationship between spring flow and groundwater level appears to be linear for the Tutaekuri-Waimate Stream (Figure 3-21.) Raupare, Mangateretere and Irongate streams (Figure 3-22 to Figure 3-24) exhibit a non-linear relationship, with the Irongate being strongly non-linear. There was limited data for Karamu, but available data also indicates a non-linear relationship. This observation is significant, as it may make numerical model setup and calibration difficult, as discussed in Section 0.

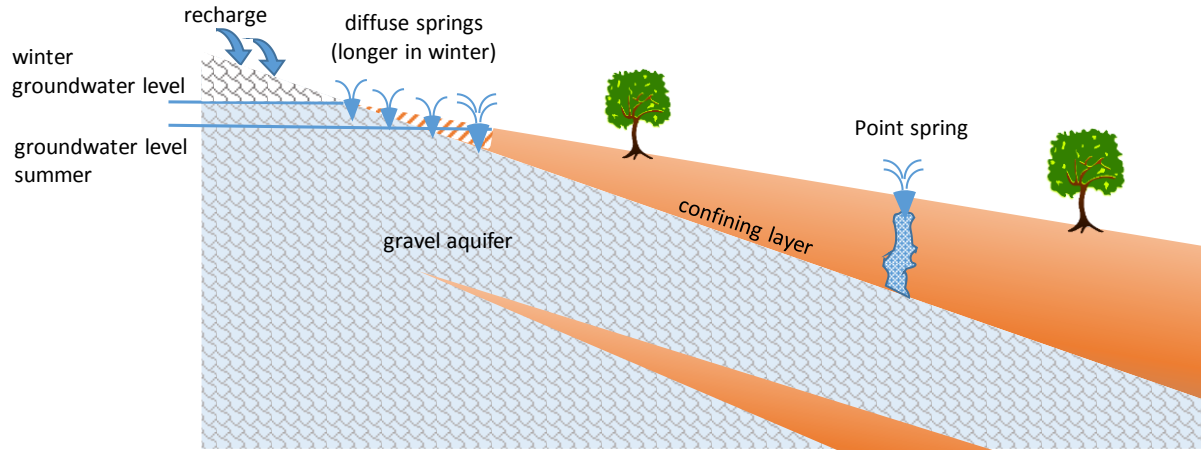

Figure 3-19: Diffuse and point springs. The length of diffuse springs can increase during winter when groundwater levels are higher, compared to the fixed location of point-springs, as demonstrated in this stylised diagram. This may result in non-linear head-spring flow relationship.

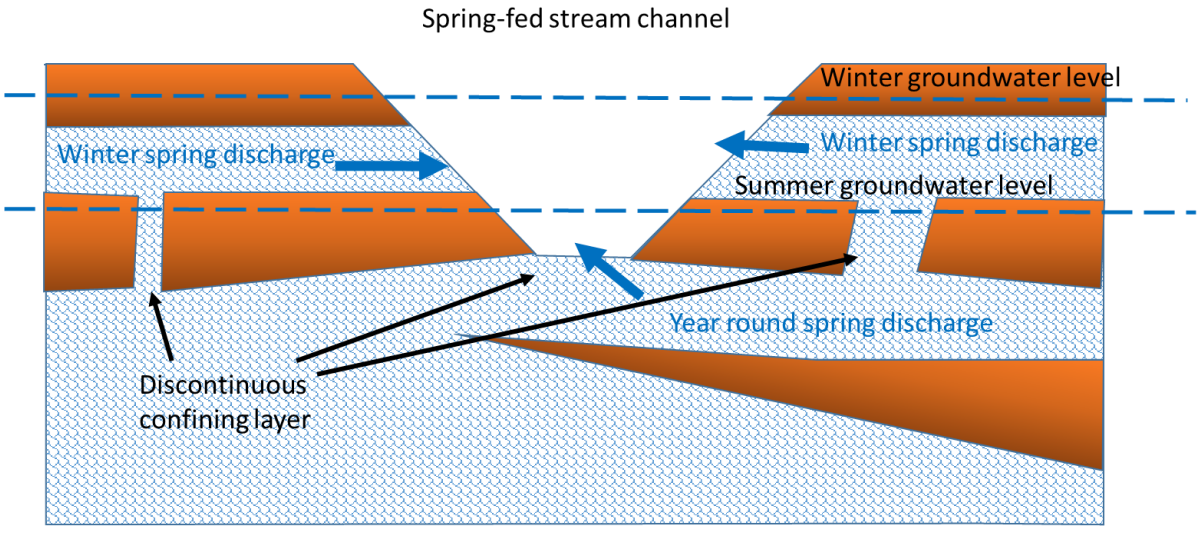

Figure 3-20: Conceptual cross-section through spring-fed stream. When water level is high (e.g. in the winter), additional higher pathways for springs water may become active, resulting in non-linear head-spring flow relationship.

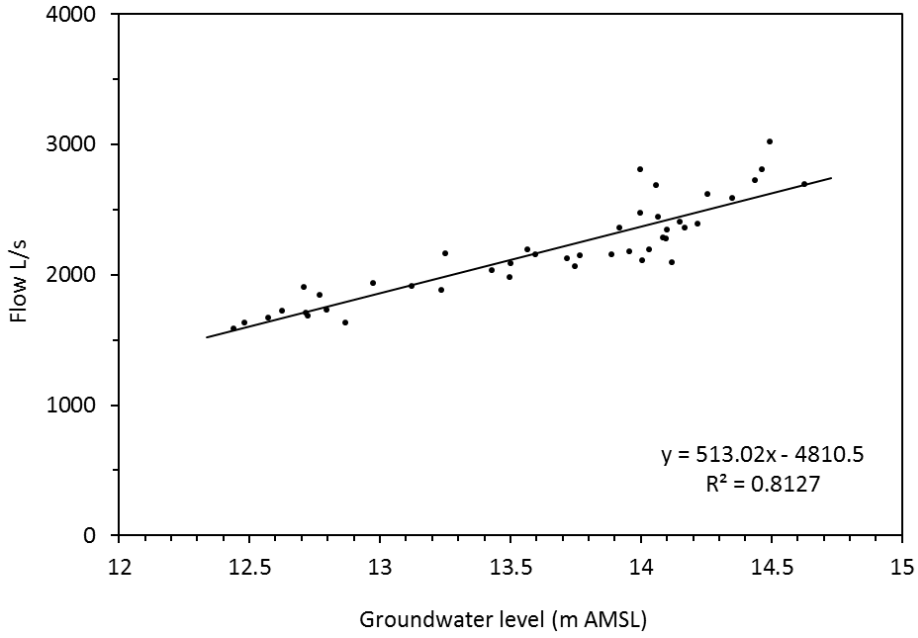

.

Figure 3-21: Tutaekuri-Waimate flow correlation with groundwater level. Flow measurements at Goods bridge are plotted against daily mean groundwater level observed at well 15006 on the day of the gauging (n=44, periods 1991-1994 and 2014-2016).

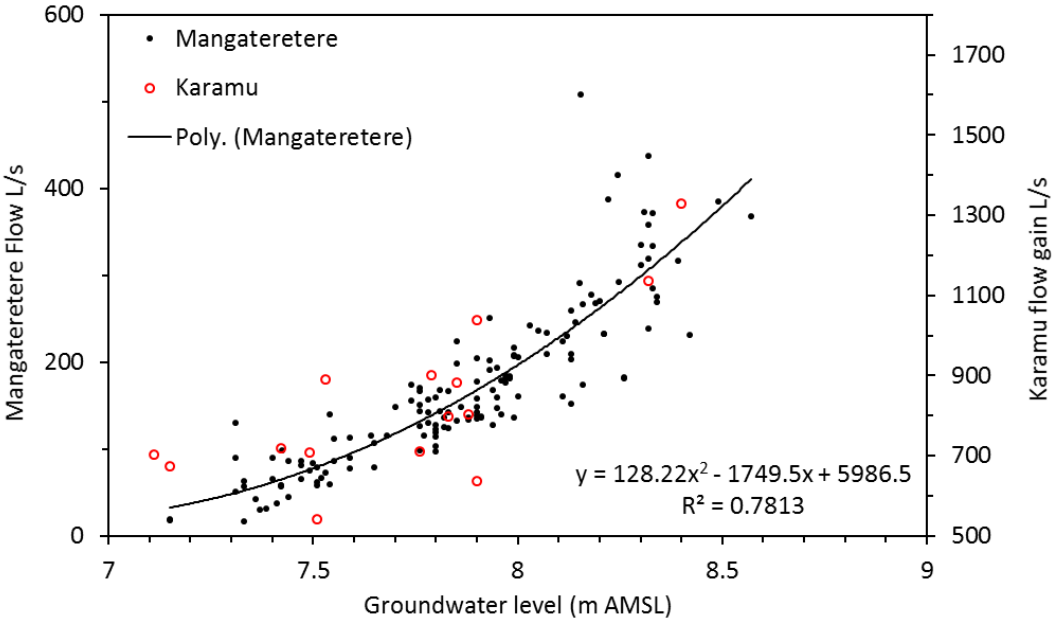

Figure 3-22: Flow in the Mangateretere and Karamu streams compared to groundwater elevation. Gauged flow for the Mangateretere Stream at Napier Road is plotted against groundwater level (metres above mean sea level) at Brookvale (well no. 10496) measured within 7 days of the gauging (from dipped groundwater level). The plot includes a polynomial curve fitted to this data. Also over-plotted as red circles are spring inflows to the Karamu Stream (estimated from concurrent gaugings), plotted against Brookvale groundwater levels.

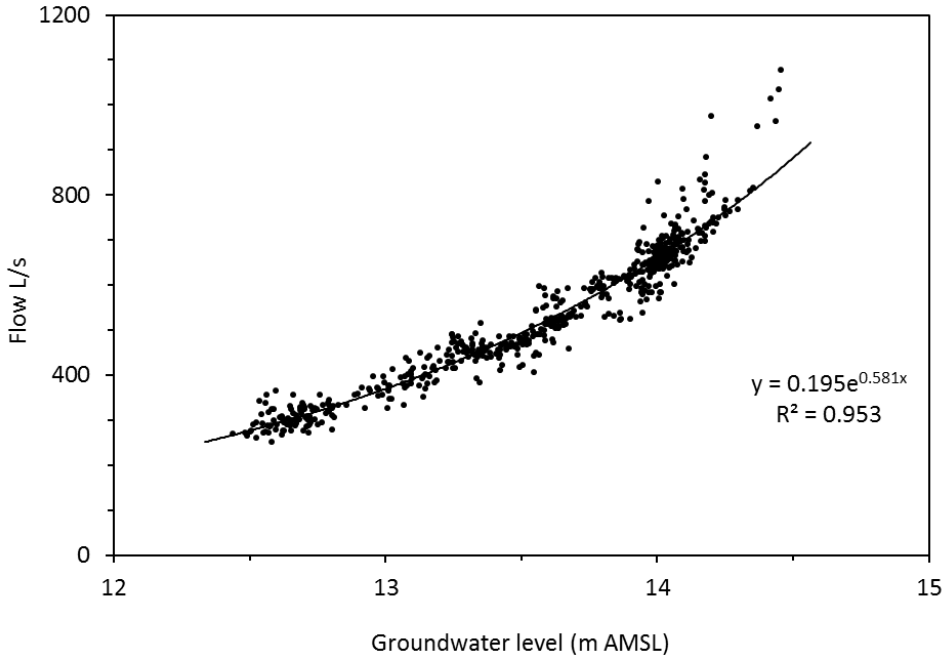

Figure 3-23: Raupare Stream flow correlation with groundwater level. The daily mean stream flow is plotted against the daily mean groundwater level observed at well 15006.

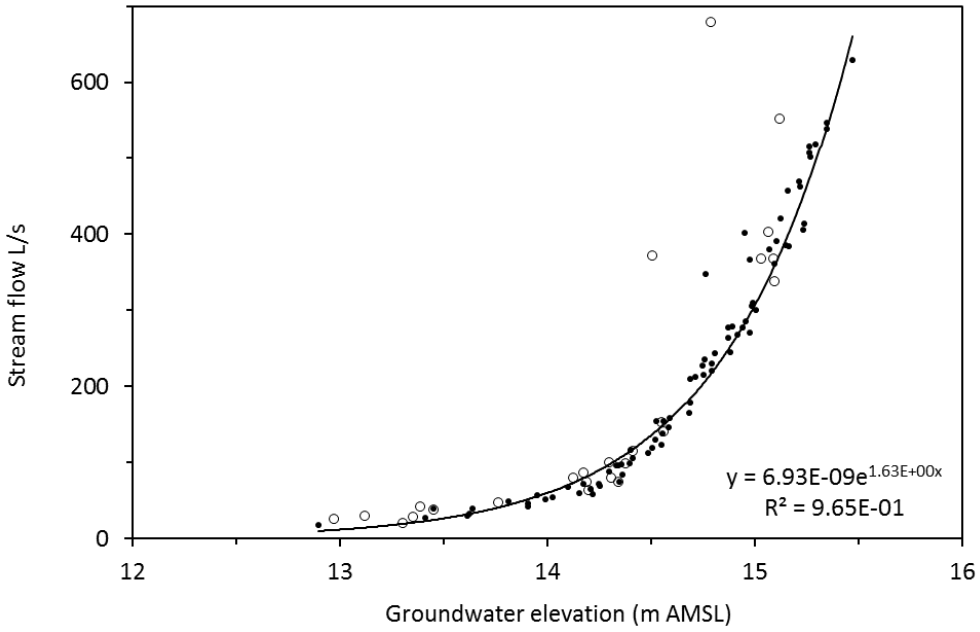

Figure 3-24: Irongate flow versus groundwater elevation. Flow for the Irongate at Clarke's weir is plotted against groundwater level in Flaxmere well (Well 3737, depth 29.2 m). Flows are plotted as open circles if there was rapid variation in flow (from rated stage to flow record) on the day of the manual flow measurement. These were isolated in case the flow measurements included rainfall runoff, which is unrelated to groundwater level.

3.4.5 Other rivers

The Ahuriri River (one of the TANK catchments) is not described here, as it is not hydraulically connected to the Heretaunga Aquifer system.

3.5 Aquifer system

Alluvial deposits underlying the Heretaunga Plains form the major aquifer, with estimated thickness of 250 m. In addition, there are other peripheral aquifers connected to this main aquifer. The aquifers forming the Heretaunga Aquifer System are shown in Figure 3-25.

The following aquifers form the aquifer system:

- Heretaunga aquifer;
- Tukituki aquifer;
- Tutaekuri and Moteo valley aquifer;
- Lower Tutaekuri aquifer (between Puketapu and Waiohiki);
- Upper Ngaruroro valley aquifer (between Whanawhana and Maraekakaho, including terraces).

Other aquifers with potential connectivity with the Heretaunga Aquifer System include:

- Peripheral limestone aquifer (e.g. at Poraiti);
- Poukawa basin aquifer;
- Okawa Basin aquifer;
- Te Awanga aquifer.

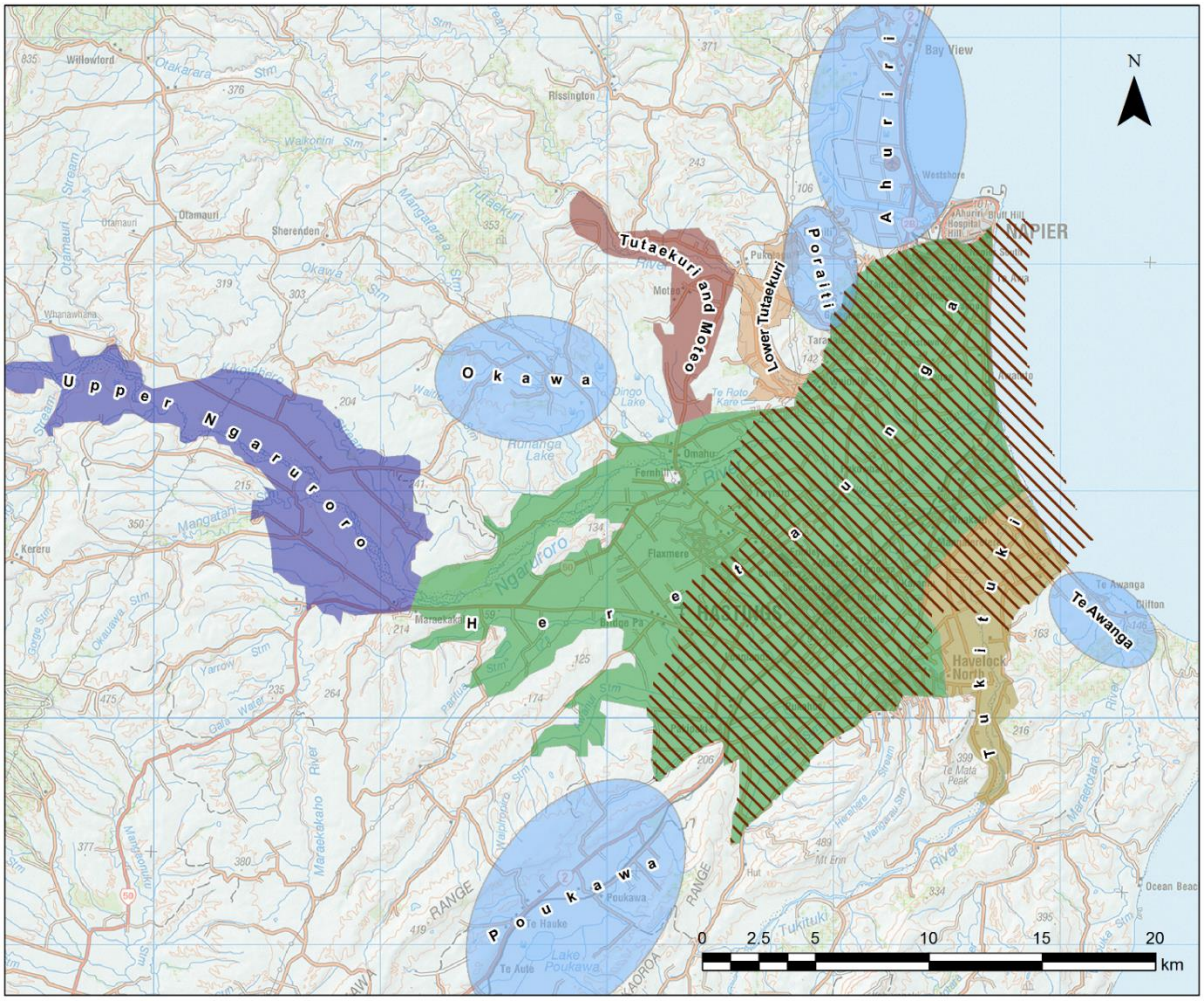

Figure 3-25: Heretaunga Aquifer System The confined area of the aquifer is shown with brown hatched lines. Aquifers that are not considered part of the Heretaunga Aquifer System are shown as blue ovals to indicate their approximate location and size.

3.5.1 Heretaunga aquifer

General Description

The Heretaunga aquifer underlies most of the Heretaunga Plains. The general geometry of the aquifer has been described by Dravid & Brown (1997) on the basis of three deep exploratory bores and other drilling data, with refinement using 3D geological modelling (Lee et al., 2014).

The aquifer is a multi-layered leaky system, formed mainly from alluvial gravels.

Aquifer type

The eastern part of the main Heretaunga aquifer is artesian. Deep exploratory bores in this area indicates 5 interconnected layers at Tollemache and 6 at Awatoto respectively. The shallowest layer of the Last Glacial Gravels is confined under a thick wedge of low permeability Holocene sediments. The eastern area of the aquifer is confined (Figure 3-25).

In the western part of the aquifer, drilling identified a shallow, unconfined aquifer, predominantly formed by gravel fans associated with major rivers, which allows for high rates of rainfall and river recharge to occur. Unconfined conditions have also been encountered where the Tukituki River enters the Heretaunga Plains (see Section 3.5.2)

Aquifer material

The top part of the aquifer is formed by Holocene alluvial gravels and Last Glacial Gravels (Q2-Q4 deposits), with deeper layers of the aquifer formed by older Quaternary sediments (Q5-Q7 deposits).

Most groundwater is used from the Holocene Gravels and Last Glacial Gravels. This part of the aquifer is highly transmissive and is likely to carry most of the groundwater flow.

The deeper part of the aquifer is formed by the older Q5-Q7 Quaternary deposits (predominantly alluvial gravels, see Section 3.3.1). However, the aquifer could potentially extend to even greater depths than have been identified in drilling logs (see following sections).

Stratification of the aquifer

The aquifer is stratified, with multiple aquifer layers identified in deep drilling bores. An exception is the eastern part of the aquifer, near the Ngaruroro recharge area, where the aquifer appears to be predominantly gravels down to 117 m depth, suggesting that different aquifer layers are connected here. Monitoring data shows head difference between shallow and deep layers, suggesting some degree of separation. However, the monitoring data also reveals similar groundwater fluctuation at different levels, suggesting connection between the layers. See section 3.7.2 for detail.

Extent of the aquifer

Vertical extent of the aquifer

Deep exploratory bores indicate that the aquifer extends to at least 250 m depth. It may extend even deeper than 250 m, but permeability can be expected to be lower at greater depths, so the aquifer is unlikely to be as productive at such depths.

Land-based aquifer boundaries

On land, the Heretaunga basin and consequently the Heretaunga aquifer is generally bounded by older rocks that have a lower permeability.

The northern extent of the basin is defined by Napier Hill.

The boundary between the hills west of Taradale and Napier Hill is difficult to define. Topographically, the Heretaunga Plains extend north of Napier and include the former Ahuriri Lagoon. In general there aren't many deep bores north of House Road and Prebensen Drive. Also, water levels in bores in this area are much lower and non-artesian; in contrast with high artesian pressures further south. This suggest that the deep Heretaunga aquifer doesn't extend north of House Road and Prebensen Drive and only a shallow aquifer, disconnected from the Heretaunga Aquifer System, is present there. This is consistent with the description by Dravid & Brown (1997), but is in contrast with the Leapfrog geological model (Lee et al., 2014) which indicates the presence of Q2-Q4 deposits north of Napier. The Leapfrog model doesn't seem to be supported by drilling data in this area.

Further southwest, the boundary is broadly defined by the hills. The basin forming the aquifer is likely to become shallower near the edge of the Heretaunga Plains and the western boundary of the Heretaunga aquifer may be set arbitrarily where the Ngaruroro valley becomes only about 1.5 km wide near Maraekakaho.

Further south and east of Maraekakaho, the aquifer boundary continues to follow the hills. East of Havelock North the aquifer connects to the Tukituki aquifer.

Smaller peripheral aquifers are hydraulically connected to the Heretaunga aquifer. These include the Moteo and Tutaekuri aquifers, the upper Ngaruroro aquifer and peripheral limestone aquifers.

Seaward extent of the aquifer

The seaward extent of the aquifer is unknown. The geological understanding is that the top part of the aquifer was deposited during the last glaciation between 12,000 and 71,000 years ago, when sea levels were as much as 150 m lower than today, and the coast was located up to 60 km further east (Dravid & Brown, 1997). This would allow for the aquifer to be deposited as far as 60 kilometres offshore, and later covered by fine marine sediments. This suggests that the aquifer extends a considerable distance east of the present coastline.

Whether or not the aquifer is hydraulically connected to the sea is uncertain. Geological understanding is that aquifer may extend far offshore, suggesting that such connection is possible. Navigational charts("NZ 56 Table Cape to Blackhead Point," 2012) indicate the presence of submarine springs perhaps 30 km offshore, citing observations from HMNZS Lachlan in 1954. However, the existence of these springs has not been confirmed, despite extensive searches of national archives, and it is not certain how they were identified.

Local well driller Russell Baylis funded an investigation that attempted to locate these springs using a vessel equipped with a salinity meter and underwater remote-controlled camera. The investigation was undertaken by MSc student Clementine Meyniel, with some assistance from HRBC staff, and is described in her Masters thesis (Meyniel, 2015). Meyniel suggested that springs were identified in her investigation. However, the evidence appears insufficient to conclude that submarine springs are present. The data could be the result of measurement errors.

Dravid & Brown (1997) suggested that upward pressures recorded in the deep Awatoto bore indicate that the deeper part of the aquifer has limited offshore extension.

High artesian head recorded at the coast indicates there is some hydraulic resistance between the sea and the aquifer. This could be due to large distance to the submarine springs (e.g. 30 km to the mapped springs), and/or the low conductivity of the springs themselves.

3.5.2 Tutaekuri and Moteo valley aquifer

General Description

The Moteo valley aquifer is located in a valley formed by an abandoned buried palaeochannel of the Tutaekuri River. This valley is about 7 km long and 2 km wide in the upstream and middle sections, with a width of only 800 m near its transition to the Heretaunga Plains. Currently the area is drained by the Tutaekuri-Waimate Stream, which is fed by groundwater springs (see Section 3.4.4 for detailed discussion). The aquifer is formed by gravelly alluvial deposits.

Connection to the Heretaunga Aquifer System

To the north, the Moteo valley connects to the Tutaekuri River valley (between Dartmoor and Puketapu), which is about 9 km long, and about 900 m wide. This area also forms an alluvial gravel aquifer. The Tutaekuri River loses approximately 800 L/s of flow through that reach and recharges the Moteo valley aquifer (see section 3.4.3)

The Tutaekuri valley also forms an aquifer downstream of Puketapu (referred to as Lower Tutaekuri aquifer), but this aquifer appears connected only by a very narrow valley. This suggests that the Lower Tutaekuri aquifer is not in full hydraulic connection with the upper Tutaekuri aquifer, or that the flow between these aquifers is limited.

To the south, the Moteo valley connects to the Heretaunga aquifer, although there is conflicting evidence regarding the nature of this connection. For example, in a recent report Morgenstern *et al.* (2018) argues that there is no connection between the Moteo valley aquifer and the Heretaunga aquifer. The available evidence regarding this connection is discussed below.

Evidence supporting the connection:

- Geologically, the Moteo valley is an abandoned buried channel of the Tutaekuri River and the aquifer is formed by alluvial gravels deposited along the valley. Conceptually, this deposition would probably result in a continuous aquifer along the valley which is connected to the Heretaunga aquifer.
- A review of groundwater well locations suggests the presence of an aquifer along the entire length of the Moteo valley without any major gaps that would indicate a discontinuity.
- Piezometric surveys in the valley suggest a continuous hydraulic gradient without any obvious discontinuities, which would otherwise be expected if the Moteo aquifer was disconnected from the Heretaunga Aquifer system.

Evidence against the connection:

- A groundwater balance suggests that most of the groundwater that enters the aquifer from the Tutaekuri River re-emerges as spring flow and the remainder may be discharged via groundwater pumping. However, this evidence is weak because accurate measurement of the water budget is not possible and the presence of at least some groundwater flow from the Moteo valley to the Heretaunga aquifer cannot be discounted using this method.
- Groundwater chemistry, stable isotopes and tritium data from Heretaunga aquifer samples did not indicate the presence of Tutaekuri River water, despite its distinct signature (Morgenstern *et al.*, 2018). However, there are no groundwater samples available in the vicinity of the Moteo valley exit, so this interpretation may be a consequence of insufficient sampling. Furthermore, after merging with the Heretaunga aquifer, water originating from the Tutaekuri River may be very diluted (assuming that only 200 L/s of Tutaekuri water enters the aquifer and mixes with 4,000 L/s of Ngaruroro water), which would make it difficult to distinguish from Ngaruroro water.

A review of data available from the Morgenstern *et al.* (2018) study also indicated that one of the bores used in the investigation, which was described as a shallow (37 m deep) bore, may be much deeper and located in tertiary sediments, but was misrecorded in a HBRC database. This bore (number 15795) is located near the exit of Moteo valley to the Heretaunga aquifer. Water age in this bore was interpreted as 230 years, suggesting old, slowly moving water. If bore 15795 was shallow, this data would support the hypothesis that throughflow does not occur. However, if the bore is deep the relatively old water age is not surprising and shallower groundwater at this location may be younger. It is recommended to sample a shallower bore at this location to resolve this.

Overall the evidence suggests that flow of groundwater between the Moteo Valley and Heretaunga aquifers is possible, albeit likely to be relatively minor (<200 L/s).

Vertical extent

While Dravid & Brown (1997) considered the Moteo valley aquifer may be 30 m deep, more recent drilling has identified that the aquifer may be deeper than previously thought. At the downstream end of the Moteo valley, gravels are present to 96 m depth in bore 15795 (reportedly, although there is

some uncertainty, as described in the previous section), and at a bore near the Tutaekuri river that identified gravels to 53 m depth. Ages of deposits have not been reported, and only basic bore logs are available, so the age and depositional environment is uncertain. Bore depth in the Tutaekuri aquifer between Dartmoor and Puketapu is typically less than 25 m, suggesting the aquifer is relatively shallow, although it is not certain if these bores have fully penetrated the aquifer depth. The Leapfrog geological model (Lee et al., 2014, 2017) appears to represent the aquifer in a very simplistic way, and there appears to be little data supporting the total depth of this aquifer.

Aquifer type

Available bore logs indicate that the aquifer is unconfined in the southern part of the Moteo valley and in the Tutaekuri valley, then becomes confined under a layer of clay and silt in the middle section of the valley. The depth of confining layer increases from about 5 m to 15 m where the Moteo valley connects to the Heretaunga Aquifer. Springs arise where the aquifer becomes confined.

The Leapfrog geological model (Lee et al., 2014, 2017) does not include a representation of this confining layer.

Aquifer recharge

The Moteo valley aquifer is recharged by the Tutaekuri River, along with rainfall in the unconfined part and some contribution from surrounding hill country (see section 3.4.4 for discussion).

Groundwater flow direction

Water flow direction is southwards in the Moteo valley. Of the 800 L/s recharge from the Tutaekuri River (excluding land surface recharge and contributions from outside of the valley, which are expected to be relatively small), approximately 600 L/s emerges as springs in the middle part of the Moteo valley. Further downstream, after the Moteo valley joins the Heretaunga Plains, a further 1,300 L/s emerges from springs in the Tutaekuri-Waimate Stream, but this water is most likely derived from the Heretaunga aquifer (see discussion in section 3.4.4). This indicates approximately 200 L/s of through flow to the Heretaunga aquifer, however most of this through flow may be intercepted by groundwater pumping.

3.5.3 Lower Tutaekuri aquifer (below Puketapu)

The Tutaekuri River downstream of Puketapu flows within a narrow valley, about 1 km wide and 6 km long. The valley forms an unconfined gravel aquifer (the Lower Tutaekuri aquifer) and is tapped by numerous wells. Most of the wells are less than 30 m deep. The full depth of the aquifer is unknown, but valley size would suggest that the aquifer is relatively shallow. The Leapfrog geological model (Lee et al., 2014, 2017) appears to represent the Lower Tutaekuri aquifer in a very simple way, and there appears to be little data to identify the total depth of this aquifer. Also, the Leapfrog modelling shows a very shallow Holocene and Q2-Q4 layer where the aquifer joins the Heretaunga aquifer, which is unsupported by bore data and appears to be an artefact of the geological modelling algorithm.

In the recently updated Leapfrog geological model (Lee et al., 2017) the authors have included Tutaekuri fan gravels, which are located within the Heretaunga aquifer system. These gravels are directly on top of the main aquifer Q2-Q4 material where the Lower Tutaekuri aquifer merges to the Heretaunga aquifer, and further east inter-fingers with confining layer deposits. This suggests that the Lower Tutaekuri aquifer is connected to the main Heretaunga aquifer.

However, other evidence suggests that this aquifer has limited connection to the Heretaunga aquifer. Hydrological data suggests that the Tutaekuri River does not lose or gain flow below Puketapu. This may be due to lack of permeable connection between the river and the aquifer, but may also indicate

that there is insufficient head difference between the river and the aquifer to generate a measurable change of river flow. Also, recent work by Morgenstern *et al.* (2018) indicates that the source of water in nearby Taradale bores can be traced to Ngaruroro recharge and is not sourced from the Tutaekuri River. This was indicated by a distinctive stable isotope signature and old water age (over 20 years) from samples taken from these bores. Again, although this suggests that significant groundwater flow does not occur between the Lower Tutaekuri aquifer and the main Heretaunga aquifer, this may be due to lack of head difference between the river and Heretaunga aquifer. The presence of some groundwater flux between the Lower Tutaekuri and Heretaunga aquifers cannot be completely discounted.

Water level surveys show a lack of appreciable groundwater level changes between the Lower Tutaekuri aquifer and the Heretaunga aquifer, indicating no connection exists.

Water levels recorded in bores where the modelled fan gravel lies directly on top of the main Heretaunga aquifer mostly exhibit a lack of artesian conditions. Consistently artesian conditions would indicate that local rainfall recharge and river leakage to the main aquifer do not occur, but lack of artesian conditions cannot be used to indicate that that the connection exists.

Overall, the evidence (in particular hydrological and isotope results) suggests that the Lower Tutaekuri aquifer is disconnected from the Heretaunga Aquifer System, or the connection is limited. However, existing data are such that some uncertainty exists.

3.5.4 Tukituki aquifer

The Tukituki aquifer has been described by Dravid & Brown (1997) as a distinct shallow aquifer, formed by Holocene gravel deposits, but hydraulically connected to the Heretaunga aquifer and underlain by it. This aquifer is described as the "Te Mata aquifer" in recent reports related to a contamination outbreak for public water supply bores (DIA, 2017).

The Leapfrog geological model (Lee et al., 2014, 2017) indicates that this shallow aquifer formed by Tukituki gravel fan is underlain by a deeper aquifer of Last Glacial Gravels. Further evidence from a new 150 m bore drilled near Havelock North indicates that a deep aquifer system is present closer to the edge of hill country than indicated by the geological model (see Section 3.3.1). This suggests that the deep aquifer may underlie the shallow Tukituki aquifer.

Analysis of water sources in the Karamu Stream and spring-fed Mangateretere stream (see Section 3.4.4) identified the Tukituki River as a primary source of water, but with possible Ngaruroro River inputs as well. This also indicates a connection between the Heretaunga and Tukituki aquifers.

Based on this, it may be more appropriate to refer to the Tukituki aquifer in this area on the southern part of the Plain as a part of the Heretaunga Aquifer System, rather than as a distinct aquifer unit.

Dravid & Brown (1997) describe the aquifer in this area as semi-confined to confined, however the presence of significant flow losses from the Tukituki river (800 L/s, see Section 3.4.4) and mapping of the surface expression of Tukituki fan gravels (Figure 3-10) for the purpose of a geological model (Lee et al., 2014, 2017), would indicate that at least part of the aquifer is unconfined. This transition from unconfined to semi-confined to confined aquifer character of the Tukituki aquifer in this area is consistent with the Heretaunga Aquifer System character generally.

3.5.5 Upper Ngaruroro

The Ngaruroro River upstream of the Heretaunga Plains, between Whanawhana and Maraekakaho, flows in a wide valley curved against surrounding hill country. In this section, the valley is

approximately 21 km long, and of variable width ranging from 1.5 km to 8 km. Upstream of Whanawhana the river valley becomes very narrow and gorges are present.

The aquifers in this area are formed in the river terraces and in gravel deposits of the river floodplain. There are bores in this area located both in terraces and the floodplain. Overall the aquifer doesn't form a significant water resource, due to limited depth and extent, but may provide recharge and the potential for contaminant transport to the downgradient Heretaunga aquifer.

The aquifers in this area can be divided into the following parts:

- Ngaruroro floodplain;
- Kikowhero terrace;
- Pigsty flats terraces;
- Maraekakaho terrace.

Ngaruroro floodplain

The river bed and surrounding floodplain form an alluvial gravel aquifer. The floodplain is approximately 1.5 km wide near Maraekakaho and further upstream reduces to approximately 700 m width, while it is only 300 m wide near Whanawhana. There are several bores that tap this aquifer: most of them very shallow at approximately 10 m depth. River gaugings have not identified any significant gain or loss in this Ngaruroro River reach because observed longitudinal differences in flow are relatively small and may be a consequence of gauging error (see Section 3.4.3).

Kikowhero terrace

Kikowhero terrace is located on the northern side of the Ngaruroro River. This terrace is approximately 12 km long and 2 km wide. The terrace is elevated above the floodplain, which increases from about 20 m elevation at the eastern end to nearly 50 m at the western end. The terrace is formed by Last Glacial Gravels (Q2-Q4) with a thickness up to 15 m (Lee et al., 2014). These gravel materials form an aquifer utilised by several groundwater production wells. Deeper aquifers also appear to occur in the underlying bedrock and are tapped by several deeper wells with depths down to 90 m.

This aquifer is likely to be recharged by local rainfall, with possible contributions from surrounding hill country runoff and losses from the Kikowhero stream (see sections 3.4.4).

This terrace aquifer appears to be mostly disconnected from the floodplain aquifer and perched above the Ngaruroro floodplain. It is possible that some springs emerge where the aquifer is terminated at the cliff edge, although this was not investigated for the present study. There is a large head difference between water levels in this aquifer and floodplains. For example, bores in the middle section of the terrace have groundwater levels of approximately 155 m asl, whilst the Ngaruroro river bed is at elevation of about 120 m asl in this area). Any hydraulic connection is likely to occur at the eastern (downstream) end of the terrace.

Maraekakaho terrace

Maraekakaho terraces are located on the southern side of the Ngaruroro River, just upstream of Maraekakaho. These terraces are much less pronounced than Kikowhero terrace, and form a series of smaller terraces with maximum height approximately 30 m above the floodplain. The Maraekakaho terraces are approximately 7.5 km long and up to 2.5 km wide. Groundwater levels within the terrace appear to be equivalent to water level within the floodplain aquifer. The description of the Maraekakaho terraces aquifer by Rosen (1996) appears to confirm that this. Bore logs indicate gravel

deposits to depth of approximately 40 m. Overall it appears that this aquifer may be in hydraulic continuity with the floodplain aquifer.

Pigsty flats terrace

Also on the southern side of the Ngaruroro River there is another small terrace (approximately 2 km by 3 km), of the same age as Kikowhero terrace (Q2-Q4). There are several water wells here, with gravels recorded at depths of approximately 40 m. Groundwater levels at the terrace are much higher compared to Ngaruroro River levels, suggesting that the aquifer is perched above and partially separated from the floodplain aquifer, similar to the Kikowhero aquifer.

3.5.6 Peripheral limestone

Groundwater is also present in limestone deposits around the Heretaunga Plains. The limestone deposits consist of sequences of weakly to moderately cemented muddy and sandy limestone, separated by mudstone beds (Dravid & Brown, 1997).

Most of the bores in peripheral limestone aquifers tap into the Poraiti area at the northern end of the Heretaunga Plains. The number of bores in Poraiti is probably more related to a greater number of properties in this area, rather than favourable aquifer properties. A piezometric survey in the Poraiti area identified much lower water levels near the edge of the Heretaunga Plains than the nearby Heretaunga aquifer. This suggests that the limestone aquifer near Poraiti is not well connected to the main Heretaunga Aquifer.

In other areas there is only limited data available that would allow for identification of the productive limestone aquifers. Overall it appears unlikely that a large groundwater resource exists outside of and connected to the Heretaunga Aquifer System, but nevertheless there may be some resources of local significance such as in Poraiti.

3.5.7 Te Awanga

Te Awanga is located at the coast, near the south-eastern edge of the Heretaunga Plains and this area contains a shallow gravel aquifer. Most bores at Te Awanga have gravels present to depths of approximately 20 m. The Leapfrog geological model (Lee et al., 2014, 2017) shows beach gravel deposits near the surface in this area. LiDAR elevation data indicates that this area is partially separated from the rest of Heretaunga Plains by an older terrace structure. Analysis of groundwater level data indicates a significant head difference between the Te Awanga area and nearby Haumoana bores. This difference is about 5 m over just 1 km. This difference indicates that the shallow aquifer around Te Awanga is not well connected hydraulically to the main Heretaunga Aquifer.

The Leapfrog model (Lee et al., 2014, 2017) indicated that beach gravels are directly underlain by the Last Glacial Gravels aquifer, but the geological model structures don't appear to match bore logs in this area very well (the geological model doesn't seem to be very accurate in this area). Actual bore logs for some deeper bores, for example bore 2953, show gravels at depths below 50 m, but separated from the shallower deposits by a thick layer of clay. This might suggest that a deeper aquifer connected to the Heretaunga aquifer may be present at depth here.

Overall, most of the bores seem to tap the shallower beach gravel aquifer separated from the deeper system.

3.5.8 Poukawa

The Poukawa catchment is approximately 15 km south of Hastings and is a small basin, 3 km to 4 km wide and 8 km long. The catchment occupies a depression formed by a faulted syncline, filled with

Quaternary fine-grained sands and silty clays up to 40 m thick and overlain with peat. (O'Shaughnessy, 1988). The dominant features of the catchment are limestone ridges up to 300 m high that surround the catchment.

Poukawa Lake occupies the low-lying land in the centre of the basin and is approximately 1.5 km in diameter with a depth less than 1 m. The Poukawa Lake and Pekapeka Swamp, located further north in the basin, form peat wetlands.

The lake drains into Poukawa Stream which then continues to the Heretaunga Plains, although the drainage flow is regulated by a control gate (O'Shaughnessy, 1988).

Poukawa groundwater resources are probably limited in comparison to the Heretaunga Plains, although there are several irrigation bores in the basin. The aquifer is present in limestone, sandstone and siltstone sediments, along with Quaternary sediments that infill the basin.

The hydraulic connection to the Heretaunga plains is likely to be limited. Groundwater outflow is constrained by a narrow valley, and was estimated by Cameron (2011) to be in the order of 5 L/s.

3.5.9 Okawa basin

Okawa basin is located several kilometres north of the Heretaunga Plains in a tectonic depression. Groundwater occurs here in several water bearing units, and these are described by Cameron (2003). There are multiple bores within the basin that utilise these aquifers. The basin is drained by Okawa Stream, which further downstream becomes Ohiwia Stream and joins the Heretaunga Plains. The connection to the Heretaunga aquifer is likely to be restricted, because the productive aquifer appears to be limited to an isolated depression, with only a narrow valley connecting it to the Heretaunga aquifer.

3.6 Aquifer Properties

Hydraulic properties of the Heretaunga aquifer, including transmissivity (T), horizontal hydraulic conductivity (K) and storativity (S) are known from pumping tests. Pumping test results available from the Heretaunga Plains have been compiled and summarised, with the hydraulic conductivity (Figure 3-26), transmissivity and storage maps developed in a separate assessment (Perwick, 2014).

Perwick (2014) analysed more than 100 pumping tests to estimate transmissivity and hydraulic conductivity throughout the Heretaunga Aquifer System. The reliability of these tests was also assessed and it was it was found to be variable, with only a third of the pumping tests considered to be highly reliable. Analysis indicated the presence of a high transmissivity zone in the central area of the Heretaunga Plains. However, the analysis also showed high variability of hydraulic conductivity, changing between 100 m/d to 3,000 m/d over a short distance in multiple locations. This is not surprising, as in alluvial systems such as the Heretaunga aquifer, high hydraulic conductivity zones can be associated with small-scale features such as buried river palaeochannels or open framework gravels that are likely to be spatially variable. The delineated zones appear somewhat arbitrary. For example, there are points where hydraulic conductivity values are estimated to have high confidence, which do not match values in delineated zones, but the zones seem to represent the general pattern of permeability in the aquifer reasonably well.

Most of the data for the hydraulic conductivity analysis was from relatively shallow depths, with only 9 bores that are greater than 60 m deep in the Heretaunga aquifer. There were no bores greater than 100 m deep.

It is worth noting that the pumping test analysis methods typically assume a fully penetrating well, or require some prior knowledge of the total thickness of the aquifer tested. The Heretaunga aquifer system is at least 250 m deep and several aquifer layers have been identified in some places, as described in Section 3.5.1. Most of the bores tested have screen lengths less than 10 m, which means that the tested vertical section of the aquifer may be relatively small (i.e. most bores do not fully penetrate the aquifer). Consequently, because the fully penetrating assumption is not valid, and the full depth of the aquifer or aquifer layer may be unknown, pumping tests may be not representative of the total transmissivity of the aquifer (the product of hydraulic conductivity with saturated thickness). For example, the pumping test may provide an estimate of properties for a 10 m thick aquifer layer, when at depth there may be another more (or less) permeable layer.

Another potential issue is success bias. That is, when well drilling encounters low hydraulic conductivity aquifer materials and is unsuccessful at tapping a productive aquifer, pumping tests may not be undertaken or reported. Depending on the frequency of these events, the analysis of hydraulic conductivity zones may be confounded by data that is biased towards higher conductivity values.

The above considerations mean that although aquifer properties and maps reported by Perwick (2014) are technically robust and defensible, they may not be representative of the entire Heretaunga aquifer thickness.

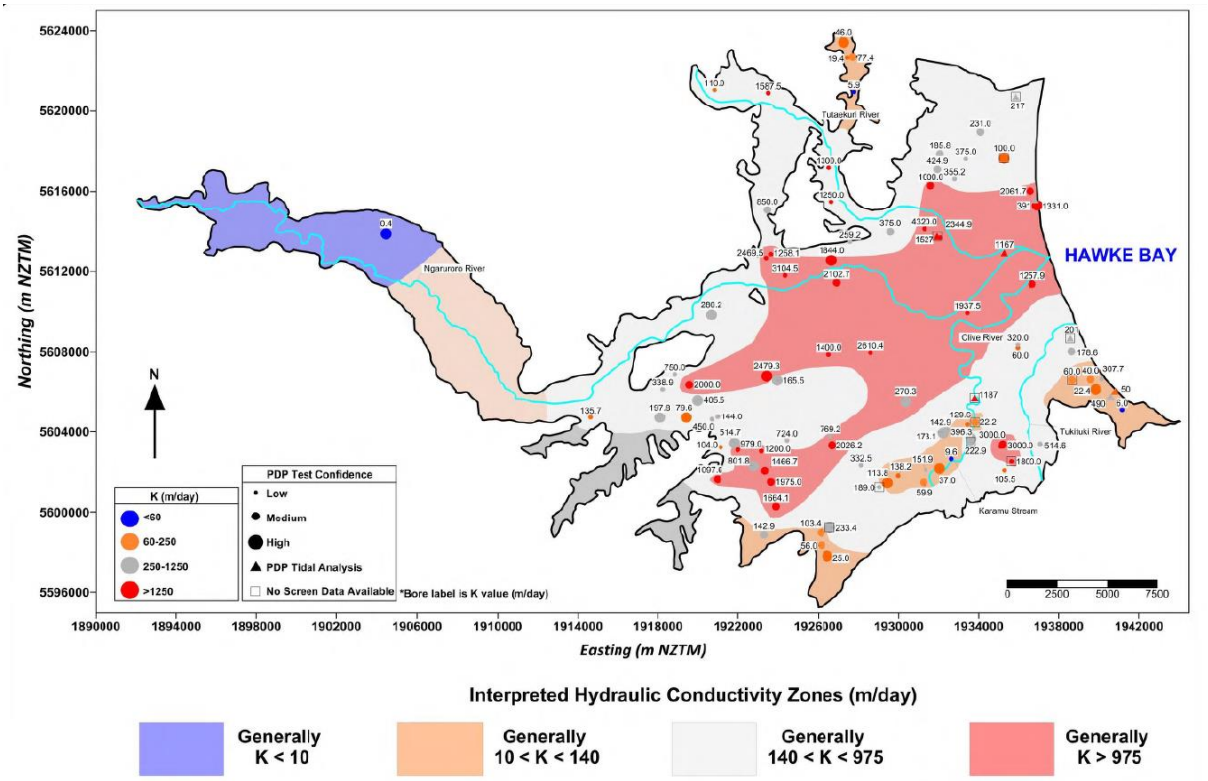

Figure 3-26: Interpreted aquifer hydraulic conductivity (after Perwick (2014)).

3.7 Groundwater levels

3.7.1 Piezometric contours

Piezometric maps (groundwater level contour maps) are useful for understanding the pattern and direction of groundwater flow. Because of significant seasonal variability of groundwater levels (typically 2 m), the presence of long-term trends (up to 2 m decline over 10 to 20 years) and short

term effects (e.g. due to pumping), piezometric contour maps for the Heretaunga Plains should be based on surveys undertaken within a short period (i.e. no more than one day).

Dravid & Brown (1997) provided piezometric contour maps for summer 1995 and an "average winter, 1974-77". However, these maps don't include all areas of the Heretaunga Aquifer System (for example, Upper Ngaruroro aquifers are excluded). Also, newer data is available that could potentially be used to produce a more recent piezometric map.

Piezometric survey data

Piezometric surveys have been undertaken several times in the Heretaunga Plains Aquifer system area.

Available data includes:

- January 1974;
- August 1974;
- September 1976;
- February 1995;
- May 2014;
- December 2014.

Survey data from 1974 and 1976 is difficult to interpret, due to uncertainties about exact locations and elevations at measuring points.

The best spatial coverage and data quality is available from the February 1995 survey. While the method for measuring elevation is not clearly established, the survey appears to have been completed using a GPS device with resolution presumably of ±1 cm (based on tabulated data available). The survey was undertaken at the end of February, which is near the end of the irrigation season. Dravid & Brown (1997) noted that this survey was undertaken after a prolonged drought. However, the monitoring data demonstrate recovery of groundwater levels in January, which is most likely due to reduction of groundwater pumping (see Figure 3-29).

Survey data from 2014 are more sparse. Only about 100 bores were surveyed in 2014, compared to 300 bores during the 1995 survey. Furthermore, bores were not surveyed in the Napier area during 2014, which is problematic as there are large abstractions for Napier's public water supply that would have created localised cones of depression (analysis of 1995 contours identified this). In addition, the 2014 survey appears to contain erroneous data (e.g. very low water levels, possibly affected by localised pumping), but does include survey data from the peripheral valleys around Heretaunga plains.

Elevation data of the 2014 survey is based on LiDAR, which may introduce significant error to calculations of groundwater elevations. Recorded groundwater elevations in December 2014 appear to be 1.5 m lower than those recorded in February 1995, despite the 2014 survey being undertaken at the beginning of the irrigation season. A review of independent monitoring data indicates that the February 1995 water levels were 1 m higher than December 2014 levels, and during February 2015 water level declined by a further 0.5 m (Figure 3-28). The 2014-2015 irrigation season appears to have been wetter than during the 1995 survey period. However, there was more groundwater pumping during the more recent survey (Figure 3-29), which may explain lower groundwater levels at the end

of the 2014-2015 irrigation season. The above shows the importance of timing with piezometric data collection.

In general, there is uncertainty related to data gathered during all of these surveys. However, the available data allowed for development of a piezometric map that was useful to understand the pattern of groundwater flow, even though the map may only represent a specific time (c.f. "typical" conditions) and is subject to uncertainty.

Data collected during the February 1995 survey appears to have the best coverage and accuracy; therefore, it was used as a basis for the piezometric map. The 1995 data was supplemented by observations recorded during December 2014 in the areas outside of the Heretaunga Plains. In addition, data was also supplemented by water levels in the Ngaruroro River upstream of Maraekakaho. This was necessary due to lack of groundwater level data in this area. River water level can be a good approximation of aquifer level, especially in this case where the aquifer is relatively small and the river is large, with a braided river character suggesting good connection between the river and aquifer. This map is considered to provide the best possible representation of groundwater flow pattern in the Heretaunga Plains.

Because data recorded during 2014 indicated lower groundwater levels than in 1995, the piezometric contour map doesn't identify the lowest ever recorded water levels, which may be perhaps 1.5 m lower.

Delineation of Contours

The data has been contoured using an automated contouring algorithm. It is challenging to generate piezometric contours in the upper Ngaruroro River valley, as groundwater level in the terraces appears to be partially disconnected from the valley floor aquifer. The contouring was undertaken using the Kernel Smoothing with Barriers method (available in ArcMap Geostatistical Analyst), which allows for contouring with barriers (Figure 3-30).

Flow field in Heretaunga Aquifer system

Main Aquifer

The piezometric results reveal that groundwater flow direction in the main Heretaunga aquifer is predominantly from the recharge area in the unconfined aquifer zone in the west, to the coast in the east. Gradients are very steep near the losing section of the Ngaruroro River between Fernhill and Roys Hill (indicating river and rainfall recharge), but then becomes much less steep towards the coast. The map also reveals flow of groundwater towards the north in the Napier area. The conceptual understanding is that the aquifer does not continue to the north past Napier Hill, and the only possible outflow that in this area is groundwater pumping; mostly from Napier City Council's public water supply bores (pumping is discussed further in Section 3.9).

Groundwater contours near the Tukituki River mouth suggest a preferential pathway that allows draining of the aquifer to the sea in this area. This drainage could be explained by the Tukituki gravels that were identified by the Leapfrog geological model (Lee et al., 2014, 2017), as there are no significant spring discharges to surface water. Some of this drainage may also be explained by the Hastings District Council (HDC) public water supply bores near Brookvale that may have contributed to lower water levels in this area.

Near the southern boundary of the Heretaunga Plains near Pakipaki, groundwater appears to flow in a southerly direction, which could be caused by additional drainage of the aquifer in this area, perhaps

a consequence of groundwater pumping, or by unknown hydrogeological structure, such as palaeochannel.

A notable feature of the Heretaunga Plains flow field is the absence of visible impacts from spring discharges on groundwater contours. Usually, where springs or spring-fed streams are present, groundwater contours appear to bend as groundwater is intercepted by the springs. However, this is not apparent in the piezometric contour map (Figure 3-30), even for large springs flowing at several hundred litres per second. This indicates very high transmissivity of the aquifer.

Upper Ngaruroro

Piezometric contours are also useful to visualise the groundwater flow pattern in the Ngaruroro river valley between Whanawhana and Maraekakaho. The contours show a discontinuity in groundwater levels between Kikowhero Terrace and the Ngaruroro floodplains, where water levels are up to 40 m higher in the terrace aquifer. The water level also appears to be disconnected in the Pigsty terrace aquifer, where groundwater is perched up to 50 m above the floodplain aquifer.

Moteo Valley

Groundwater gradients in the Moteo valley are much steeper than in the main Heretaunga aquifer, and the groundwater flow direction is from the Tutaekuri valley in the north towards the Ngaruroro River in the south.

Artesian conditions

Flowing artesian conditions, where groundwater head is higher than ground level occur in most of the eastern part of the Heretaunga Aquifer.

The exact boundary between artesian and unconfined conditions is dependent on groundwater levels at any given time, because the groundwater level is subject to seasonal variability of 2 m or more.

The extent of flowing artesian conditions was estimated for winter 1976 and summer 2014 conditions (using piezometric and topographical data). The position of artesian conditions varies by several hundred metres between winter and the summer (Figure 3-27.) This variation may be even greater during more extreme conditions, such at the end of the 2013 summer.

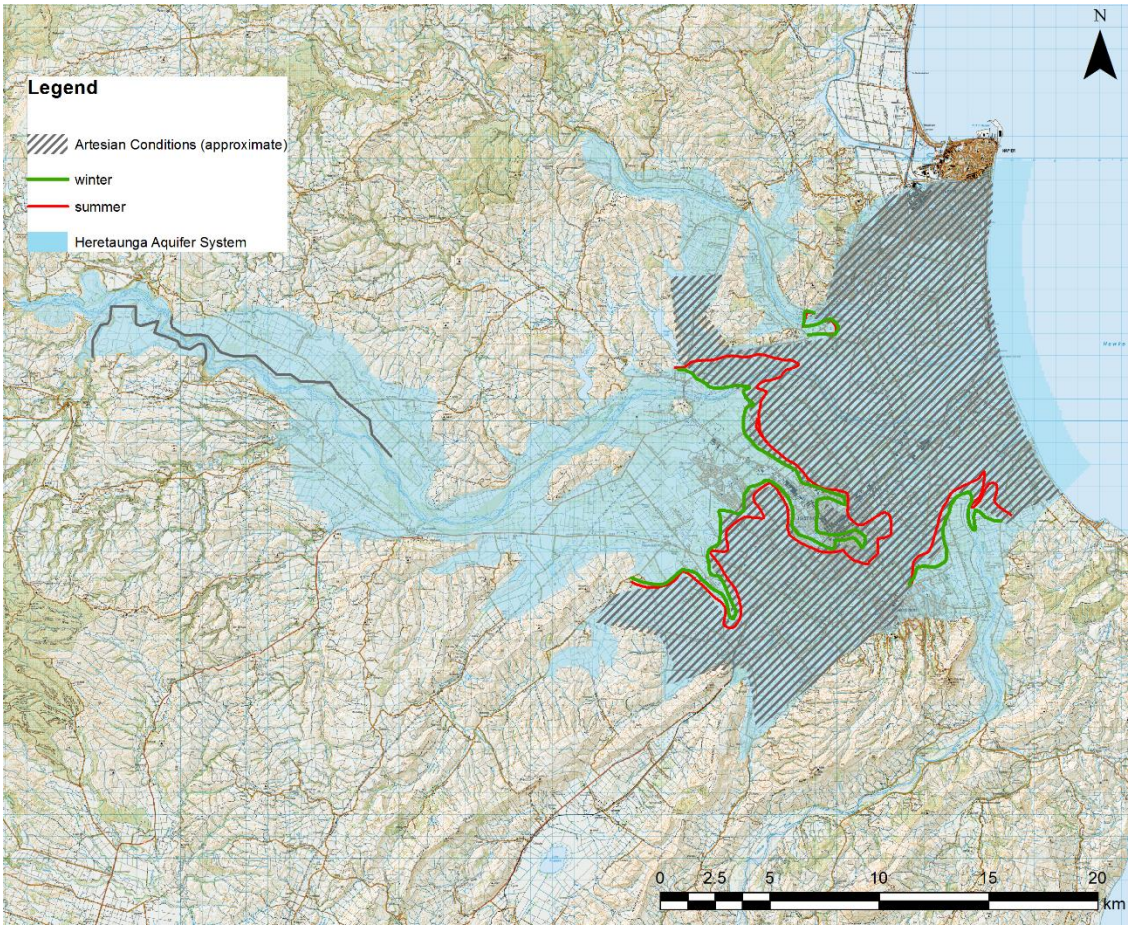

Figure 3-27: Flowing artesian conditions in the Heretaunga Aquifer.

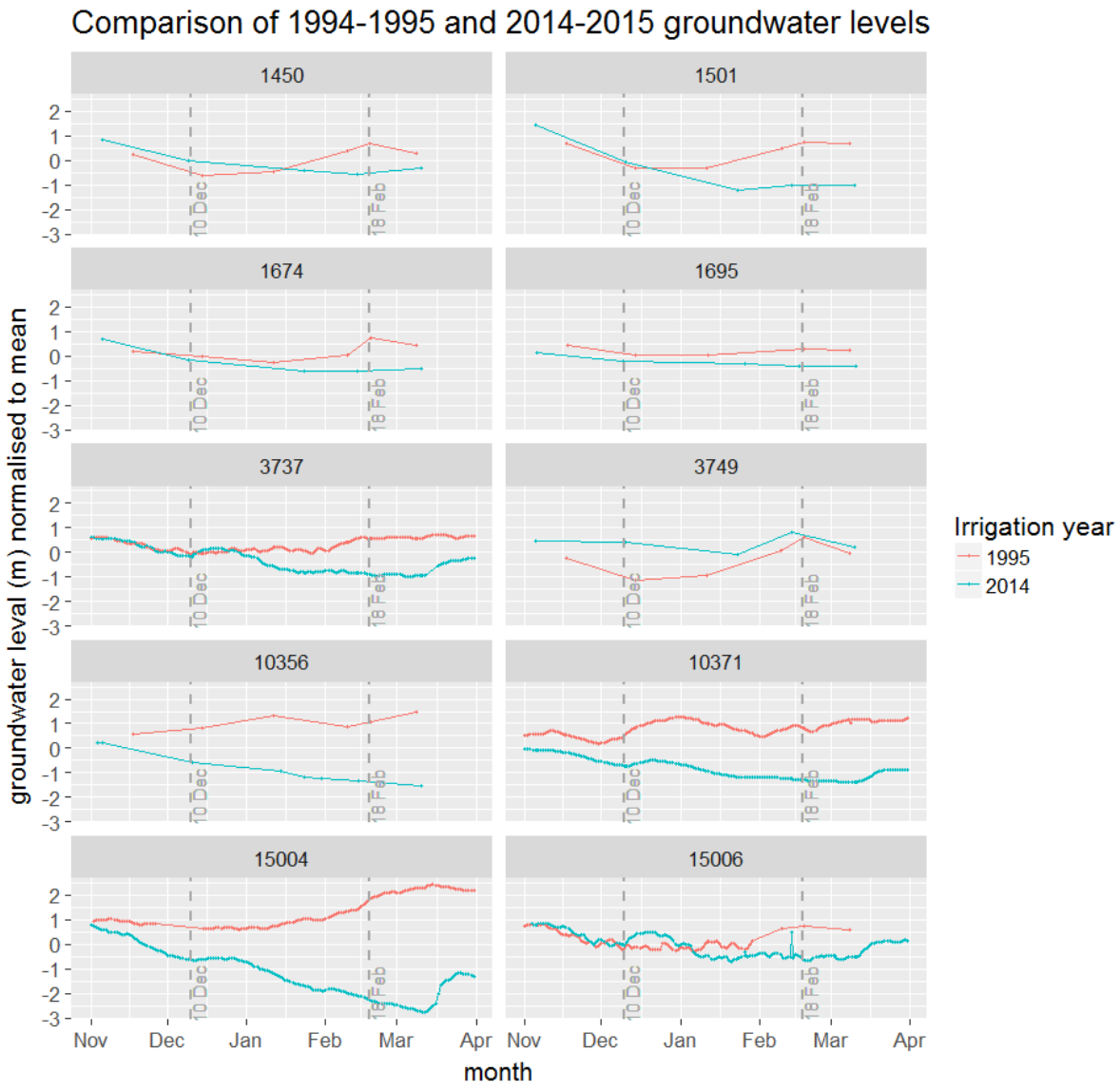

Figure 3-28: Comparison of groundwater levels between 1994-1995 and 2014-2015 irrigation seasons.

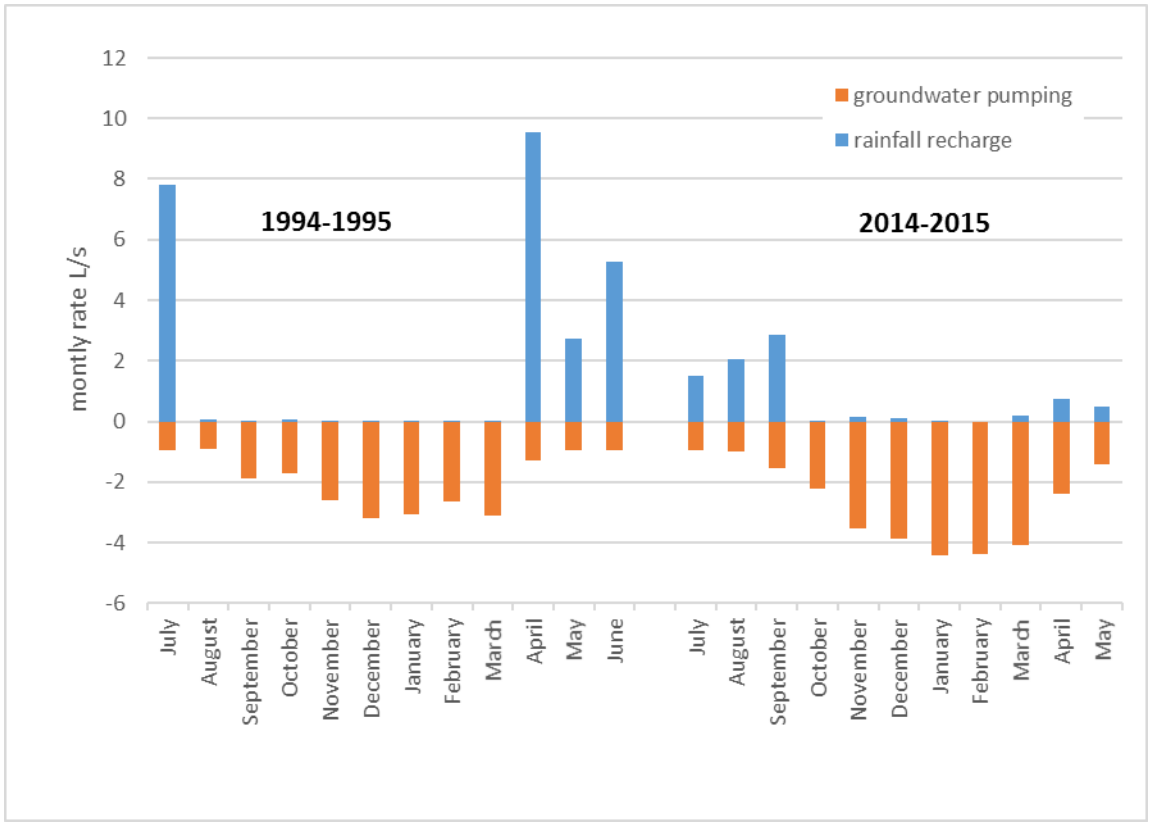

Figure 3-29: Comparison of monthly rates of land surface recharge and groundwater pumping between the 1994-1995 and 2014-2015 irrigation seasons.

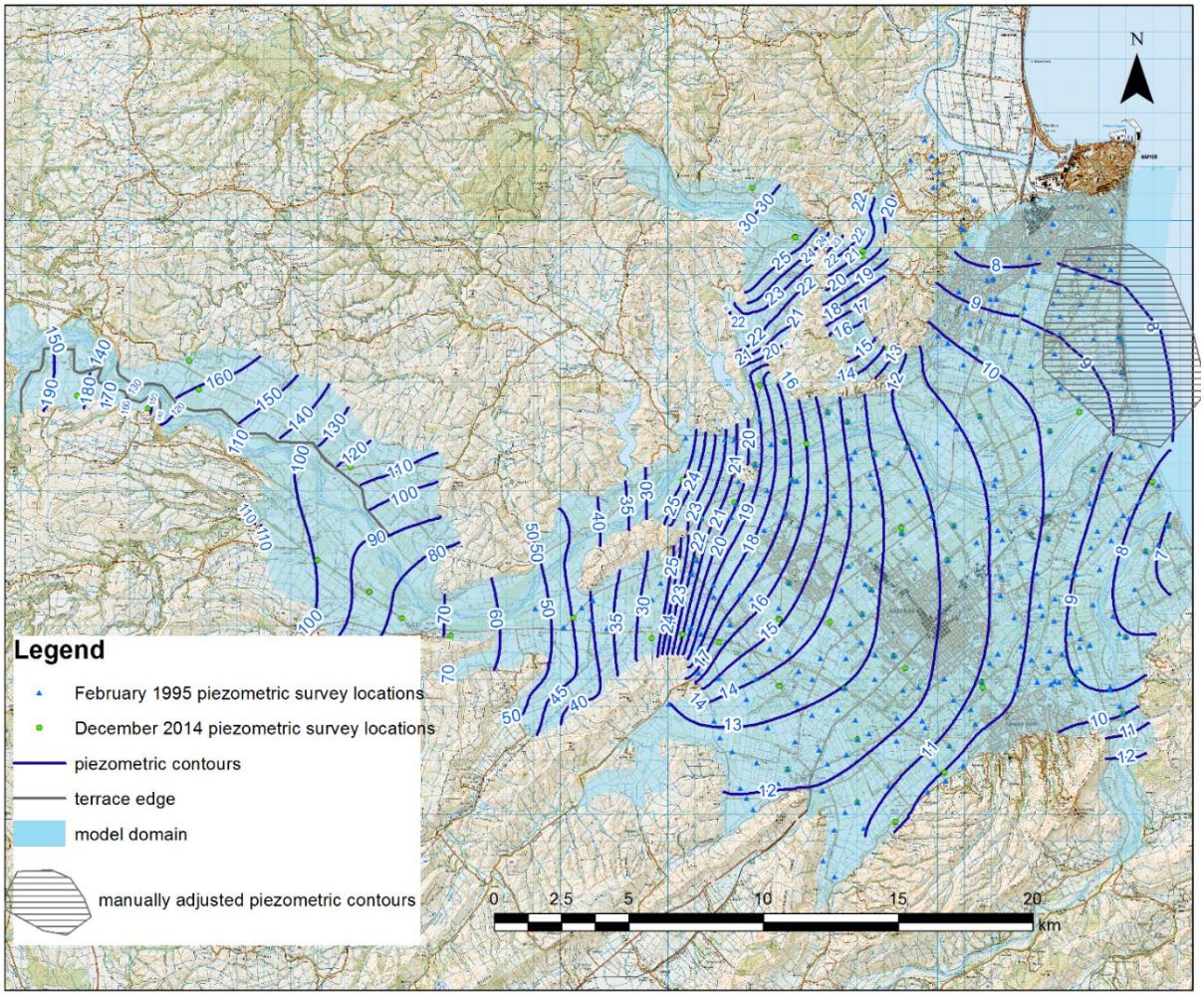

Figure 3-30: Piezometric map of the Heretaunga Aquifer system during summer. Contours are based on data recorded in February 1995 (Heretaunga Plains), December 2014 (Moteo Valley, Upper Ngaruroro Valley), and river elevation in the Upper Ngaruroro valley The blue outline represents the Heretaunga Aquifer System. Grey lines in Ngaruroro valley represent edges of terraces that create a barrier to groundwater flow.

3.7.2 Groundwater level changes

Groundwater level monitoring

Groundwater levels in the Heretaunga aquifer have been extensively monitored. For this study, 101 monitoring points (locations shown on Figure 3-31) with corresponding time series data sets were compiled. The data was derived mainly from the State of the Environment (SoE) monitoring network maintained by HBRC (67 sites), along with compliance monitoring sites maintained by consent holders (21 sites) and other sites. These time series data have variable coverage, monitoring frequency and quality. Some sites have continuous automated recorder data since before 1980, while other sites may only have a few years of data. A graphic representation of data availability is shown in Figure 3-31 and more details are provided in Figure 3-33. Prior to 1990, data availability is limited to five wells, while the number of monitoring wells increased to greater than 30 in 1991 and continued to expand in subsequent years (Figure 3-32). Only 50 wells have a data record for 10 years or longer, while 26 wells have records exceeding 20 years, mostly starting after 1995.

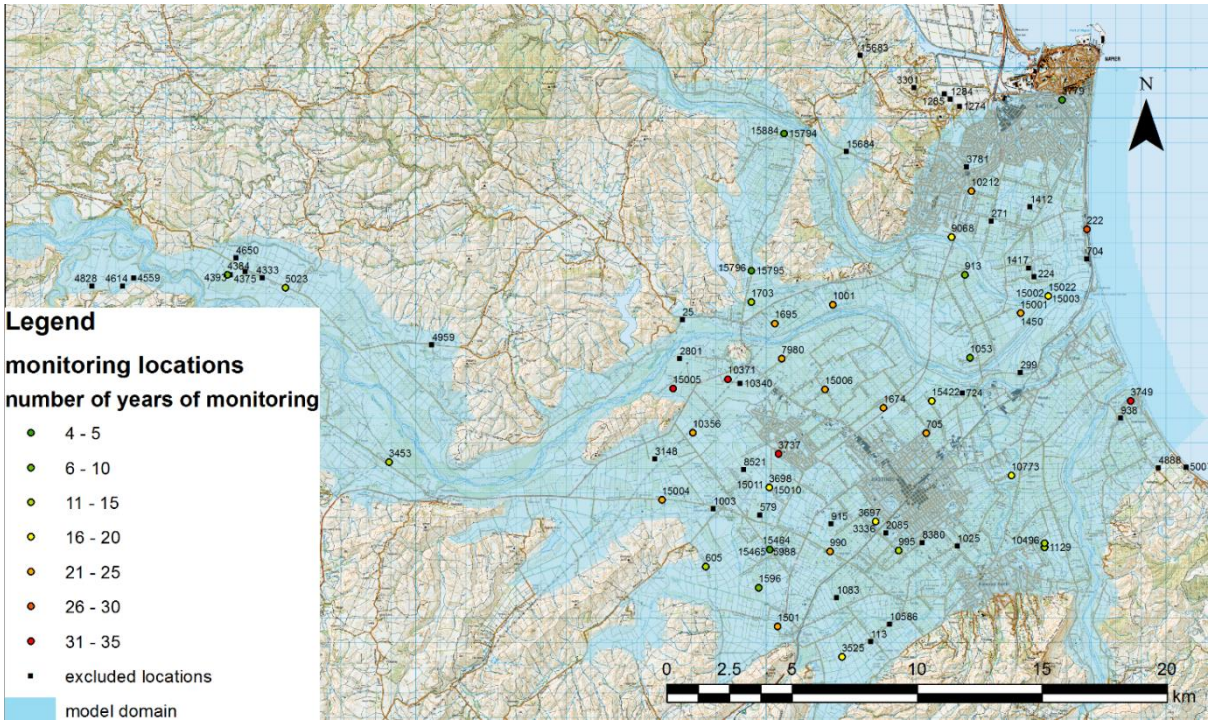

Figure 3-31: Groundwater level monitoring locations and available data.

Selection of data for model calibration:

Some of the data was removed from analysis in this study, including the following:

- Sites that have fallen outside of the final domain of the study, or were in an aquifer considered to be disconnected from the Heretaunga Aquifer System;
- Locations where data was available from various depths (e.g. nested piezometers) and appears to be closely correlated, so using any more than one of the records was considered redundant;
- Sites with poor data quality that were located near sites with better data quality;
- Sites that had insufficient data density or quality.

Consequently, 43 groundwater monitoring sites were selected for use in this study and model calibration.

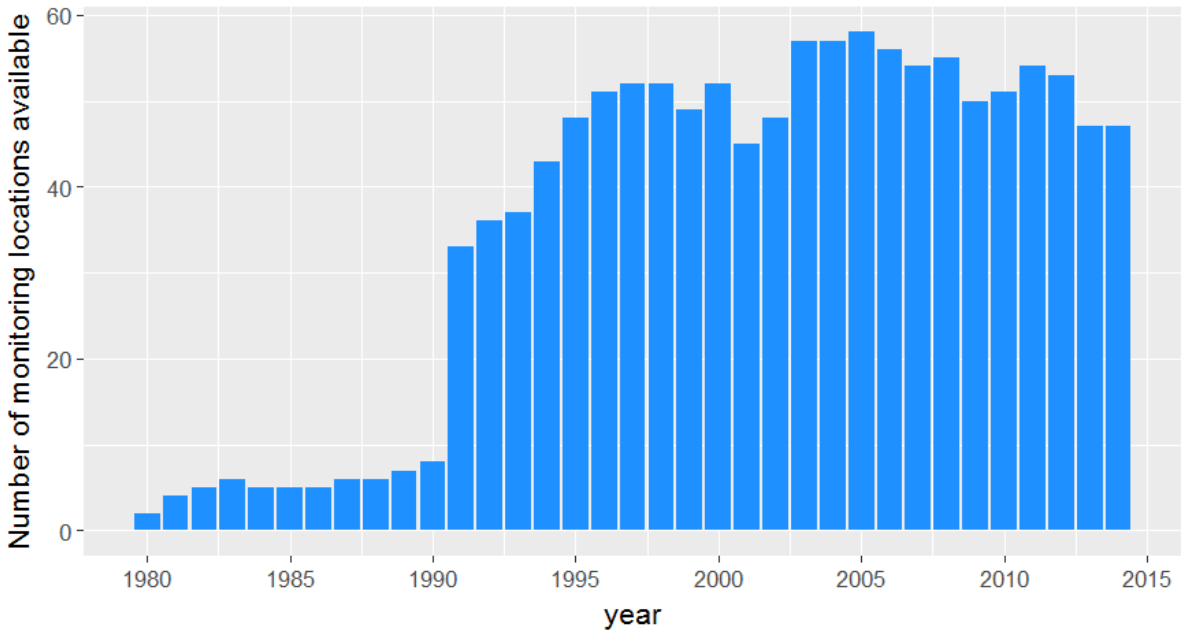

Figure 3-32: Availability of HBRC groundwater monitoring locations.

Figure 3-33: Annual availability of groundwater level monitoring data.

Seasonal groundwater level variations and long-term trends

Groundwater levels in the Heretaunga plains show a strong seasonality, with groundwater level changes of approximately 2 m between summer and winter. Some of the monitoring locations also show long-term water level changes (e.g. 10371 shows a decline, 3749 shows a rising trend, and the others show no sustained trend). Figure 3-34 shows a section of available data.

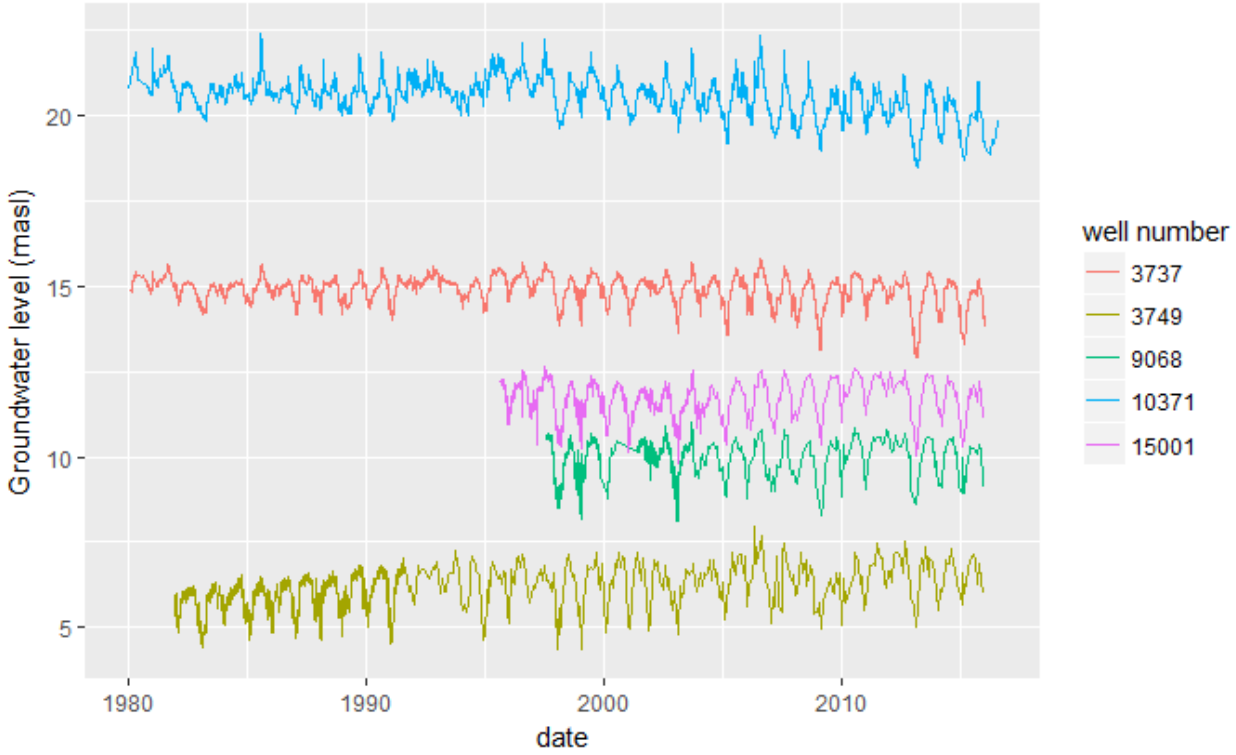

Figure 3-34: Selected long-term groundwater monitoring records.

The data has recently been analysed by Harper (2015), who identified statistically significant trends since 1994 for localised bores in the unconfined aquifer area, near the Ngaruroro River losing reach (Figure 3-35). The maximum trend detected was -0.1 m/year in one location, which is equivalent to a 2 m decline over 20 years, and smaller declining trends in other locations. Over the majority of the Heretaunga Plains, statistically significant trends were not detected. The longest continuous record, since 1968, is available for well 10371 near Fernhill and indicates an average decline of 3 cm/year, which is equivalent to 1.4 metres since 1968 (Figure 3-36).

Harper (2015) also analysed changes to seasonality over time, and concluded that for most wells, the amplitude between February and August water levels has increased by approximately 0.3 m to 0.7 m over 20 years. Harper (2015) considered that observed declining groundwater levels and increasing seasonal amplitude is most likely due to changes in groundwater pumping. This interpretation is largely based on a premise that allocated groundwater abstraction has increased significantly over the years. Groundwater pumping will be further discussed in Section 3.9.

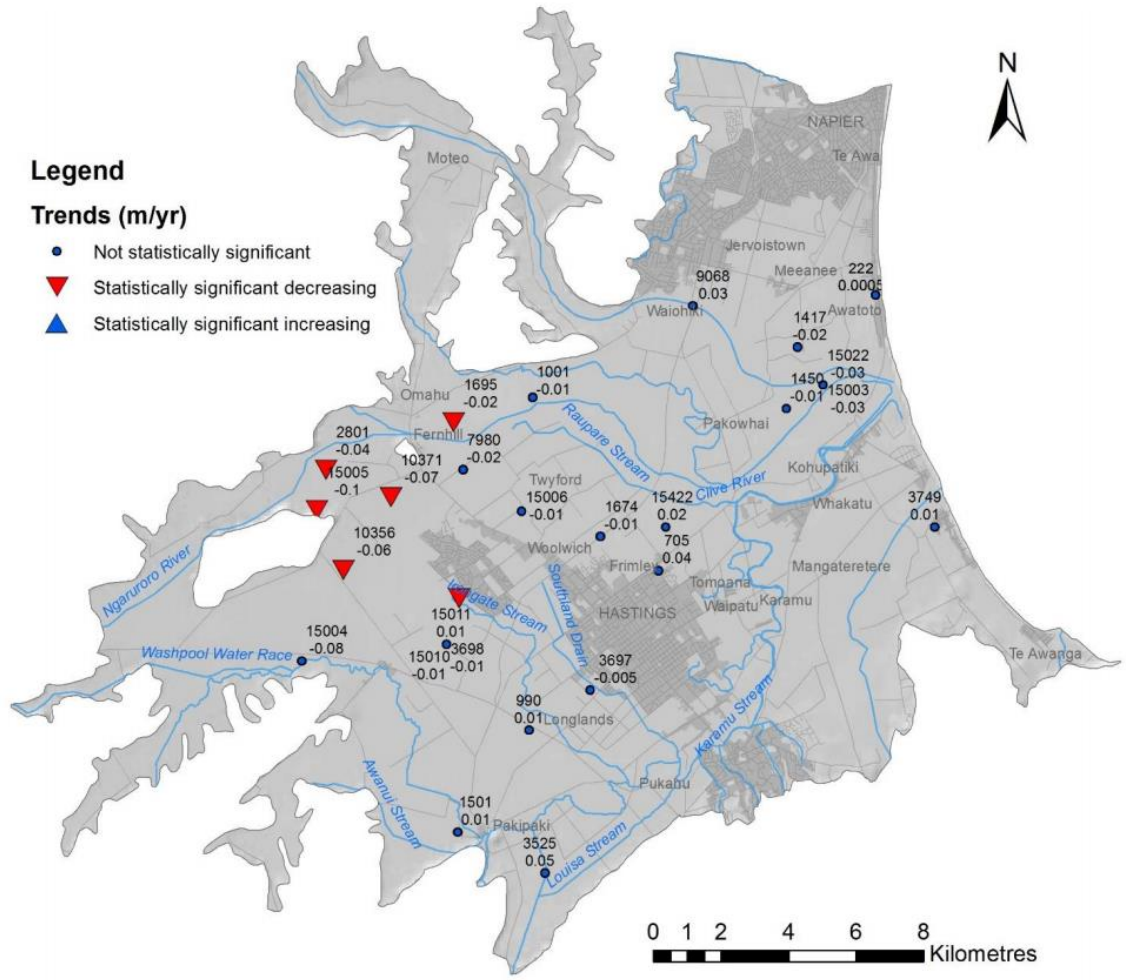

Figure 3-35: Groundwater level trends in Heretaunga Aquifer (after Harper, 2015).

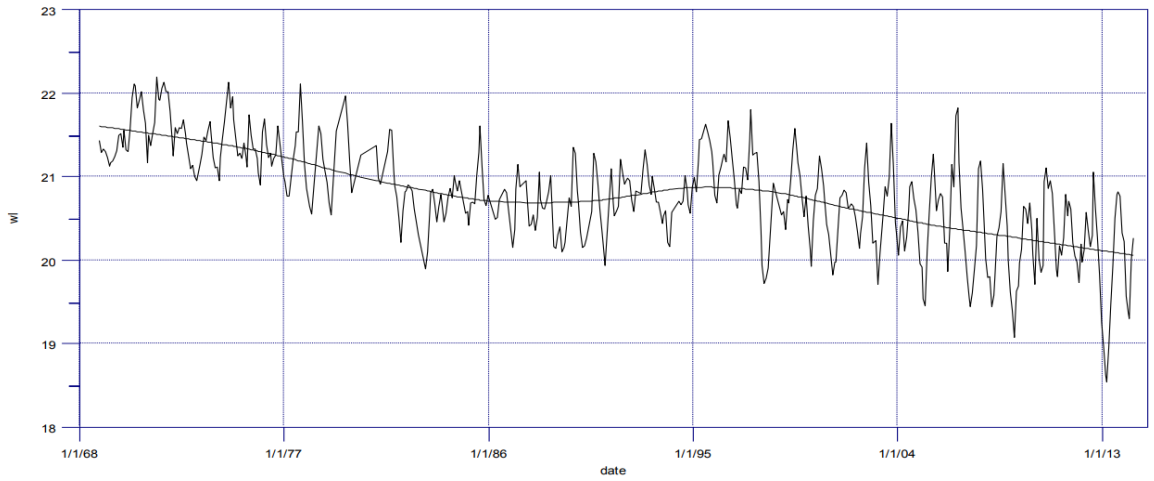

Figure 3-36: Longest groundwater level monitoring record at well 10371 at Fernhill (after Harper, 2015).
The y-axis is groundwater elevation in metres asl.

Vertical head gradients

The understanding of groundwater flow patterns in the Heretaunga aquifer would not be complete without analysis of vertical head distribution. Unfortunately, most of the groundwater level data for identifying piezometric contours is from relatively shallow depths, with limited data from greater depths. There are a few locations available where water levels are available from different depths (Figure 3-37) and vertical head differences were calculated for those sites.

Results indicated negative vertical gradients (lower head at deeper depths) near the recharge area of the aquifer (unconfined aquifer east of Hastings, and near Havelock North). This phenomenon is typically expected in recharge areas where groundwater moves downwards from the recharge source at the surface. A positive head gradient was observed in the Awatoto bore located near the coast, which indicates greater heads at depths and upwards groundwater movement, and is typical at locations where discharge of groundwater occurs to the surface (e.g. through springs).

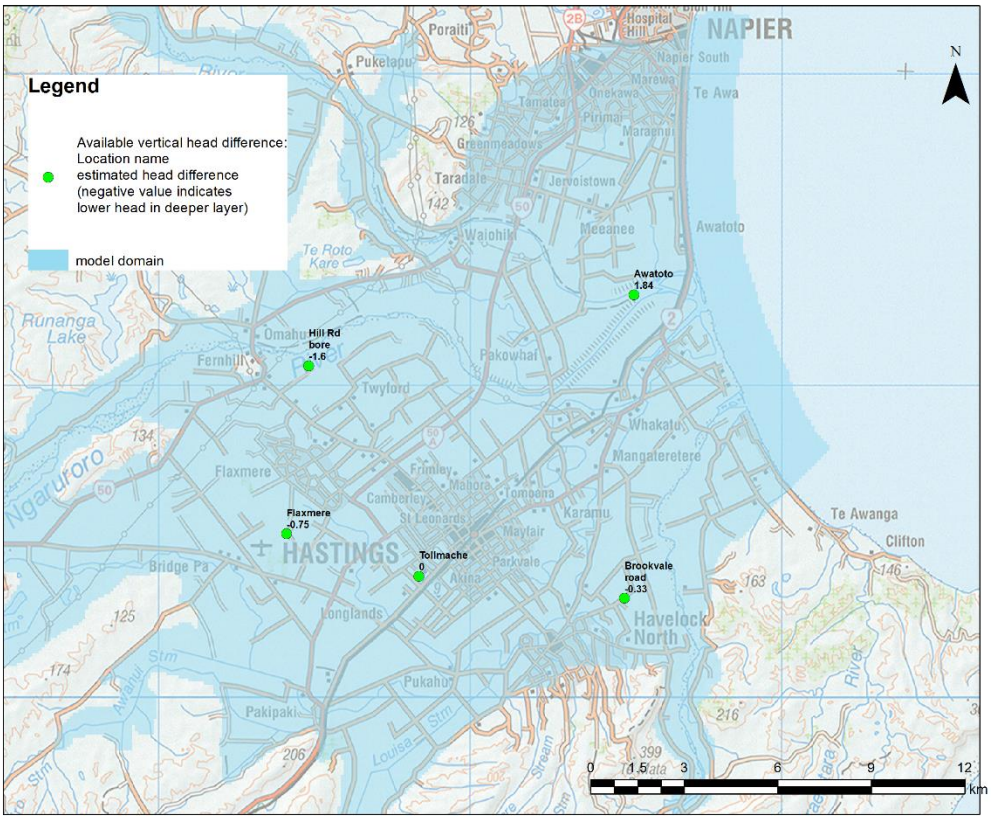

Figure 3-37: Locations of vertical head difference data available.

Groundwater level changes following river flooding events

A review of monitoring data revealed that groundwater levels in some wells respond to flooding events that occur in the Ngaruroro and Tutaekuri Rivers. These observations can be useful, as they may be used in model calibration.

The response can only be observed when automatic recorder data is available, as manual records do not have sufficient frequency. Most of the continuous data was available for the Ngaruroro River.

The analysis has focused on responses observed in bores located near the Ngaruroro River, where recorder data was available. A number of groundwater level records have been reviewed and compared with river stage recorded at Fernhill. Locations of these bores are shown on Figure 3-38.

The data has been analysed for the following high flow events: 3/07/1997, 17/09/1998, 24/05/2001, 21/06/2015 and 20/09/2015. Analysis of multiple periods was necessary to maximise the number of monitoring locations per event, as automatic recording was discontinued in some locations, whilst new locations became available more recently. Rainfall and soil moisture deficit based on NIWA's Virtual Climate Network (VCN) data for nearby locations was also included in the review, to verify if direct rainfall recharge was likely to occur at these times. To indicate this, if the soil moisture deficit was negative, direct recharge of the aquifer was considered unlikely and any response in groundwater was attributed to river levels. Summary of this analysis is presented in Table 3-5, while detailed analysis charts are presented in Figure 3-39 and Figure 3-40.

Analysis shows that groundwater levels near the Ngaruroro River respond to flooding events. As expected, the largest response was observed in bores closest to the river (i.e. bores 15005, 2801, 16360 and 16361, located less than 1,000 m from the river). However, some response appears to be present at significant distance from the river. For example, in bore 10371 (1,600 m from the river), and even further away in bores 15004 and 3737 (located more than 4 km from the river). In these distant bores the response is weaker, and there is less certainty that this response may be exclusively attributed to the river flooding. The response in bore 15004 is very variable between different flood events, which suggests that the aquifer response may be caused by factors other than Ngaruroro flood events. For example, the groundwater response in bore 15004 might be a consequence of an event in Karewarewa Stream, but this cannot be determined due to insufficient data.

For the multilevel bore 16300, 16360 and 16361, the shallower levels (down to 65 m depth) showed a uniform response, whilst the deeper installation (98 m depth) showed a subdued response, suggesting some degree of separation between the deeper aquifer and the shallow aquifer system.

Table 3-5: Groundwater response to Ngaruroro flooding, summary table. Responses have been converted to unit responses via division of the groundwater level response by Ngaruroro River water level change, to allow comparison between events of different magnitude.

			Groundwater level change (m) per 1m Ngaruroro change per flooding event:						
Bore id	Bore depth	Distance from the Ngaruroro River (m)	3/07/1997	17/09/1998	21/05/2001	20/06/2015	20/09/2015	Median	Expected groundwater level change (m) per typical Ngaruroro stage change of 1.5 m
2801	7.9	360	0.59	0.41	0.30			0.35	0.53
3737	29.2	4300	0.13	0.02	0.06	0.03		0.03	0.05
15004	25.0	4600	0.89	0.01	0.03			0.02	0.02
15005	12.9	650	0.15	0.46	0.36			0.41	0.62
10371	13.4	1600	0.38		0.03	0.06		0.05	0.07
16300	98.0	360				0.03	0.01	0.02	0.03
16360	65.3	360				0.16	0.37	0.26	0.39
16361	23.9	360				0.14	0.37	0.25	0.38

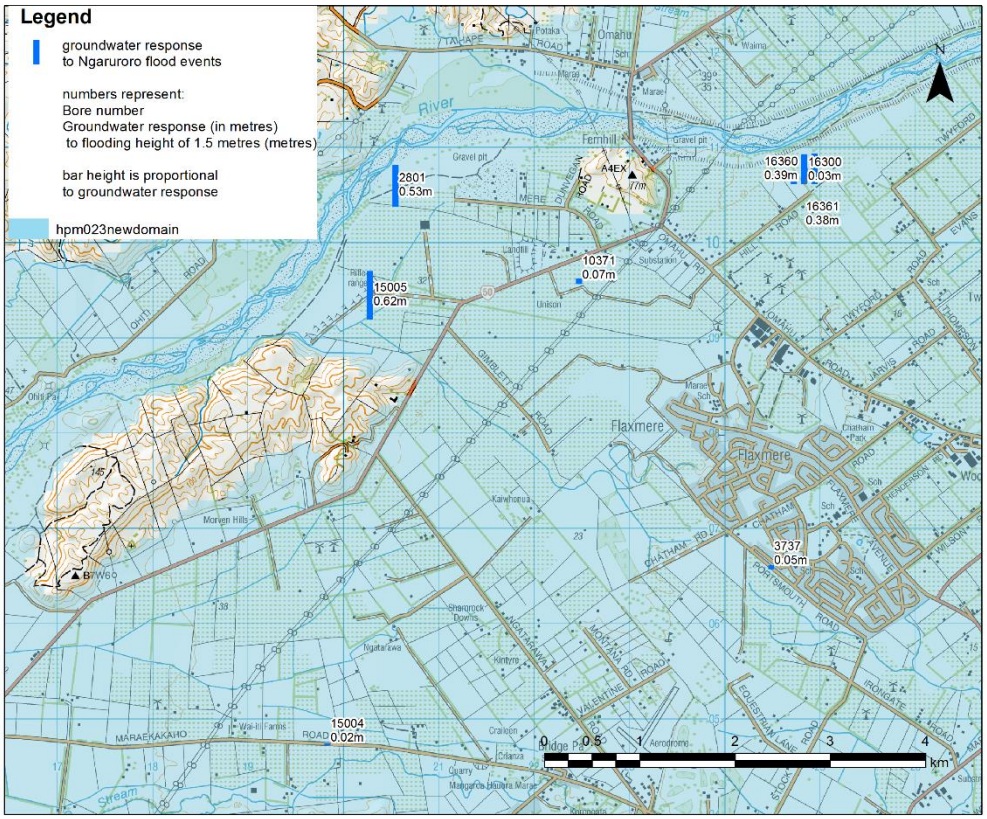

Figure 3-38: Ngaruroro flooding response analysis.

River stage, groundwater levels, rainfall	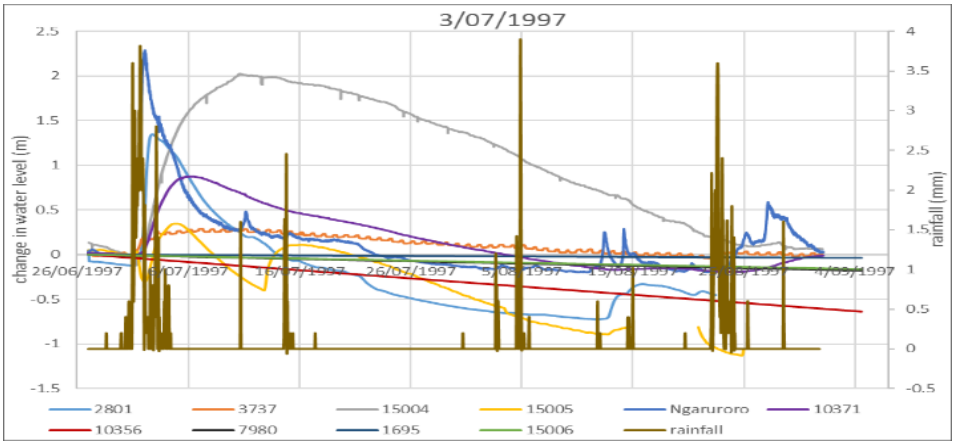
Soil moisture deficit	
River stage, groundwater levels, rainfall	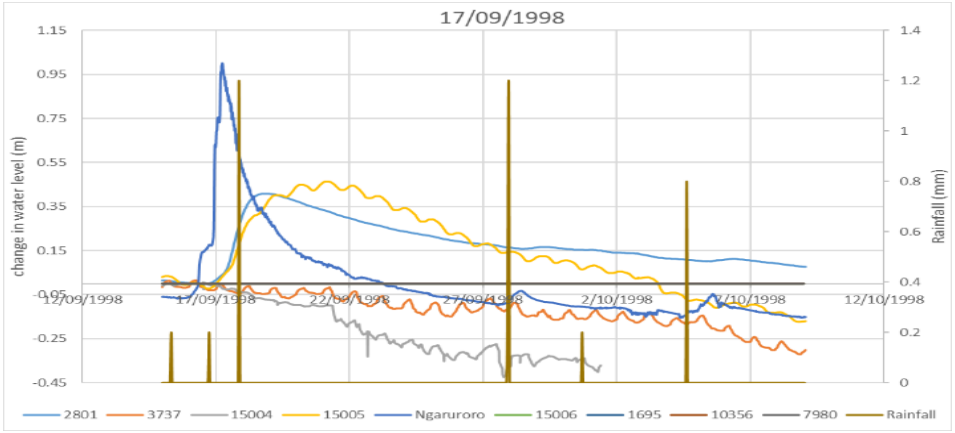
Soil moisture deficit	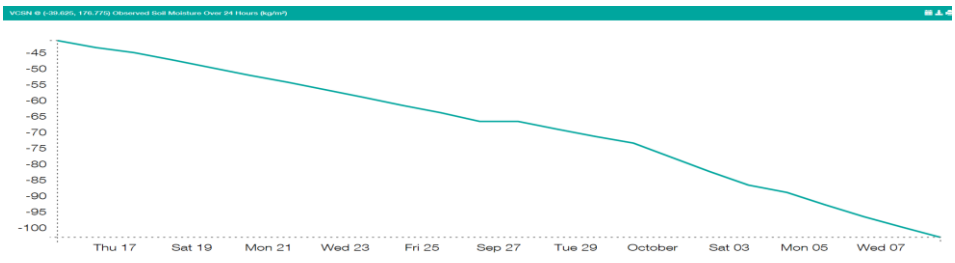

Figure 3-39: Groundwater level response to Ngaruroro flood events (part 1).

River stage, groundwater levels, rainfall	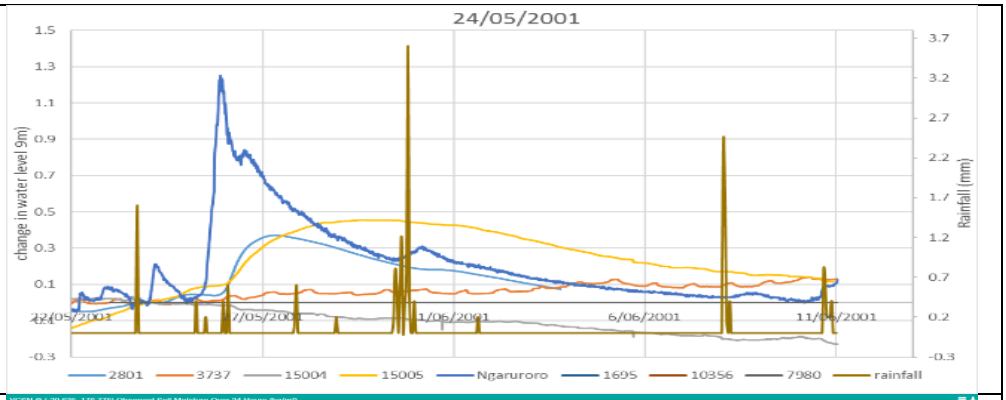
Soil moisture deficit	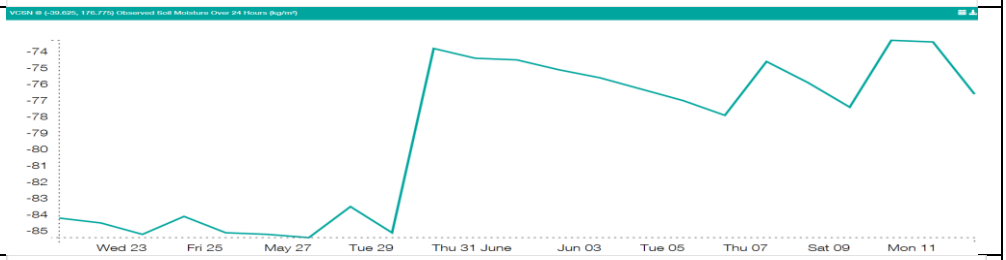
River stage, groundwater levels, rainfall	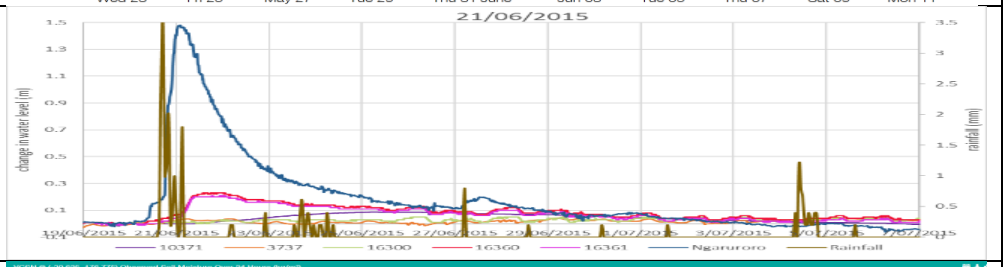
Soil moisture deficit	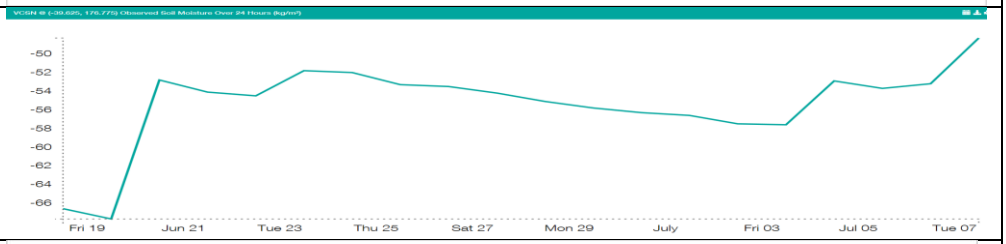
River stage, groundwater levels, rainfall	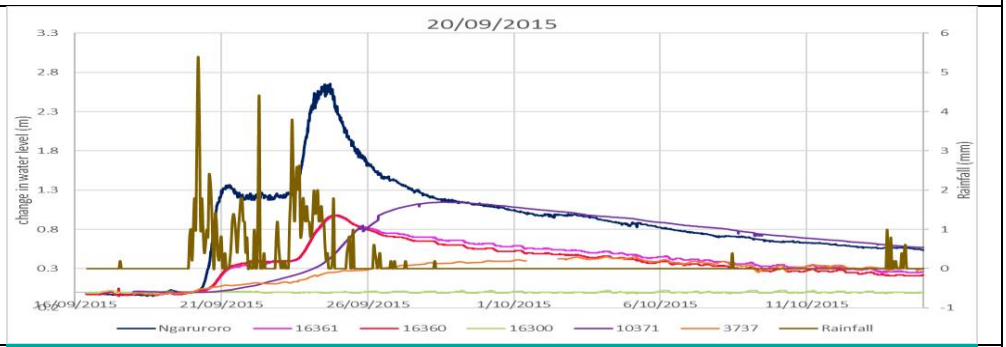
Soil moisture deficit	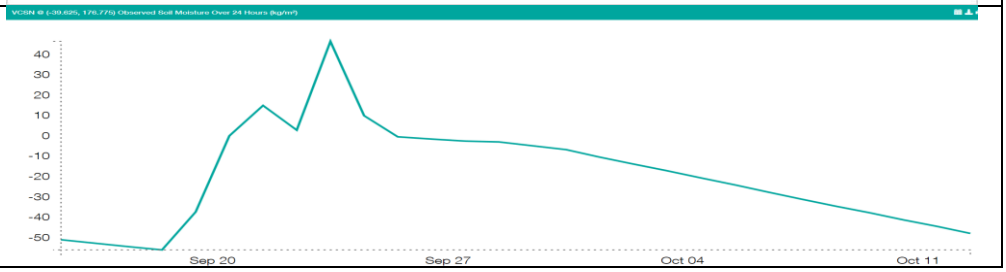

Figure 3-40: Groundwater level response to Ngaruroro flood events (part 2).

3.8 Land surface recharge

Rainfall recharge only occurs in the unconfined area of the aquifer (see Section 3.5.1). Recharge in the confined aquifer area is limited by the presence of impermeable marine sediments that form a confining layer, which is a physical barrier to recharge. Artesian conditions (see Section 3.7.1) also mean that groundwater within the aquifer is under pressure, forcing upward seepage of groundwater to the surface and preventing any recharge from penetrating the aquifer.

The amount of rainfall recharge to the aquifer is dependent on many factors, such as rainfall frequency and intensity, evaporation, soil properties and land cover. In the Heretaunga Plains, the presence or absence of irrigation can also be an important factor. When irrigation activities are considered along with rainfall inputs to groundwater, it is appropriate to refer to the combined input as land surface recharge.

Land surface recharge (LSR) was calculated for this study by Aqualinc Research Ltd (Rajanayaka & Fisk, 2016b), as part of their irrigation demand assessment for the Heretaunga Plains.

The LSR study has relied on the following data sets:

- Soil data based on the Fundamental Soils Layer (Landcare Research, 2000) (4 classes of soil);
- Daily Virtual Climate Network (VCN) climate data 1972-2015 for 22 stations;
- 10 crop types with different irrigation requirements;
- Irrigated area based on HBRC's consents database and land use surveys (1791 consents).

LSR (and irrigation demand) was calculated daily for each combination of the above variables, which resulted in 3,108 recharge daily time series.

The calculations were undertaken using Aqualinc's Irricalc daily soil water balance model, which is accepted and field verified both internationally and within New Zealand. The domain of the Aqualinc study included the entire Heretaunga Plains, despite recharge to the aquifer not occurring in the confined aquifer area. Recharge that was calculated over the confined aquifer does not enter the main aquifer system, but may be generating local runoff or recharging a shallow aquifer that flows to lowland streams. The spatial distribution of recharge is shown on Figure 3-41

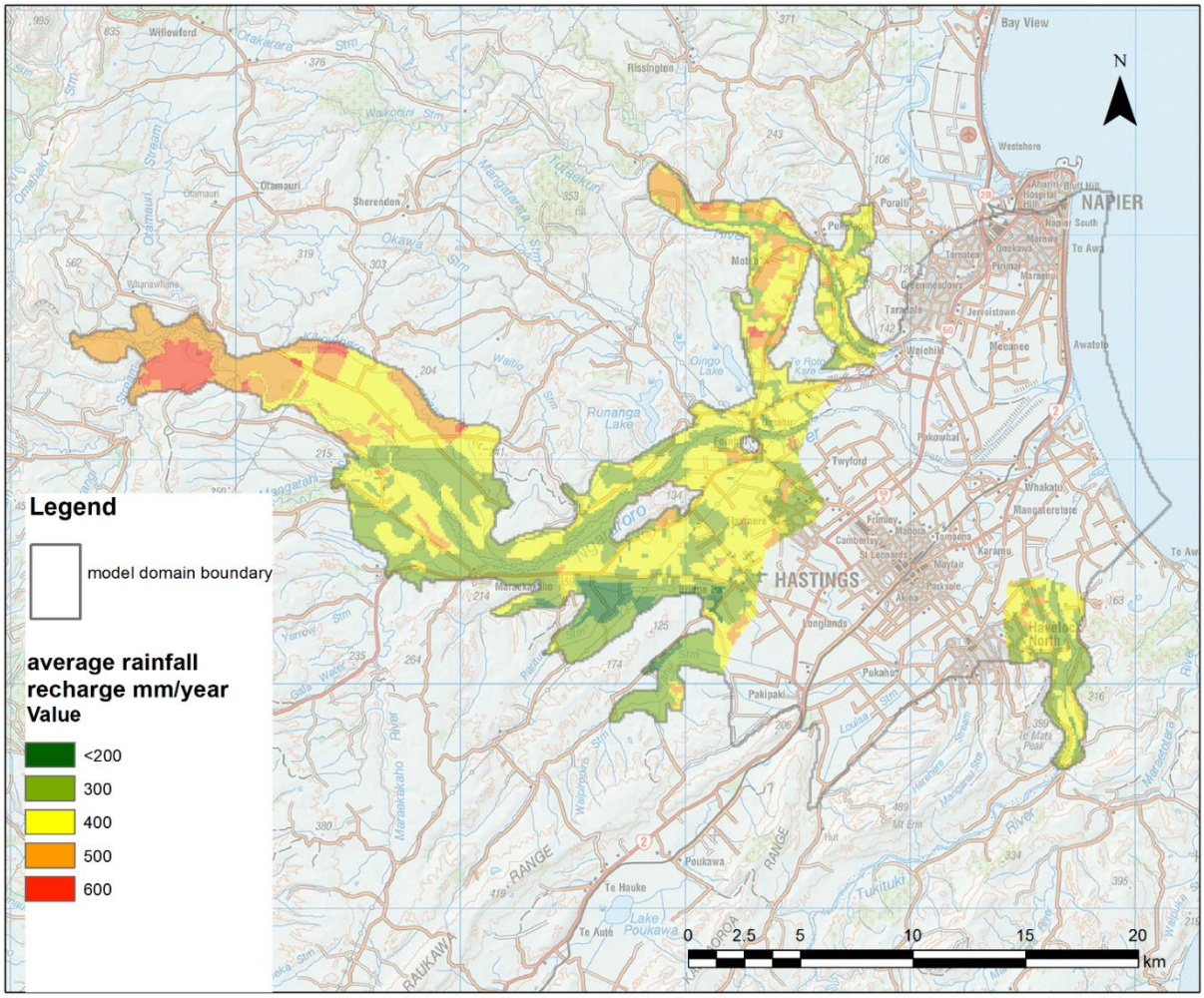

Figure 3-41: Distribution of average annual (2005-2015) land surface recharge (mm/year).

LSR is highly variable over time, with most of this recharge occurring in winter months, but much less LSR occurring during the summer period (see Figure 3-42 and Figure 3-43). There is also variation between years, depending on the rainfall. For example, there was a prolonged period with practically no LSR in summer 2012-2013, whilst in other years some LSR occurred in the summer (Figure 3-43).

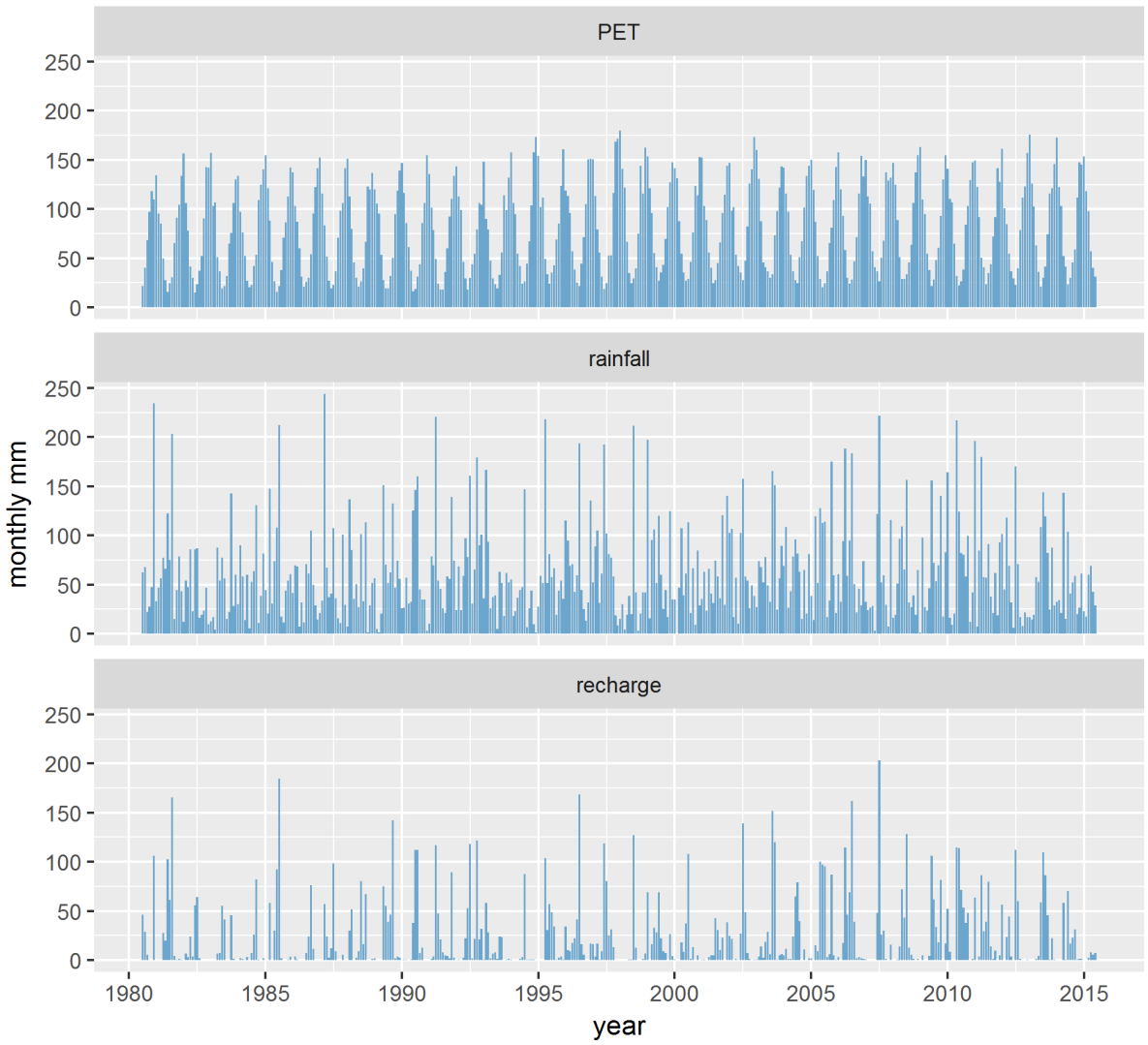

Figure 3-42: Monthly PET, rainfall and land surface recharge on the Heretaunga Plains.

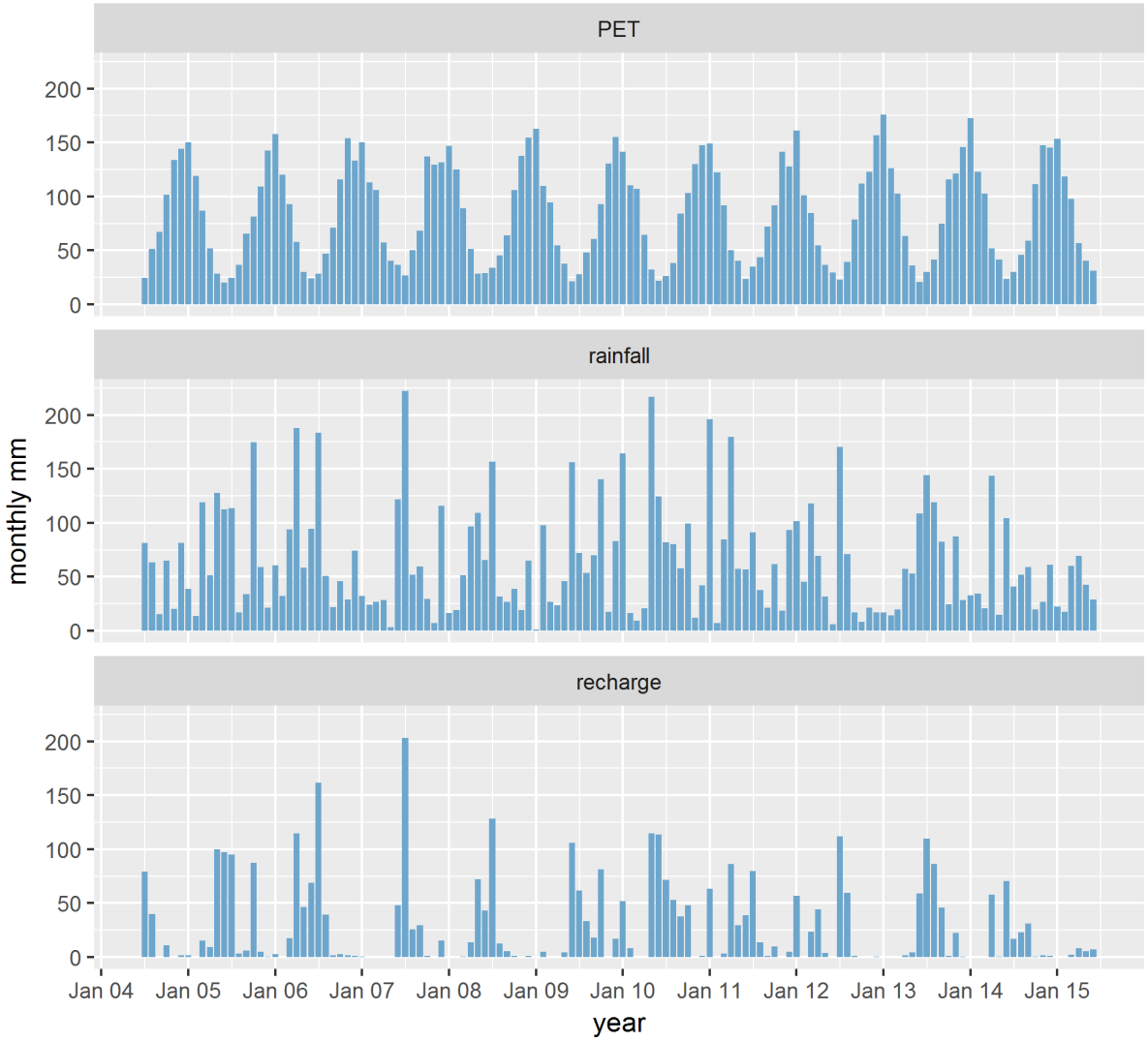

Figure 3-43: Monthly PET, rainfall and land surface recharge 2010-2015.

To provide context, recharge is presented with rainfall rate and Potential Evapotranspiration (PET) shown on Figure 3-42, Figure 3-43 and Figure 3-44. Recharge presented here is recharge as used in the model, but PET and rainfall area based on a VCN station in the central part of the recharge area.

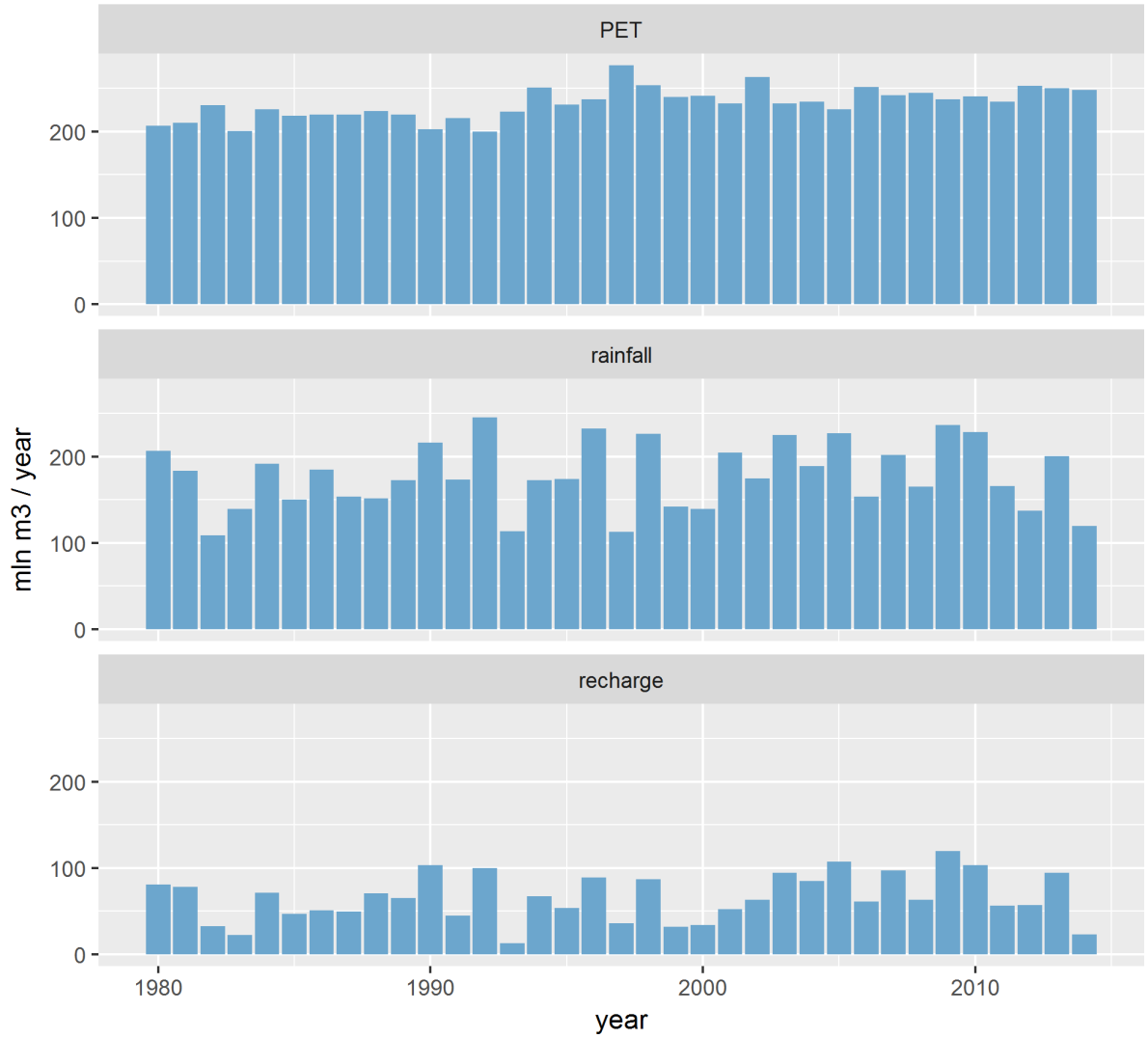

Figure 3-44: Cumulative yearly PET, rainfall and land surface recharge.

The average LSR between 2005 and 2015 is 330 mm/year, which is equivalent to 78.9 Mm^3/year.

Average rainfall in this period was 769 mm, which means that recharge is 42% of rainfall (on average).

However, this proportion is variable, for example in July 2007 rainfall was about 220 mm whilst recharge was calculated as 200 mm, about 90 % of rainfall. This is very high proportion of rainfall, and perhaps is unrealistically high.

The calculation of recharge rate is primarily based on the daily soil moisture balance calculation, and is dependent on number of factors, including rainfall, PET and quick flow run-off threshold (as documented in Rajanayaka & Fisk (2016a). For this study, as there was very limited data available to estimate the quickflow run-off threshold value, the authors have applied a generic approach and set the quickflow run-off threshold such that it provides about 5% quickflow contribution of the total recharge. This method is simple, and could possibly overestimate recharge especially in high rainfall events. However, model calibration using this recharge data gave a good match to observed groundwater levels at most times (as described in Section 0), including in the high rainfall event in July 2007, which tends to validate that high recharge event. Further work may be required in the future to investigate more complex recharge models and uncertainty issues during high rainfall events.

Total annual LSR is also variable, ranging between approximately 25 Mm^3/year and 120 Mm^3/year (Figure 3-44).

A notable feature of this dataset is that it shows an apparent increase in aquifer recharge since around the year 2000. This increase may have been caused by climatic variation, although an increased irrigated land area (which would result in more LSR when irrigation is present) is also a plausible explanation.

The estimated aquifer recharge is higher than recharge estimated by Dravid & Brown (1997), who estimated recharge between 7 and 22 M m^3/year. However, Dravid & Brown's estimate considered a much smaller LSR area of only 69 km^2 of the unconfined aquifer area, compared to 239 km^2 identified in this assessment. When Aqualinc's average LSR is applied to the 69 km^2 area considered by Dravid & Brown, the yearly total is 18 Mm^3/year, which is at the upper end of the range estimated by Dravid & Brown, which suggests the two estimated LSR are similar.

The largest difference between these estimates seems to be a consequence of the larger recharge area in the present study, which includes the upper Ngaruroro valley, Moteo valley, and the Tukituki area (see Figure 3-45). These areas contribute a significant portion of LSR to the aquifer. Figure 3-45 shows that most LSR occurs in the unconfined aquifer and the upper Ngaruroro valley (each 30 Mm^3/year). However, the inclusion of areas outside the unconfined area in this study is justified, as these areas are underlain by hydraulically connected unconsolidated aquifers.

Dravid & Brown's (1997) analysis was much more limited in terms of the numbers of soil, crop and climate classes considered. The Aqualinc methodology is internationally and nationally recognised, so the Aqualinc estimate is likely to be more representative of LSR for the Heretaunga Plains.

Losing rivers contribute approximately 185 Mm^3 of water per year to the aquifer, so the estimated average LSR of 79 Mm^3/year is a relatively smaller proportion of total recharge.

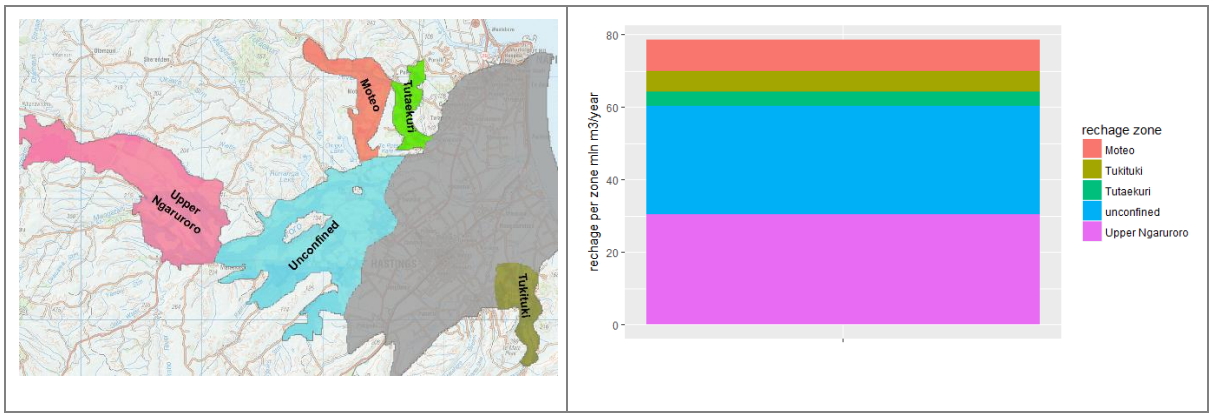

Figure 3-45: Recharge contribution from different recharge zones. There is no recharge to the confined zone (grey area)

3.9 Groundwater pumping

3.9.1 General considerations

Groundwater pumping is a significant component of the groundwater budget for the Heretaunga Aquifer System. Groundwater abstraction is mainly used for public water supply, industrial and irrigation uses, with smaller volumes of water abstracted for frost protection, stock water, and for domestic purposes.

A major review of metered pumping data was undertaken for the purpose of model development. Numerous problems were encountered with retrieving this data, including issues related to data storage, availability and quality.

3.9.2 Data sources

A variety of sources were used to obtain data on pumping rates (Table 3-6).

Abstraction for irrigation is a significant part of overall groundwater use in the Heretaunga Plains. Irrigation data used in modelling is based on the irrigation demand modelling, due to poor quality and availability of recorded data. Some data from metered groundwater pumping for irrigation was of suitable quality for validating the Aqualinc irrigation demand modelling and this process is described by Rajanayaka and Fisk (2016b).

Public water supply and industrial groundwater use data is available from HBRC databases.

The methodology used to estimate Frost Protection, Stock Water and Domestic is described in Appendix A.

Table 3-6: Pumping data sources.

Pumping type	data source	Data type	comment	reference
Irrigation	irrigation demand modelling	estimate	daily estimate 1980 - 2015	(Rajanayaka & Fisk, 2016b)
	HBRC database	data	poor data availability and numerous quality issues. Irrigation modelling data used instead.	
Public water supply	HBRC database	data	good quality data, some issues with individual bore flow before 1990	
Industrial	HBRC database	data	good quality data for major users after 1990	
Frost Protection	estimate of requirement in a typical year based on current consents	estimate	monthly flows for typical year	(Harper, 2016a) Appendix A
Stock Water	estimate of requirement in a typical year based on current consents	estimate	typical flows steady state	(Harper, 2016b) Appendix A
Domestic	estimate of requirement in a typical year based on pollution and typical used	estimate	typical flows steady state	(Harper, 2016b) Appendix A

3.9.3 Pumping data description

Groundwater abstraction for public water supply is approximately 22 Mm^3/year and has been relatively stable since 1980, with a reasonably good record of abstraction available since that year. Water abstraction occurs through a number of public water supply borefields in Napier, Hastings and Havelock North (Figure 3-49).

Industrial use appears to have stabilised in the year 2000 at a level of 13 Mm^3/year, after increasing from approximately 4 Mm^3/year between 1990 and 2000. Data quality before the year 2000 is subject to uncertainty, with some conflicting data occurring. Some of the apparent increase between 1990

and 2000 may be a consequence of improved reporting and record keeping, rather than an actual increase of groundwater use. Data available before year 1990 is scarce and may not be representative of actual industrial use.

Approximately 50 Mm^3/year is estimated to be abstracted for irrigation, but only a small proportion of this is metered and only during recent years. Therefore, groundwater use for irrigation required estimation by calculating irrigation demand for consented takes. The estimation of irrigation water use was undertaken as part of the LSR assessment (Rajanayaka & Fisk, 2016b) and used the same combinations of soil types, climate data, crop types, and consented irrigation areas, resulting in more than 3000 combinations.

Groundwater use for irrigation has steadily increased since 1980 (Figure 3-46). This increase is related to a similar increase in the number of resource consents to abstract groundwater for irrigation. There appears to be some inter-annual variation, which is most likely caused by climatic variation that increases irrigation demand during dry summers (e.g. 1997, 2012).

Abstraction from the aquifer system is highly seasonal, with largest abstraction volumes in the summer, when more than 50% of groundwater abstraction is for irrigation (Figure 3-47 and Figure 3-48). There is also considerable variability between the different years

Spatial distribution shows large, concentrated abstractions for public water supply and industrial takes, in contrast to a large number of relatively evenly distributed irrigation takes during the summer (Figure 3-49 and Figure 3-50). Increase of irrigation over time is apparent when different years are compared (Figure 3-50).

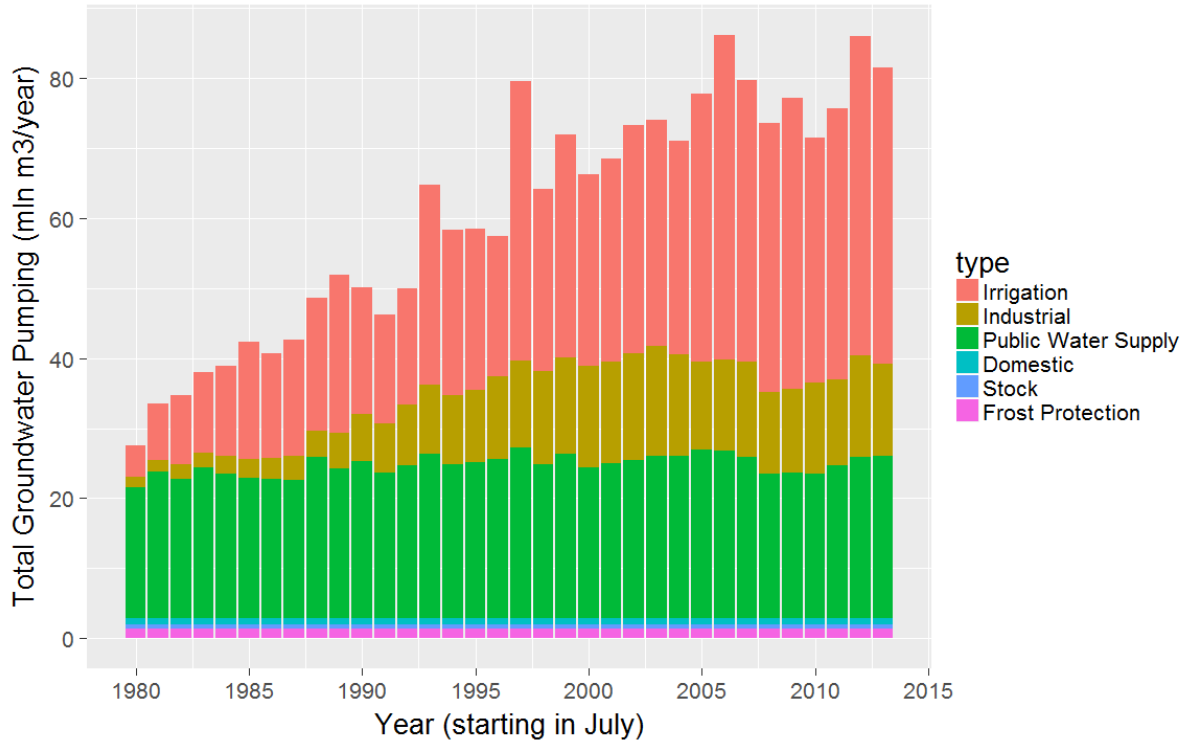

Figure 3-46: Annual groundwater abstraction from Heretaunga Aquifer System.

Figure 3-47: Monthly groundwater abstraction from the Heretaunga Aquifer System (2005 - 2015).

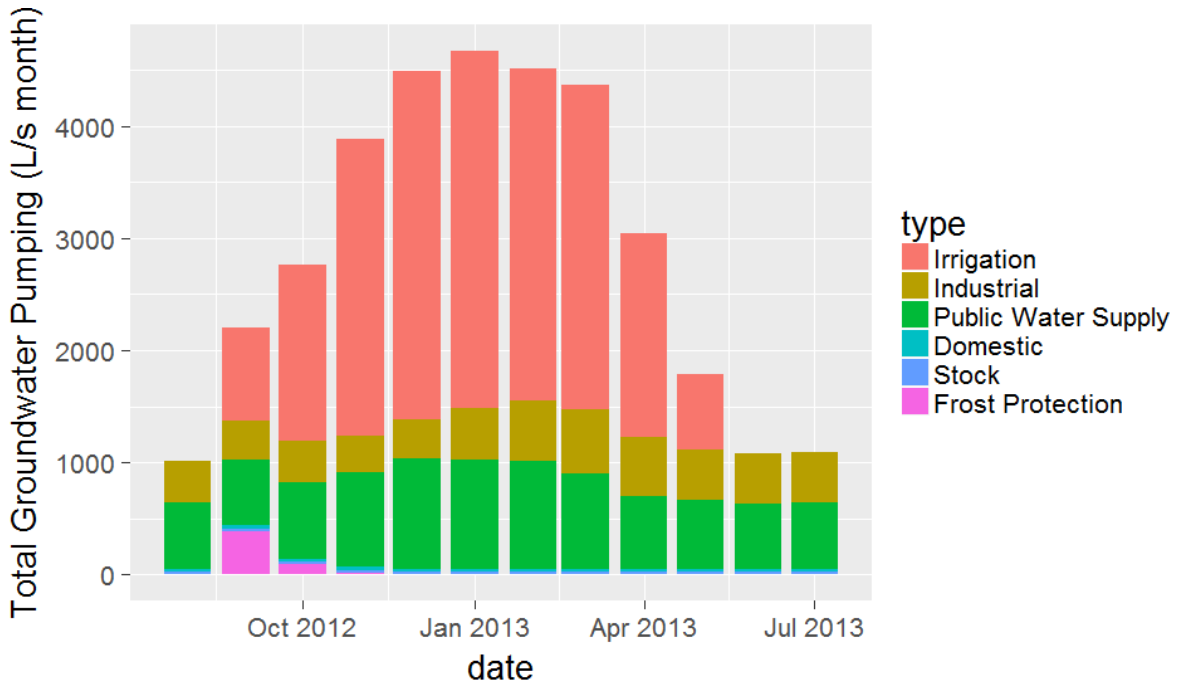

Figure 3-48: Monthly groundwater abstraction during the 2012/2013 irrigation season.

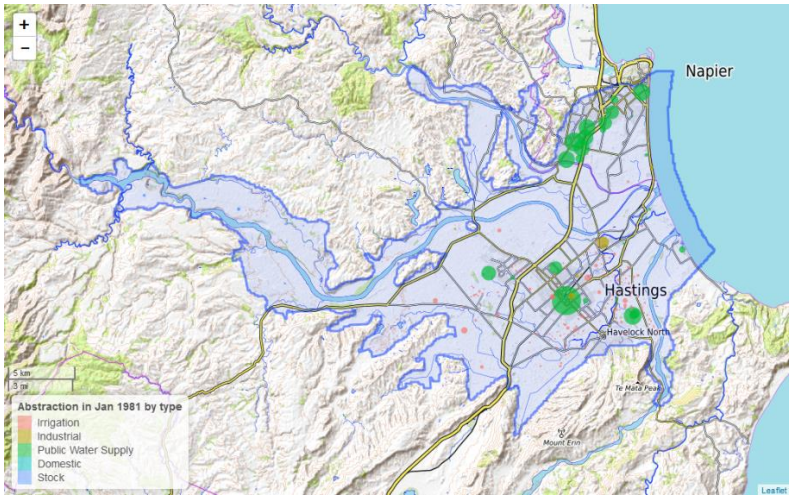	January 1981
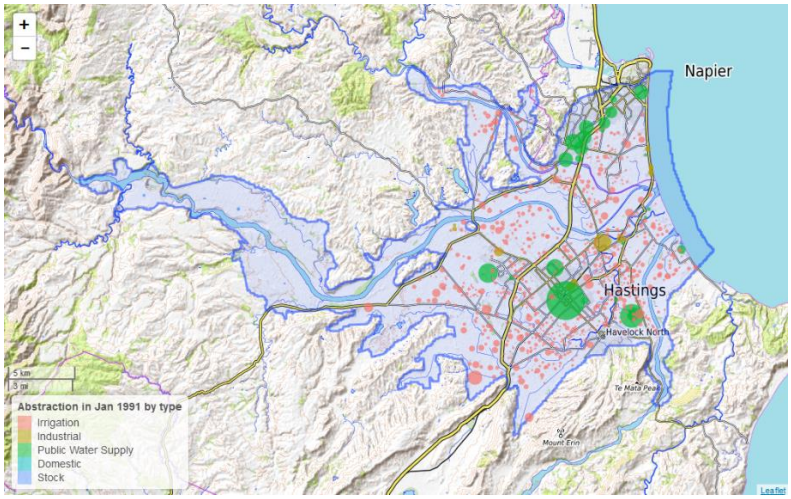	January 1991
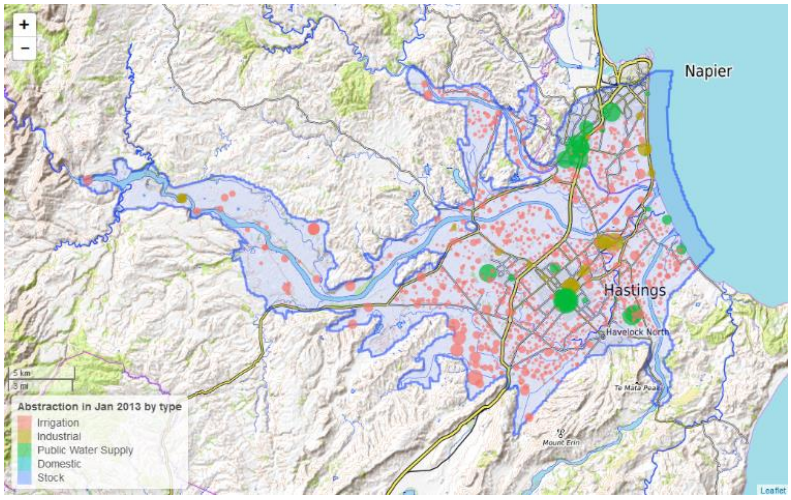	January 2013

Figure 3-49: Distribution of groundwater pumping from the Heretaunga Aquifer System during summer periods (January 1981, 1991 and 2013) by type. Dot area is proportional to take size, such that individual small domestic and stock water takes are indiscernible.

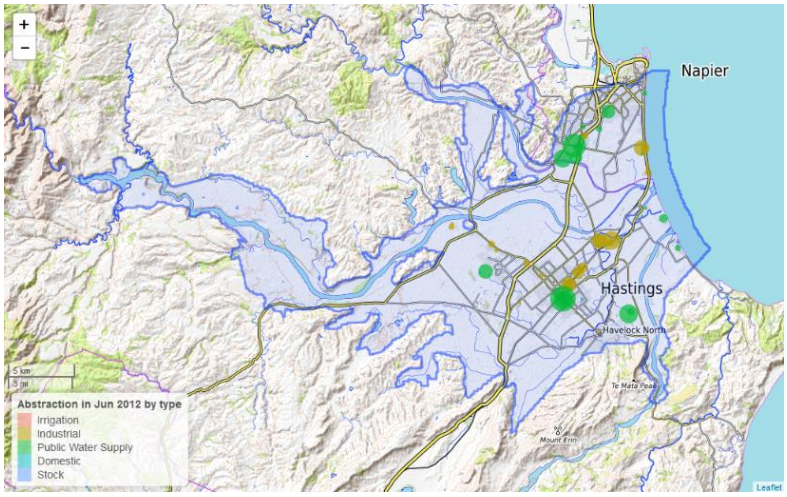	June 2012
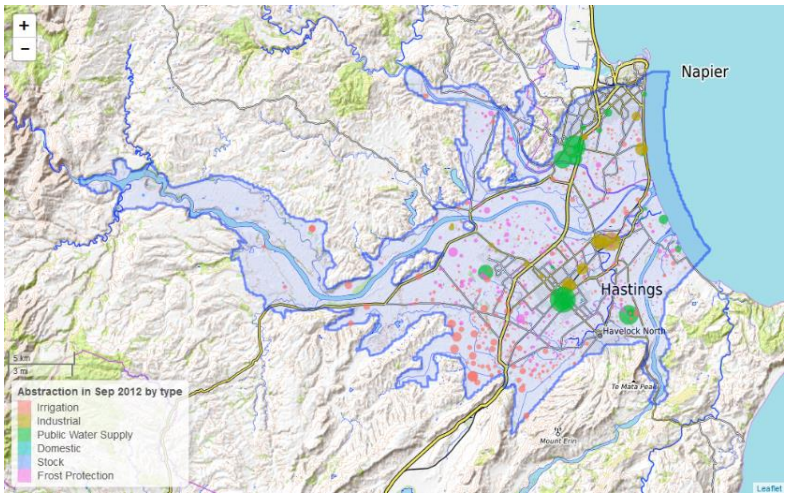	September 2012
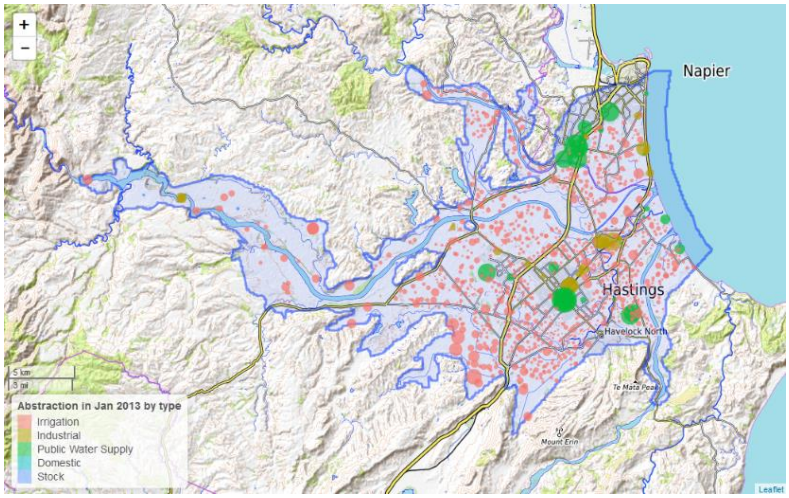	January 2013

Figure 3-50: Distribution of groundwater pumping from the Heretaunga Aquifer System during different seasons. Dot area is proportional to take size, such that individual small domestic and stock water takes are indiscernible.

3.10 Geochemistry

3.10.1 Overview of the study

GNS Science, with collaboration from HBRC, completed an investigation of groundwater age along with the isotopic and hydrochemical composition of water in the Heretaunga Aquifer System (Morgenstern *et al.*, 2018). The aims of the investigation were to explore rates of groundwater flow through the aquifer, along with interaction of groundwater with streams and rivers. The study used available age tracer data for the Heretaunga Plains, including tritium, CFCs, SF_6, δ^2H, $\delta^{18}O$, Ar, N_2, CH_4, radon and major/minor ion hydrochemistry data.

At a time of writing this report, the geochemistry study was subject to a final report review. Consequently, some of the findings of the geochemistry study were not available when this modelling work was completed and could not be fully integrated into the groundwater models.

Some of the findings of the geochemistry study have been discussed in earlier sections (3.4 and 3.5) of this report (e.g. sources of water in lowland springs, along with interconnection between various parts of the aquifer). In this section (below), other relevant elements of the geochemistry investigation are discussed.

3.10.2 Sources of Aquifer Recharge

Napier area

The geochemistry study concluded that groundwater in the Napier area originates from the Ngaruroro River, with no contribution from the Tutaekuri River or rainfall recharge. This conclusion is based mainly on stable isotopes of oxygen ($\delta^{18}O$) and major/minor ion hydrochemistry data. The conclusion appears to be supported by strong evidence, with strong contrast between chemistry of water in this area compared to other parts of the aquifer (Figure 3-51 and Figure 3-52).

This conclusion is not surprising, given that there is no unconfined aquifer area between the Ngaruroro River and Napier that could contribute rainfall recharge and there is a lack of detectable Tutaekuri river losses (see discussion in Section 3.4). However, it is remarkable that Ngaruroro River water can be clearly identified in groundwater more than 10 kilometres from the source.

Southern Part of Heretaunga Plains

The southern part of the Heretaunga aquifer has a distinct water chemistry signature that indicates limestone geology (see Figure 3-52) and local rainfall recharge (Figure 3-53). The interpretation of Morgenstern *et al.* (2018) is that this entire area is primarily recharged only by rainfall. However, there is not enough contrast in water chemistry to distinguish recharge from the Tukituki River water and rainfall recharge. Moreover, there is evidence that the Tukituki River recharges this area (see discussion in Section 3.4) and there is also evidence for a contribution from the Ngaruroro River (Wilding, 2017).

Morgenstern *et al.* (2018) do not discuss potential mixing of water from different sources. Wilding (2017) discussed this issue and estimated that as little as 10% hill country derived water may significantly alter the composition of aquifer water in this area. This may mean that the contribution of recharge from nearby hill country may be relatively minor, but a limestone geology signature may still be observed in groundwater samples.

Unconfined Aquifer between Maraekakaho and Roys Hill

The interpretation by Morgenstern *et al.* (2018) is that there is no contribution from the Ngaruroro river to the unconfined aquifer between Maraekakaho and Roys Hill (as indicated in the Figure 3-53 by red crosses). However, this interpretation appears to be based on a water sample from only one bore in this area that indicated very old water. Minor water losses from Ngaruroro River have been recorded in this area, indicating that a connection with groundwater is possible. It is also possible that the river water has not been detected in groundwater due to: 1) insufficient sampling locations and/or depths; or 2) mixing of river recharge with local rainfall water.

Unconfined aquifer between Roys Hill and Fernhill

In this area major losses from the Ngaruroro River occur. The interpretation by Morgenstern *et al.* (2018) is that some of this lost water travels south east, and then directly east towards the coast (Figure 3-53), which is consistent with the interpretation of Dravid & Brown (1997). However, Morgenstern *et al.* (2018) suggest that in this area there is also rainfall recharged water, distinct from river sourced water. This is not unexpected, as this is an unconfined area that receives recharge from direct rainfall. However, Morgenstern's interpretation (see Figure 3-53) shows river and rainfall sourced water moving in different directions and crossing paths. Whilst this pattern of movement is possible, it is not supported by any piezometric data and it appears unrealistic especially in the unconfined area where the aquifer is known not to include aquitards that could separate different aquifer layers and allow for different travel directions. The interpretation appears to be based on $\delta^{18}O$ measurements, which indicates the presence of Ngaruroro River water along a zone from east of Hastings to the coast, with some rainfall recharged water detected to the north and south of Hastings (Figure 3-51). An alternative explanation is that there is some vertical separation in the aquifer, as discussed below.

Central part of the confined Heretaunga Aquifer

Morgenstern *et al.* (2018) interpreted a distinct geographical separation of river and rainfall derived water. In this interpretation there is a narrow (approximately 2 km) band of river derived water along the zone from east of Hastings to the coast, with rainfall recharged water both to the north and south, separated from river derived water in the Napier area (see blue outlines on Figure 3-51). This suggests preferential flow of river water along a palaeochannel.

However, a clear distinction does not seem to be fully supported by the data. For example, in the rainfall recharged zone north of Hastings there are three bores that have clear indicators of rainfall recharge and six bores with mixed river/rainfall indicators near the edges of this zone. In the palaeochannel zone there are also several bores with a rainfall recharge interpretation and there is interpreted river water outside of this zone. Another consideration is a possible vertical separation of water derived from different sources, such as rainwater perched on top of river water. In this case, if the water was sampled from the same location but from different depths, the samples could indicate different sources of water. This would make it difficult to delineate any zones, if depth is not factored into the analysis (for example, most bores would target the shallower aquifer to reduce drilling costs, which would introduce bias towards shallower rainfall water).

It is also possible that these results could be produced by the mixing of water from different sources.

Other work also contradicts the geochemistry analysis, including the overall water budget. Figure 3-53 (from Morgenstern *et al.*, 2018) suggests that most of the Heretaunga Plains is recharged by rainfall. However, it is known from other work that most recharge occurs through river (see Section 3.12).

The above consideration suggests that delineation of river recharged water as presented by Morgenstern *et al.* (2018) may be an oversimplification. There is clearly evidence for the presence of Ngaruroro sources water in the central part of the Heretaunga Aquifer, but this water may be to some degree mixed and possibly separated vertically from rainfall recharge water.

Inflows from Moteo Valley and Tutaekuri River

The interpretation by Morgenstern *et al.* (2018) is that there is no contribution from the Moteo Valley and Tutaekuri River to the Heretaunga Aquifer (as indicated in Figure 3-53 by red crosses). However, there is other evidence for this connection, in particular from Moteo Valley (see Section 3.5).

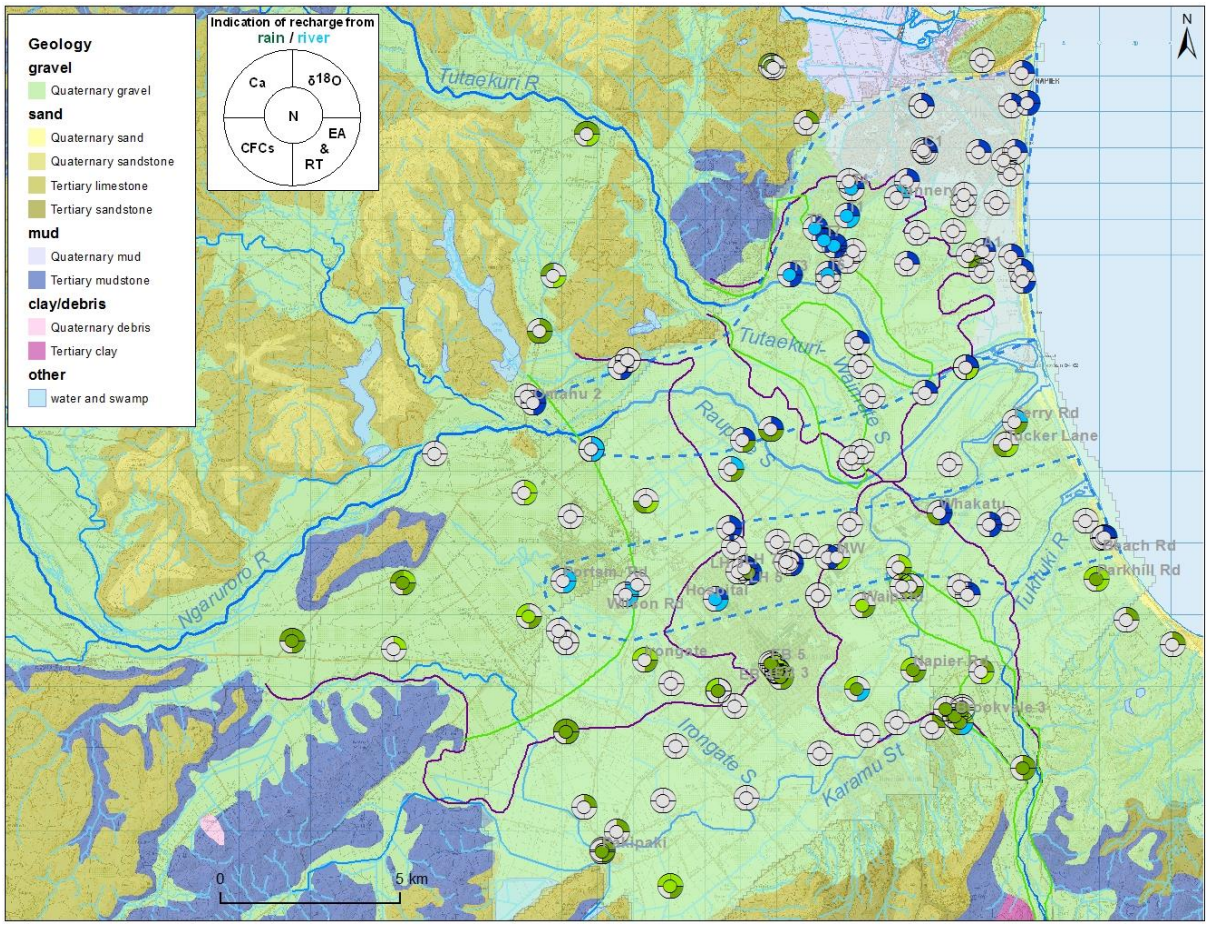

Figure 3-51: Map of indicators for groundwater recharge source. Green represents local rain, and blue represents river/stream recharge. Darker colours show stronger indication (Morgenstern *et al.*, 2018).

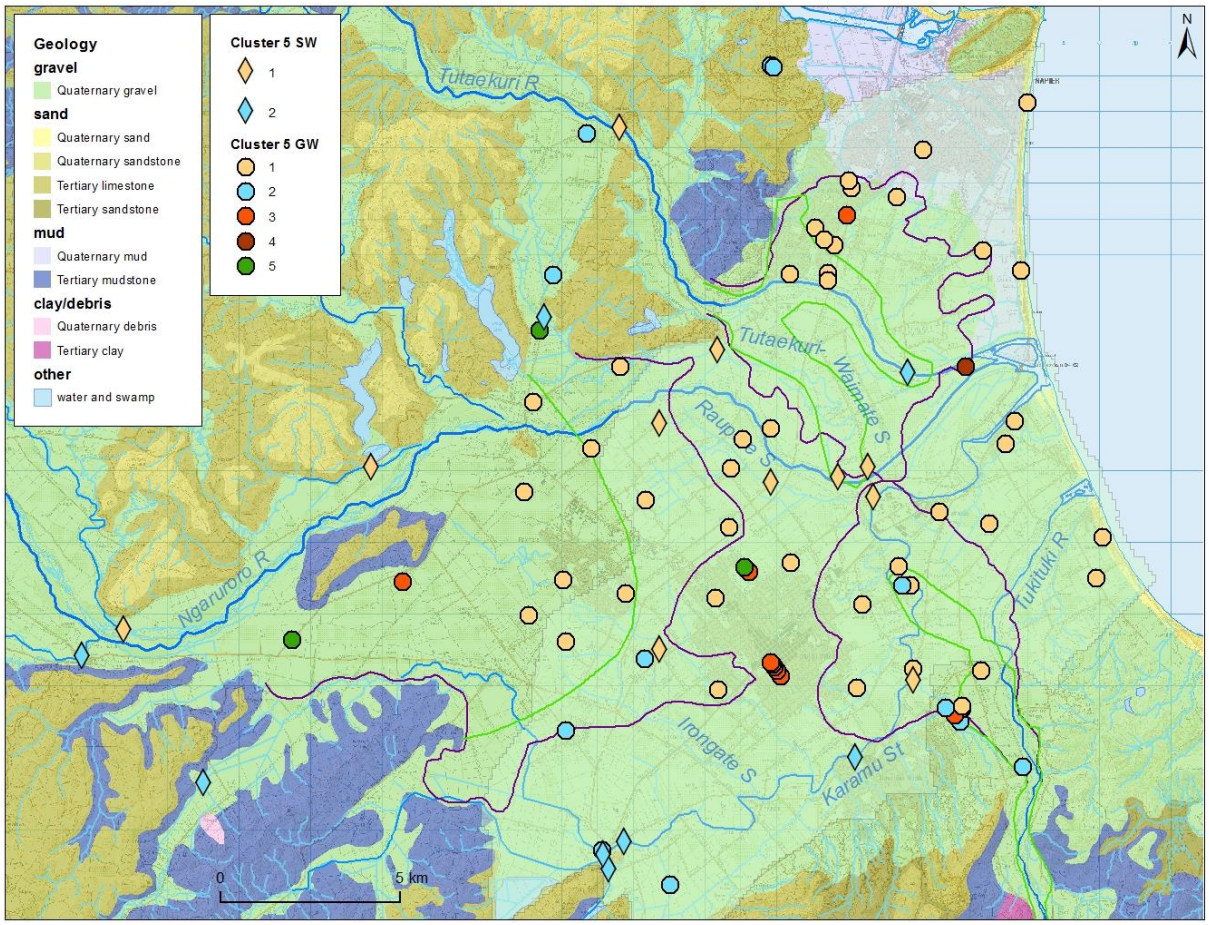

Figure 3-52: Map of hydrochemical cluster assignments for groundwater (circles) and surface water (diamonds) sites considered in this study. Groundwater cluster one (yellow circles) is interpreted as river recharged waters with low nutrients. Groundwater cluster two (blue circles) is interpreted as associated with limestone geology. For other clusters and more detail refer to the source (Morgenstern *et al.* 2018).

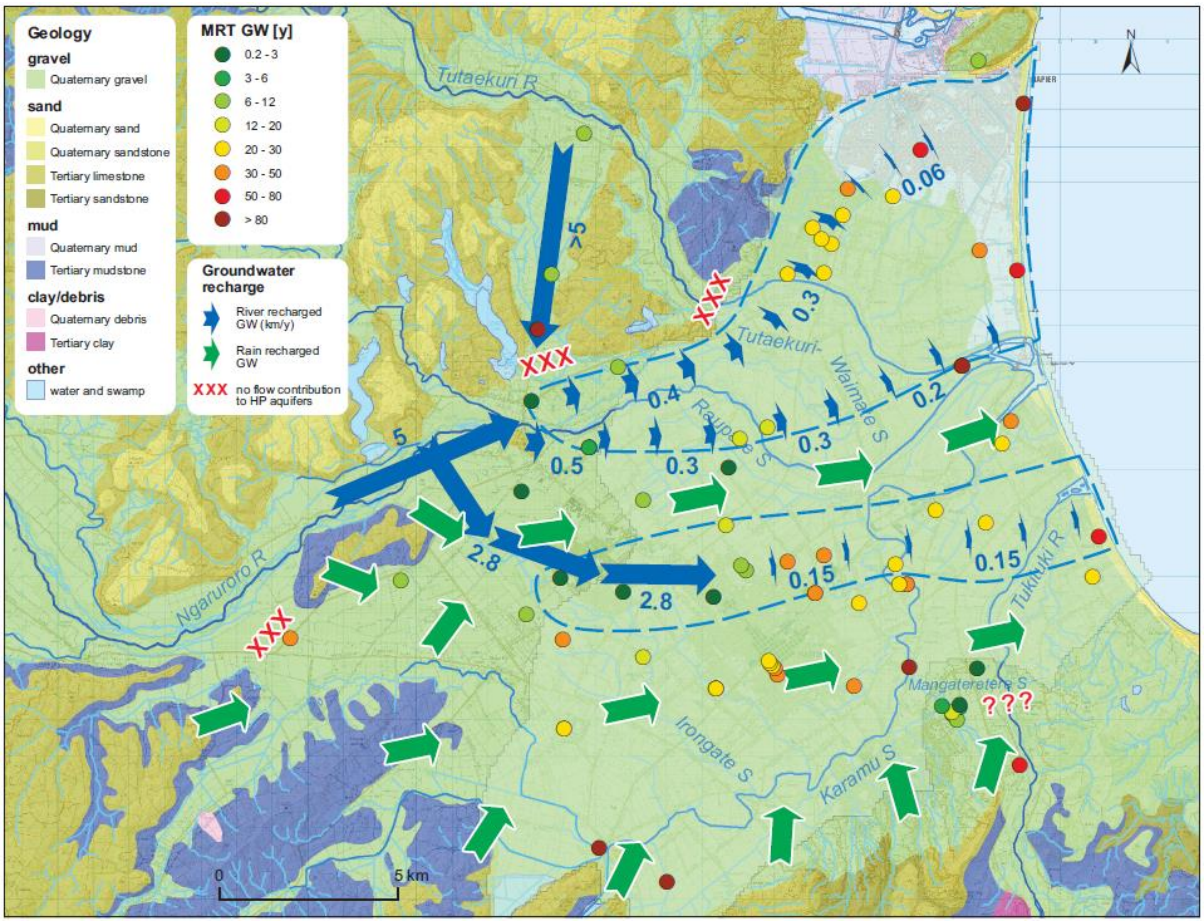

Figure 3-53: Water dynamics in the Heretaunga Plains hydrologic system inferred from groundwater ages (circles). Green arrows indicate rain recharged groundwater flow direction in general, without information on flow velocity. Red crosses indicate no connection of potentially lost surface water to the main aquifer. Red question marks indicate unknown contribution of the river to the main aquifer due to lack of data. The two areas indicated by blue dotted lines are the areas of clear Ngaruroro River-recharge signature (after Morgenstern *et al.*, 2018).

3.10.3 Age of water

The age of water based on tritium analysis (Figure 3-53) gives an indication of velocity and travel times of water through the aquifer.

Figure 3-53 shows very young water entering the aquifer in the unconfined zone, through Land Surface Recharge to the main unconfined aquifer area west of Hastings, the unconfined area near Tukituki River and the Moteo Valley area, along with river leakage from Ngaruroro, Tutaekuri and Tukituki Rivers.

Ngaruroro River water moves rapidly through the aquifer towards Hastings with velocity of approximately 3 km/year, resulting in relatively young groundwater in Hastings water supply bores, even at depths below 60 m. Further east beyond Hastings, the velocity decreases significantly to about 0.15 km/year.

The velocity of water flowing toward Napier is much less, resulting in much older groundwater being present there.

Morgenstern *et al.* (2018) reports that tritium, which is an indicator of young water, occurs at significantly greater depth in Heretaunga Plains aquifers, than in other New Zealand aquifers (Figure

3-54). Morgenstern *et al.* (2018) interpret this as an indicator of higher hydraulic conductivities in the Heretaunga Plains aquifer.

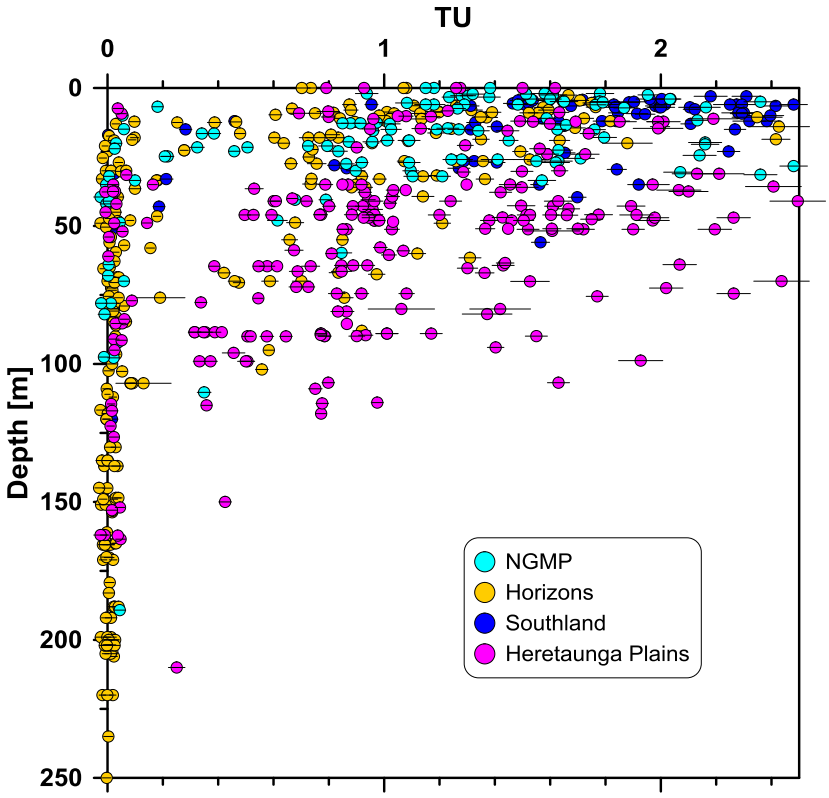

Figure 3-54: Tritium versus well-depth, for the Heretaunga Plains aquifer compared to other New Zealand aquifers. after Morgenstern *et al.* (2018)

3.11 Managed Aquifer Recharge

A Managed Aquifer Recharge (MAR) scheme in the Heretaunga Plains was commissioned in 1988 and transferred water from the Ngaruroro River to recharge ponds near Roys Hill, before the scheme was abandoned in 2008 (Gordon, 2009b). The location of the recharge scheme is shown in Figure 3-55 (after Gordon, 2009b).

The purpose of the scheme was to prevent decline of groundwater levels in the Heretaunga Aquifer.

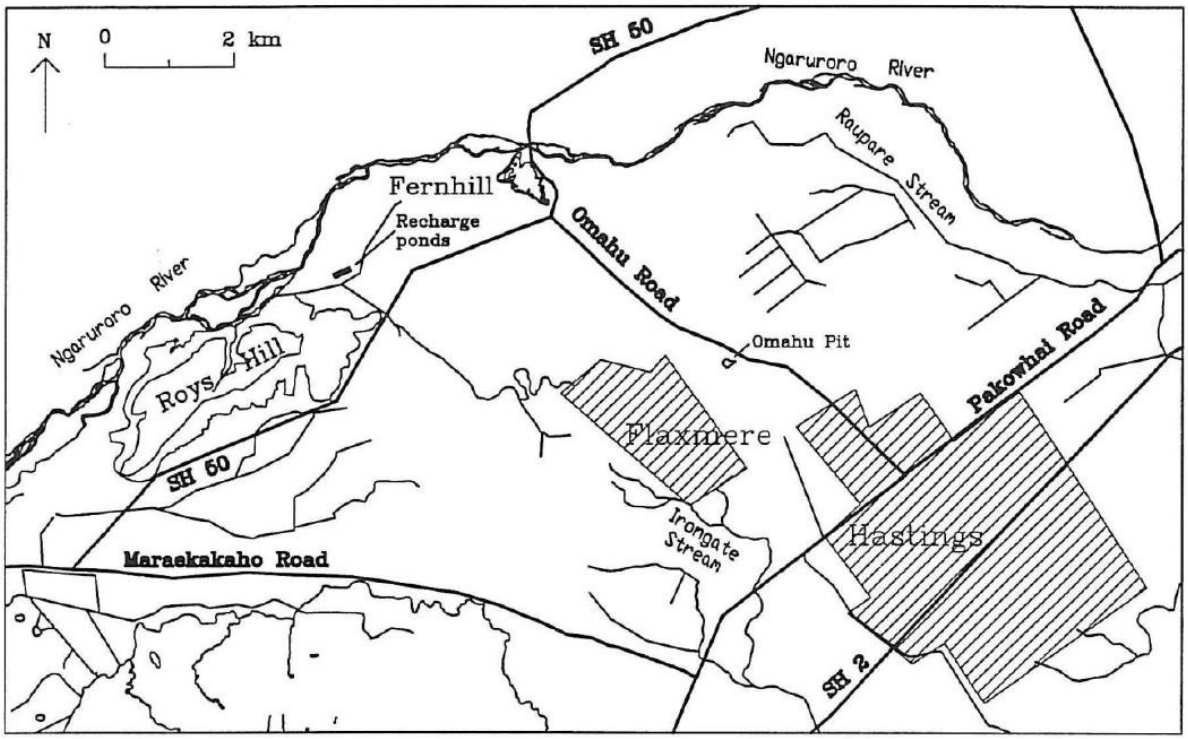

Figure 3-55: Managed Aquifer Recharge at Roys Hill. (After Gordon, 2009b)

Spot gauging data recorded between 1990 and 1998 show that the intake flow for the MAR scheme was highly variable during this time, between 100 L/s and 2,700 L/s (Figure 3-56).

The MAR scheme was commissioned in 1988, with resource consent allowing abstraction up to 3,000 L/s when river flow was greater than 3,500 L/s, along with a maximum take of 850 L/s when river flow was between 2,800 L/s and 3,500 L/s. Until the resource consent was renewed in 1995, siltation of the recharge ponds was a problem and abstraction often ceased during high flows to avoid this issue.

To overcome the siltation issue, a collection channel was constructed adjacent to the river channel and in 1995, when the resource consent was renewed, the maximum take was reduced to 600 L/s with a minimum flow of 2,800 L/s. The minimum flow was increased to 5,000 L/s in 1997 and the scheme was abandoned in 2008.

Recharge via the MAR scheme is a significant portion of the groundwater budget and requires inclusion in the groundwater model. Continuous records of abstraction for MAR from 1998 to 2008 are appropriate for representing MAR in the groundwater model. The average recharge rate was 300 L/s during that time (Figure 3-57). Prior to 1998, there are insufficient data to inform the groundwater model development. Instead, monthly ensemble averages (1998 to 2008) were used to represent MAR for each month between 1988 and 1998 (Figure 3-57).

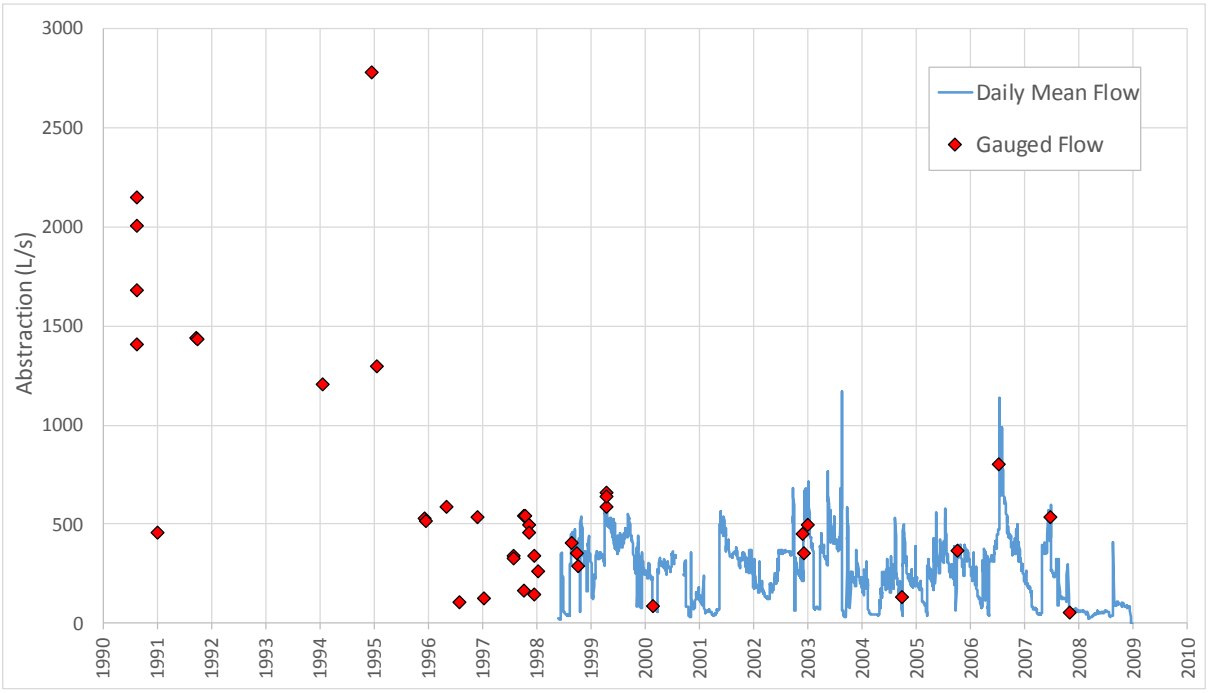

Figure 3-56: Abstraction flow records for the MAR race at Roys Hill. Blue line shows continuous flow data and red diamonds are flow gauging records.

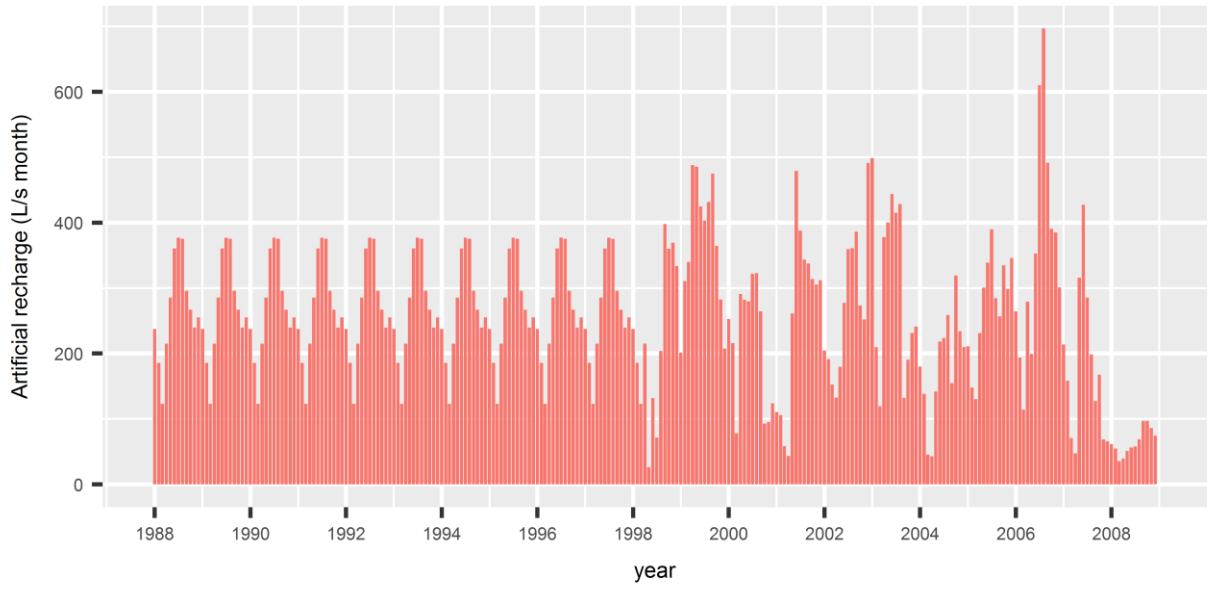

Figure 3-57: Artificial recharge rate used for modelling. Due to unavailability of data, rates before 1998 are based on 1998-2008 averaged rates for corresponding months.

3.12 Groundwater balance

The groundwater budget for the Heretaunga Plains is shown in Table 3-7 and Figure 3-58. The water budget is calculated as the average for the 2005 – 2015 period. This budget approximates average or typical conditions, however it needs to be noted that spring discharges are representative of average summer discharge, as winter spring discharges are difficult to measure.

The budget is presented in both L/s to allow for easy comparison with river flow which are typically recorded in this unit, and million m^3/year (Mm^3/year) which is often used when discussing water allocation.

Inputs

River recharge is based on observations, as described in Section 3.4.3.

Rainfall recharge is based on average recharge for period 2005-2015 estimated by Aqualinc, as described in Section 3.8.

Artificial recharge is excluded from the budget, as it discontinued in 2008.

The budget shows that 71% of recharge to the aquifer is from rivers rather than directly from rainfall. A previous water budget by Dravid & Brown (1997) identified a similar estimate of river recharge, but a much smaller estimate for land surface recharge.

Outputs

Spring discharges are based on observed summer spring discharges as discussed in Section 3.4.4.

Annual pumping volume is based on measured and estimated flows (average 2005-2015), as described in Section 3.9.

The best available information is that 111 m^3/year (or 55% of output) is discharged via springs and spring-fed streams each year. This is similar to the 120 Mm^3/year estimated by Dravid & Brown (1997).

A significant proportion (29% of outputs or 78 Mm^3/year) of groundwater is leaving the system through pumping. This is greater than pumping estimated by Dravid & Brown (1997), who suggested annual average pumping of 66 Mm^3/year. However, the value of 78 Mm^3/year is based on annual average pumping between 2005 and 2015, whilst Dravid & Brown's (1997) estimate is for part of the year 1994-1995 and, when corresponding periods are compared, abstracted volumes are very similar. Pumping volumes are greater during drier years, when abstraction is estimated to be as large as 90 Mm^3/year.

Most of the outflow appears to be through springs and spring-fed streams. In fact, this proportion is likely to be higher than shown in the budget, due to higher discharges during the winter.

There is approximately 78 Mm^3/year unaccounted in the groundwater budget, which may be exiting the aquifer system via offshore submarine springs, although there are no observations that could confirm this. It is possible that some (or even all) of this water may be exiting through winter spring flows, or undetected spring discharges (for example in tidal areas, where measurements are not possible). However, the recent study (Wilding, 2017) has already identified the major springs of the Heretaunga Plains, so any additional spring discharges are likely to be relatively minor. The most plausible explanation is that the unaccounted discharge exits the aquifer system through submarine springs.

	Type	Description	Mm^3/year	L/s	
INFLOWS	River Recharge (to groundwater)	Total river recharge to groundwater (based on observed major river losses by HBRC) including: Ngaruroro loss Tukituki losing Tutaekuri losing	**188.6** 138.8 24.6 25.2	**5,980** 4,400 780 800	71%
	Land Surface Recharge from rainfall	LSR calculated by Aqualinc for the unconfined area	78.5	2,489	29%
	TOTAL INFLOWS		**267.1**	**8,469**	
OUTFLOWS	Spring discharges	Measured summer discharges	111.0	3,520	42%
	Groundwater pumping	Some data and estimated from demand modelling	78.1	2,475	29%
	Sea discharge	No observations	78.0	2,474	29%
	TOTAL OUTFLOW		**267.1**	**8,469**	

Table 3-7: Groundwater budget for the Heretaunga Aquifer System. Artificial recharge is not shown as the MAR scheme was abandoned in 2008.

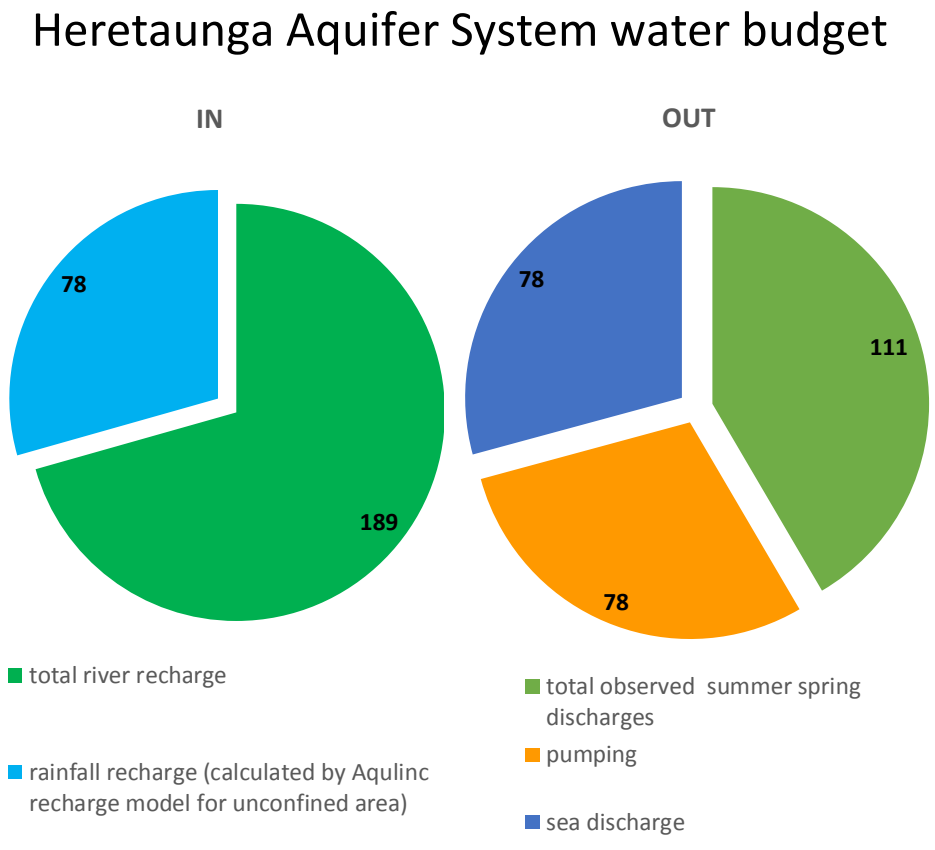

Figure 3-58: Average Water budget for the Heretaunga Aquifer system.

3.13 Conceptual model summary

The Heretaunga Aquifer System includes the main Heretaunga aquifer (including the Tukituki aquifer) within the Heretaunga Plains area, along with hydraulically connected surrounding valley aquifer systems in the Moteo valley, the Tutaekuri valley and the upper Ngaruroro valley. The Heretaunga aquifer is formed by highly transmissive alluvial gravels. The aquifer is stratified, although there is some degree of connection between deeper and shallower aquifer layers.

The main aquifer is confined and artesian in the eastern part, while it is unconfined in the western part and also near the Tukituki River (Figure 3-59).

Most (71%) recharge to the aquifer occurs through river losses; most of which is from the Ngaruroro River and the remainder from the Tukituki and Tutaekuri rivers (Figure 3-60). Land surface recharge provides the other 29% of recharge and occurs in the unconfined area of the aquifer. Discharge from the aquifer occurs through springs and spring-fed streams (42%) along with groundwater pumping (29%), with the remainder most likely occurring via submarine springs.

Groundwater pumping forms a significant part of the water budget, especially during the summer irrigation season, and is likely to affect other parts of the water budget, such as spring discharges.

The groundwater flow direction is eastwards towards the coast from the recharge area in the west, with pumping and spring discharges having some effect on flow pattern.

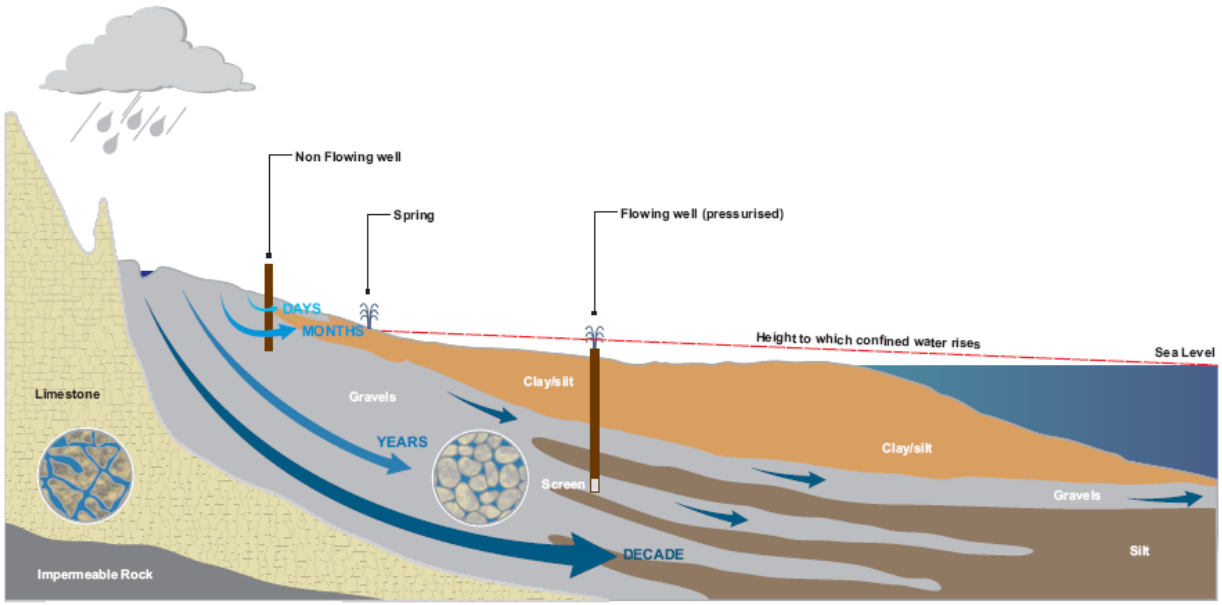

Figure 3-59: Conceptual cross-section through Heretaunga Plains.

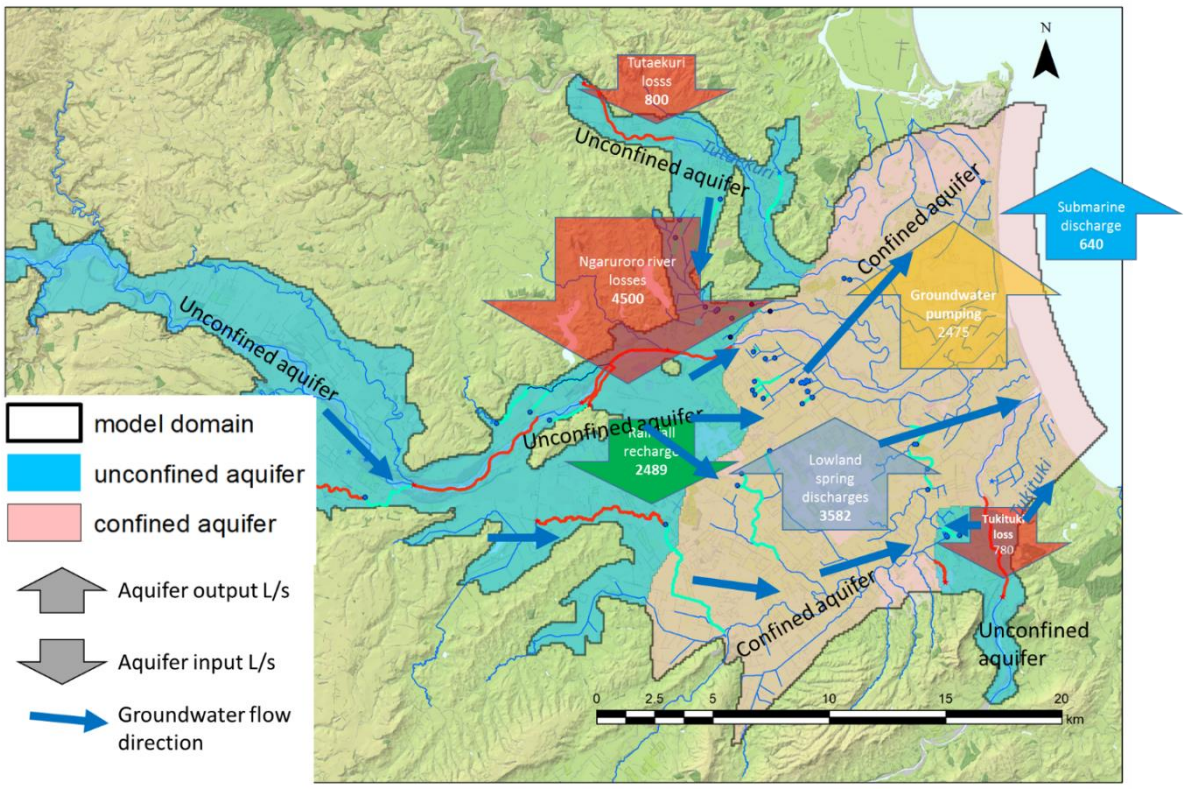

Figure 3-60: Main features of the Heretaunga aquifer Arrows show typical flow components in L/s, for explanation refer to section 3.12

4 Model design

4.1 Overall modelling approach

4.2 Modelling code

MODFLOW-2005 (Harbaugh et al., 2017) was used to simulate groundwater flow under both steady-state and transient conditions. The model was setup using Groundwater Vistas 6 user interface, and further modified using scripting in Python and R.

4.3 Model discretisation

4.3.1 Model time discretisation

The model was designed to cover the period from 1 July 1980 until 30 June 2015, with a monthly stress period.

For model calibration purposes this time discretisation was modified to reduce model run time, as described in Section 0.

4.3.2 Model domain

The model covers the area of the Heretaunga Plains and surrounding river valleys (Figure 4-4) that are considered to contain aquifers in hydraulic connection with the Heretaunga Aquifer (see Section 3.5). The model domain was extended approximately 1.5 km east, to include the sea and enable simulation of submarine springs. The total active area is 506 km^2, which is larger than the Heretaunga Plains area of 300km^2, because the model area includes valley aquifers and the offshore part of the aquifer.

The upper Ngaruroro River (upstream of Maraekakaho) was included in the domain. This area is probably connected to the main Heretaunga aquifer and may provide aquifer recharge along with pathways for contaminants, despite not representing a major groundwater resource.

Ngaruroro River terraces were included in the domain, despite a degree of separation from the aquifer. This is justified as some connection is possible and these areas may provide recharge and pathways for contaminants.

The Moteo Valley and Tutaekuri aquifer (upstream of Puketapu) was included in the domain, despite some uncertainty regarding the nature of connection, because the connection appears likely – as described in Section 3.5.2.

The Tutaekuri aquifer downstream of Puketapu was also included in the domain. In this case there is also some conflicting evidence about the nature of the hydraulic connection, although the connection does appear unlikely. However, this valley was included in the domain to allow for this potential pathway to be included in the model, if required.

Other valleys aquifers discussed in Section 3.5 are also excluded in the domain, because connection to the main aquifer is unlikely.

4.3.3 Model spatial discretisation

The model area is discretised into a 100 m x 100 m uniform grid (Figure 4-4). The grid consists of 302 rows and 501 columns and the domain contains 87,594 active cells. The total number of cells (including inactive cells) is 302,604.

4.3.4 Model vertical discretisation

The aquifer was discretised vertically into 2 model layers.

Layer 1 represents the combined Holocene gravels (mainly fan gravels where present in the unconfined area) and the underlying Last Glacial Gravels (Q2-Q4 deposits).

Layer 2 represents the deeper deposits of the main Heretaunga aquifer (geologically defined as Deposits below the Last Glacial Gravels or Q5-Q7 deposits), to a maximum depth of 250 m.

Both layers are set as Type 3 using the BCF package, which allows for conversion between confined and unconfined conditions.

An aquitard separating the two aquifer layers was not explicitly modelled, due to insufficient data that could be used to adequately delineate it. Instead, vertical conductivity (represented by horizontal/vertical anisotropy) was used to simulate the hydraulic separation between layers

4.3.5 Confining layer

The confining layer above the Heretaunga aquifer, consisting predominantly of low permeability marine clays and silts, was not included in the model layer thicknesses. This layer is not water bearing and modelling it explicitly was not considered necessary (but the confining hydraulic effect was represented in the layer configuration).

An early version of the model included this layer. However, it has proven difficult to incorporate, due to model convergence problems and long run times, so this layer was removed.

Any flow occurring in or above the confining layer, either by localised, small-scale higher conductivity zones or natural and artificial drainage (e.g. field drains), is accounted for in a separate surface water model that has been developed using the eWater SOURCE modelling platform.

4.3.6 Layer elevation

Layer elevations are based on a 3D geological model developed by GNS for the Heretaunga aquifer (Lee *et al.*, 2014). The elevations and thicknesses are shown in Figure 4-2 and Figure 4-3 respectively, while the model extent and boundaries are shown in Figure 4-4.

In converting the geological model to layers in the numerical model, some adjustments were necessary. This is because of simplifications and interpolations of the geological model (especially in areas where data is limited) that sometimes generate unrealistic results (e.g. discontinuous units). Consequently, simplifications were necessary for the numerical modelling. This included ensuring that the model layers are continuous and relatively flat.

The schematic showing how the model layers area defined is shown on Figure 4-1.

The top of Layer 1 is defined differently in confined areas (generally eastern parts of the main aquifer) and unconfined areas (generally western parts of the aquifer). For detailed locations of confined and unconfined areas refer to Figure 3-25. In the unconfined area, the top of the layer is based on ground elevation. The eastern part of the aquifer is confined under a thick wedge of low permeability Holocene sediments, and in this area the top of Layer 1 is defined by base of these low permeability sediments. This base of the confining layer is relatively well defined via abundant drilling logs from water supply bores that penetrate this layer.

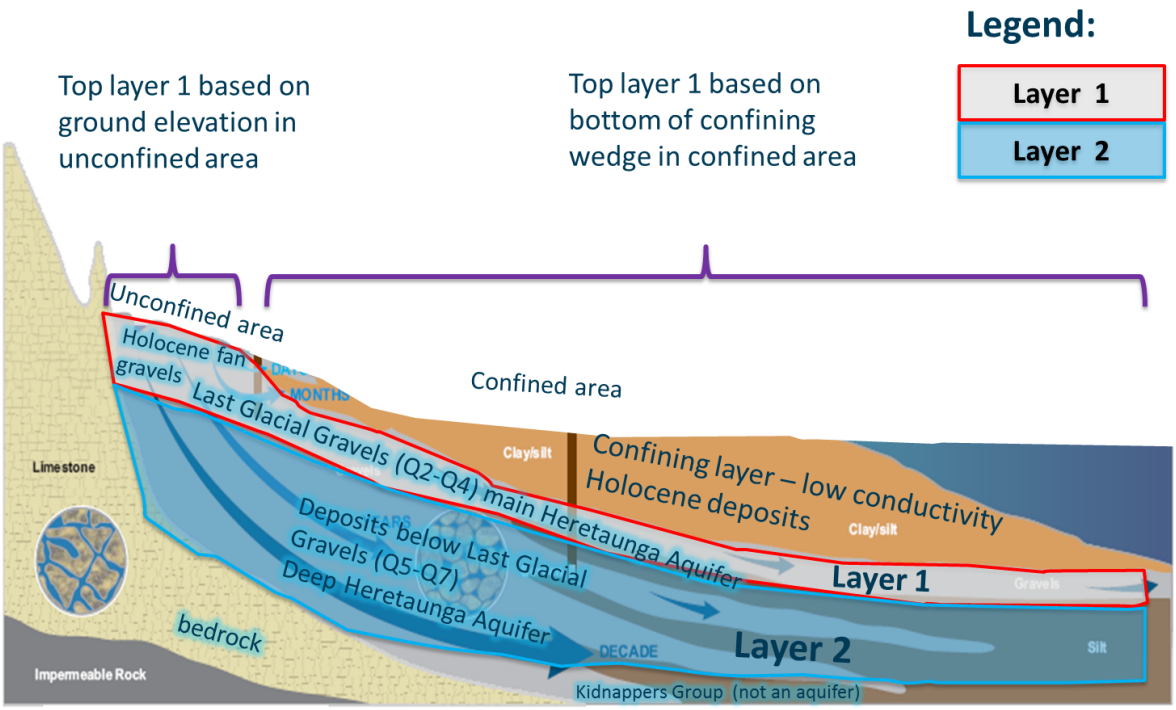

Figure 4-1: Model layer discretisation diagram.

The bottom of Layer 1 is identified from the base of Last Glacial Gravels (Q2-Q4) Quaternary deposits derived from the 3D geological model. The bottom of this layer is at roughly 100 metres below ground level (mbgl) in the centre of Heretaunga Plains and 20-40 mbgl at the perimeter of the plains and in adjacent valleys. The thickness of Layer 1 is variable: roughly between 20 m and 60 m. A minimum thickness of 20 m was enforced in the model.

The bottom of Layer 2 is based on the lower extent of Q7 deposits identified in the 3D geological model. The bottom of this layer is at the maximum depth of about 250 mbgl, while thickness is variable – increasing from about 50 m at the edges of the basin to 150 m thickness in the centre of the Plains.

The bottoms of layers 1 and 2 are much less well defined by the geological model, because much less data is available (most drilled wells do not fully penetrate the deep aquifer because this is not necessary to achieve water production).

Model layer elevation and thicknesses are shown in Figure 4-2 and Figure 4-3 respectively.

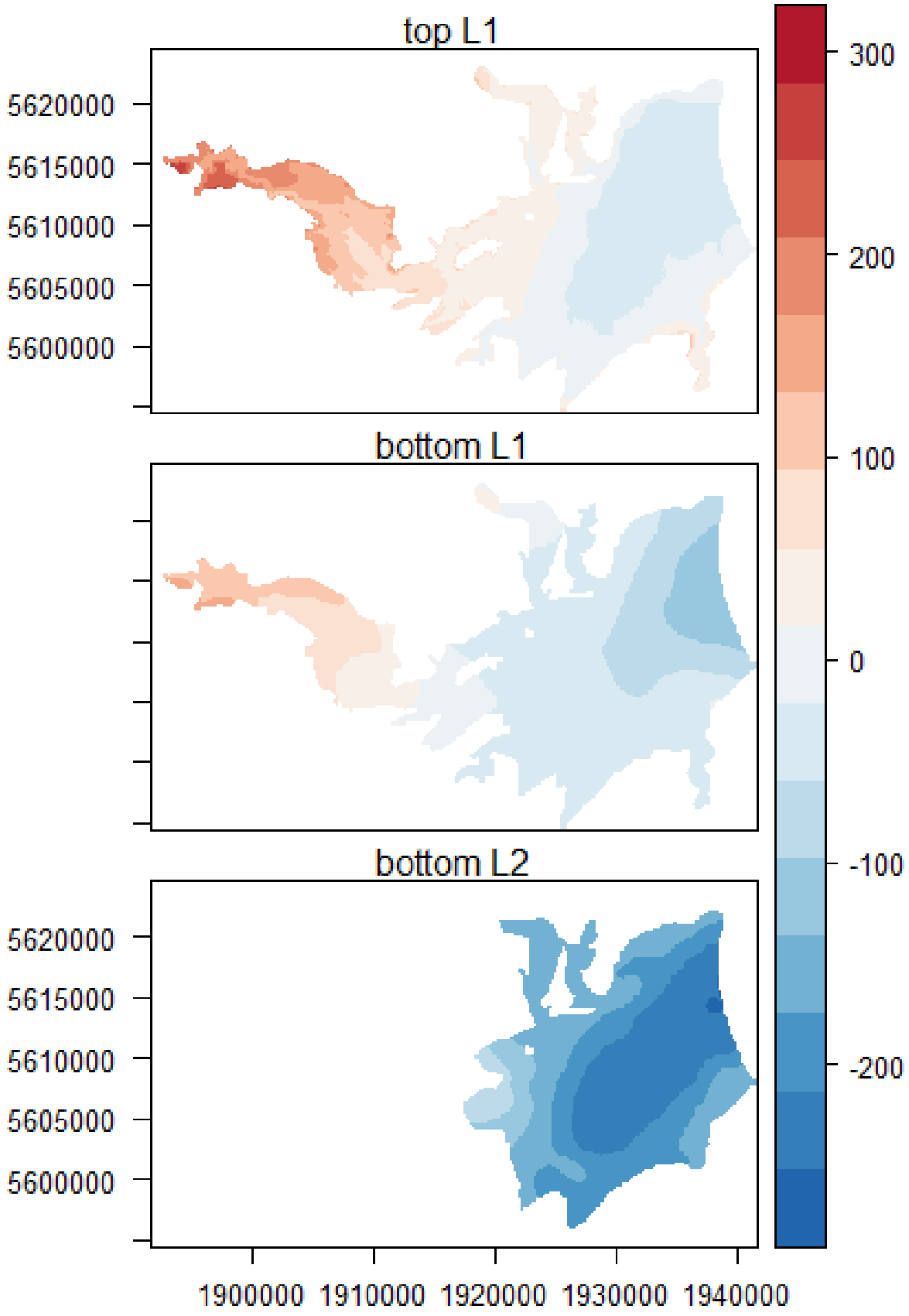

Figure 4-2: Grid elevations (m asl) for Layer 1 (L1) and Layer 2 (L2) of the Heretaunga groundwater model.

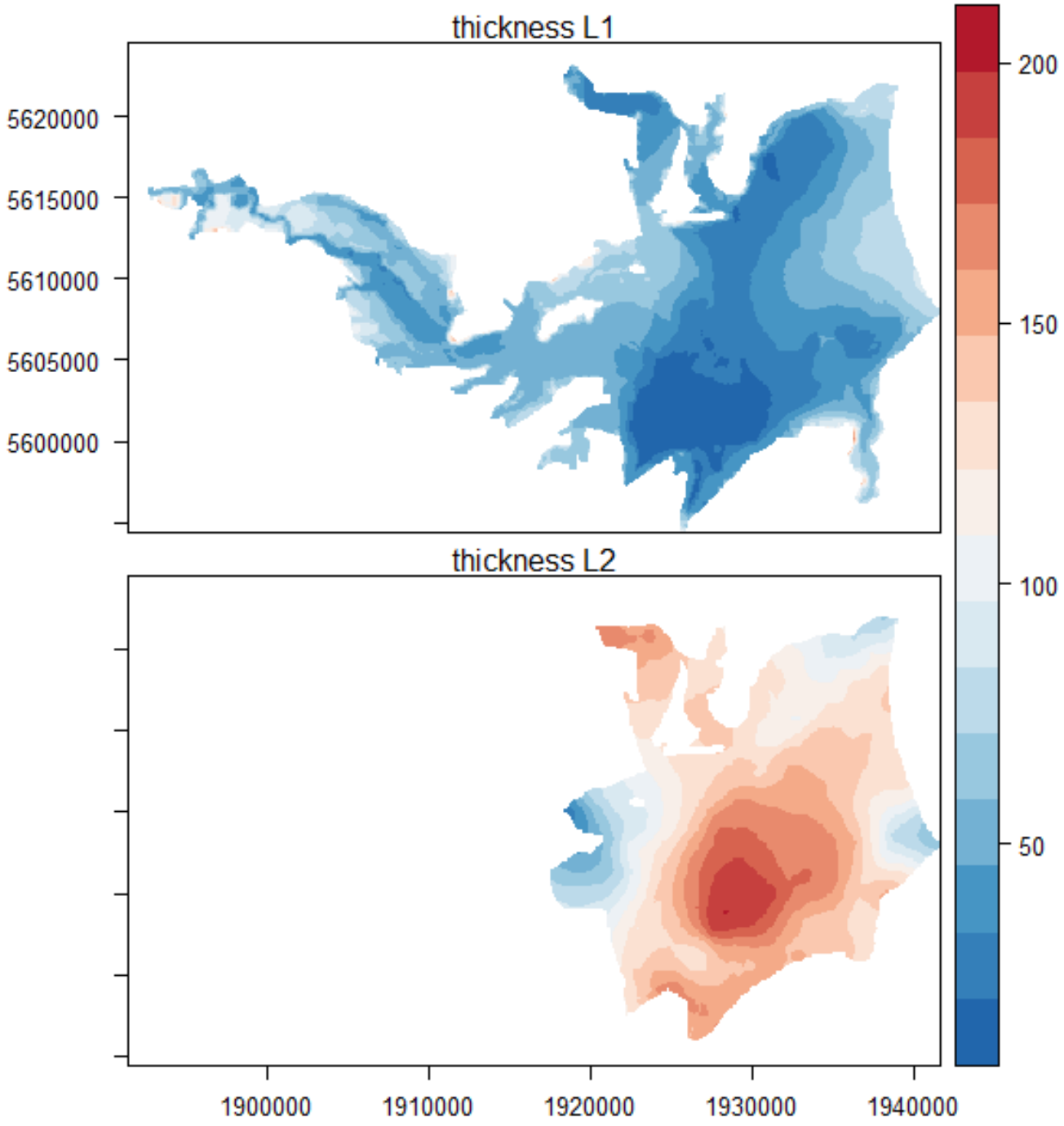

Figure 4-3: Layer thicknesses (m) for Layer 1 (L1) and Layer 2 (L2) of the Heretaunga groundwater model.

4.4 Boundary conditions

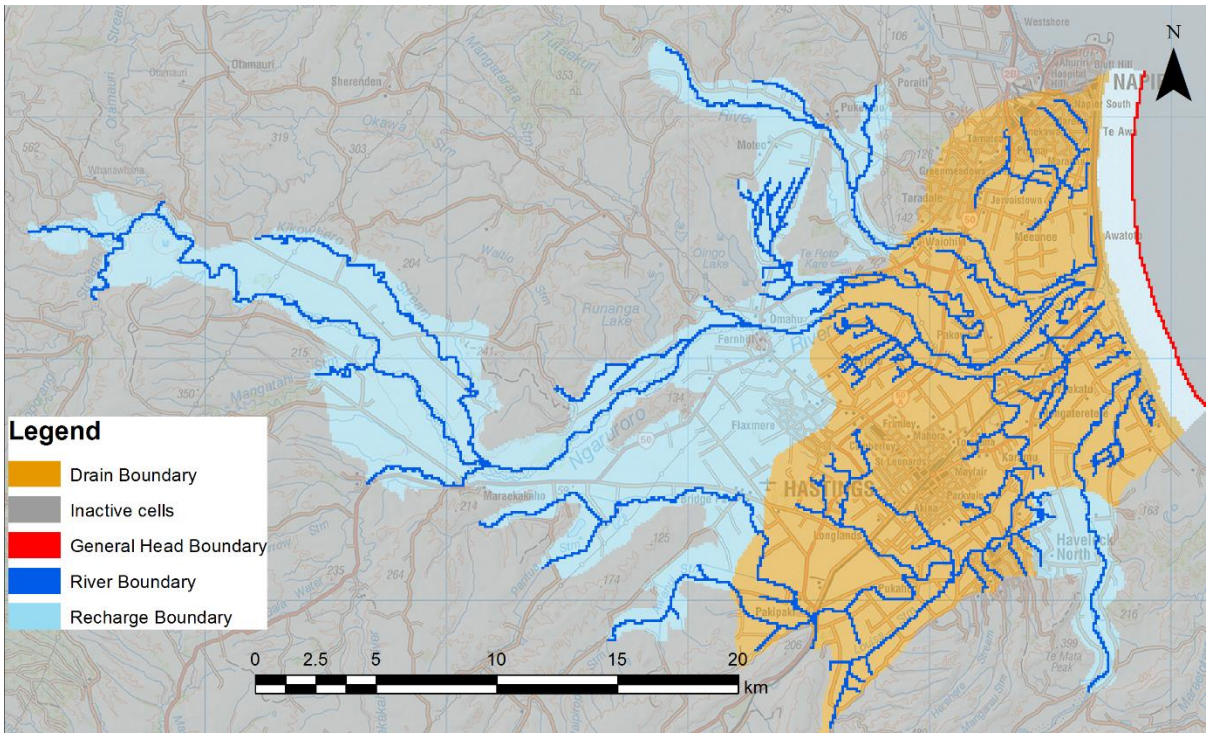

Figure 4-4: Model domain and boundary conditions.

4.4.1 Rivers

Boundary condition

Rivers, streams and springs are represented using the "River" boundary condition (RIV) (Figure 4-4). This boundary condition allows representation of river/aquifer interaction and simulation of river losses to the aquifer, along with gaining river sections and springs. This includes the ability to switch between losing and gaining conditions. It is also capable of simulating both hydraulically connected conditions (where flow between river and aquifer is dependent on head difference between river and aquifer) and perched conditions (where flow is independent of head difference between river and aquifer). RIV is also capable of dynamically switching between these conditions. These characteristics make the river boundary condition a suitable tool for simulating both losing and gaining sections of rivers, including the assessment of effects from groundwater pumping on river flow and spring discharges as required by the modelling objectives.

However, it also has some limitations:

- Inability to simulate changes in river level in response to flow conditions (but changes in river levels can be pre-set during model construction);
- Inability to represent drying of losing reaches;
- Inability to represent drying of springs;
- If the groundwater level drops below spring elevations the modelled spring feature becomes losing; for streams fed exclusively by spring flow, this may be unrealistic;
- Inability to represent increased river width (and thus the increased stream bed conductance) during floods.

Observations indicate that complete drying of main losing reaches, or complete drying of springs, does not normally occur and water level changes in springs are relatively small compared to changes in groundwater level. Therefore, it was considered that the above limitations are acceptable, except for some extreme modelling scenarios; e.g. with extremely high pumping rates. Variability of stream bed conductance in floods may be better modelled in the Modflow Stream Flow Routing (SFR) package, although this would require significantly more data to set up.

An advantage with using the River boundary condition as opposed to more sophisticated boundary conditions such as SFR is much more simple set up. RIV also has less data requirements (for example surface water inflows from catchments outside the model domain and runoff inside the model domain are required for SFR package) and RIV has shorter run times and model convergence is more readily achieved. The SFR boundary condition was initially proposed to be used in the assessment. However, during the trials this boundary condition was problematic due to convergence and run time issues.

The river network was derived on the basis of the BRS network, and was modified to include existing springs and losing-gaining sections.

Model setup

The river network included in the model consists of 338 river reaches, with 70 reaches representing 54 rivers, springs, spring-fed streams and drains that have been identified as having active surface water – aquifer interaction (see discussion in Section 3.4).The data sources and assumptions used to derive the network have been described in a Section 3.4.2. The river network has been provided in a GIS shapefile and imported into the Groundwater Vistas program to generate Modflow River (RIV) boundary conditions. Later, the river package was processed further:

- To duplicate boundary conditions in model cells that have been removed.
- To apply variable river stage and time variable conductance (see below).

Variable river stage

The main rivers (Ngaruroro, Tukituki, Tutaekuri) had a time-variable head stage applied, based on observed river stage (level). This variable stage is “fixed” in the model run. Due to changes in stage-flow relationship over the years (resulting from river bed changes), a composite stage was used. This was derived from calibrated flows in the river (calibrated flows is defined as flow recorded automatically using stage measurement, converted to flow using an established flow–stage relationship which is regularly calibrated to river gaugings to account to river bed changes).

Time variable river conductance

Spring discharges for some springs display a non-linear relationship between spring flow and groundwater level, as discussed in Section 3.4.4. However, the river boundary condition assumes a linear relationship between discharge and head difference between the river and aquifer. This means that if the model was calibrated to summer spring discharges, it could significantly underestimate discharges during the winter. This in turn could have a significant effect on the groundwater budget and compromise the ability of the model to represent groundwater dynamics.

This problem could potentially be resolved by using different boundary conditions type (for example Drain or SFR) and possibly with additional model layers, but only if additional data was available to adequately delineate springs and parametrise model layers. Due to lack of this data, an alternative solution was proposed using the standard River package.

The proposed solution uses seasonally variable river conductance, using higher conductance in the winter months to approximate the non-linear spring discharge relationship. A limitation of this method is that river conductance is time dependent in the model, rather than stage dependent, which may be not always realistic (for example there may be a very dry winter when groundwater levels, and therefore conductance, remain low). A better method may be to have river conductance dependent on groundwater stage, but this would require a modification to package code. This was considered unachievable due to limitations of time and resources. Furthermore, the proposed method is considered appropriate for typical conditions on the Heretaunga Plains.

The method was implemented by applying multipliers to conductance for selected springs (Irongate, Raupare, Karamu, Mangateretere, Karewarewa and Tutaekuri-Waimate) during winter months between May and November. To achieve a smoother transition between summer and winter conductance, in April and December a smaller multiplier (half the value of the winter multiplier) was applied. The value of the multiplier was identified as part of the calibration process (as discussed in Section 0.

4.4.2 Coastal boundary

The Coastal boundary was represented as line of "General Head Boundary" (GHB) cells, representing the head-dependent flow conditions, located about 1.5 km offshore (Figure 4-4). The existing evidence suggest a possible discharge that occurs 30 km offshore (see Section 3.5.1), and there is no evidence that there is any discharge within 1.5 km of the shoreline. Extension of the model grid 30 km offshore to include this discharge location would not be practical, as it would cause a large computational burden. Instead a 1 km distance has been selected arbitrarily to minimise any boundary effects, and the GHB boundary type allows simulation of the remote boundary by adjusting boundary conductance. The boundary condition was set at sea level and adjusted for saline water density. This boundary condition allows for simulating an exchange between the aquifer and the sea and it allows for simulating a variable degree of connection (both good connection and separation), by adjusting conductance of the boundary cells. High conductance would represent the presence of submarine springs, whilst lowering this conductance to a very low level would approximate the absence of offshore springs.

4.4.3 Land surface recharge

Land surface rainfall and/or irrigation recharge is represented by the "Recharge" (RCH) boundary condition. Model recharge was applied in the unconfined area of the aquifer only (Figure 3-41). Model recharge was used with a monthly stress period, on the basis of daily recharge calculated as part of the irrigation and recharge study described in Section 3.8.

There is some evidence for additional recharge contribution from surrounding hill country, mainly from the water quality data. This applies to the Moteo Valley and the southern part of the Heretaunga Plains (see discussion in Sections 3.4.4 and 3.10.2). However, contributions to the southern part of Heretaunga Plains appear to be relatively minor, as explained in Section 3.10.2. The contribution of total outflow from the Moteo Valley is already relatively low (see Section 3.5.2), and the additional recharge from the surrounding limestone hills is likely to be a relatively minor contribution to the Heretaunga Aquifer System water budget. Accordingly, this recharge component has not been incorporated in the model.

4.4.4 Groundwater Pumping

Pumping from the aquifer was simulated using the MODFLOW "Well" package (WEL).

Pumping applied in the model is based on measured and estimated data, as described in Section 3.9. This data has been applied with a monthly stress period.

Due to the many pumping locations (in particular irrigation, domestic and stock water takes), a well package was generated with an R script that converted data to an appropriate format.

4.4.5 Managed aquifer recharge

Managed aquifer recharge was introduced as three positive rate wells in model Layer 1 using the MODFLOW "Well" package (WEL) along with other pumping wells.

4.4.6 Diffuse drainage

Aquifer discharges through the known springs in the confined area have been measured (as described in Section 3.4.4). However, it is possible that some additional discharge occurs through tile drains or similar, although this is not captured by the measured discharges due to the small and distributed volumes of these discharges. The volume of this diffuse drainage is unknown, but it was arbitrarily set to be a maximum of 20% of the combined measured discharge of lowland springs (Karamu, Irongate, Raupare), applied over the entire confined area, which is approximately 200 L/s.

This diffuse drainage in the confined aquifer was represented using the "Drain" package (DRN), by applying a drainage layer everywhere in the confined area of the aquifer (only the Heretaunga Plains area). The drainage elevation was assumed equal to ground level. The conductance of the drain was determined in the calibration process.

4.5 Aquifer Properties

Hydraulic properties for the Heretaunga Aquifer System have been described in Section 3.6.

Available data is limited to horizontal conductivity (Kh) and confined storage (S; the product of specific storage Ss with aquifer thickness), with the majority of data from relatively shallow depths and of variable quality. Vertical hydraulic conductivity (Kz) was not available.

Parameterisation of spatial variability in Kh, Sy, and Ss was achieved using Pilot Points (Certes & de Marsily, 1991). This technique facilitates generation of a smooth parameter field, whilst allowing for variability, and does not require specification of arbitrary zones. The method is based on assigning property values at arbitrary points (for example in grid cells) and interpolating (typically using kriging) in areas between the points to achieve a smooth field.

Initial parameter values for Kh were based on interpreted hydraulic conductivity values as shown in Figure 3-26.

Vertical hydraulic conductivity was represented in the model using vertical conductivity anisotropy (Kh/Kz). This technique is particularly useful when undertaking automated parameter estimation, as it allows the constraint of vertical conductivity value to realistic limits. This is because when vertical anisotropy is used as calibration parameter, the lower parameter bound can be set to 1, consequently preventing vertical conductivity from ever becoming higher then horizontal.

The distribution of Kh pilot points is shown in Figure 4-5. The figure only shows Kh pilot points in Layer 1 of the model, however pilot points for Layer 2 and for Kz type are in the same locations (except where Layer 2 is absent). Pilot points are generally arranged in a regular grid and spaced every 2 km (Figure 4-5.) In some locations there are additional points spaced less regularly and closer together, to help with model calibration.

The distribution of storage pilot points (unconfined storage Sy and confined storage S) is shown on Figure 4-6.

The use of both Sy and S in both layers is necessary due to use of MODFLOW Layer Property Flow package (LPF) and "convertible" layer type in both layers 1 and 2, which allows for dynamic conversion between confined and unconfined condition, depending on the calculated water level in relation to top of the layer.

Unconfined storage Sy pilot points are more sparsely distributed in the unconfined area of the aquifer (in Layer 2 there is only a single pilot point) (Figure 4-6). Similarly, the confined storage parameter is more sparsely distributed in the unconfined area of the aquifer in Ngaruroro valley. The reason for such distributions is to reduce computation burden during calibration. The zones shown on Figure 4-5 represent zones where pilot points are interpolated to generate smooth fields within the zones.

During the calibration process it became apparent that high groundwater water levels in the Kikowhero and Pigsty terraces in relation to Ngaruroro valley water levels are very difficult to simulate. The pilot point technique would require a large number of pilot points to allow water levels to be retained at these terraces. To overcome this difficulty, additional zones have been created to represent the terraces, along with barriers between the terraces and the Ngaruroro valley. Pilot points were then placed in these zones and in the terraces.

The "barrier" zones that form lines around Kikowhero and Pigsty terraces were introduced to represent zones of lower conductivity.

Parameter fields generated in the process of calibration are presented in Section 0.

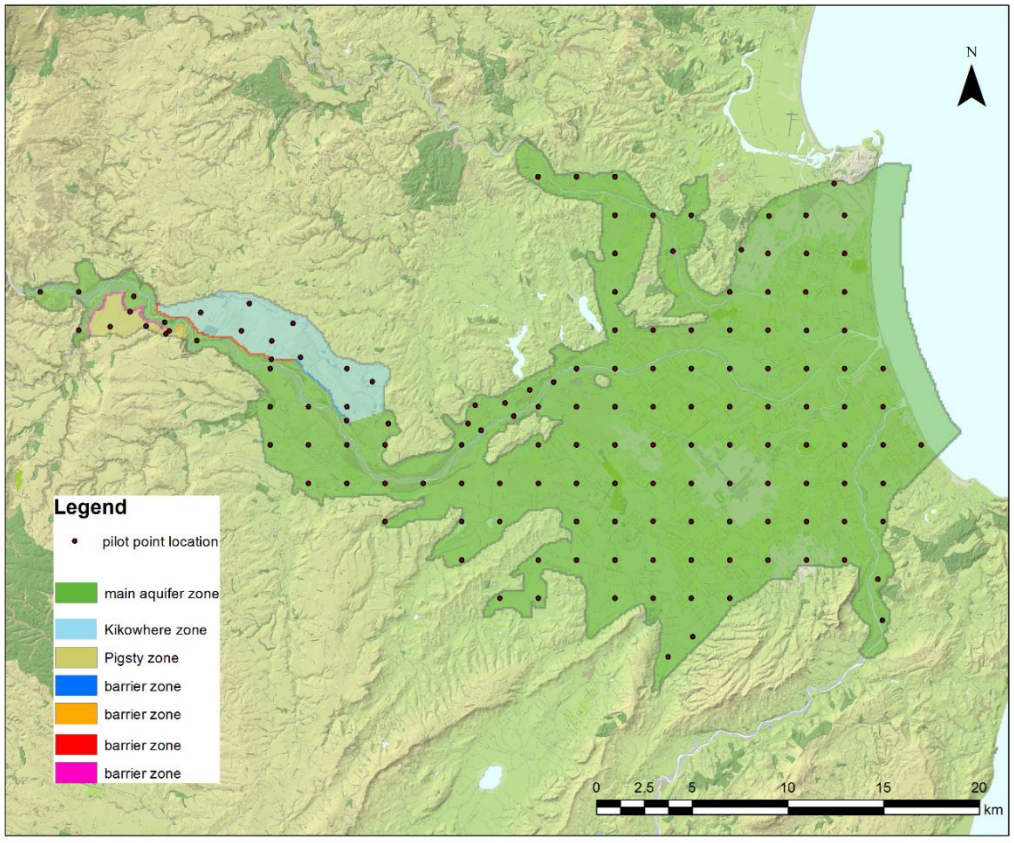

Figure 4-5: Horizontal hydraulic conductivity Pilot Points in Layer 1.

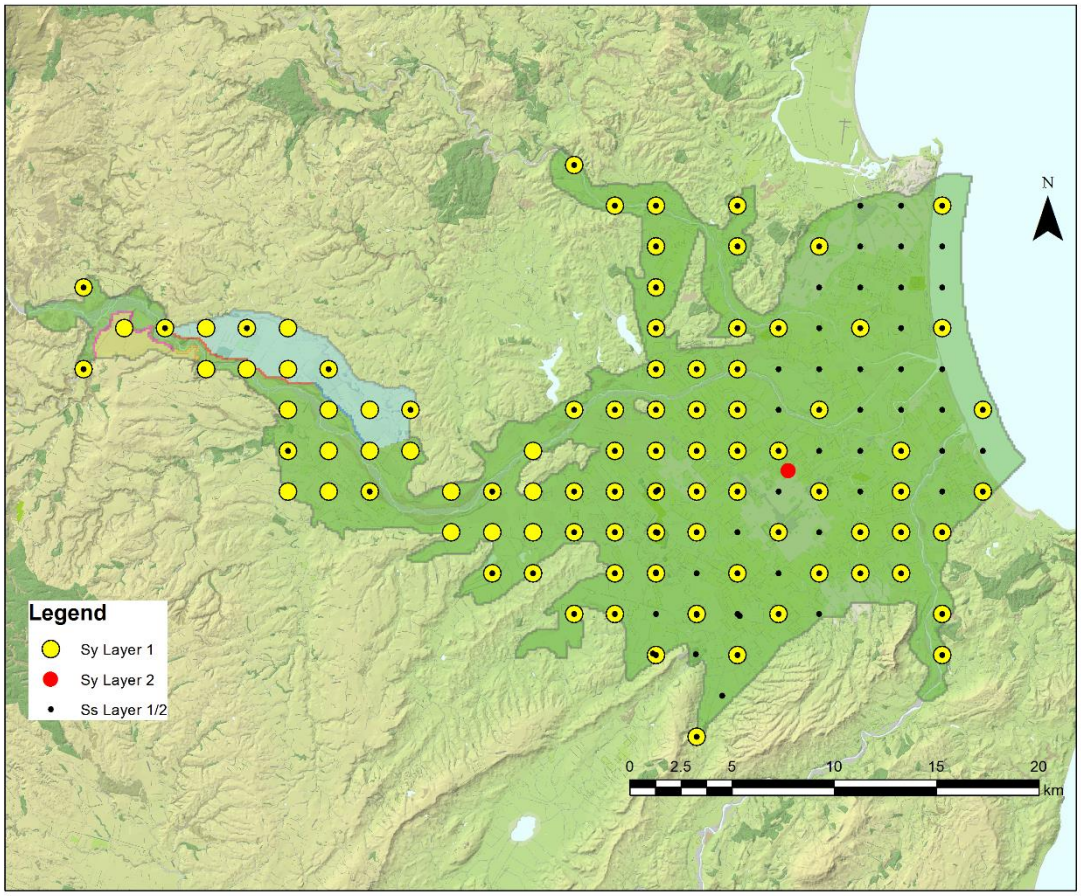

Figure 4-6: Storage Pilot Points.

5 Model calibration

5.1 Methodology

Estimation of model parameters through calibration was performed using the industry-standard Parameter Estimation software PEST (Doherty, 2016b,a). PEST adopts a gradient (or "local") search algorithm (i.e., the Gauss-Marquardt-Levenberg method) to minimise a sum-of-squared-weighted-residuals objective function. PEST_HP (Doherty, 2017) is a parallel version of PEST currently being developed and was applied here to reduce the computational burden associated with highly parameterised model calibration problems. PEST_HP is an advancement on previous parallel versions of PEST such as BeoPEST (Schreüder, 2009), due to its enhanced parallelisation of the parameter-upgrade testing process.

5.2 Model configuration for PEST runs

5.2.1 Combined model

Initial model design anticipated a monthly model running from 1980 to 2015. However, the run time of this model was expected to be excessive, due to the large number of stress periods. Additional data was available for calibration to flooding events in the river, which required finer time steps of duration less than one day.

To accommodate and minimise the number of these additional stress periods, a model was divided into several sub models with different time periods and lengths of stress periods, including steady state models. These models were then run together using common model parameters (e.g. same aquifer properties). This minimised the number of model stress periods and model run times.

The assumption of steady-state conditions is considered to be a reasonable approximation of groundwater levels averaged over the periods July 1980–June 1990 (i.e. "historic" conditions) and July 2005–June 2015 (i.e., "contemporary" conditions), giving rise to models referred to herein as "HPM_80" and "HPM", respectively.
Transient simulations were set up as following:

- Yearly stress period model, representing the average hydrological conditions for each consecutive year spanning the period July 1980 – June 2015 ("HPM_A"), i.e. representative variability between successive years during this period;
- Monthly stress period models, representing the average hydrological condition in each consecutive month, spanning April 1997–March 1999 ("HPM_M1") and April 2011–March 2015 ("HPM_M2"), i.e. representative variability between successive months and years during this period (e.g. April 1997 stresses are different from April 1998 stresses);
- Short-term responses to flooding events: 7 days starting 1/07/1997 ("HPM_E1"), 7 days starting 25/05/2001 ("HPM_E2") and 25 days starting 20/09/2015 ("HPM_E3"), each with 14 variable length stress periods representative of the variable river stage (while other hydrological conditions such as recharge and pumping are constant for these short periods).

Table 5-1 summarises the different models employed.

Monthly average model time periods were selected to have maximum availability and coverage of transient data.

Initial conditions for the HPM_A model are specified as per the output head distribution from the HPM_80 model.

Initial conditions for the HPM_E1, HPM_E2 and HPM_E3 models are specified as per the output head distribution from the HPM model.

For the HPM_M1 and HPM_M2 models, the initial head conditions are obtained from the HPM_A output head distributions at the HPM_A model time-step(s) closest to the HPM_M1 and HPM_M2 models simulation start-time.

Table 5-1: Summary of different models.

Model ID	Type (SS/Tr)[a]	Temporal resolution[b]	No. stress periods	Simulation period (Date range)	Model stress period	Model purpose
HPM	SS	-	1	10 years (2005–2015)	Time-averaged conditions for period 2005–2015.	Calibrate to contemporary typical conditions (water levels)
HPM_80	SS	-	1	10 years (1980–1990)	Time-averaged conditions for period 1980–1990.	Generate starting conditions for HPM_A and HPM_E1, HPM_E2, HPM_E3
HPM_A	Tr	Annual	35	35 years (1 Jul 1980– 30 Jun 2015)	average conditions in each consecutive year	Capture long-term groundwater trends. Generate starting conditions for monthly models
HPM_M1	Tr	Monthly	24	2 years (1 Apr 1997–31 Mar 1999)	average conditions in each consecutive month	Capture seasonal fluctuations.
HPM_M2	Tr	Monthly	48	4 years (1 Apr 2011–31 Mar 2015)	average conditions in each consecutive month	Capture seasonal fluctuations.
HPM_E1	Tr	Sub-daily	14	7 days (1/07/1997)	Short-term flood-event responses to flooding events.	Capture river – aquifer dynamics for major river recharge zone
HPM_E2	Tr	Sub-daily	14	7 days (25/05/2001)	Short-term flood-event responses to flooding events.	Capture river – aquifer dynamics for major river recharge zone
HPM_E3	Tr	Sub-daily	14	21 days (20/09/2015)	Short-term flood-event responses to flooding events.	Capture river – aquifer dynamics for major river recharge zone

[a] SS – steady state, Tr – Transient

[b] This represents the stress-period temporal resolution.

5.2.2 Observations

Overall, 6433 observations of different types were used. These observation types are described below.

Steady State Observations

Observation data used as calibration targets for the steady-state HPM model include:

(1) Time-averaged groundwater heads based on long-term monitoring data 2005-2015, 31 targets.
(2) Single groundwater levels (secondary group). This group was set up to supplement calibration with data where long-term monitoring was not available. In some areas, for example in the Moteo valley, long-term averages were not available but piezometric survey data was. This data is considered of lower quality, but cannot be ignored. Lower quality was reflected by assigning significantly lower weight to these observations.
(3) Upper valley head observations. This group is based on shorter term records from the location in the upper catchments of Ngaruroro. Due to a shorter record, this group is considered to be of lower reliability.
(4) Vertical groundwater level differences between aquifers (5 sites in total).
(5) Deep aquifer levels (2 bores).
(6) A single diffuse drainage flux.

The location of observation wells is shown in Figure 5-1.

Head observation targets are based on groundwater monitoring and piezometric surveys as described in Section 3.7.

Given that diffuse drainage flux values as described in Section 4.4.6 are accompanied by a large degree of uncertainty, an approach is adopted whereby only drainage fluxes that do not lie within a range of reasonable values (in this case, between 5,000 m^3/d and 30,000 m^3/d) lead to contributions to the objective function. This was achieved using the Groundwater Data Utility program OBS2OBS (Doherty, 2015).

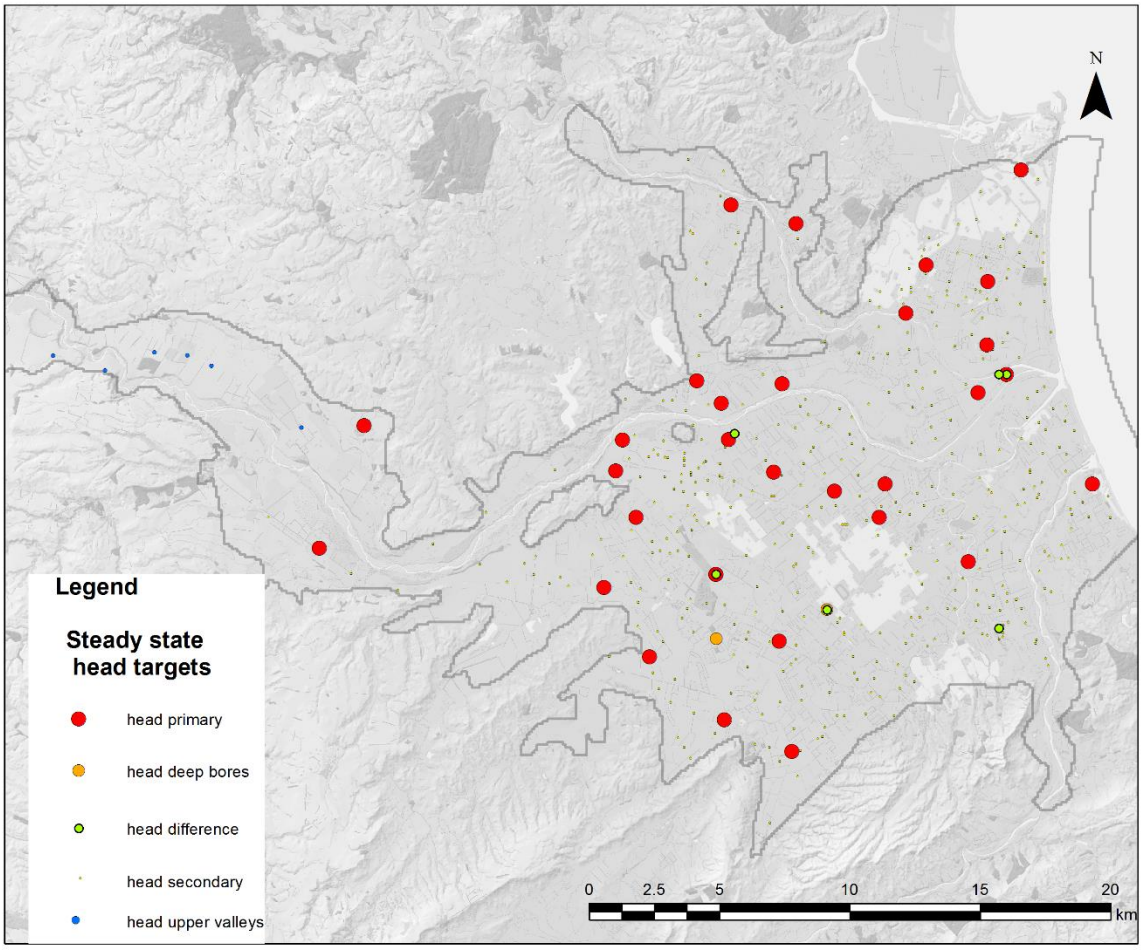

Figure 5-1: Steady state head calibration targets.

Transient Observations

Observation data serving as calibration targets for the transient models include:
(1) Temporal groundwater level differences;
(2) Absolute groundwater levels;
(3) Llong-term groundwater level trends; and
(4) River and spring fluxes at specific times.

Water level differences

Water level differences in time are used as targets to help calibrate aquifer storage parameters. Such differences are calculated using the Groundwater Utilities program SMPDIFF. The number of water level difference targets and absolute water level targets for the HPM_A (annual water levels), HPM_M1 and HPM_M2 (monthly water levels) models is 710, 721 and 1332 respectively.

For the HPM_E1, HPM_E2 and HPM_E3 models, only water level difference targets are used (of which there are 39, 38 and 125 respectively), and no absolute level targets were used in these models. The location of observation wells where transient water level targets are situated is shown in Figure 5-2.

Trends

Calibration targets representing long-term groundwater level trends (i.e. declines, as discussed in Section 3.7.2) are based on the slope of the regression line through the annual-average water levels, as well as the long-term differences in annual average levels.

Trends in 19 observation wells are used as targets (Figure 2b). The period over which the slope and the long-term difference is calculated is 01/01/1995– 01/01/2016, and the calculation is applied to observed and model-calculated annual average water levels. The script TRENDCALC was used to automate the calculation of the slope and the difference.

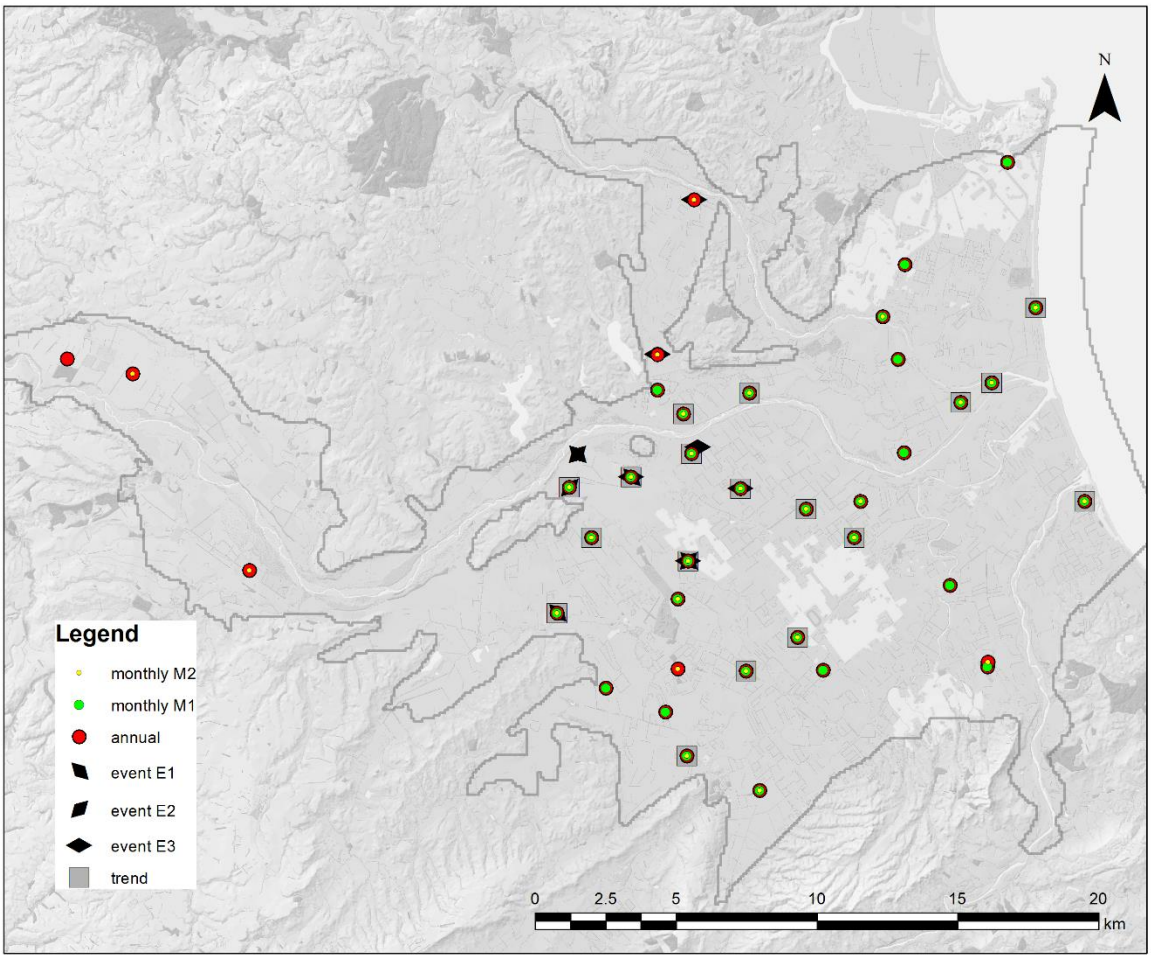

Figure 5-2: Locations of transient modelling targets.

River and spring fluxes at specific times

Calibration targets representing river gains and losses are based on identified losing and gaining reaches (see Section 3.4). Out of 64 identified gain or loss locations, 54 calibration targets were created (some locations were excluded due to lack of flow data, or due to being outside of the model domain). These calibration targets are based on observations during specific times, representative of dry and wet conditions. The use of two separate wet and dry condition targets was necessary due to observed non-linearity in the spring flow response to water level, indicating variable spring conductance in different conditions, as described in Section 3.4.4. Monitoring locations are shown in Figure 5-3.

Dry condition targets are recorded in 28/02/2013 for 54 locations. Spring discharges and river losses from individual reaches were known, as discussed in Section 3.4.4, but these individual discharges have been reported as MALF (mean annual low flow). Individual discharges were not known for specific days and were calculated instead. For example, on 28/02/2013, combined discharges for spring-fed streams were measured at downstream flow recorder sites ($Qcombined_{rec}$). MALF is also known for the combined spring discharges at the flow recorder site ($MALFcombined_{rec}$). This allowed for estimation of discharges from individual springs on a selected day ($Qspring_{calc}$), by multiplying MALF for the spring (MALFspring) with the ratio of $MALFcombined_{rec}$ to $Qcombined_{rec}$ (see Equation 5-1).

Equation 5-1: Spring discharge calculation for a specific day

$$Qspring_{calc} = MALFspring \times \frac{Qcombined_{rec}}{MALFcombined_{rec}}$$

Wet condition targets were recorded on 9/11/2011. This date was selected because at this time most gauging data was available, allowing for accounting of surface water inflows and thus for calculation of combined discharge for nine spring-fed streams and rivers.

In addition to known springs and losing rivers, there may be locations where gain or loss of water occurs locally, but without large-scale overall water exchange with the aquifer. In other words, a river may lose water to the aquifer through one reach, then gain the same volume of water through a downstream reach, resulting in no net exchange over the combined reaches of that river. To account for such cases, the water gains and losses have also been accounted for in the model outputs. This was done by having combined flow target for all rivers (excluding 54 known gain/loss sections), with observed value of combined surface water –aquifer exchange for these rivers of zero.

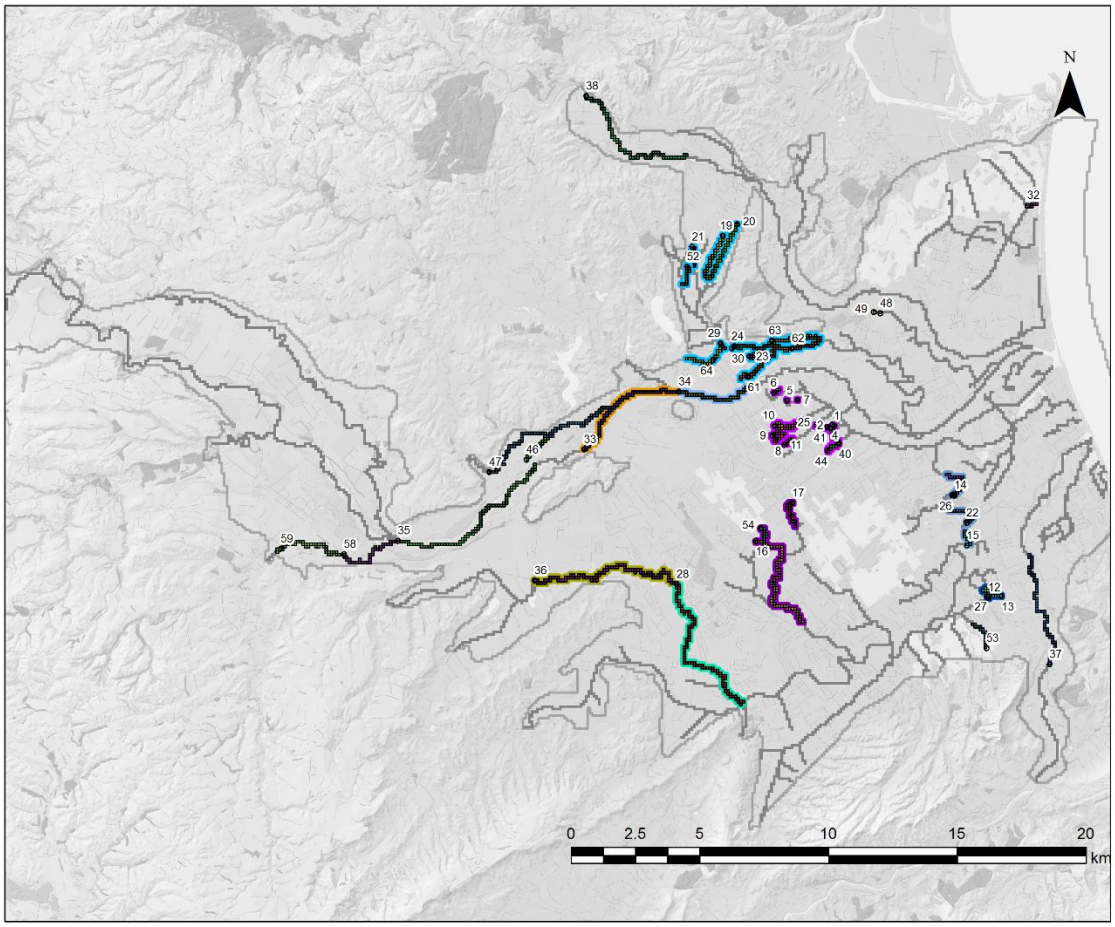

Figure 5-3: Locations of spring and river observations. Coloured cells represent locations where spring flow was used for observations. Numbers represent a spring identification number. Cells with outline represent winter spring observations, in most cases for a group of springs (e.g. Raupare). Grey coloured cells represent a combined flow target of zero for location where no surface water – aquifer flow has been identified.

Observation weights

PEST requires the specification of weights for observation targets. During the calibration process the PEST algorithm uses weights when calculating contributions to the objective function.

Weights were set up so that they reflect:

- Reliability of the data.
  For example, long-term water level averages were considered more reliable than one-off measurements, so the weights for this observation group were set higher.
- Importance of the data.
  For example, spring flow observation were considered more important than head observations, so they were assigned greater weight.
- Contribution of observations of different types to the objective function.
  Calculated contribution to the objective function is always related to units of measurements. For observations of different types, the units of measurements are different (for example m vs m^3/d for head and flow targets respectively) and weights can be set to ensure that different observation groups have similar contributions.

The weights were adjusted multiple times using a trial and error approach during the calibration.

5.2.3 Parameters

Model parameters estimated as part of the calibration process include:

- Aquifer parameters:
  - horizontal hydraulic conductivity (K_h);
  - vertical K anisotropy factor (K_h/K_z);
  - unconfined specific yield (S_y);
  - confined specific storage (S_s);
- Recharge and irrigation demand multipliers:
  - Rainfall recharge rate multiplier (RM);
  - Irrigation well extraction rate multiplier (QM_{irr});
- River conductance parameters
  - River bed conductance (C_{riv});
  - River seasonal conductance multiplier ($C_{rivMult}$)
- Coastal boundary conductance (C_{sea});
- Drain conductance (C_{drain}).

A total of 822 adjustable parameters were used.

Aquifer parameters

Parameterisation of the spatial variability in K_h, K_h/K_z, S_y, and S_s is achieved using pilot points (Certes & de Marsily, 1991) as described in Section 4.5.

Land surface recharge and irrigation demand multipliers

To account for uncertainty related to land surface recharge and irrigation demand estimation (which has been undertaken in a separate assessment described in Sections 3.5.2 and 3.9), and allow more flexibility in calibration, additional multiplier parameters for total recharge and total irrigation demand have been applied (RM and QM_{irr}).

Irrigation demand is of particular importance here, because irrigation consists of a considerable part of the aquifer's water budget. Whilst important, the irrigation rate applied in the model is only based on calculations (and not metered data) and is subject to large potential error due to assumptions and simplification required in the estimation. The use of an irrigation multiplier parameter is designed to help compensate for this data uncertainty. For example, if irrigation demand was underestimated in the assessment, PEST could compensate for this during calibration by adjusting the multiplier value.

A multiplier was not used for abstraction types other than irrigation. This is because public water supply data and industrial use data is based on actual measurements and therefore considered reliable, whilst other uses are relatively small and their contribution to flow uncertainty is considered low.

River bed conductance

The river network delineated for modelling included 338 river reaches, with 70 reaches representing 54 locations where groundwater-surface water interaction was identified. River bed conductances for these reaches have been used as parameters in calibration. However, some of these parameters have been tied with other parameters, which keeps the number of adjustable parameters to minimum. All the parameters related to known river gains and losses (70 reaches) remained non-tied. In addition, other river reaches (30) have been designated as non-tied parameters. These reaches were selected to represent a group of similar reaches (for example, all reaches of the upper Ngaruroro River), which were then tied to the selected reaches. In total 100 river reaches are represented by 100 adjustable conductance parameters.

In addition, some reaches have temporally variable conductance (see discussion in Section 4.4.1), which are specified as a multiplier of conductance for winter months. There are seven PEST multiplier parameters of this type.

Coastal boundary

The coastal boundary is represented by the General Head Boundary Condition (head-dependent flux boundary) type, as explained in Section 4.4.2. The boundary was divided into seven sections of approximately equal length in each layer, to allow for spatial variability. This gave a total of 14 sections of boundary. Conductance in each section was then used as a PEST parameter.

Drain conductance

The conductance term for the diffuse drainage layer (described in Section 4.4.6) was used as a single PEST parameter.

Parameter bounds and initial values

Parameter bounds and initial values are listed in Table 2.

Table 5-2: Model parameterisation set-up.

Parameter	Method	NPAR[a]	Bounds	Initial value	Preferred value
K_h (m/d)	Pilot points	235	10^{-4}-10^{4} [d]	0.1 - 2000, [b,c]	0.1 - 2000[c,d]
K_{xy}/K_z (-)	Pilot points	187	1-1000	10^{b}	10
S_y (-)	Pilot points	91	10^{-4}-0.20	0.1	0.1
S_s (1/m)	Pilot points	185	10^{-7}-10^{-3}	10^{-6}	10^{-6}
RM (-)	Single value	1	0.80-1.20	1.0[b]	1.0
QM_{irr} (-)	Single value	1	0.80-1.20	1.0[b]	1.0
C_{riv} (m^2/d)	Reach-by-reach	100	10^{-3}-5.0×10^{5}	-	-
$C_{rivMult}$ (-)	Selected reaches	7	1-20	1	-
C_{sea} (m^2/d)	Zone-by-zone	14	10^{-3}-10^{5}	-	-
C_{drain} (m^2/d)	Single value	1	10^{-3}-10^{2}	-	-

[a]NPAR represents the number of adjustable parameters
[b]Initial values represent those used for calibration of the HPM model prior to the joint calibration
[c]Multiple values reflect expert knowledge relating to spatial variability in hydraulic parameters, as explained below.
[d]Bounds and initial values are spatially distributed, as explained below

Hydraulic conductivity – spatial distribution of bounds and preferred values

Spatial distribution of parameter bounds and preferred values of hydraulic conductivity is presented in Figure 5-4. This distribution is based on conductivity zones delineated from pumping tests (see Section 3.6). The high conductivity zone had a preferred value of 2000 m/d in the central part of Heretaunga Plains. Model Layer 2 (deep Heretaunga aquifer) was assigned value of 500, which is based on the assumption that deeper layers of the Heretaunga aquifer are likely to have lower conductivities due to consolidation with depth.

The lower preferred value is also along the edges of the Heretaunga Plains, and in the upper valleys. Very low preferred values in the upper valleys represent “barrier” zones for Ngaruroro Terraces (see section 4.5 for explanation). Lower and upper bounds result in a large range of values across the aquifer. This large range is justified by large variability seen in the pumping test results (see Section 3.6).

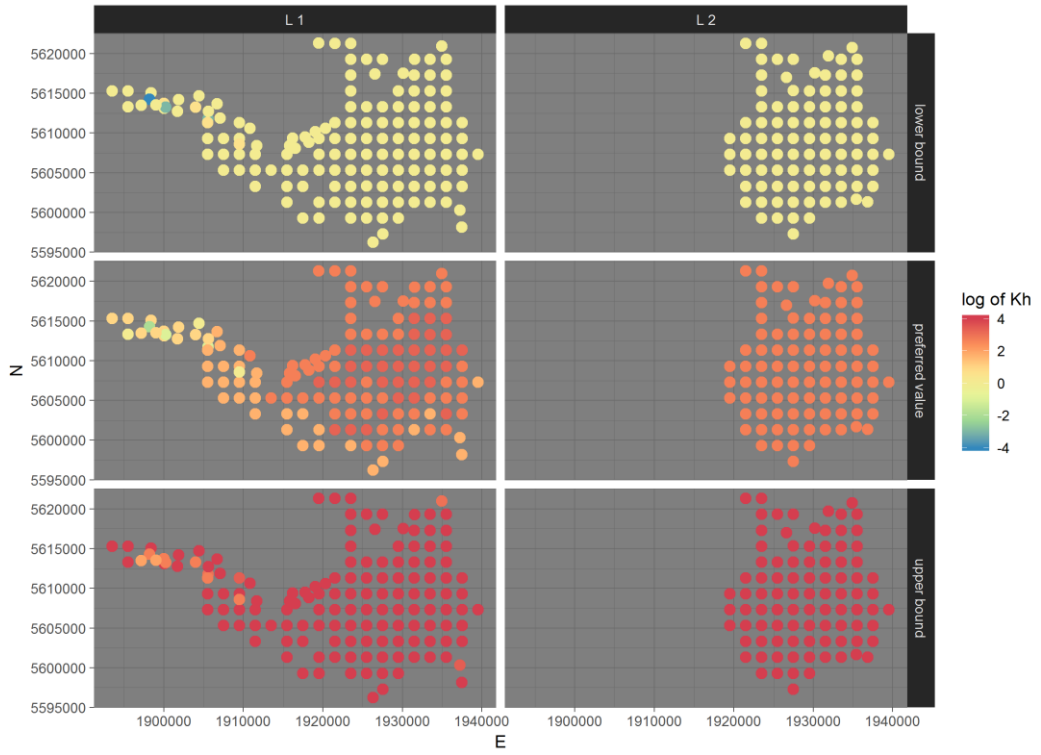

Figure 5-4: Spatial distribution of upper and lower bounds and preferred values for horizontal hydraulic conductivity (m/d).

Regularisation

Inverse problems, such as parameter estimation (calibration) of a complex groundwater model, often have non-unique solutions, which means that there are many possible parameter sets that will result in a calibrated model (Doherty, 2016a).

Regularisation is a term used to describe the process whereby a large number of parameters can be simultaneously estimated without incurring the numerical instability that normally accompanies parameter non-uniqueness. (Doherty, 2005)

PEST implements several types of regularisation. Methods used in this study are as described below.

Tikhonov Regularisation

Tikhonov Regularisation is a technique that works by supplementing the calibration dataset with expert knowledge about the parameters. This allows for specifying "default" values for parameters. The default value can be a specific value such as known aquifer conductivity (this is referred as "preferred value method"), or a relation to other parameters such as maintaining homogeneity ("preferred homogeneity"). In the calibration process the parameter will remain in this default position, unless the calibration data set contains the information that the parameter value should be different (Doherty, 2016a).

In this study the "preferred value" method was used, with preferred values shown in Table 5-2.

Singular Value Decomposition (SVD)

Singular Value Decomposition (SVD) is another regularisation technique implemented in PEST. It works by subtracting parameter combinations where the calibration dataset does not inform to the

calibration process.[1] This allows for a reduction in the computational burden of the calibration process. This technique is used in this study.

SVD-Assist

To reduce the computational burden of the calibration process, the SVD-Assist methodology was used. The method is part of the PEST suite and is described by Doherty (2016b) . The method works by replacing model parameters with a smaller number of "super parameters", and estimating these instead of the original parameter, and thus considerably reducing the number of model runs.

5.2.4 Model pre- and post-processing.

Model pre- and post-processing involves the use of several programs. While most of these programs are available within the PEST and Groundwater Data Utilities suite (Doherty, 2015), four programs were written as part of the current work to address specific tasks including data processing and formatting: (1) WELGEN (); (2) RIVGEN (); RIVERREAD(3); and TRENDCALC (4).

WELLGEN

This program applies a multiplier parameter QM_{irr} to the irrigation pumping. The program is written in R scripting language (R Core Team, 2018), using dplyr package (Wickham *et al.*, 2017) and is a custom function that allows for generation of the MODFLOW well package file. The program generates a well file for each of the sub models.

RIVERGEN

This program applies a multiplier parameter ($C_{rivMult}$) to the river boundary condition. The program is written in R scripting language (R Core Team, 2018), using dplyr package (Wickham *et al.*, 2017) and is a custom function that generates a MODFLOW river package file for each of the sub models.

RIVERREAD

This post-processing program facilitates calculation of total winter spring flow per group of springs, used as a PEST observation. The program is written in R scripting language (R Core Team, 2018).

TRENDCALC

This post-processing program calculates groundwater level trends in selected locations to be used as PEST observation. The program is written in R scripting language (R Core Team, 2018).

The integration of all pre- and post-model run processing steps, and a list of the programs executed within the calibration process, is summarised schematically in Figure 5-5.

[1] http://www.pesthomepage.org PEST FAQ accessed 12/04/2018

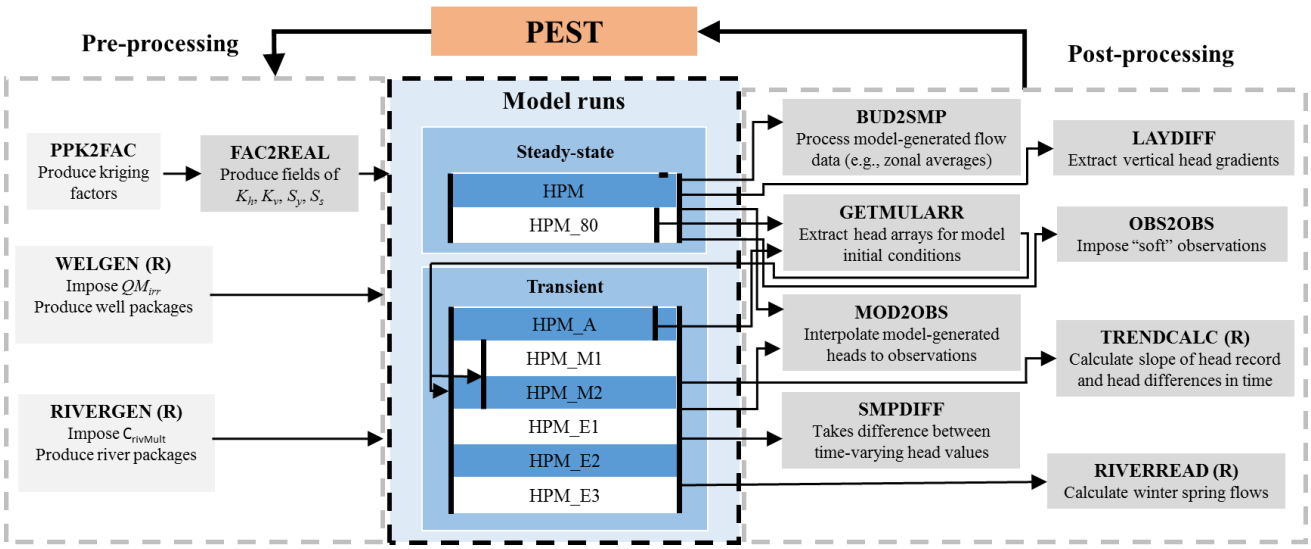

Figure 5-5: Flowchart illustrating pre-processing, model run and post-processing steps within the model calibration process.

5.3 PEST runs

Due to long model run times and a large number of parameters, PEST runs had to be undertaken using a high performance computing facility.

The New Zealand National eScience Infrastructure (NeSI) cluster hosted by University of Auckland was used. Ref. http://www.eresearch.auckland.ac.nz/

The cluster consists of more than 6,000 processing cores and allows for highly efficient computing of even large PEST runs. Typically, 200 cores were used during the calibration process and total of nearly 50,000 processing hours was used during PEST runs.

The cluster runs on a Linux operating system, so all model and PEST processing programs had to be recompiled to Linux for the calibration runs.

Multiple PEST runs have been undertaken, during which various model, and PEST setups were used (such as parameter and observation definitions, observations weights, regularisation and other options), until a satisfactory PEST performance was achieved. Each PEST runs consists of thousands of iterations of a model run.

5.4 Calibration results – match to observed values

5.4.1 Spring flow observations

The results show very good calibration to observed river gains, spring discharges and river losses for both winter and summer conditions (Figure 5-6). This indicates that the model is capable of representing surface water – groundwater flows and consequently is capable of estimating changes to these flows in response to various forces (for example groundwater pumping).

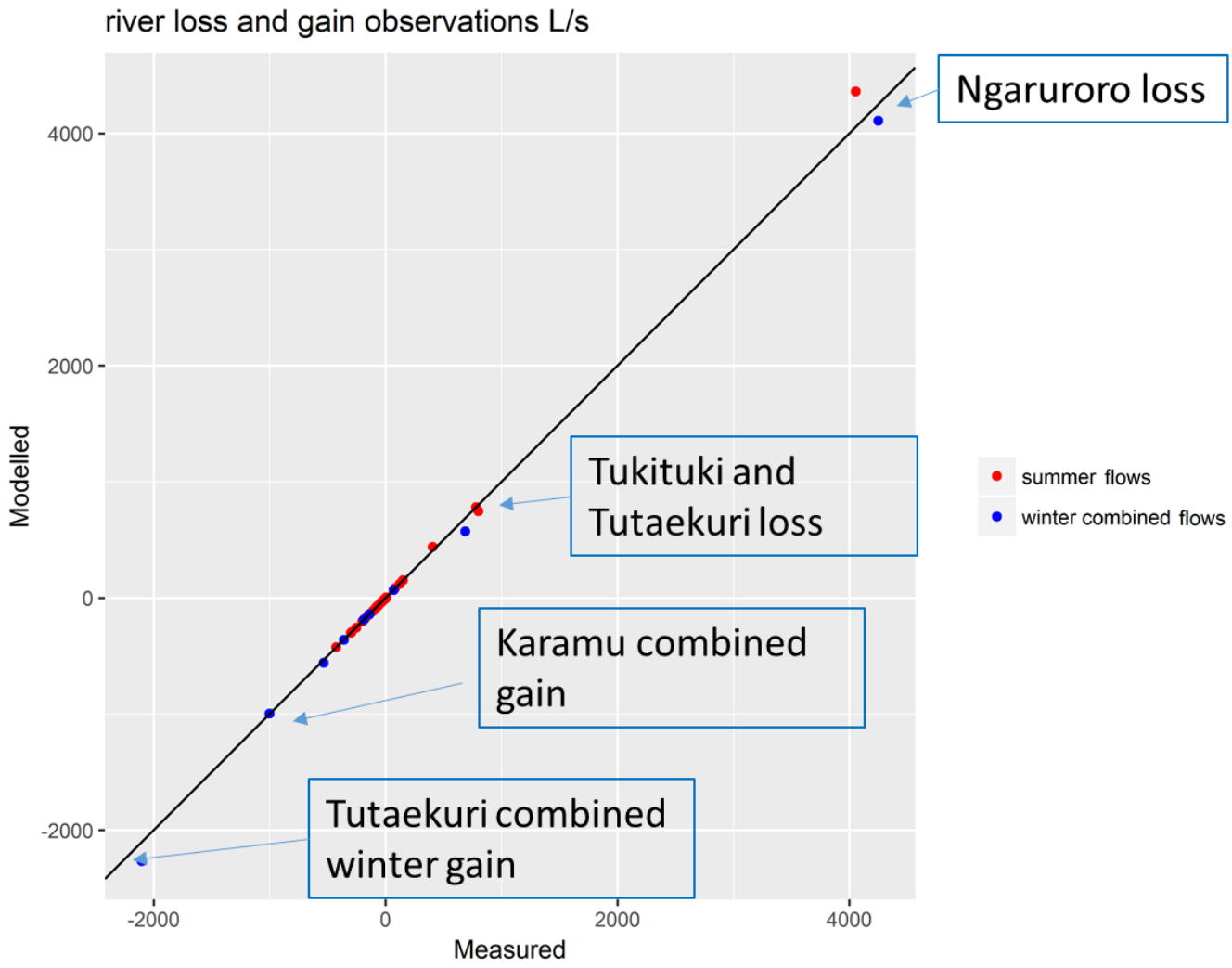

Figure 5-6: Measured vs Modelled river losses and gains, including springs

5.4.2 Steady state head observations

The steady state head observation results show a good match for the primary observation group and a reasonable match (with some scatter around slope 1) for the less reliable secondary and upper catchment groups (Figure 5-7 and Figure 5-8).

The goodness of fit is often measured using simple statistics such as Root Mean Squared (RMS) error and Scaled Root Mean Squared error (SRMS). Australian Modelling Guidelines (Barnett *et al.*, 2012) suggest using an SRMS value of less than 5% (or not more than 10%). Table 5-3 shows that the SRMS is slightly above a value of 5% for the primary head observation group.

Results (Figure 5-7) reveal a model bias to over-estimate high levels (>20 m) and to underestimate low levels (<20 m), particularly for the secondary observation group, although the secondary observation group has much lower confidence than the primary group (see discussion in Section 5.2.2). Since these observations are from the steady state model, there are limits as to how well this model can represent the transient groundwater flow process. A primary purpose of this model was to enable use of observations that could not be easily achieved in a transient model, such as average water levels, or water levels recorded in timeframes outside of the transient model temporal domain. Observations from the transient model, discussed in the next section, further enhance the observation data set. In this context, the nominal model bias is acceptable.

Overall, the results identify that the model is capable of representing the general flow pattern in the Heretaunga Aquifer System.

Table 5-3: Head calibration statistics.

Group	RMS (m)	Range (m)	SRMS %
Primary head group	1.19	21.48	5.54
Secondary head group	1.52	96.23	1.58
Upper valley head group	1.08	88.69	1.22

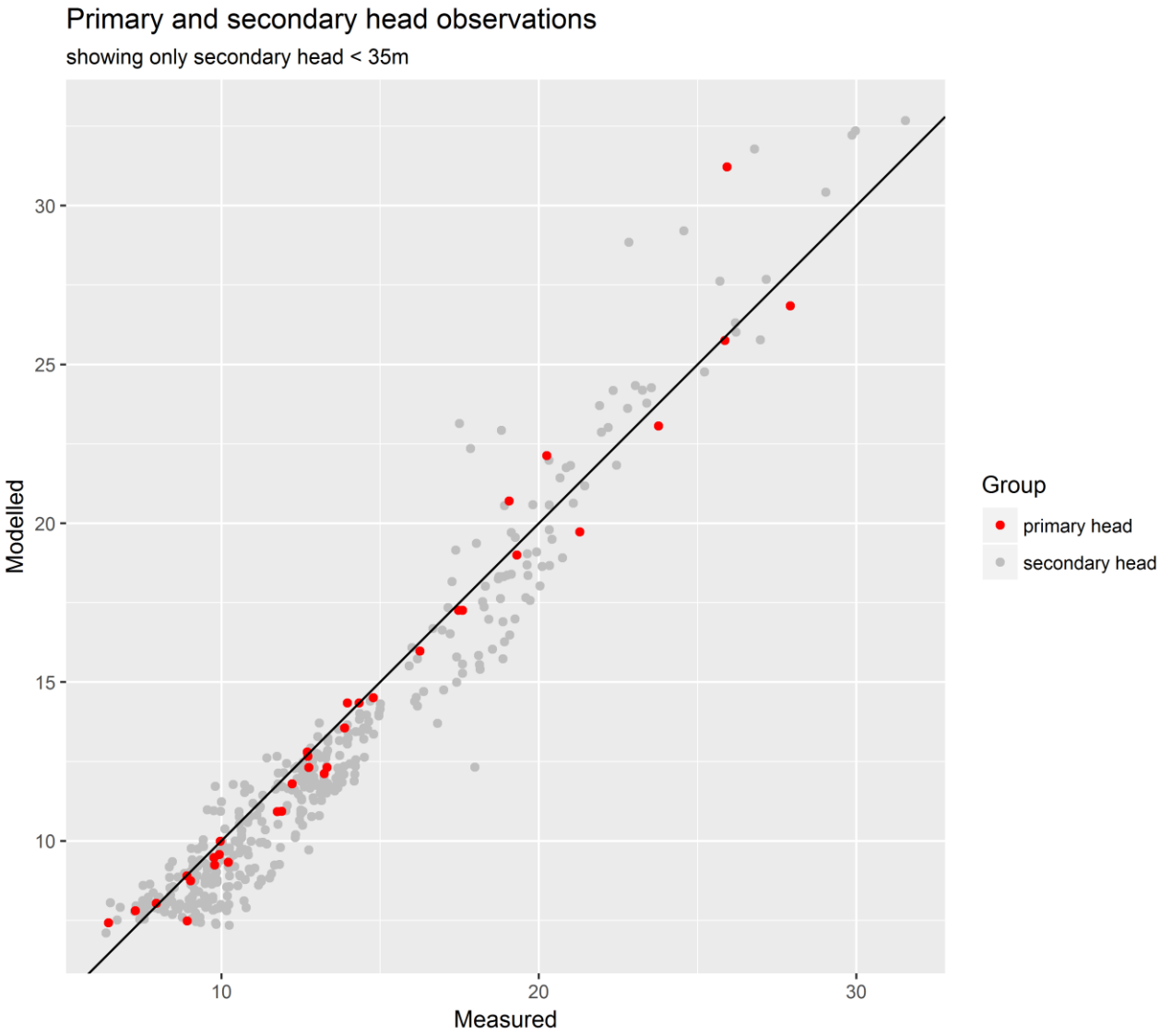

Figure 5-7: Measured and modelled heads for steady state observation groups.

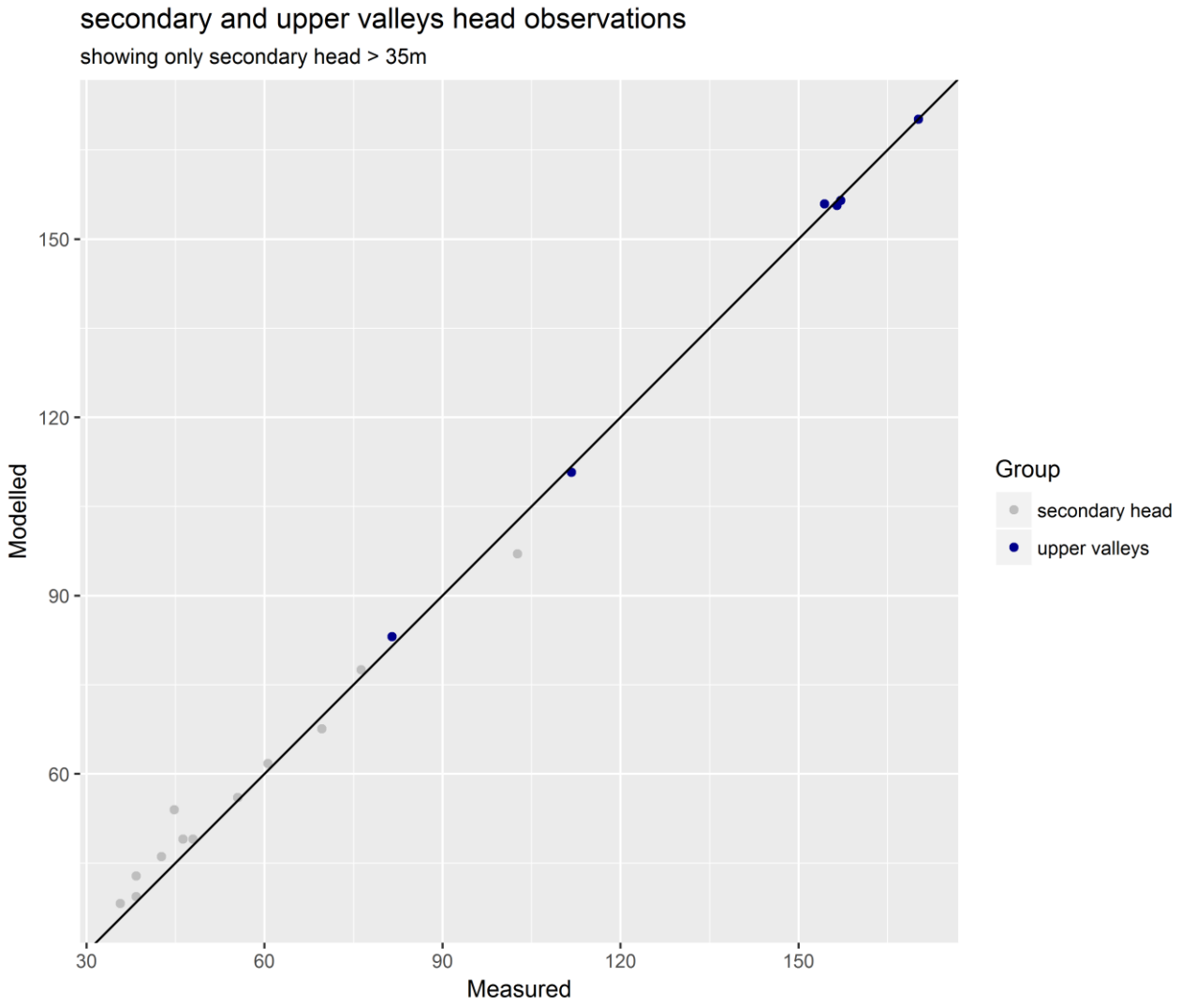

Figure 5-8: Measured and modelled heads for the steady state observation group - upper valleys.

5.4.3 Transient Calibration

Seasonal water level changes

Calibration to seasonal water level changes was assessed using results from the M1 and M2 models. These models run with monthly stress periods spanning April 1997–March 1999 ("HPM_M1") and April 2011–March 2015 ("HPM_M2"). Hydrographs comparing measured and modelled heads for these models are shown in Figure 5-9, Figure 5-10, Figure 5-11 and Figure 5-12.

These figures show that seasonal variation is generally well represented by the model for most of the monitoring locations, in terms of amplitude, timing and absolute groundwater level.

In some locations, where high frequency monitoring data is available (for example wells 3225, 3697), there are rapid water level fluctuations (particularly during summer) that cannot be fully represented by the model with monthly stress periods. Nevertheless, the overall patterns appear reasonable.

In some cases, the model shows a good calibration to seasonal amplitude and timing, but modelled absolute groundwater levels do not match the observed (for example well 10371).

In the bores 15794, 15795, 15796 and 15884, which are located in Moteo Valley, the calibration is deficient both in term of amplitude of fluctuations and absolute groundwater levels. The model over predicts water level fluctuations, and over predicts absolute water levels. This is likely to be a consequence of insufficient parameterisation (for example insufficient number of pilot points used), inadequate conceptual understanding of the Moteo Valley system, or possibly erroneous data (some additional information became available recently indicating that bores 15795 and 15796 might have been mislabelled in a database, which could explain some differences).

This deficiency in calibration is considered acceptable for the model purpose, however the uncertainty of predictions in the Moteo Valley is expected to be higher. This area of the aquifer is under relatively low stress in terms of the impacts of groundwater pumping on surface water flows, e.g. Tutaekuri –Waimate does not normally drop below critical levels, so more uncertainty in this area is acceptable.

To improve the calibration in the Moteo Valley area, the following is suggested:

- Increasing weights of observations in the Moteo Valley bores;
- Verification of appropriate layer designation in these bores;
- Introduction of additional pilot points for k and Sy/S.

Annual average water level

Annual average water level can be useful in improving overall calibration to:

- Absolute water level;
- Longer term water level changes (e.g. wet versus dry year, or long-term declines).

This is visualised on the basis of submodel A, which was run using yearly stress period from 1980 to 2015, as shown in Figure 5-13, Figure 5-14 and Figure 5-15. Visual assessment indicates a variable match of modelled and measured groundwater levels. In all locations the charts have been subjectively assessed and ranked. Of 43 plotted locations:

- Nearly half of locations show good calibration both in terms of absolute groundwater levels and water level changes;
- Most show good or reasonably close calibration to absolute groundwater levels;
- Most show good or reasonably close calibration to water level changes;
- Only several show poor calibration, both in terms of absolute groundwater levels and water level changes. These locations are described in Table 5-4

Overall, the annual average water level is predicted well by the model, and is acceptable for the modelling objectives, with calibration deficiencies mostly having local impacts. Some of the deficiencies could be addressed in the future.

Table 5-4: Annual model calibration deficiencies.

Bore	Location	Problem Description	Possible Reason	Impact on Model Prediction	Possible Solution
10371	Unconfined aquifer between Fernhill and Roys Hill	Model over predicts by about 1m and does not show declining trend	Insufficient parametrisation, weighting strategy	Local impact on absolute water level prediction, underprediction of trend	Increase number of pilot points in the area
3749	Coastal area	Model over predicts and shows opposite trend direction	Opposite trend direction is probably caused by deficiency of pumping data (e.g. there was pumping in this area that cause decline, that is not included in available pumping data)	Mostly affects historical scenario	Not likely to be resolved due to lack of historic pumping data
15795, 15796, 15884	Moteo valley	Shows poor calibration to absolute level	Insufficient parametrisation, weighting strategy, erroneous data	Local impact on predictions for Moteo Valley	Increase number of pilot points in the area, weighting strategy, data checks
5023	Located higher in a catchment	Model shows water level increase by about 15 metres, not shown in model data	Opposite trend direction is probably caused by deficiency of pumping data (e.g. there was pumping in this area that cause decline, that is not included in available pumping data)	Mostly affects historical scenario	Not likely to be resolved due to lack of historic pumping data
10371	Unconfined aquifer between Fernhill and Roys Hill	Model over predicts by about 1m and does not show declining trend	Insufficient parametrisation, weighting strategy	Local impact in unconfined zone	Increase number of pilot points in the area

Trends

Calibration to observed groundwater level trends is shown in Figure 5-16. This figure shows average annual groundwater levels, measured and modelled (for selected locations where data between 1995 and 2015 was available) and linear trend lines calculated for these datasets. In all but two locations, the model correctly predicts the observed declining trend. In about half of the cases, the trend predicted by the model is similar to the observed trend (i.e. slope of the trend lines are similar, for example at bore 15006). There is a good match in the location with the highest observed trend (bore 15005), but the model underestimated trends in other locations where a notable trend was observed, such as bores 15004 (the model predicts no trend), 10356 and 10371. In locations 705 and 3749 the model failed to replicate an observed rising trend.

Overall, the model appears capable of representing observed declining trends in most areas, particularly in the area where the largest trend was detected, but this was not achieved everywhere. The reasons for this might be as follows:

- Deficiency in model parametrisation (e.g. insufficient number of pilot points)
- Insufficient boundary condition setup (e.g. trend may be driven by changes to processes that cannot be adequately represented in the model, such as river bed erosion).
- Insufficient or erroneous pumping data used in the model.

Current data availability and resource limitations for this assessment did not allow for improvement in calibration to trends at this time, but future work programs should target and aim to improve those few areas of poor model performance.

Event based water level changes

Calibration to events (Figure 5-17) shows that to some degree, the model is able to replicate observed responses of groundwater levels as a result of flooding events in the Ngaruroro River. In some locations (e.g. bore 16360) the match is very good both in terms of amplitude and timing. There are however some discrepancies. For example, bore 10371 shows a response, but the modelled response is attenuated. In bore 2801, there is a good match in the event E2 in May 2001, but a poorer match to event E1 during July 1991. In general, the model appears to adequately match responses to river flooding at most key bores but at some sites/times it underestimates the peak. Achieving a better match would likely require more refined parametrisation and possibly a more realistic boundary condition, type such as stream flow routing (Modflow SFR package).

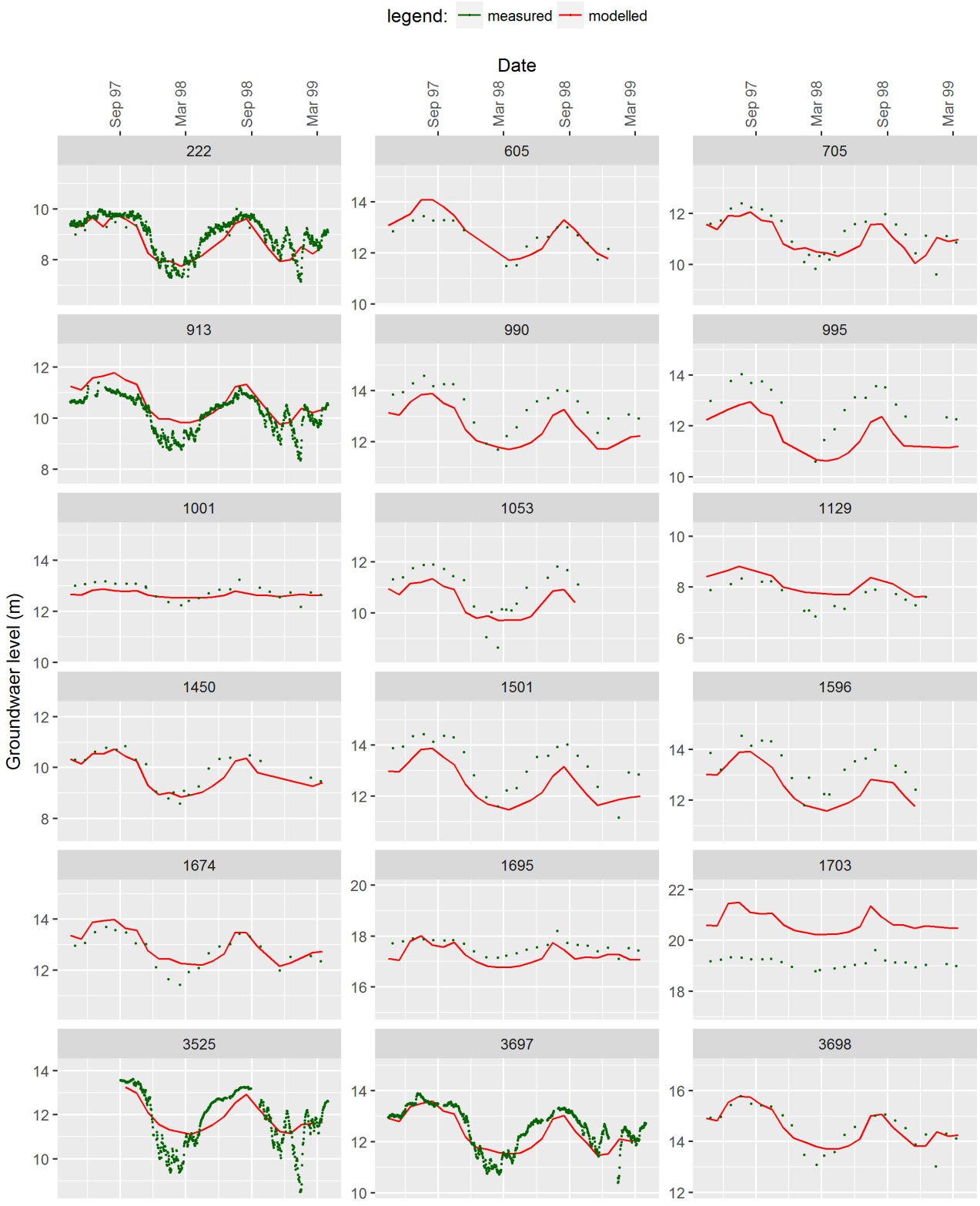

Figure 5-9: Hydrograph of measured and modelled head for M1 submodel (part1).

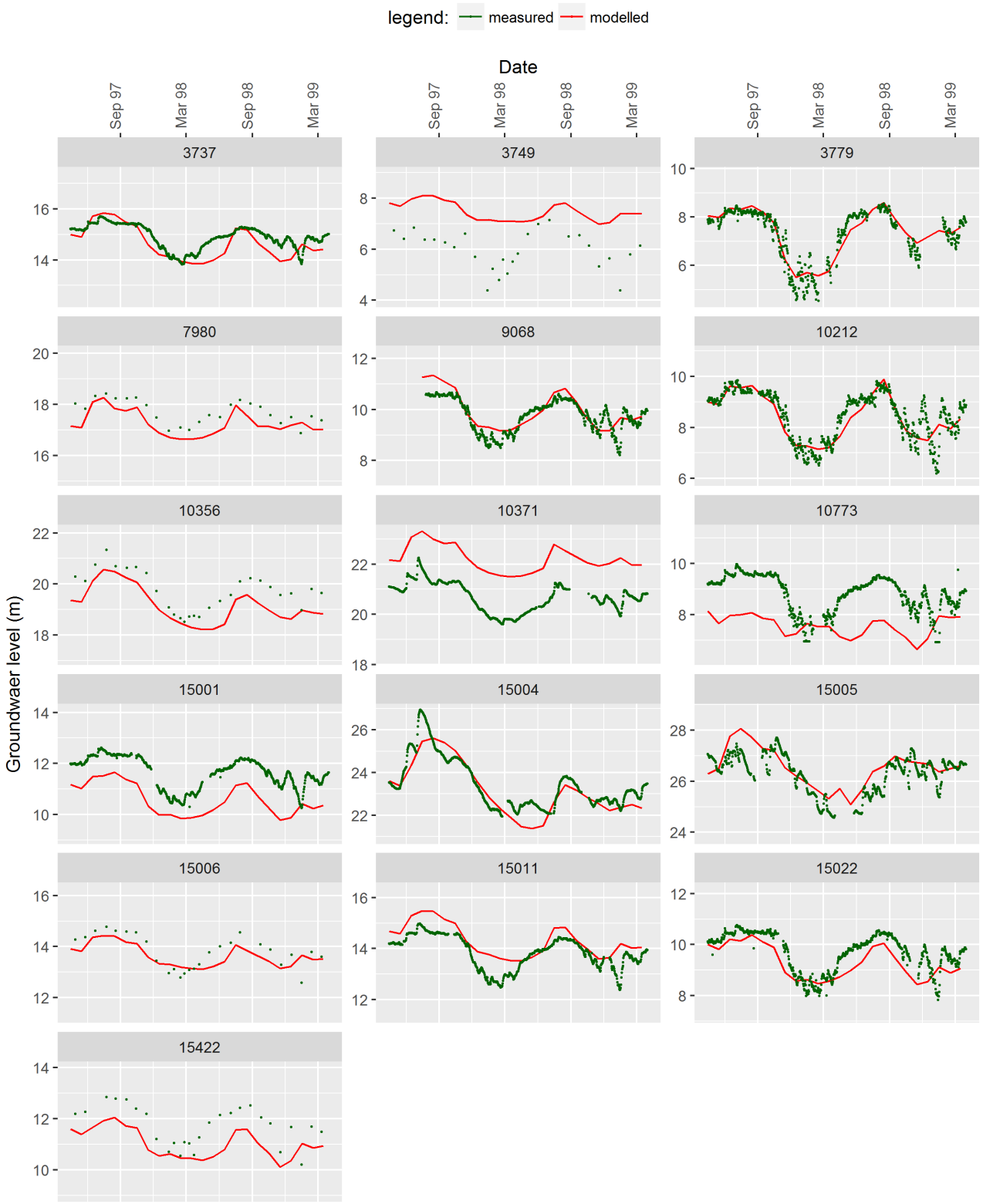

Figure 5-10: Hydrograph of measured and modelled head for M1 submodel (part2) .

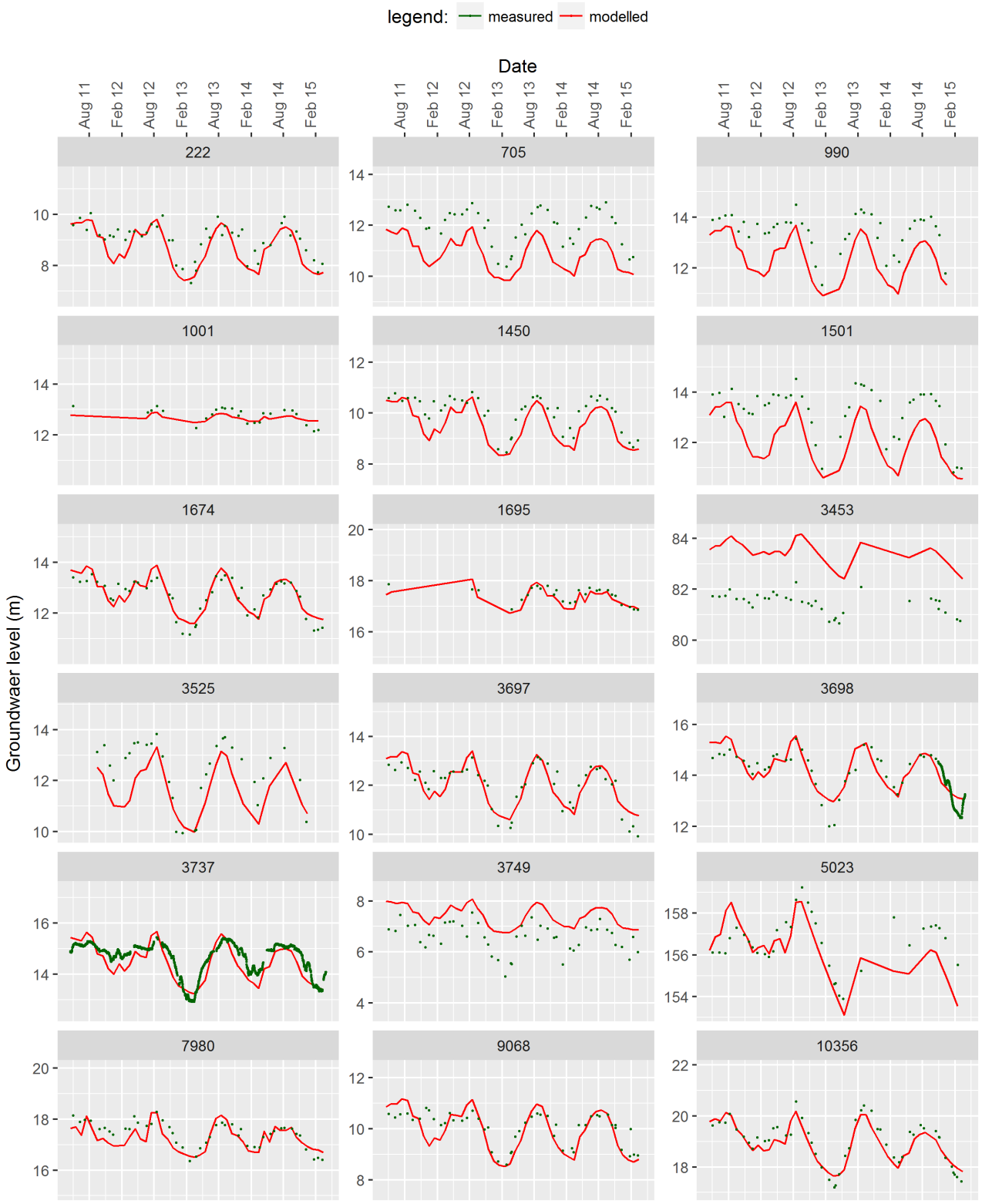

Figure 5-11: Hydrograph of measured and modelled head for M2 submodel (part1) .

Figure 5-12: Hydrograph of measured and modelled head for M2 submodel (part2).

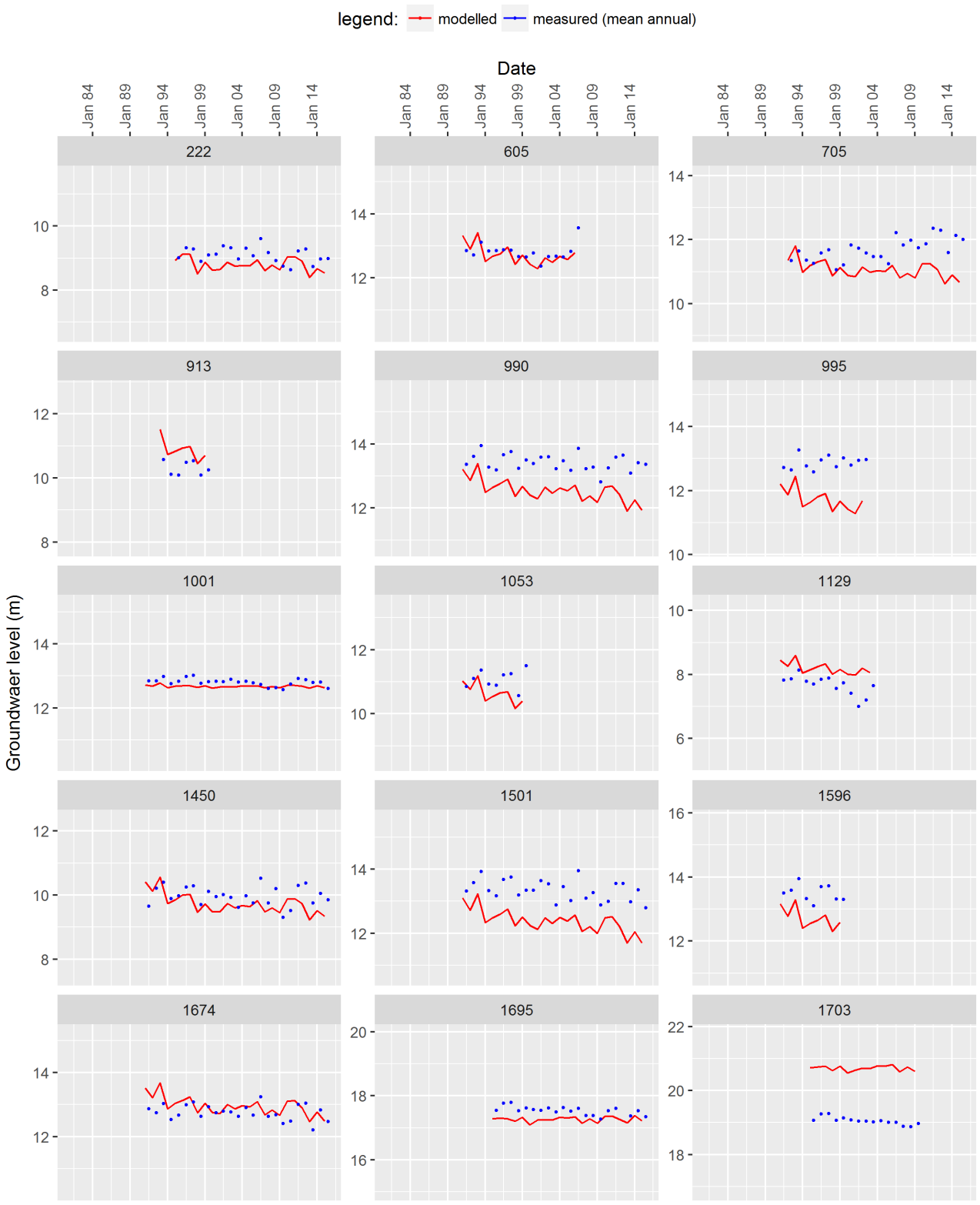

Figure 5-13: Hydrograph of measured and modelled head for A (annual) submodel (part 1) .

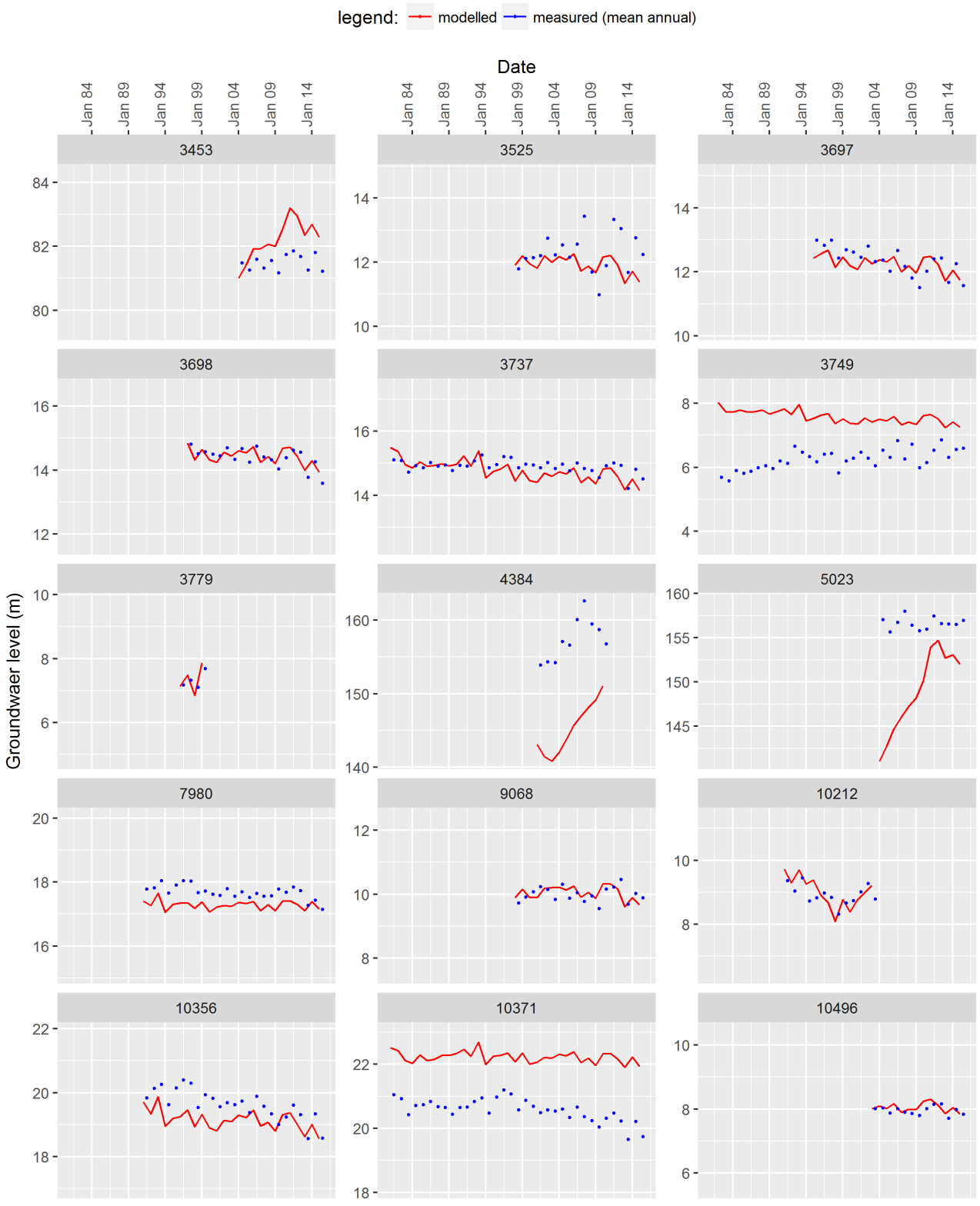

Figure 5-14: Hydrograph of measured and modelled head for A (annual) submodel (part 2).

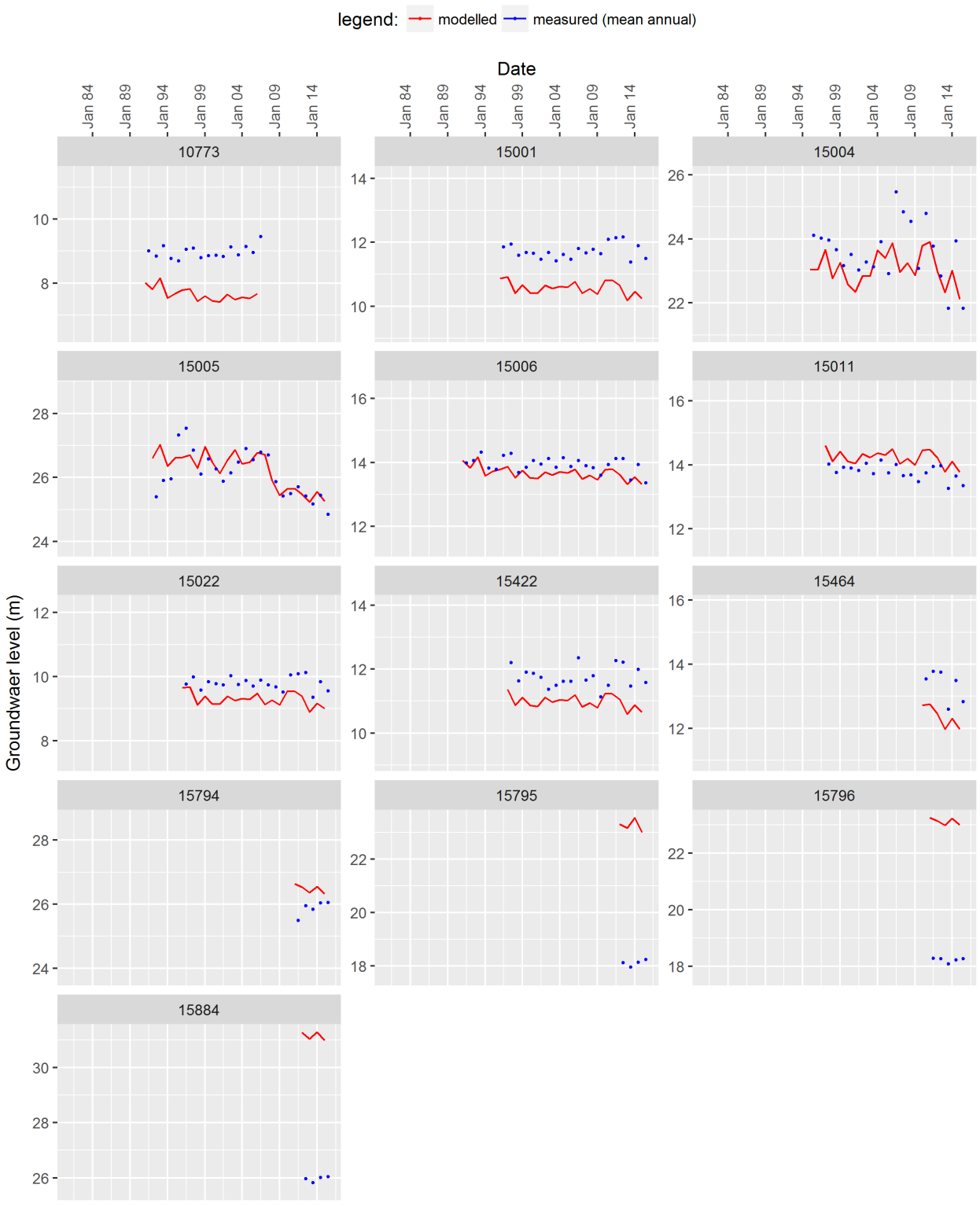

Figure 5-15: Hydrograph of measured and modelled head for A (annual) submodel (part 3).

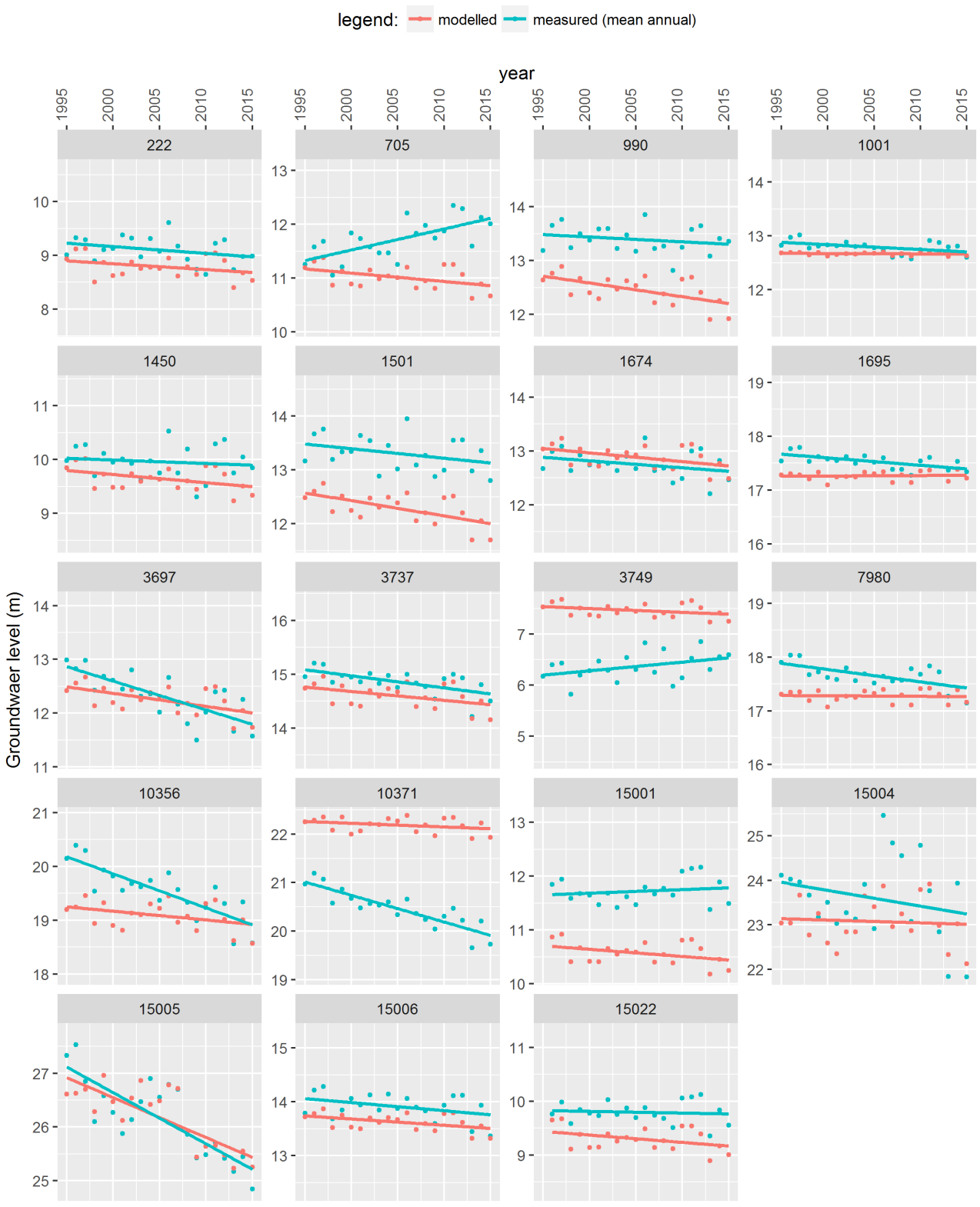

Figure 5-16: Observed and simulated trends in groundwater levels.

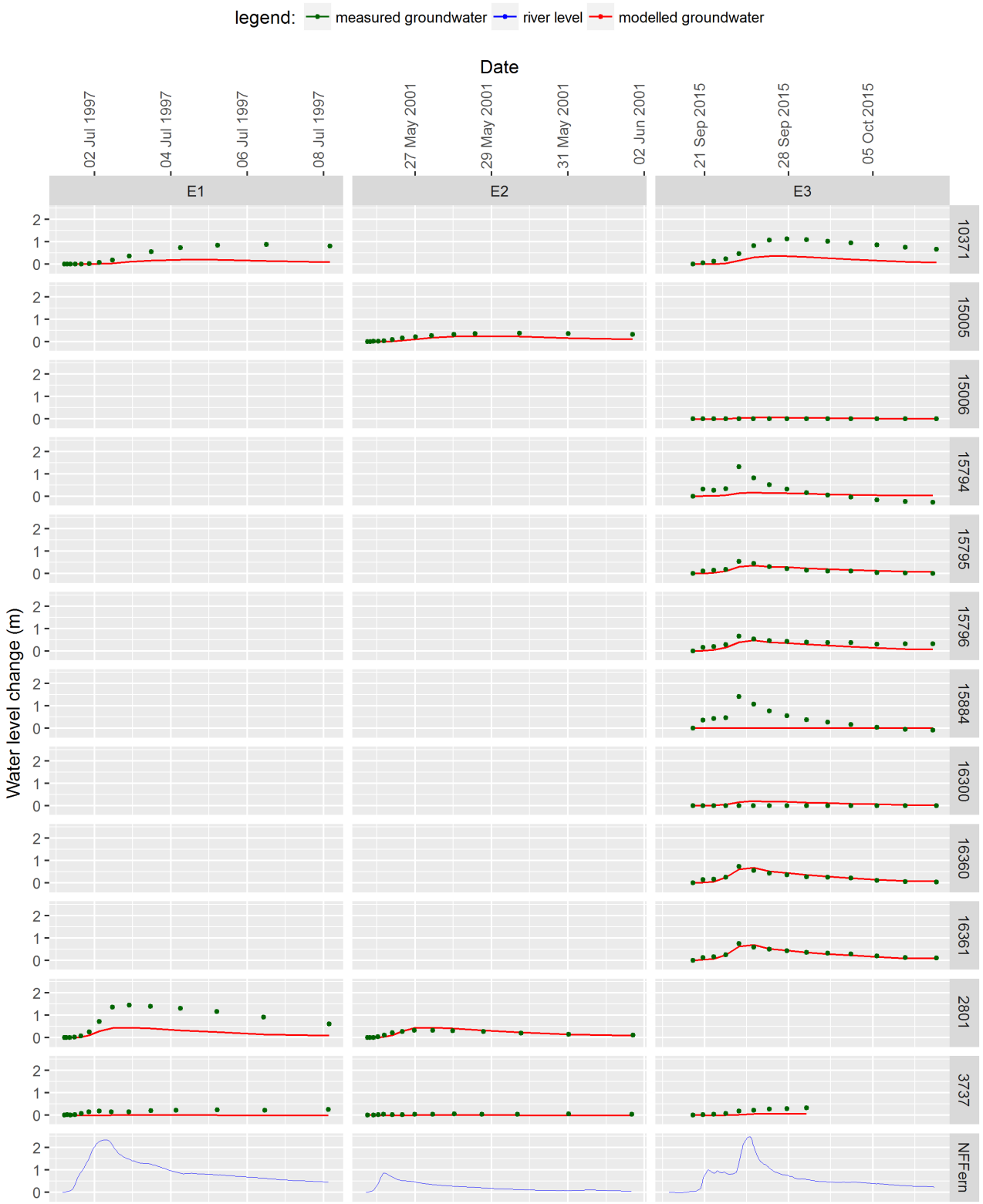

Figure 5-17: Calibration to river flooding events. Hydrographs of water level change in metres per observation well including Fernhill river stage (NFern) are shown in rows for three events (columns).

5.4.4 Model verification

After the calibration, using a set of combined models with varying time scales and time discretisation (as explained in Section 5.2.1), the model was reassembled into a single transient model simulation run at a monthly stress period from 1980 to 2015 (this simulation is referred to as “M3” model). The base case uses the same stresses (pumping, recharge) as the calibration model, but a monthly stress period was applied. The results of this model run were then used for model verification.

The results indicate that the model represents observed groundwater level dynamics well, as shown in 43 hydrographs presented in Figure 5-18, Figure 5-19, Figure 5-20 and Figure 5-21. Both absolute groundwater levels and groundwater level variations are represented well in most cases. For example, the model managed to replicate small variations in water levels as observed in bore 1001 and much larger variation in bore 990. In some cases the model replicates observed longer term changes, such as in bores 15005 and 10356 where a groundwater decline is replicated.

However, there are still some discrepancies, for example absolute groundwater level is not matched in some wells, such as 10371 near Fernhill, and the pairs of bores in the Moteo valley (15794 & 15884; 15795 & 15796).

5.4.5 Future model improvements

Possible ways to improve the model calibration have been suggested in earlier paragraphs. These measures are likely to improve the calibration, however full success cannot be guaranteed. The effort to achieve any improvement is significant due to the complexity of the model setup. Consequently, due to time and budget constraints, this work has been deferred.

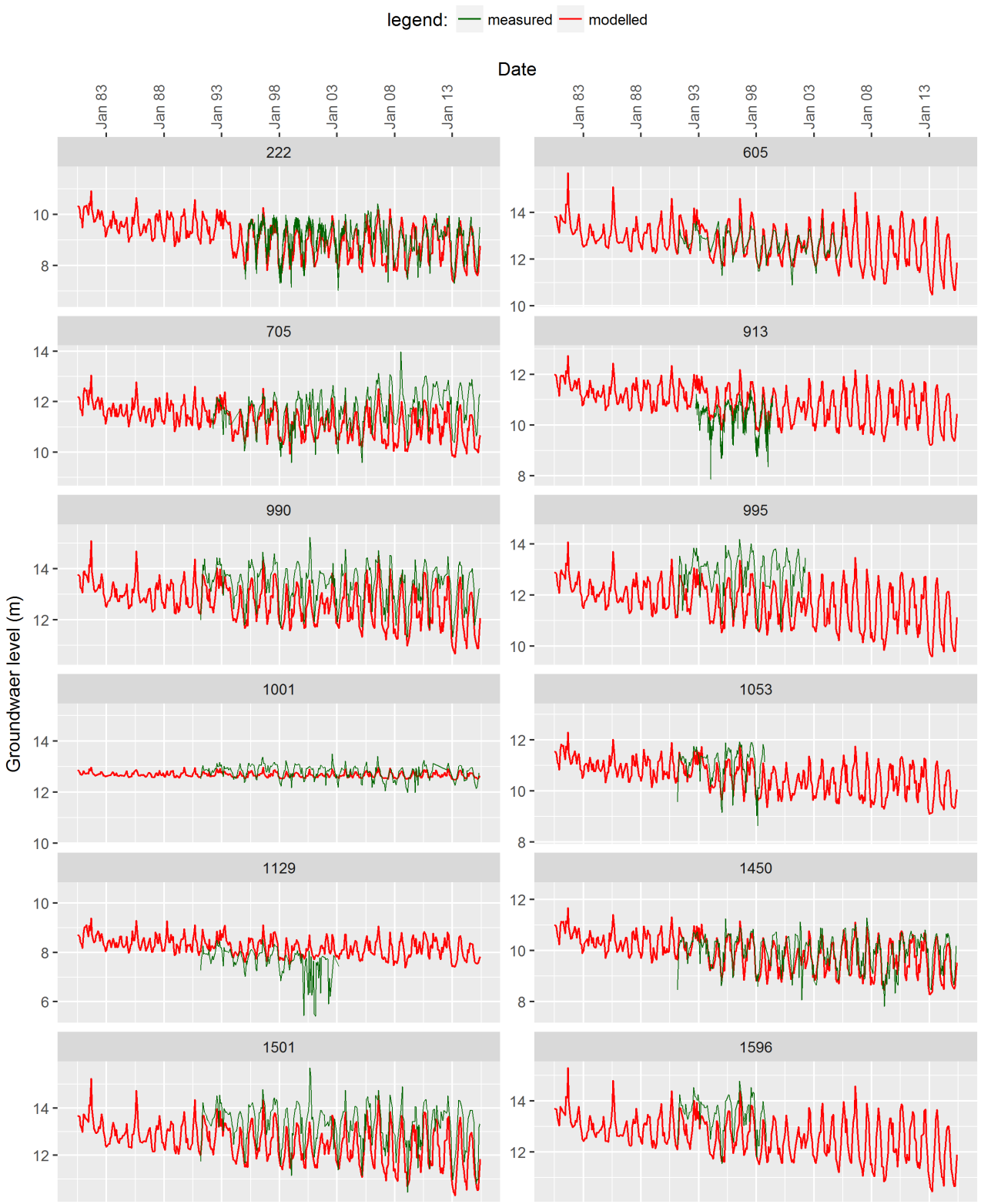

Figure 5-18: Model verification groundwater hydrographs (part 1).

Figure 5-19: Model verification groundwater hydrographs (part 2).

Figure 5-20: Model verification groundwater hydrographs (part 3).

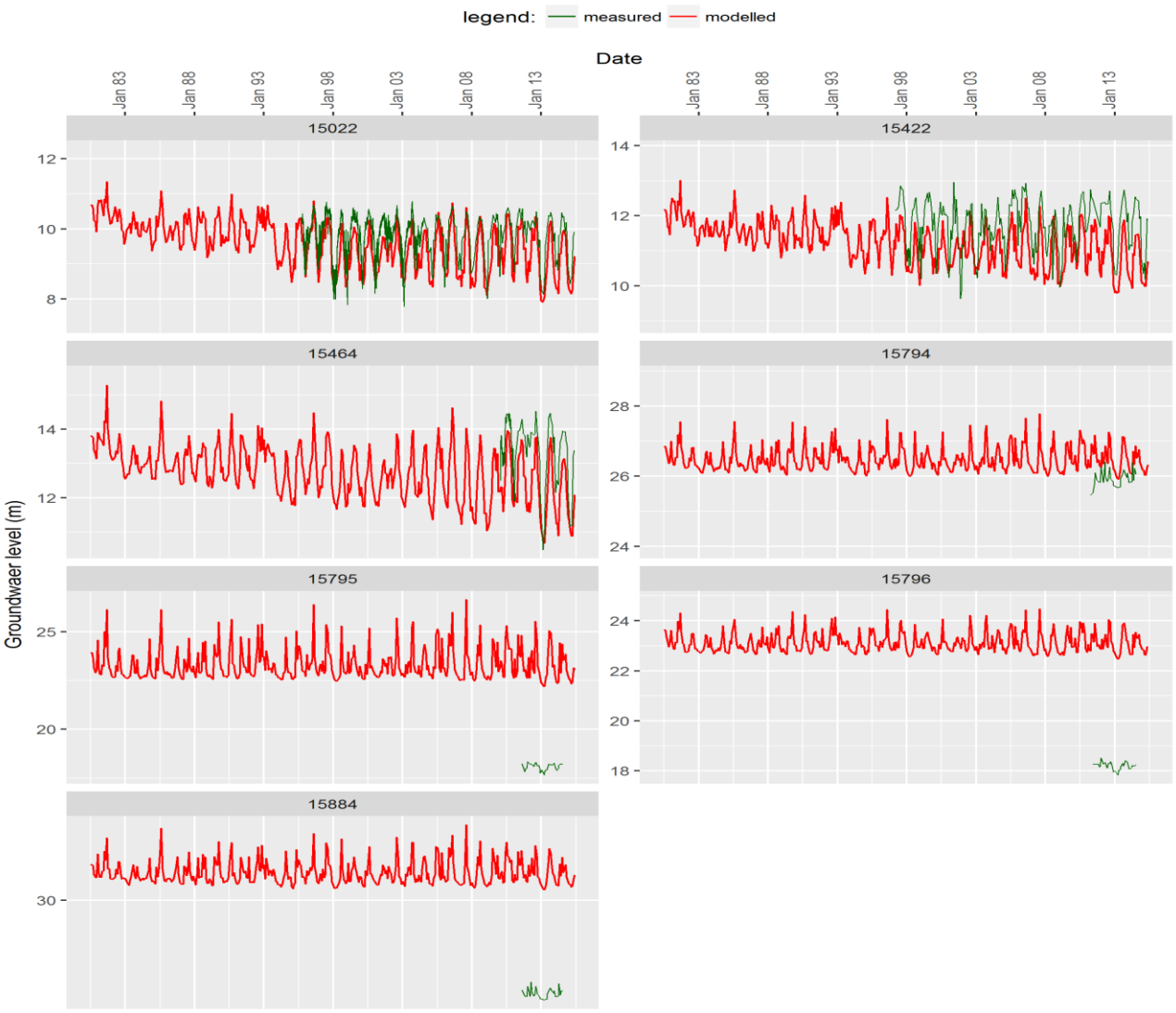

Figure 5-21: Model verification groundwater hydrographs (part 4).

5.5 Final calibrated model

5.5.1 Model version

The model set-up and calibration process was recorded in a comprehensive modelling log. This modelling log is not provided here because of its large size, which makes it difficult to print. The log will be made available with the electronic version of the model.

The final calibrated model described here has version number HPM035. Specifically, most of the model scenarios, which will be described in a separate report, are based on monthly 1980-2015 verification simulation (referred to as "M3" as described in section **Error! Reference source not found.**).

5.5.2 Aquifer Parameters

Horizontal Hydraulic Conductivity

Figure 5-22 shows the calibrated horizontal hydraulic conductivity field and demonstrates significant spatial variability of aquifer conductivity. Figures 4-1 and 4-2 present the top and bottom elevations and the thickness of the two layers.

When compared with the hydraulic conductivity measured from pumping test data (Figure 3-26), the calibrated conductivity shows more variability, although there is resemblance in the distribution. For example:

- The central part of the plains exhibits high aquifer conductivity;
- There is an area of high conductivity near the southern edge of the plains;
- Lower conductivity occurs at the Kikowhero terrace, around Paritua stream, and in Layer 1 in near Tukituki River;
- Very low hydraulic conductivity in Layer 1 at zones that separate terraces from the Ngaruroro River valley (as expected because this is required to achieve the observed head difference between terraces and the river valley).

Notable differences in distribution are:

- The calibrated model shows an area of very high conductivity and unconfined storage near the Tutaekuri River loss area;
- Lower conductivity in Layer 1 in the Twyford area.

Vertical Hydraulic Anisotropy

Figure 5-23 shows the calibrated hydraulic anisotropy field (ratio of horizontal to vertical conductivity Kh/Kz). Higher values indicate highly anisotropic conditions with vertical hydraulic conductivity being much lower than horizontal, resulting in restricted vertical flow. The vertical anisotropy distribution indicates high anisotropy in Layer 2 (and therefore lower vertical conductivity) in the central part of the Heretaunga aquifer and in the Moteo Valley, with lower anisotropy in the southern part of the aquifer. This is consistent with the vertical head difference data that indicated head difference near the coast and near Fernhill.

Unconfined storage

Figure 5-24 shows the calibrated unconfined storage field, which exhibits significant variability in unconfined storage for Layer 1. Notable features are low storage near the Ngaruroro recharge area between Fernhill and

Roys Hill, which is less than the preferred storage parameter set in PEST. This is unexpected, as conditions in this area are likely to remain unconfined, and the gravel aquifer may be expected to have relatively high storage. The low storage value may be a consequence of calibration to a river flooding event, which required a low storage parameter to achieve a match with observed response to river flood and reduction of the objective function.

The calibrated unconfined storage field shows some variability in the confined area of the aquifer (an explanation of why the unconfined storage parameter is used in the confined area of the aquifer is provided in Section 4.5). This is unexpected because this area of the aquifer remains fully saturated throughout the simulation, which means the model calibration should not be sensitive to unconfined storage. Normally regularisation using a "preferred value" method would result in the calibrated value remaining at the preferred value. It appears that a reason for this behaviour in the northern part of the aquifer might be due a minor error in model setup, namely in two locations a preferred value has not been set up, which could have allowed the parameter value to deviate from a realistic value unexpectedly. Whatever the reason for this behaviour, it is unlikely to have an impact on any modelling scenarios, provided that the confined aquifer remains saturated, which would be expected in most scenarios.

Layer 2 was only represented by one parameter, which remained at the preferred value of 0.1. This parameter should not have any effect unless under extreme scenarios if desaturation of this layer occurred.

Confined Storage

Figure 5-25 shows the calibrated confined storage (Specific Storage) field, which exhibits spatial variability of confined storage for both model layers.

5.5.3 Other parameters

Rainfall recharge and Irrigation multiplier

Table 5-5 shows calibrated land surface recharge and irrigation multiplier parameters. Values of these parameters did not change substantially during the calibration and remained within 1% of the original value of 1.

This may mean that:

- Parameters are applied as global multipliers and because of that, the objective function was not sensitive to these parameters (i.e. spatial and temporal differentiation of these parameters could have resulted in more sensitivity);
- The original values for recharge and estimates based on irrigation demand applied in the model are close to the actual (i.e. accurately estimated).

Additional work has been undertaken to explore uncertainties related to model parameters, including recharge and irrigation multipliers, and this will be documented in subsequent reports.

Multiplier	**Calibrated value**
Irrigation pumping	0.989
Land surface recharge	0.994

Table 5-5: Land surface recharge and irrigation pumping multiplier - calibrated values

River Conductance

Figure 5-26 shows calibrated river conductance values for winter and summer conditions. The highest conductance values are in locations of major river-aquifer interactions, such as losing sections of the Ngaruroro, Tukituki and Tutaekuri rivers, along with spring-fed streams (such as the Karamu, Tutaekuri-Waimate and Raupare).

Coastal Boundary

Figure 5-27 shows the calibrated coastal boundary GHB conductance. The most notable feature is very high conductance near the southern edge of the model, with much lower conductance elsewhere. This is not entirely unexpected, because of the presence of generally lower groundwater levels in the south-eastern section of the aquifer, with an absence of any groundwater discharge area (such as surface springs or major pumping), which could suggest offshore discharge. This appears to be in agreement with the geological understanding of this area (i.e. the presence of Tukituki River gravel deposits), as described in the Leapfrog model (Lee *et al.*, 2014).

Drain Conductance

The calibrated value of distributed drain conductance is 5.2×10^{-3} m^2/d.

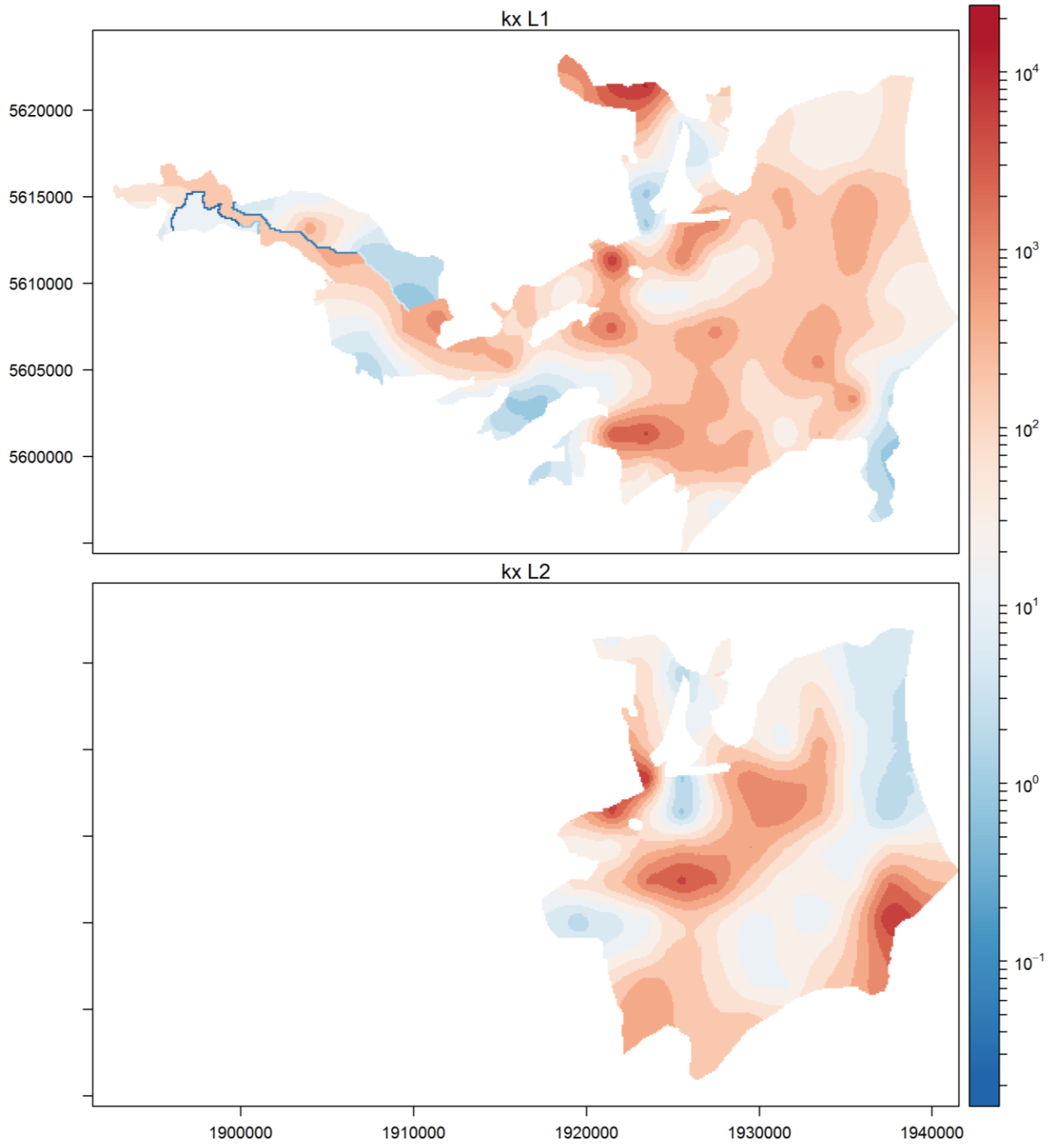

Figure 5-22: Calibrated parameter fields for horizontal hydraulic conductivity (m/d).

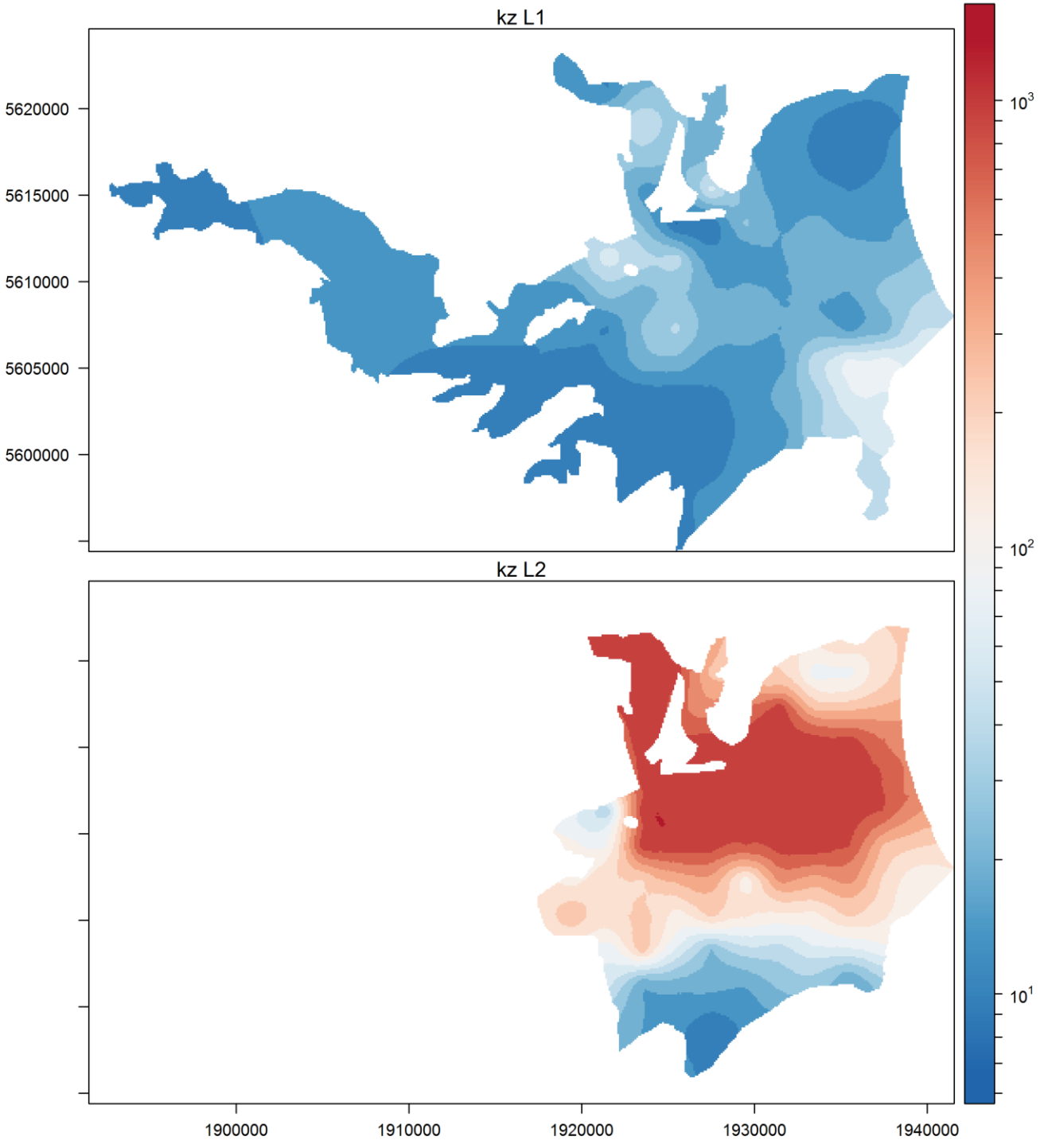

Figure 5-23: Calibrated parameters field for vertical hydraulic anisotropy.

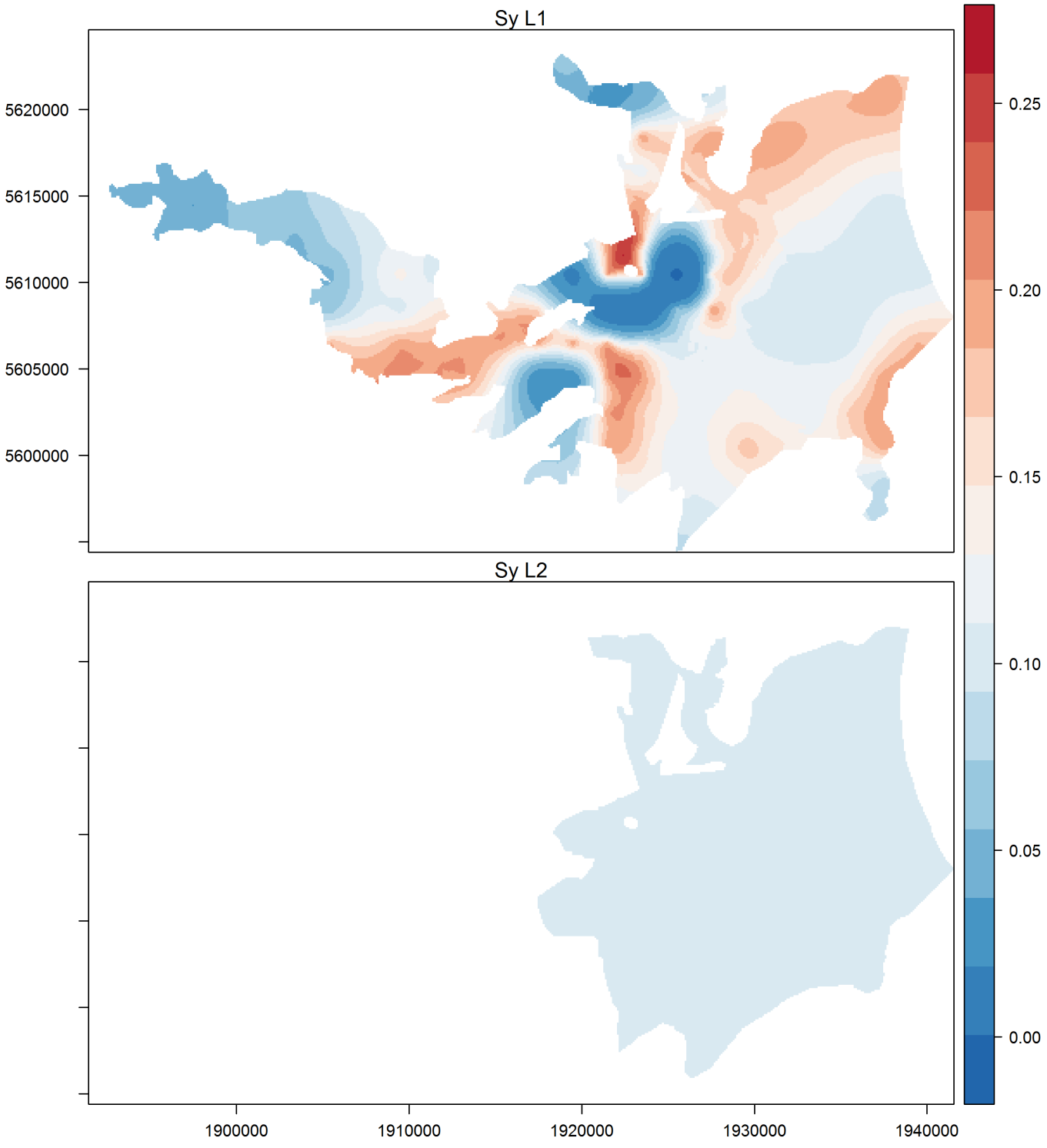

Figure 5-24: Calibrated unconfined storage Sy.

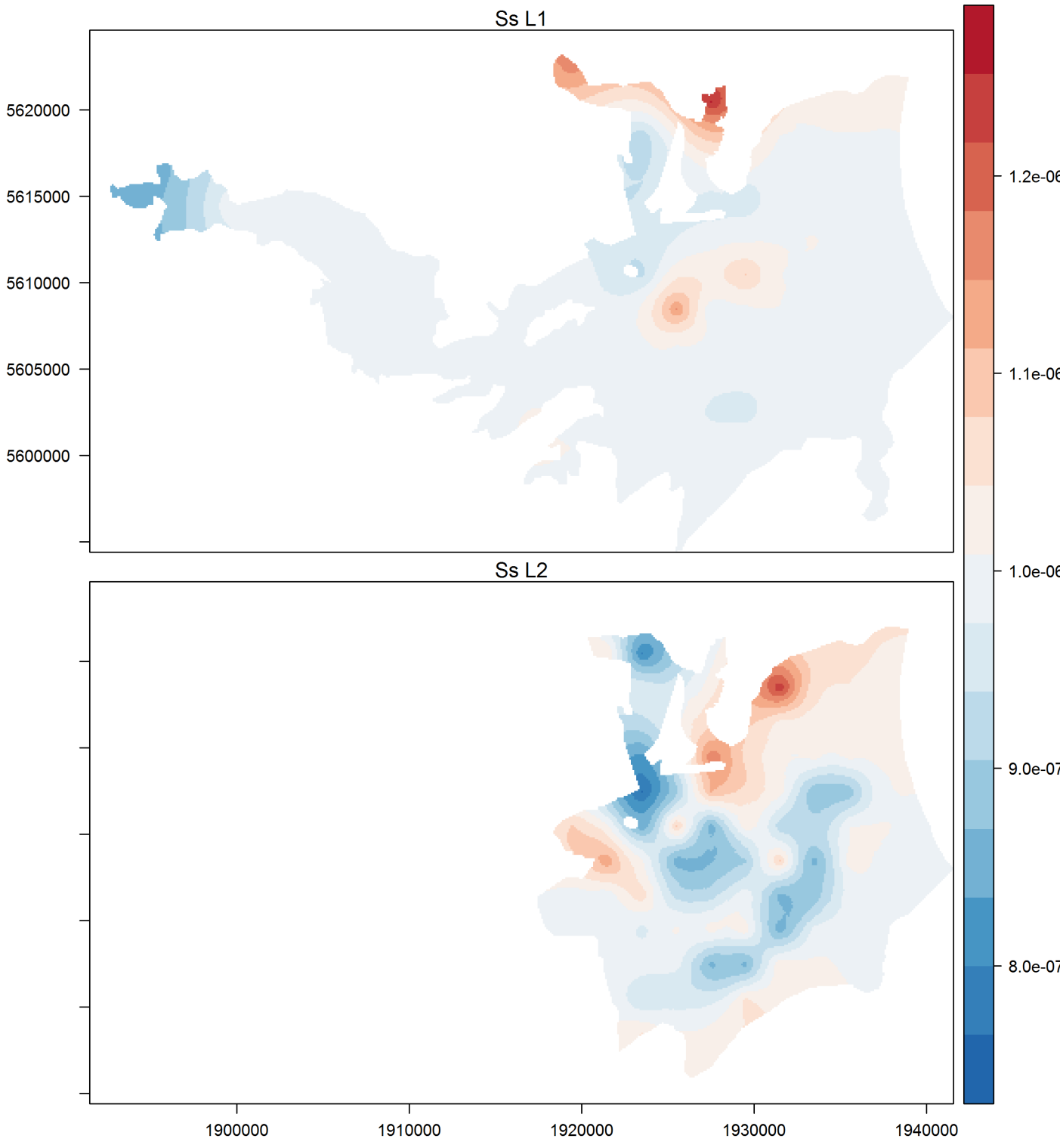

Figure 5-25: Calibrated Specific Storage Ss (1/m).

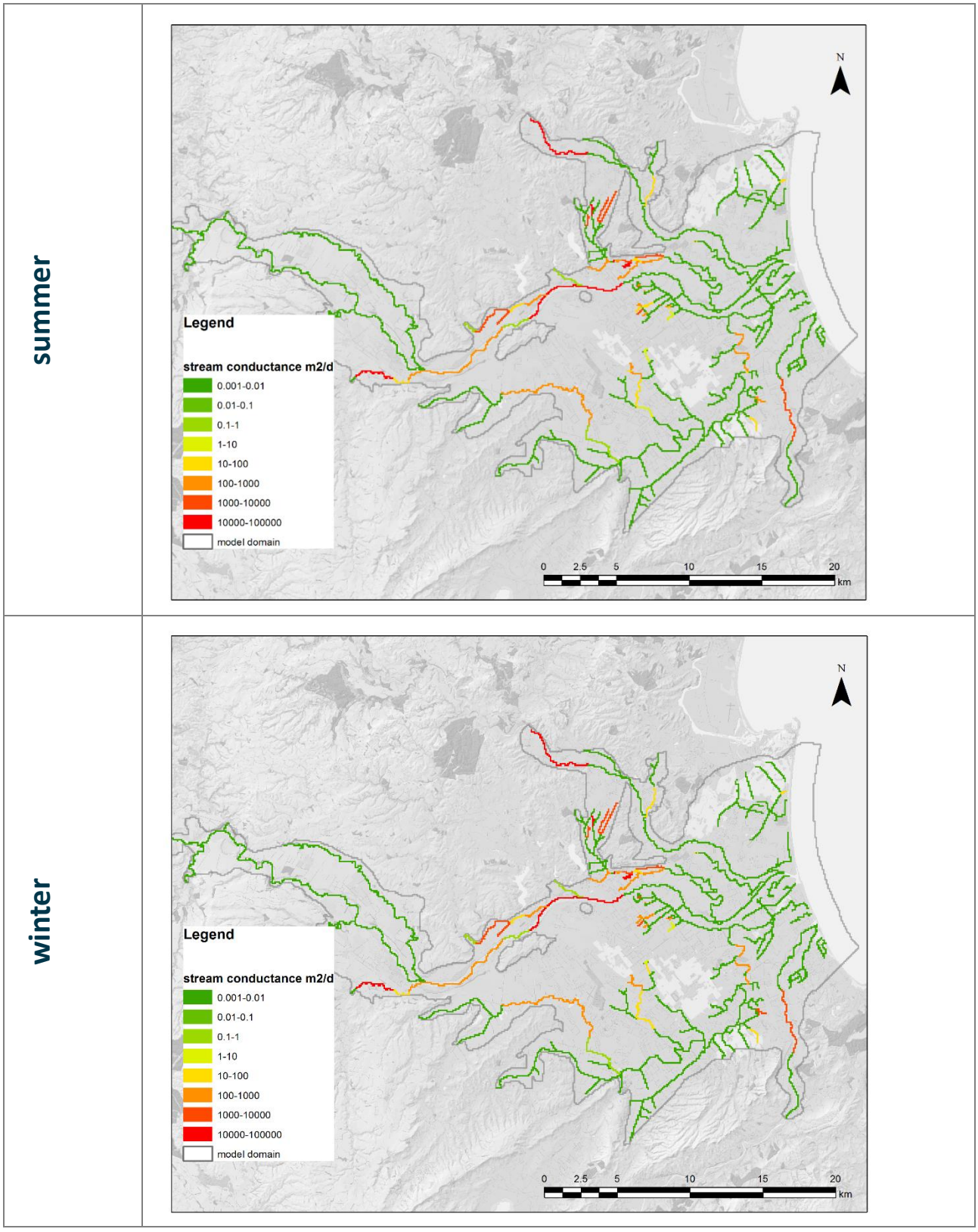

Figure 5-26: Calibrated river conductance (summer and winter).

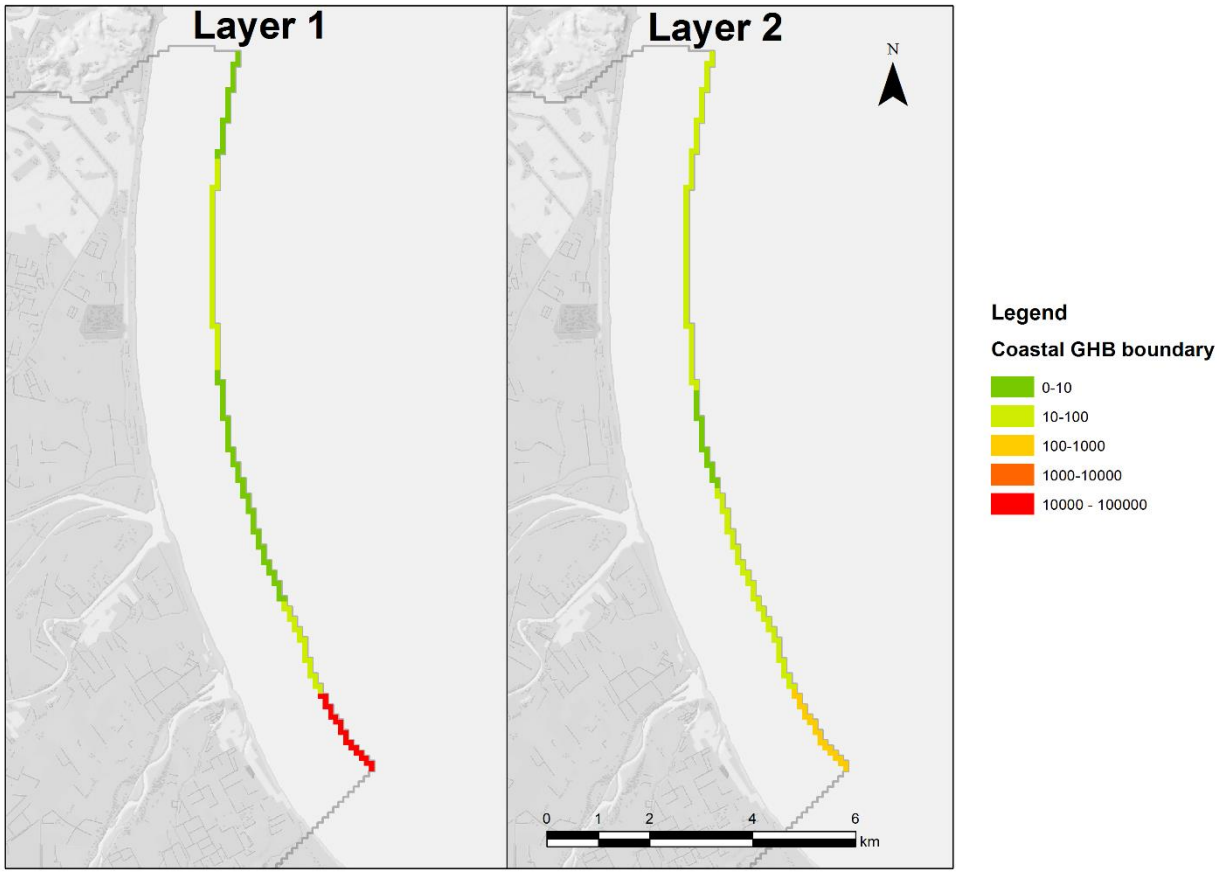

Figure 5-27: Calibrated GHB boundary. Colours represent boundary conductance m^2/d.

6 Model limitations and capability

6.1 Capability

The calibration has achieved a good match to observed spring flows and river losses, along with seasonal and long-term water level changes. Therefore, the model can be considered suitable for simulating the effects of groundwater pumping on river flows, along with and seasonal and long-term changes of groundwater levels. Potential management scenarios that may be informed by these simulations include:

- Estimation of stream depletion effects on known springs due to groundwater pumping anywhere in the model domain, including effects on individual springs;
- Estimating the potentially beneficial effects of mitigation strategies (such as pumping bans, MAR, etc) on stream flows and groundwater levels;
- Estimation of cumulative stream depletion effects from multiple groundwater users;
- Estimation of changes in stream flow and groundwater levels as a consequence of changing groundwater abstraction or changes in climate.

This means that the model is able to fulfil modelling objectives 1 to 6 as specified in Section 0.

Because the calibration has been undertaken using PEST, the model can form a basis to undertake uncertainty analysis in PEST, which will fulfil objective 7 as specified in Section 0.

The model is also able to represent general groundwater flow direction. This means that it may be used for:

- Contaminant transport modelling using MT3D;
- Flow path analysis (for water age or source protection zones assessment);
- Seawater intrusion modelling.

The model may also be used as a basis for other models that may subsequently fulfil modelling objectives 8 to 10 as specified in Section 0.

6.2 Limitations

6.2.1 Uniqueness of model calibration

Although the model is well calibrated, this does not necessarily mean that there is no uncertainty in model parameters and consequently predictions. In particular, the calibrated solution is likely to be non-unique, which means that there may be other different parameter combinations that may result in similarly calibrated models. Doherty (2016a) gives a detailed discussion of this problem.

This means that despite a reasonable calibration, there is a residual uncertainty remaining. This is a common issue in all groundwater models. Uncertainties have been explored using a calibration-constrained Monte Carlo analysis (Knowling, 2018) and the impacts on model predictions will be explored in a subsequent report.

6.2.2 Limitation of model calibration

Poor match to observation data

As described in Section 0, the model match to observed data is not perfect and in some locations or time periods the model does not completely represent groundwater levels or dynamics. This is particularly the

case for the Moteo Valley area, where poor calibration to groundwater level and seasonal change occurred. In this area, accuracy of the model (especially in terms of groundwater levels and groundwater level changes) is likely to be low.

Model calibration to observed long-term trends was only partially successful. The model appears to be capable of representing overall trend direction but not in detail, so the predictions of long-term trends are best to be treated as indicative.

In general, the model is capable of representing the groundwater dynamics reasonably well, but not in full detail everywhere.

Recharge during high flow events

As explained in Section 4.4.3 there is some uncertainty related to rate of recharge during high rainfall events. Follow up work may be required to confirm recharge rates in high flow events.

Data gaps

In some areas there is not enough data for fully constraining model parameters. For example, in the upper part of the Ngaruroro Valley upstream of Maraekakaho, there is limited gauging data or well drilling logs. In this area, the ability of the model to predict river interactions and detailed groundwater flow patterns is limited.

In particular there is limited data available on the deeper layer of the Heretaunga Aquifer.

Conceptual uncertainty

In some areas there is uncertainty related to conceptual understanding. For example, in the Tutaekuri valley downstream of Puketapu there is some evidence that this area is not connected to the Heretaunga Aquifer System. Despite this, this area has been included in the model domain to allow for a potential connection if this is discovered in the future. River losses or gains have not been detected either in this area, leading to the calibration algorithm assigning a low river conductance parameter in this area. In reality, the river may be hydraulically connected to the local aquifer and this is not represented in the model. This could mean that effects of abstraction on river flow are not represented correctly in this area.

Similarly, there is some conflicting evidence on the nature of the connection between the Moteo Valley aquifer and the Heretaunga aquifer (see discussion in Section 3.5.2). The model set up allowed for a connection, but if the connection happens to be absent, this may impact the accuracy of model predictions in this area.

6.2.3 Model resolution

Scale of the model

The model has been designed primarily as a regional tool and may not be suitable for small-scale applications such as assessing local scale effects of pumping from specific bores.

Horizontal resolution

The model horizontal resolution is 100 m by 100 m. Model parameterisation reflects the 2,000 m intervals between Pilot Points. Rivers included in the model are represented using 100 m by 100 m grid cells, but are parametrised using reaches consisting of multiple cells.

This means that the model can represent stresses (such as pumping) at a scale close to 100 m, but the aquifer properties and boundary conditions are simplified at a coarser scale. This means that model does not

represent small-scale heterogeneity (less than 2,000 metres) of the aquifer. It also means that coarse model parametrisation may be not strictly consistent with properties measured locally.

The model could be improved, if required for these specific applications, both in terms of grid resolution and parametrisation. However, in recent years the necessity of building increasingly complex models is being questioned by leading modelling experts (Doherty & Moore, 2017), and it is recommended to investigate whether such refinement effort could provide any value. The uncertainty analysis undertaken for this work will be reported in subsequent reports, and may provide an alternative to further model refinements.

Vertical resolution

Vertical resolution of the model is limited to two model layers. This means that smaller scale vertical effects, such as narrow clay bands and small aquifer divisions, and vertical gradients, such as near the coastal boundary, cannot be represented.

The vertical resolution could be made finer, which may be required for detailed saline intrusion modelling or contaminant transport modelling. Work has been undertaken for contaminant transport modelling in the Heretaunga by others (eg, Knowling *et al.*, 2018) where the existing 2 model layers have been subdivided into a total of 6 layers.

Temporal resolution

The temporal resolution of the model is one month. This may be a limitation for model scenarios that require finer time scale (for example assessing the environmental benefits of pumping bans). However, this could easily be resolved for model simulations at finer time scales.

7 Acknowledgements

Many people and organisation have contributed to this study. All published publications relied on in this report are referenced, but there is also a number of people who contributed to the study, but are not mentioned in the list of authors.

Special thanks to GNS scientists Catherine Moore for providing valuable advice on model calibration, and to Mike Toews for his great contribution to the model and PEST setups.

Thanks to Hugh Middlemis for an independent review which has greatly improved this report.

Thanks to HBRC scientists Simon Harper, Rob Waldron, and Thomas Wilding for their valuable input in data preparation and advice on Heretaunga Plains hydrology, with special thanks to Jeff Smith for management and technical overview of the project.

Thanks to technical advisory panel members Vince Bidwell, Hugh Middlemis, Catherine Moore, and David Scott for their valuable advice.

The list of contributors includes:

First Name	Surname	Institution	Contribution
Vince	Bidwell	Lincoln University	technical advisor
Vicky	Bloomer	HBRC	preparation of pumping data
Andrew	Bobst		high performance facility set up
Wesley	Burrows		PEST setup
John	Doherty	Watermark Numerical Computing	advice on PEST and providing PEST software
Dougall	Gordon	HBRC	advice on Heretaunga Aquifer
Robert	Greer		high performance facility set up
Simon	Harper	HBRC	advice on Heretaunga Aquifer
Hugh	Middlemis	HydroGeoLogic Pty Ltd	technical advisor
Catherine	Moore	GNS	technical advisor / advice on PEST and MODLOW setup
Uwe	Morgenstern	GNS	geochemistry and isotope study
David	Scott	ESR	technical advisor
Flore	Sergeant	HBRC	data preparation and processing
Stephen	Swabey	HBRC	technical overview of the project
Mike	Toews	GNS	model and pest setup
Mark	Trewartha	HBRC	initiation and management of the project
Rob	Waldron	HBRC	providing surface water data
Thomas	Wilding	HBRC	work on Heretaunga Springs

8 Glossary of abbreviations and terms

term or abbreviation	description
abstraction	Pumping of groundwater from the aquifer.
alluvium	Sediment (gravel, sand, silt) deposited by rivers and streams.
aquiclude	A geological formation that absorbs and holds water but does not transmit it at a sufficient rate to supply springs, wells.
aquifer	An underground layer of water-bearing permeable rock, rock fractures or unconsolidated materials.
aquitard	A geological formation of a semi-pervious nature that transmits water at slower rates than an aquifer.
artesian aquifer	A confined aquifer containing groundwater under positive pressure. This causes the water level in a well to rise to a point where hydrostatic equilibrium has been reached. A well drilled into such an aquifer is called an artesian well. If water reaches the ground surface under the natural pressure of the aquifer, the well is called a flowing artesian well.
conductivity (electrical)	The degree to which a specified material conducts electricity, in groundwater electrical conductivity is related to dissolved mineral content.
conductivity (hydraulic)	Ability of aquifer material to transmit water.
confined aquifer	see artesian aquifer
drawdown	The reduction in hydraulic head observed at a well in an aquifer, typically due to pumping.
GW	groundwater
HBRC	Hawke's Bay Regional Council
HDC	Hasting District Council
Hydraulic head	Hydraulic head or piezometric head is a measurement of groundwater pressure above a datum (in this report mean sea level is used a s datum). Sometimes groundwater level term is used instead.
IRRICALC	Irrigation demand and recharge model.
LSR	Land Surface Recharge
MODFLOW	Groundwater modelling software
MODPATH	Particle-tracking model that computes three-dimensional flow paths.
MT3D, MT3DMS	A modular three-dimensional transport model for the simulation of advection, dispersion, and chemical reactions of dissolved constituents in groundwater systems.
NCC	Napier City Council
OVERSEER	An agricultural management tool, based on a nutrient budget, which assists in examining nutrient use and movement within a farm, to optimise production and reduce nutrients losses from the farm.

PEST	Parameter Estimation software
PET	Potential Evapotranspiration
piezometer	An observation well designed to measure elevation of water table of hydraulic head.
Q2-7	Quaternary deposits
recharge	Recharge is precipitation, river bed seepage, flooding and other natural forms of water that enter the groundwater system.
SOURCE	Surface water modelling software
specific storage	The specific storage is the amount of water that a portion of an aquifer releases from storage, per unit mass or volume of aquifer, per unit change in hydraulic head, while remaining fully saturated.
specific yield	Specific yield, also known as the drainable porosity, is a ratio, less than or equal to the effective porosity, indicating the volumetric fraction of the bulk aquifer volume that a given aquifer will yield when all the water is allowed to drain out of it under the forces of gravity.
spring	A location where water flows naturally from an aquifer to the Earth's surface.
storativity	Storativity or the storage coefficient is the volume of water released from storage per unit decline in hydraulic head in the aquifer, per unit area of the aquifer. Storativity is a dimensionless quantity.
TANK	Tutaekuri, Ahuriri, Ngaruroro and Karamu Rivers' catchment.
Transmissivity	Ability of aquifer unit to transmit water, product of hydraulic conductivity and thickness.
Unconfined aquifer	An aquifer whose upper water surface (water table) is at atmospheric pressure, and thus is able to rise and fall.
VCN	Virtual Climate Network
well	An structure created in the ground by digging, driving, boring, or drilling to access groundwater in underground aquifers.

9 References

AEI (1991) *A model for assessing the impact of Regional Water Plans on irrigated agriculture.* Agricultural Engineering Institute.

Barnett B., Townley L., Post V., Evans R., Hunt R., Peeters L., Richardson S., Werner A., Knapton A., Boronkay A. (2012) *Australian groundwater modelling guidelines*. Sinclair Knight Merz and National Centre for Groundwater Research and Training.

Brooks T. (1999) *Review of Roys Hill artificial recharge site*. Hawke's Bay Regional Council, Napier.

Cameron S. (2003) *Report on the flow testing of bores 4797 and 4834, Matapiro Road*. GNS.

Carr R., Podger G. (2012) "eWater Source — Australia's Next Generation IWRM Modelling Platf." *Engineers Australia*.

Certes C., de Marsily G. (1991) "Application of the pilot point method to the identification of aquifer transmissivities." *Advances in Water Resources* 14: 284–300. https://doi.org/10.1016/0309-1708(91)90040-U

Chappell P.R. (2013) *The climate and weather of Hawke's Bay, 3rd Edition*.

DIA (2017) *Report of the Havelock North drinking water inquiry: Stage 1*. The Department of Internal Affairs.

Diack E., Williamson J. (2018) *Development of a model for simulating runoff and nutrient transport in the Tutaekuri, Ngaruroro and Karamu catchments using eWater SOURCE. (In Prep)*.

Doherty J. (2005) *PEST Model-Independent Parameter Estimation User Manual: 5th Edition*. Watermark Numerical Computing.

Doherty J. (2015) *PEST Groundwater Data Utilities*. Watermark Numerical Computing.

Doherty J. (2016a) "Calibration and Uncertainty Analysis for Complex Environmental Models."

Doherty J. (2016b) *PEST Model-Independent Parameter Estimation User Manual*. Watermark Numerical Computing.

Doherty J. (2017) *PEST_HP PEST for Highly Parallelized Computing EnvironmentsEST_HP*. Watermark Numerical Computing.

Doherty J., Moore C. (2017) *A Theoretical Analysis of Model Simplification*.

Dravid P.N., Brown L.J. (1997) *Heretaunga Plain Groundwater Study*. GNS,HBRC.

Gordon D. (2009a) *Roys Hill aquifer recharge review*. Hawke's Bay Regional Council, Napier.

Gordon D. (2009b) *Roys Hill recharge review*. HBRC.

Grant P.J. (1965) "Ground waters of the Heretaunga Plains. 1. Ngaruroro River as a major recharge source." *Journal of Hydrology (NZ)* 4: 65–80.

Harbaugh A.W., Langevin C.D., Hughes J.D., Niswonger R.G., Konikow L.F. (2017) “MODFLOW-2005: USGS three-dimensional finite-difference groundwater model.”

Harper S. (2015) *Groundwater level changes in the Heretaunga and Ruataniwha Basins from 1994-2014*.

Harper S. (2016a) *FROST PROTECTION DATA SET FOR THE HERETAUNGA MODEL*. HBRC.

Harper S. (2016b) *Permitted takes*. HBRC.

Hughes B. (2009a) *Statement of evidence of Mr Brydon Hughes. Appendix 3 in Resource Consent Hearing WP080487T*. Hawke’s Bay Regional Council, Napier.

Hughes B. (2009b) *Review of Paritua Stream Depletion Assessment Report*. Liquid Earth ltd: Rangiora.

Knowling M. (2018) *Heretaunga Aquifer groundwater model: Uncertainty Analysis and model calibration to groundwater age and nutrient concentrations.(In Prep)*.

Knowling M., Hayley K., Moore C.R., Rakowski P., Hemmings B.J.C. (2018) *Calibration-constrained Monte Carlo uncertainty analysis of groundwater flow and contaminant transport models of the Heretaunga Plains*. GNS.

Landcare Research (2000) “New Zealand Land Resource Inventory version 2”. GIS spatial data.”

Lee J.M., Begg J.G., Jones K.. (2017) *Geology and geomorphology of urban Napier-Hastings, Hawke’s Bay (in prep)*. GNS.

Lee J.M., Begg J.G., Tschritter C. (2014) *A 3D geological model of the greater Heretaunga/Ahuriri Groundwater Management Zone, Hawke’s Bay*.

Levy A. (2016) *Groundwater – surface water investigation Moteo Valley, Fernhill, Hawke’s Bay*. Lattey Group for Nuprop Ltd and Hamish Goodwin (resource consent WP060032Tb & WP160115T), Hastings.

Meyniel C. (2015) *Studies in the Heretaunga aquifer to the research of Sea Groundwater Discharges in Hawke’s Bay region.*

Millner I. (2017) *Catchment scale Nutrient modelling for the Tutaekuri, Ahuriri, Ngaruroro, Karamu (TANK) catchment’s (DRAFT)*.

Morgenstern U., Moreau M., Stewart M., Brown L., Franzblau, J Begg, H Martindale, M Toews, D Gordon, T Wilding, R van der Raaij, C Daughney, V Trompetter, J Kaiser, P Rakowski, J Smith, Knowling M. (2018) *Heretaunga Plains Aquifers: Groundwater Dynamics, Source and Hydrochemical Processes as Inferred from Age, Chemistry, and Stable Isotope Tracer Data*. GNS Science, Lower Hutt.

“NZ 56 Table Cape to Blackhead Point” (2012)

O’Shaughnessy H.J. (1988) *The Poukawa catchment water and soil resource management plan*. Hawke’s Bay Regional Council, Napier.

Perwick A. (2014) *Heretaunga Plains Transmissivity and Storativity Maps*. PDP Paddle Delamore Partners Ltd.

Pollock D.W. (2012) *User guide for MODPATH version 6—A particle-tracking model for MODFLOW: U.S. Geological Survey Techniques and Methods, book 6, chap. A41, 58 p.* USGS.

R Core Team (2018) *R: A Language and Environment for Statistical Computing*. R Foundation for Statistical Computing, Vienna, Austria.

Rabbitte S. (2009) *Paritua Stream depletion assessment*. EAM Environmental Consultants, Napier.

Rajanayaka C., Fisk L. (2016a) *IRRIGATION DEMAND MODELLING FOR TANK UPPER CATCHMENT (draft)*. Aqualinc.

Rajanayaka C., Fisk L. (2016b) *IRRIGATION WATER DEMAND & LAND SURFACE RECHARGE ASSESSMENT FOR HERETAUNGA PLAINS(draft)*. Aqualinc.

Rakowski P. (2018) *Heretaunga Aquifer Groundwater Model Executive Summary of Development Report*. HBRC.

Rosen M.R. (1996) "Hydrogeology, water quality, and nitrate movement in the unconfined gravel aquifer beneath the Maraekakaho sheep feedlot, Hawke's Bay, New Zealand." *Journal of Hydrology (New Zealand)* 35: 29–49.

Rushton K.R. (2004) *Groundwater Hydrology: Conceptual and Computational Models*. John Wiley & Sons.

S. Cameron, M. Gusyev, C. Meilhac, G. Minni, G. Zemansky (2011) *Pseudo-transient groundwater-stream interaction model for determination of the effect of groundwater abstraction on spring-fed stream flow in the Poukawa Basin, Hawke's Bay*.

Schreüder W.A. (2009) *BeoPEST documentation*.

Trewartha M. (2014) *Heretaunga Plains Groundwater Model Scoping Report (draft)*. HBRC.

Waldron R., Kozyniak K. (2017) *Hawke's Bay hydrological data 2008-2014 - State of the Environment technical report*. HBRC.

Watkins N., Selbie D. (2015) *Technical Description of OVERSEER for Regional Councils*.

Wickham H., Francois R., Henry L., Müller K. (2017) *dplyr: A Grammar of Data Manipulation*.

Wilding T.K. (2014) *Karamu Characterisation Report - Supporting Information for Water Allocation*. Hawke's Bay Regional Council, Napier.

Wilding T.K. (2017) *Heretaunga Springs: Gains and losses of stream flow to groundwater on the Heretaunga Plains*. HBRC.

Zheng C. (2010) *MT3DMS v5.3 Supplemental User's Guide*.

Zheng C., Wang P. (1999) *MT3DMS, A modular three-dimensional multi-species transport model for simulation of advection, dispersion and chemical reactions of contaminants in groundwater systems; documentation and user¡¯s guide*.

Appendix A Supporting memos

MEMO

To:	Pawel Rakowski
From:	Simon Harper
Date:	4th July 2016
Subject:	**FROST PROTECTION DATA SET FOR THE HERETAUNGA MODEL**
File Ref:	
Cc:	

This memo outlines the methodology used to compile frost protection takes for use in the Heretaunga groundwater model.

ASSUMPTIONS USED:

- A frost event is defined as any day where the daily minimum temperature is equal or below 0.0 degrees Celsius (NIWA; 2003)
- Frost protection occurs only during frost events and instantaneously at the maximum consented pumping rate
- Frost protection occurs only from frost protection consents
- The frequency and duration of frost protection on the Heretaunga Plains is limited to September, October and November.
- The average frequency of frost days and frost duration for each month is representative of all sites across the Heretaunga Plains.

FREQUENCY OF FROST DAYS

1. Number of days per month were calculated for selected climate sites on the Heretaunga Plains using frost probabilities (Niwa; 2003. Table 5). For example if the probability of a frost occurring in September is 24.6% the number of frost days is calculated as 30days x 24.6% = 7.38 days.

Site	Frost days in September	Frost days in October	Frost days in November
Bridge Pa	7	1	0
Hastings	3	0	0
Hasting FS	3	0	0
Havelock North	16	5	1
Napier Airport	3	0	0
Napier Nelson Park	2	0	0
Pakowhai	5	1	0
Roys Hill	4	0	0
Taradale	3	0	0
AVERAGE	**5**	**2**	**1**

DURATION OF FROST EVENTS

1. The duration of the frost events for each month were based on the frost duration maps by NIWA (NIWA, 2008).
2. The upper limit of the 1 in 5 year high (80^{th} percentile) located over Bridge Pa was to represent the average frost duration for the Heretaunga Plains. The frost durations were round up to the nearest day.

Summary of interpretation from frost duration maps

Map	September (hours)	October (hours)	November (hours)
80^{th} percentile	5	3	1

ESTIMATED VOLUMES

1. The volume of groundwater pumped for each month is calculated as follows:

Max take rate (m3/hr) X frost duration (hours) X number of frost days

e.g. 360 m3/hr X 5 hr/day = 1800 m3/day X 3 day/month = 5400 m3/month

RESULTS

Type	No consent	September	October	November	Annual total
Surface water	21	431,820	103,636.8	17,272.8	552,729.60
Groundwater	253	851,705.1	204,409.22	34,068.2	1,090,182.53
Total	274	1,283,525	308,046.02	51,341	1,642,912.13

DISCUSSION

1. The number of days frost protection occurs is likely to be greater than the number of days temperature is equal or below 0. In practise frost protection begins before a frost event. Therefore the frequency of frost days used in this methodology most likely underestimates the number of day's groundwater is used for frost protection.
2. Because pumping likely occurs before a frost event the duration of pumping for frost protection is also likely to be underestimated.
3. The frost probabilities indicated frosts on the Heretaunga Plains are likely to vary considerably in time and space. Therefore using the global average to represent all frost protection consents may not be appropriate.
4. The calculations assume only frost protection consents operated during frost events, however other consented takes are known to operate during frost events without frost permits.

QUERY USED TO OBTAIN FROST PROTECTION WELLS

Data source:
HBRC_SDE_DYNAMIC.SDEADMIN.VW_GDBCONSENTWATERTAKESUMMARY

1. Query consent layer to obtain groundwater and surface water current and section 124 consents

(StatusID = 'C' or StatusID = '124') and (SubTypeID = 'UNDERTAKE' OR SubTypeID = 'STREAMDEP' or SubTypeID = 'Take')

2. Selection consents from model boundary
3. Add frost protection consents to current selection

UseDetailID in ('IRRIGFROST', 'FROSTPRN', 'Damfill')

4. Review consents purpose and manually remove Damfill consents not used for frost protection.

Average frost duration in September - 1-in-5 year high (80th percentile)

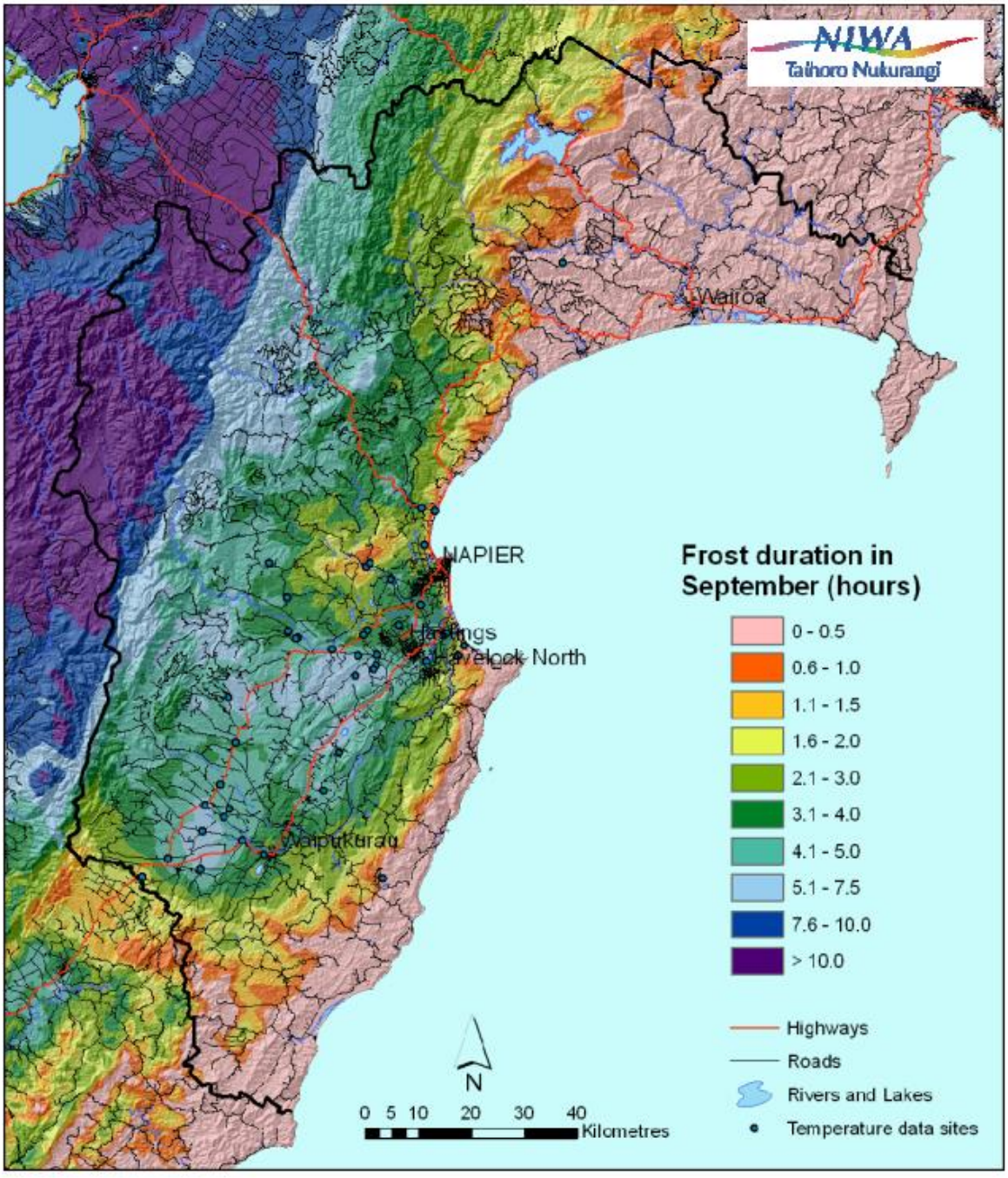

Average frost duration in October - 1-in-5 year high (80th percentile)

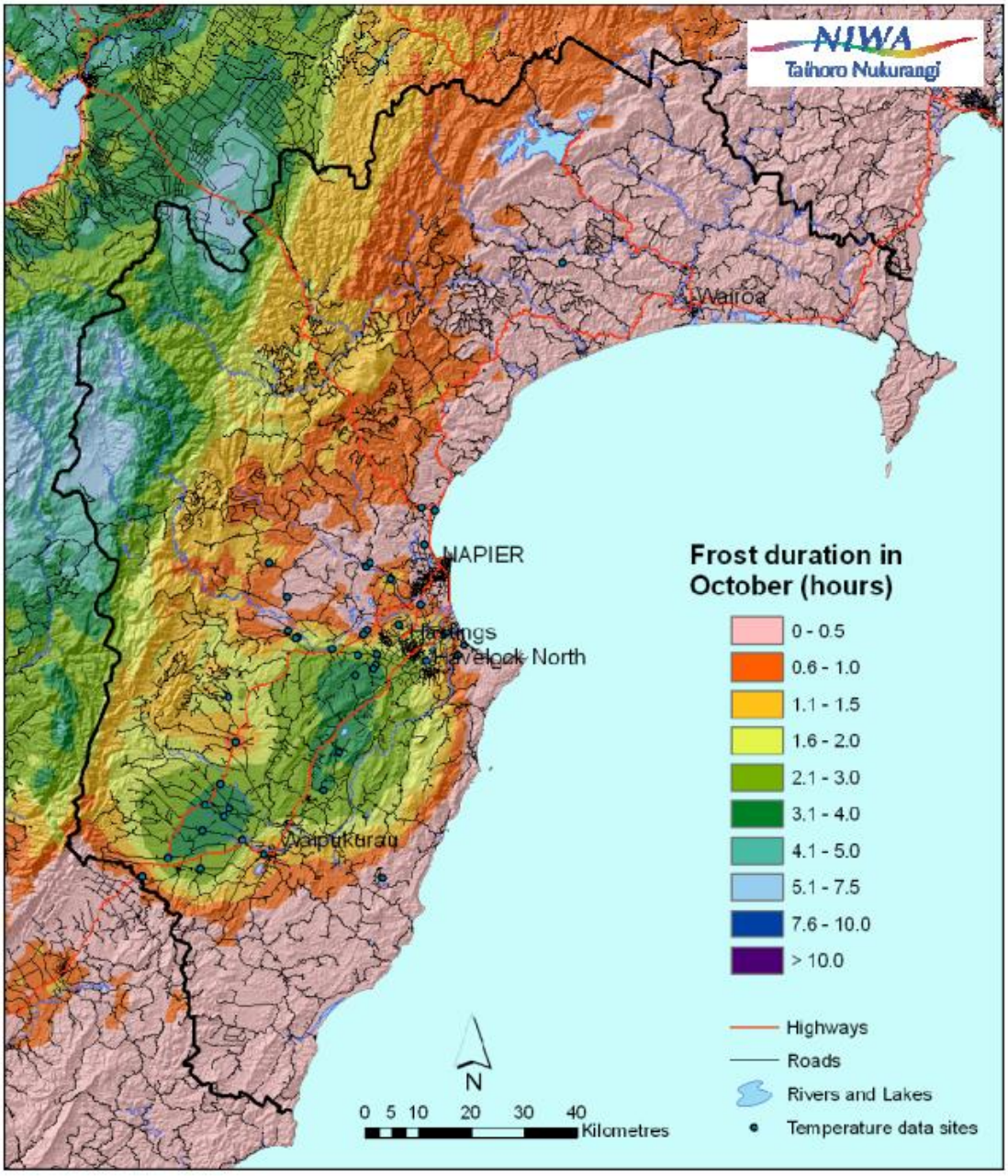

Average frost duration in November - 1-in-5 year high (80th percentile)

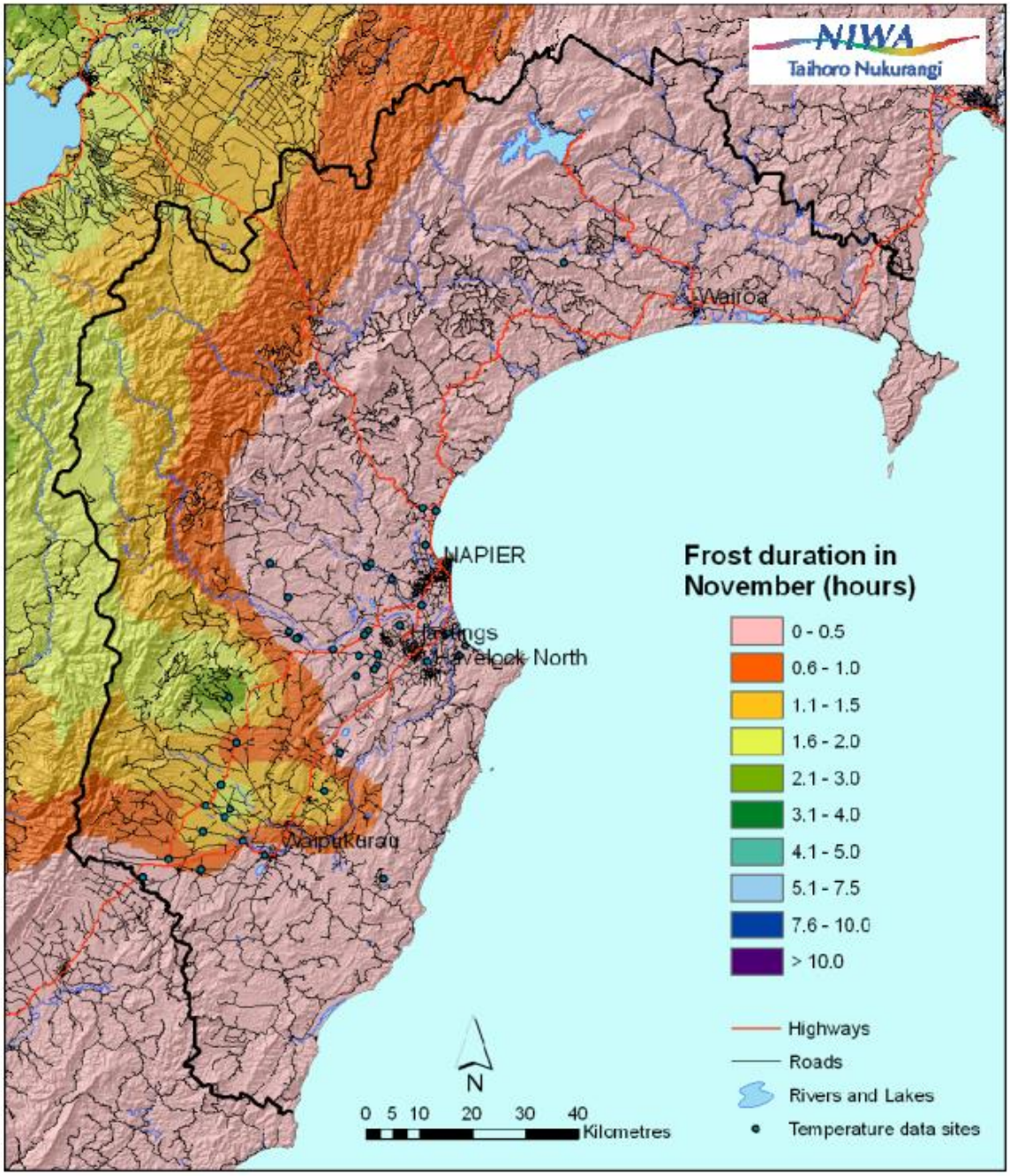

MEMO

To:	Pawel Rakowski
From:	Simon Harper
Date:	11/08/2016
Subject:	**PERMITTED TAKES**
File Ref:	
Cc:	

This memo briefly describes the methodology taken to estimate the volume of groundwater used by permitted takes in the Heretaunga model domain. In general the method follows the approach taken by Buchanan (Buchanan, 2011).

Permitted takes were divided into 3 main categories for estimating permitted groundwater volumes

1. Domestic requirements
2. Stock water
3. Dairy shed wash down and cooling.

INCLUSIONS AND EXCLUSIONS

- Only properties within 100 metres of a well were included in the estimates. All other takes were assumed to source water from either rainwater of surface water.
- Napier and Hastings ratings database were used to exclude properties linked to mains water supply.

DOMESTIC REQUIREMENTS

- To estimate groundwater used for domestic purposes an estimate of the number of people per household was multiplied by a rate of 300 l/h/d. This rate was used in the Buchanan report and considered appropriate for the typical Peak Daily Demand in Hawke's Bay (Buchanan, 2011)
- The population was obtained from the 2006 census meshblocks (NZ statistics).The mesh blocks extended beyond the model boundary and therefore a pro rata approach needed to be used.
- To determine the population per house hold the population in each meshblock was divided by the number of address locations to provide the average number of people living at each address.
- This approach assumes the population across the mesh block is evenly spread.
- A rate of 300 L/s was then multiplied by the number of people per household for all locations within the model domain to determine the domestic use.
- The address locations were then assumed to represent the point of take for groundwater use.

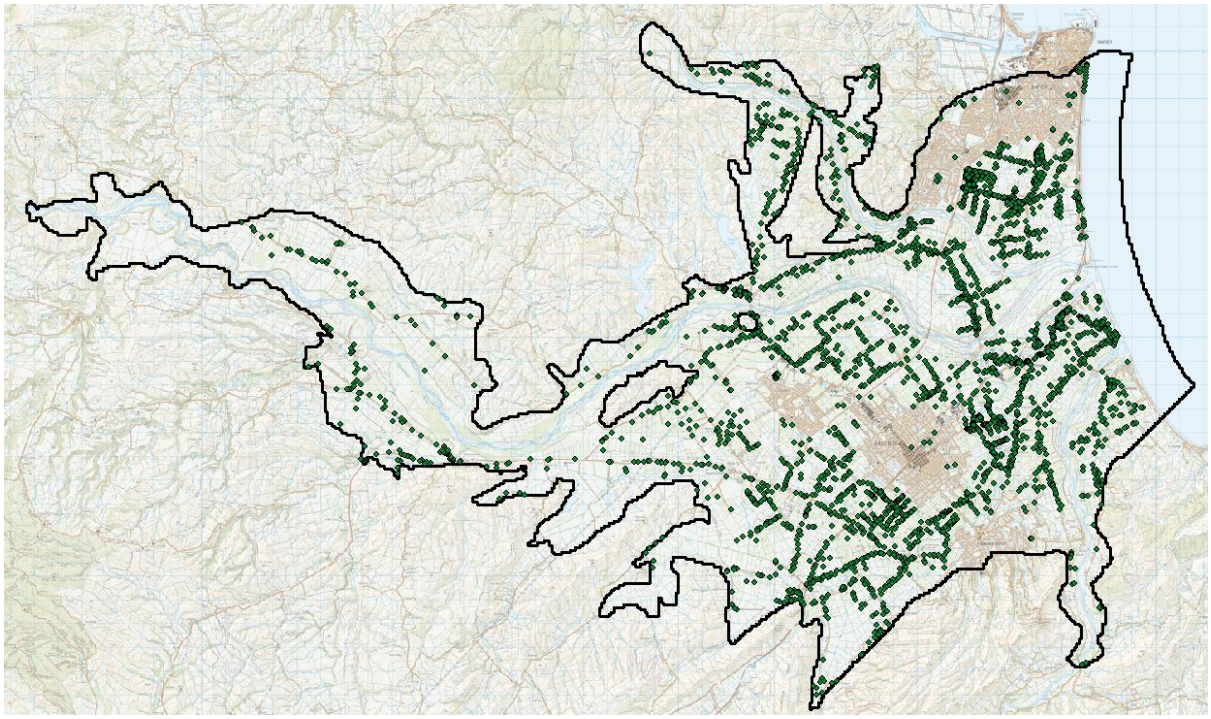

Location of domestic takes.

Results

- There are about 8000 people within the catchment using groundwater for permitted domestic needs.
- The total groundwater usage for permitted domestic needs is 2,448,392 l/day or 28.3 l/s or 893,663.08 m^3/year

STOCK WATER

- The 2015 AgriBase data set was used to determine the type of animals and stocking numbers for farms which intercepted the model boundary
- Farms were clipped to the model boundary and stock numbers recalculated based on the proportion of the farm within the model domain.
- The number of stock for each category were multiplied using estimates of Peak Daily Demand consumption rates (Buchannan, 2011). Guesses were made for animals not provided in the list based on estimates for other animals.
- Property centroid locations were used to represent pumping sites for Stock water use

Table 1: Stock water consumption volumes used to estimate permitted volumes

Description	rate (l/h/d)
Beef cattle numbers	55
Camelids (Alpacas and Llamas)	20
Dairy Cattle numbers	70
Deer numbers	12
Dogs	3
Donkeys	20
Ducks	0.3
Emus	3
Goats farmed	10
Horse numbers	70
Other Animals	10
Ostrich numbers	5
Pig numbers	35
Poultry birds	0.45
Sheep numbers	4.5

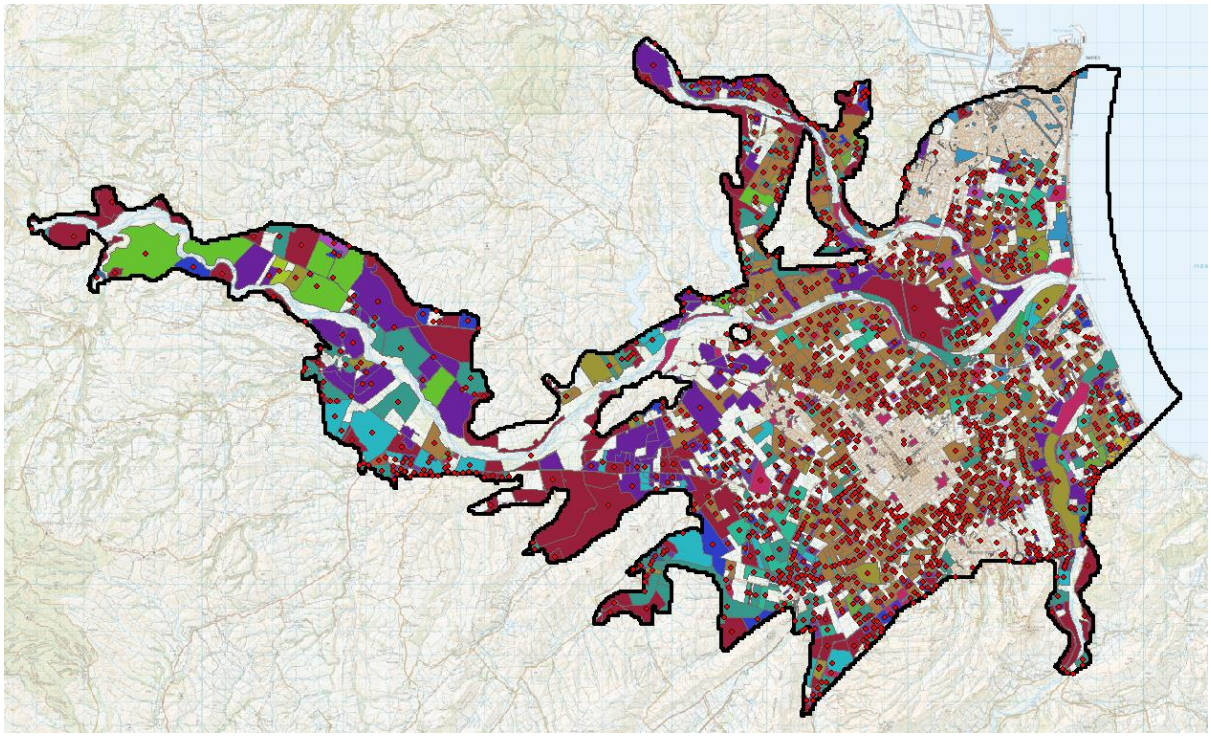

Location of farms with stock numbers.

Results

- Groundwater for animal drinking water was estimated at a Peak Daily Demand of 1,404,692 l/d or 16.25 L/s or 512,712 m^3/yr.
- The largest volumes were from Beef and Dairy farms which reflected not only the larger animal water requirements but also the larger farm size.

DAIRY SHED WASHDOWN AND COOLING

- The 2015 AgriBase data set was used to identify Dairy farms within the model boundary.
- Only farms without groundwater or surface consents were used to calculate permitted volumes.
- Farms were clipped to the model boundary and stock numbers recalculated based on the proportion of the farm within the model domain.
- Permitted volumes were calculated based on 70 l/h/d (Buchannan, 2011)
- Property centroid locations were used to represent pumping sites for Dairyshed washdown and cooling use

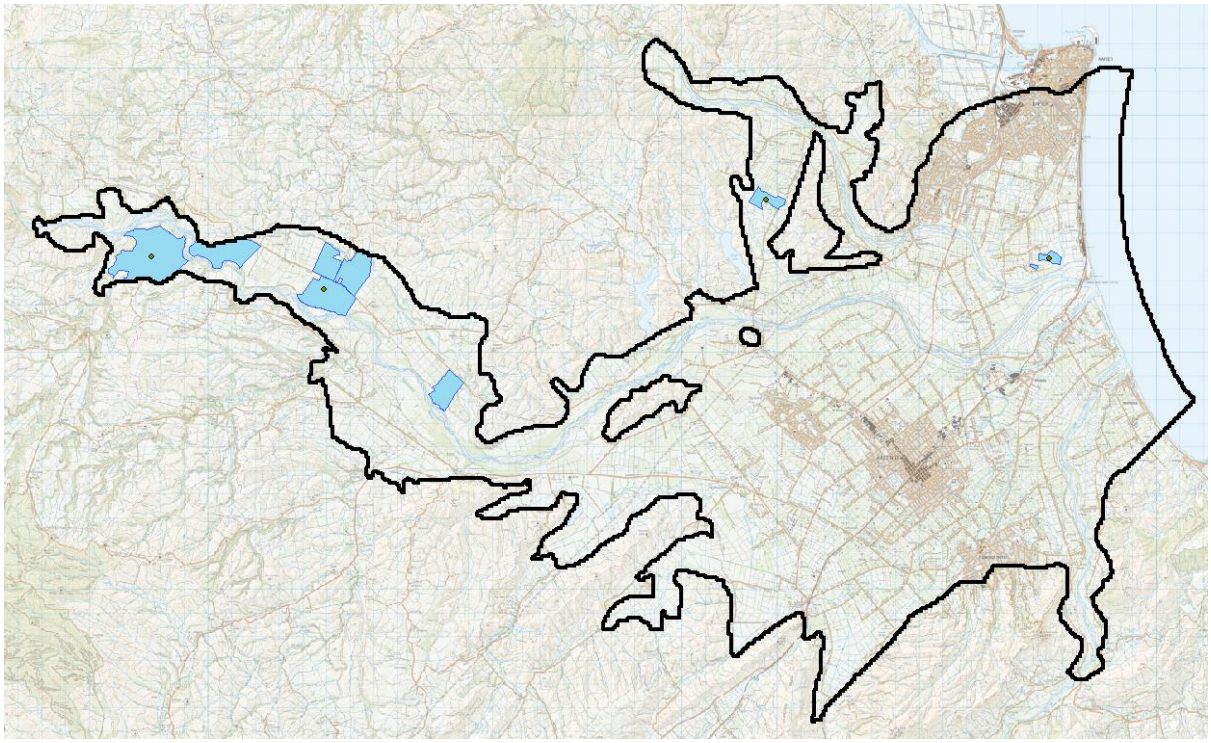

Location of Dairy farms and centroids used to represent permitted takes in these areas.

Results

- A total of 5 Dairy farms were identified within the catchment. Four were included in the permitted calculation. One farm was excluded because there was no evidence of a dairy shed.
- A total of 327,250 l/d or 3 l/s or 119,446 m3/yr was estimated for dairy shed wash down and cooling

Summary

Approximately 1.5 million m3/yr of groundwater is estimated to be used for permitted use in the model domain.

Type of use	Use (m3/yr)
Domestic	893,663
Stock	512,712
Dairy shed washdown	119,446
TOTAL	1,525,821